DOCTOR OF PHILOSOPHY

Development of a New Test Protocol for the Permit Ion Migration Test

Nanukuttan, Sreejith V.

Award date:
2007

Awarding institution:
Queen's University Belfast

DEVELOPMENT OF A NEW TEST PROTOCOL FOR THE PERMIT ION MIGRATION TEST

by

Sreejith V. Nanukuttan

B.Tech

Thesis submitted to

Queen's University of Belfast

for

The degree of Doctor of Philosophy

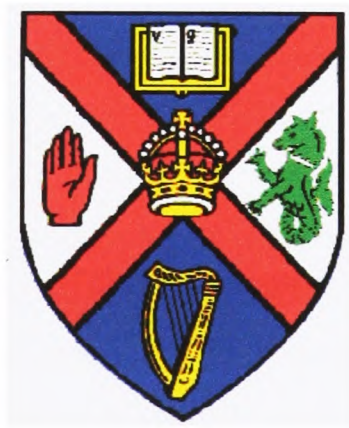

Faculty of Engineering and Physical Sciences

School of Planning, Architecture and Civil Engineering

March 2007

Abstract

Chloride induced corrosion of steel in concrete is one of the most common reasons for the deterioration of reinforced concrete in both marine and transportation structures. In order to assess the chloride penetration resistance of concrete, the common practice is to remove cores from the structure and test them in a laboratory to determine the chloride diffusion coefficient using the steady state diffusion test. This test is not popular due to its long test duration to achieve a steady state of flow of chlorides through the test specimen, which is used to calculate the diffusion coefficient. Therefore, applied voltage tests (known as migration tests) have become quite common, in which the transport of chlorides ions through the test specimens is accelerated by applying a potential difference across them. The measurements during either the non-steady state condition or the steady state condition are used to calculate a chloride migration coefficient, which has been reported to correlate well with the corresponding coefficient from the diffusion based tests. The chloride diffusion coefficient of concrete can also be predicted more rapidly using other indirect methods, such as the electrical resistivity test.

By following the principle of the migration test, a new *in situ* migration test (called the Permit ion migration test) was developed at Queen's University Belfast in the late 90s. The validity of this test was established for concretes containing normal Portland cement, by comparing the *in situ* migration coefficient with both the coefficient of diffusion (from both steady state and non-steady state diffusion tests) and the migration coefficient from the steady state migration test. However, it was considered to be necessary to broaden its applicability for testing concretes containing supplementary cementitious materials, by repeating the validation study on concretes containing such materials. Furthermore, there was a need to redesign the apparatus to make it more reliable and user-friendly for site applications. Therefore, a detailed investigation was carried out, initially as part of a European Round Robin Test programme (viz. EU FP5 Growth Programme - Chlortest) to identify the most reliable laboratory-based methods for assessing the chloride diffusivity of concretes which are commonly used in practice. This was followed by a detailed laboratory study on concretes containing supplementary cementitious materials, such as microsilica (ms), pulverised fuel ash (pfa) and ground granulated blast furnace slag (ggbs), in addition to normal Portland cement (opc) as a control. In this investigation, not only the tests identified in the initial investigation were used, but also were additional tests such as the new Permit ion migration test and the Wenner four probe resistivity test. The results from these investigations were used to establish the validity of the Permit ion migration test for testing concretes containing supplementary cementitious materials and to improve its test protocol.

As part of the Chlortest programme, a non-steady state diffusion test (to act as a reference method), a non-steady state migration test, a steady state migration test and a resistivity test were selected and a comparative (reliability) study was carried out using concretes, manufactured by four different EU countries, containing opc, pfa, ggbs and ms as binders. The results indicated that both the non-steady state migration test and the bulk resistivity test are the most reliable tests in assessing the chloride diffusivity of these. The results from the steady state migration test were found to be affected by the use of a thickness of the test sample less than the maximum size of the coarse aggregate.

In the validation study that was carried out using the Permit ion migration test, the *in situ* migration coefficient correlated well with the non-steady state migration coefficient, the steady state migration coefficient and the bulk resistivity for a range of concrete mixes containing different types of binders, such as opc, ms, pfa and ggbs. For the determination of the onset of the steady state condition and the estimation of the steady state chloride flux, it was found that the conductivity of the anolyte could effectively be used, which in turn could eliminate the need for sampling chloride solutions from the anolyte periodically. Further, there existed an excellent degree of correlation between the peak current and the steady state migration coefficient from both the steady state migration test and the Permit ion migration test, which indicated that the former could be used to predict the latter, with much lesser effort and complexity of the test protocol.

On the basis of the findings from both sets of investigation, a new test protocol was developed for the Permit ion migration test and the Permit was redesigned. The new test protocol used conductivity of the anolyte instead of the chloride concentration to identify the onset of the steady state condition and there is the option to calculate the chloride migration coefficient from either the peak current or the steady state of chloride flux. The new Permit was designed to work as a stand alone instrument on site, with little interference from the operation once the test had been started, but at any stage a computer could be connected to view the progress of the test.

Table of contents

List of symbols

a, B, q	constants
A	area of the concrete specimen
C_s	surface chloride concentration
C, C_o, C_{up}	chloride concentration of source (upstream or catholyte)
C_f or C_{free}	free chloride concentration
$C_{(x,t)}$	chloride concentration at depth x and time t
C_b or C_{bound}	bound chloride concentration
Cl^-	chloride concentration of the anolyte
C_i	initial chloride concentration
c_d	chloride concentration at colour change
C_r	reference chloride concentration
D	diffusion coefficient
D_e or D_{ssd}	effective diffusion coefficient or steady state diffusion coefficient
D_c	diffusion coefficient determined at concentration C
D_a or D_{nssd}	apparent diffusion coefficient or non-steady state diffusion coefficient
D_0	diffusion coefficient at infinite dilution
D_T	diffusion coefficient at temperature T
D_{PD}	diffusion index (from potential different test)
D_{up}	steady state migration coefficient from catholyte measurements
D_{CTH}	non-steady state migration coefficient (from CTH test method)
D_{nssm}	non-steady state migration coefficient
D_{ssm}, D_{mig}	steady state migration coefficient
$D_{in\ situ}$	*in situ* migration coefficient (from Permit ion migration test)

D_{1Dssm}	steady state migration coefficient (from conventional one-dimensional migration test)
erf	error function
ε	volumetric porosity
E_f	electric field
E, U	electrical potential applied between cathode and anode
F	Faraday's constant
i	current density
I	current
$i_{initial\text{-}1Dssm}$	initial current (from conventional one-dimensional migration test)
$i_{initial\text{-}in\ situ}$	initial current (from Permit ion migration test)
$i_{peak\text{-}1Dssm}$	peak current (from conventional one-dimensional migration test)
$i_{peak\text{-}in\ situ}$	peak current (from Permit ion migration test)
γ	activity coefficient
J	ionic flux
K_{cr}	penetration parameter
λ_{25}	conductivity of the anolyte at 25°C
λ_{Tc}	conductivity of the anolyte at T_c°C
L	thickness of concrete specimen
Q	charge passed
Q_{Cl^-}	total flow of chloride ions through the concrete
σ	conductivity of the specimen
σ_0	conductivity of the pore solution
R	Universal gas constant
R_{sp}, R_c, R_{c+sp}	electrical resistance

$R_{in\ situ}$	electrical resistance (from Permit ion migration test)
ρ_{1Dssm}	resistivity (from conventional one-dimensional migration test)
$\rho_{in\ situ}$	resistivity (from Permit ion migration test)
ρ_{Wenner}	resistivity (from Wenner four probe resistivity test)
ρ, ρ_{bulk}	bulk resistivity
t	time
T	absolute temperature
T_c	temperature of the anolyte in °C
u	mobility of ions
$\Delta\Phi$, ν	actual electrical potential across the concrete specimen
v_d	drift velocity
V_e	velocity of solution
V	volume of downstream cell
x	depth from concrete surface
X_d	depth of chloride penetration
z	valency of an ion
$\frac{dQ}{dt}$	rate of change of charge
$\frac{d\lambda_{25}}{dt}$	rate of change of conductivity
$\frac{dc}{dx}$	concentration gradient
$\frac{dQ}{dt}$	rate of change of charge
$\frac{dc}{dt}$	rate of change of concentration
$\frac{\partial C_b}{\partial C_f}$	chloride binding capacity

Acknowledgements

I would like to express my sincere appreciation to all those who contributed to the successful completion of this research programme. In particular, I would like to thank the following people:

I express my gratitude to my supervisor, Professor P.A.M. Basheer for his excellent supervision and support throughout the research. His advice and encouragement during the preparation of this thesis is sincerely appreciated. His role in developing me as a researcher will never be forgotten.

I am extremely grateful to my joint supervisor, Dr. D.J. Robinson for his guidance and support throughout the project.

Sincere thanks are also extended to Professor D.J. Cleland, Head of the School of Planning, Architecture and Civil Engineering and Mr. D. Ferguson, former Head of the School of Civil Engineering, for providing the facilities in the School to undertake this research.

The entire technical staff of the School of Civil Engineering, in particular those in the Concrete Laboratory, the Metal Workshop, the Wood Workshop and the Electronic Laboratory, for their assistance in this work. I owe special thanks to Mr. R Keag, Mr. T Crothers and Mr. W MacRoberts from the Metal Workshop and Mr. M Keegan and Mr. G Boyle from the Concrete Laboratory.

I am greatly thankful for the advice and technical support provided by Mr. A Thompson, Mr. K McDonald and Mr. K McKnight in the Electronic workshop. I am sincerely thankful to Mr. N Harmon for listening carefully to my needs, his patience with me and for responding promptly and with consideration during the design of the Permit ion migration test. Let me take this opportunity to highlight how privileged I am to work with such a great team. Their

unconditional support and enthusiasm for the instrumentation of the Permit ion migration test will always be remembered.

I thank all the postgraduate students of the School of Civil Engineering, especially Mr. K Owens, Mr. J Black, Mr. M Russell, Ms. I Liu, Ms. C Kee, Ms. J Brown and Ms. R Thom. I owe a special thanks to Dr. D McPolin, Dr. Y Bai, Mr. S Barbhuiya and Dr. L Basheer for their advice and support throughout this research project.

I am indebted to Kay Gemmert, who provided support and encouragement when it was needed the most.

Lastly, and the foremost, I express my deepest gratitude to my parents, for their advice and encouragement throughout this work. The unconditional love and support provided by them throughout all my life is sincerely appreciated.

Sreejith Nanukuttan

March 2007

Publications

1. Nanukuttan, S.V., Basheer, P.A.M., McCarter, W.J. and Robinson, D.J., The long term effect of surface coatings on chloride penetration in concrete at different exposure conditions, Bridge Engineering Research in Ireland, Proceedings of the 2004 symposium, Nov 2004, pp. 27-36.
2. Nanukuttan, S.V., Basheer, P.A.M. and Robinson, D.J., Developments on testing chloride transport of concrete on-site using Permit Ion Migration Test, International Conference on World of Innovations in Structural Engineering, Dec 2004, CD Rom.
3. Nanukuttan, S.V., Basheer, P.A.M., McCarter, W.J. and Robinson, D.J., Effect of duration and conditions of exposure on chloride diffusion, International Conference on Concrete Repair Rehabilitation and Retrofitting, Nov 2005. CD Rom, *(Received best student paper award, ICCRRR 05)*.
4. Basheer, L., Nanukuttan, S.V. and Basheer, P.A.M, An investigation into the Performance of Formtex Controlled Permeability Formwork and Effects of Its Reuse, Materials and Structures, (Being reviewed)
5. Nanukuttan, S.V., Basheer, P.A.M. and Robinson, D.J., Further developments of the Permit Ion Migration Test for determining the chloride diffusivity of concrete, Structural Faults and Repair 2006, July 2006, Edinburgh, CD Rom.
6. Nanukuttan, S.V., Basheer, L., McCarter, W.J., Robinson, D.J. and Basheer, P.A.M., Full-scale marine exposure tests on treated and untreated concretes: Initial seven year results, ACI Materials Journal, (Being reviewed)
7. Basheer, P.A.M. and Nanukuttan, S., Comparison of new in situ chloride migration test with a range of laboratory based chloride migration tests, Terry Holland Symposium, 9th CANMET/ACI International Conference on Recent Advances in Concrete Technology, Poland, May 2007.

Universities of
Cape Town and Witwatersrand

ICCRRR 2005

UNIVERSITÄT LEIPZIG
MFPA

Conference address: ICCRRR, Department of Civil Engineering, University of Cape Town
Snape Building, Private Bag, Rondebosch, 7701, South Africa
Telephone: +27 - 21 650 2603, Fax: + 27 - 21 689 7471
Email: ICCRRR@eng.uct.ac.za

Cape Town, 03.01.06

Re: Award certification ICCRRR 2005 – Best student paper

Dear Mr. Nanukuttan,

I am happy to officially congratulate you on the above award which was given to you during the International Conference on Concrete Repair, Rehabilitation and Retrofitting, ICCRRR 2005 for your outstanding paper titled "Effect of duration and conditions of exposure on chloride diffusion".

Sincerely,

Dr. Hans-Dieter Beushausen
ICCRRR co-chair

സമർപ്പണം

അക്ഷരത്തിന്റെ കനിവു പകർന്നു തന്ന അച്ഛനും
അമ്മയ്ക്കും ഗുരുക്കനമാർക്കും

Dedication

This thesis is dedicated to my parents and teachers who have inspired me throughout my life

Chapter 1

Introduction

1.1 Background to research

Chloride induced corrosion of reinforcement is considered as a major durability problem for reinforced concrete structures exposed to both marine and de-icing salt environments. Under normal conditions of exposure, a thin film of iron oxide protects the reinforcement from corrosion (Fidjestol and Tuutti, 1998). However, when the quantity of chloride ions in concrete near the reinforcement surpasses a threshold level, the break down of the oxide film occurs and the steel corrodes, with an associated volume increase of the corrosion products up to four times. As this process continues, the deposition of the expansive corrosion products on the reinforcement causes cracking and spalling and the eventual loss of the structural integrity. Expensive repair (or replacement) works need to be carried out in order to retain (or regain) the integrity of the structure (Kropp, 2002). This underlines the necessity for determining the corrosion related durability of structures.

As stated above, the presence of chloride ions at the steel-concrete interface is a pre-requisite for the chloride induced corrosion of steel in marine and de-icing salt environments. In modern concretes, where the use of calcium chloride as an accelerating admixture is not permitted, the presence of chlorides at the steel-concrete interface depends entirely on the resistance of the concrete to the ingress of chloride ions from the exposure environment (Polder, 2001). Hydrated concrete will have well developed pore network and chloride ions penetrate into the concrete through these pores. Therefore, the rate of transport of chloride ions through these pore spaces largely determines the rate of degradation and the service life of structures in chloride environments. Although chloride ions can be transported by absorption, diffusion and permeability, diffusion is considered to be the predominant

mechanism responsible for the transport of chloride ions (Zhang and Gjorv, 1995a; Kropp, 2002). Concrete imparts resistance to the diffusion of chloride ions via a combination of its characteristics, such as the pore diameter, the pore connectivity, the tortuosity and the chloride binding capacity of the binders used (Tang, 1999a). Therefore, the ability to measure the resistance of the concrete to chloride diffusion, i.e. the chloride diffusivity of the concrete, would enable the durability of the structure to be estimated in both marine and de-icing salt environments.

Conventional test methods for determining the chloride diffusivity of concrete involves removing cores from the structure and carrying out laboratory-based diffusion tests (Nilsson *et al.*, 1996). Two types of tests can be carried out, steady state diffusion test and non-steady state diffusion test. For concrete specimens the test duration for both these methods could be several months. For this reason more rapid test methods have been developed by many researchers (Tang, 1992b; Streicher and Alexander, 1995; Castellote *et al.*, 2001). The principle involves accelerating the transport of chloride ions through the concrete with the help of an electric field. The process governing the transport of chloride ions being migration, these tests are generally termed as migration tests. Due to the acceleration, the test duration could considerably be reduced, typically days. Thus, an early estimation of the chloride diffusivity could be made. However, migration tests are primarily laboratory based and, hence, they also require removing cores from structures to determine the diffusivity. This would mean that it is practically not feasible to carry out migration tests on a regular (and routine) basis to measure the chloride diffusivity of concrete structures.

Other forms of rapid tests are indirect in nature, one of which involves determining the electrical resistivity or the conductivity of the concrete. These tests are simple to perform and give repeatable results. However, further research is required in order to relate the results from these tests to the chloride diffusivity of different types of concretes.

A chloride migration test, capable of determining the diffusivity of concrete *in situ*, was developed at Queen's University Belfast (Andrews, 1999). The feasibility of the instrument was verified and the chloride diffusivity expressed in terms of an *in situ*

migration coefficient was found to correlate well with the results from other common test methods for a wide range of Portland cement mixes. Andrews (1999) showed that the *in situ* migration coefficient could be estimated in 4-10 hours for the normal Portland cement mixes he studied.

The advantage of this test over other methods of determining the chloride migration coefficient is that this test does not require removing cores from the structure. Therefore, the diffusivity of concrete can be determined non-destructively in any exposure condition within a short-time.

However, it was identified that further research is needed on the following aspects.

1. The validation study by Andrews (1999) was carried out only using normal Portland cement concretes. The use of supplementary cementitious materials, such as pulverised fuel ash (pfa), ground granulated blast furnace slag (ggbs) and microsilica (ms), in concrete is very common nowadays and the use of these materials promotes binding of chlorides and the modification of the pore structure. Therefore, compared to concretes containing normal Portland cement alone as a binder, the rate of chloride transport will be lower for these concretes. This means that there is a need to assess the performance of the new *in situ* ion migration test for a range of concrete mixes containing supplementary cementitious materials.
2. Andrews (1999) identified that the depth to which chloride ions reached were different for different concretes. This does not support the assumption that the average length, L, and the average flow area, A, used in the *in situ* ion migration test for calculating the *in situ* migration coefficient are constants. Therefore, the value of L and A used in the calculation of the ion migration coefficient needs to be studied further.
3. The test procedure proposed by Andrews (1999) requires monitoring of the chloride concentration throughout the test duration. This is performed with a chloride ion selective electrode, which requires much care and continuous calibration. Therefore, a qualified technician is required to take measurements throughout the test duration. For dense concretes, the test duration could be more than 10 hours. Not only this would increase the cost of carrying out a test, but also would increase the error associated with the measurements. Therefore, it is

necessary to adopt a test protocol involving alternative measurement techniques which can be automated.

The above limitations were addressed in this research and the associated objectives and the scope of the research programme are presented next.

1.2 Objectives and scope of the research

The overall aim of the project was to propose a scientifically supported *in situ* test for assessing the chloride transport resistance of concrete. This aim was achieved by satisfying the following objectives:

1. To identify suitable lab based test methods for assessing the chloride diffusivity of concrete, in conjunction with a European Union Round Robin Test Programme – the Chlortest, for use in comparative tests in this research.
2. To develop a new test protocol for the *in situ* ion migration test in order to address the deficiencies identified for the *in situ* ion migration test developed by Andrews (1999) and to establish experimentally the usefulness of the new test protocol for a range of mixes containing different cementitious materials.
3. To compare critically the new *in situ* ion migration test with the test methods identified from objective 1 and, thereby, to establish the validity of the new test protocol.
4. To develop a commercially viable test instrument for use on site and propose an automated test protocol.

1.3 Outline of thesis

The second and third chapters in this thesis are literature reviews. Chapter 2 introduces the different physical phenomena responsible for the chloride ingress into concrete and it identifies the different factors which affect the transport of chloride ions through concrete. Chapter 3 examines the methods for determining the chloride transport through concretes. Mainly three types of test methods were reviewed viz. diffusion-based tests, migration-based tests and indirect tests. The Chapter also provides a detailed review of the *in situ* ion migration test developed by Andrews (1999).

The fourth chapter introduces the experimental programme and describes two different test programmes which were carried out to achieve the objectives set out above. Details of the test methods and the materials used are included in this chapter.

The fifth chapter evaluates four rapid test methods used to determine the chloride diffusivity of concrete in the European project. The effect of the mix variables on the diffusivity parameters were analysed and the performance of the different test methods were studied based on the diffusivity parameters. Furthermore, relationships between different diffusivity parameters were critically analysed. The latter part of the chapter provides details of the formulation of a new test protocol for the *in situ* ion migration test.

The sixth chapter validates the new test protocol for the *in situ* ion migration test. The chapter elaborates the relationship between the test parameters from the *in situ* ion migration test and other tests. The findings of this chapter were used to refine the new test protocol of the *in situ* ion migration test with a view of automating the measurement procedure, which is detailed in the seventh chapter. Chapter seven also provides a summary of the different stages involved in the development of the *in situ* ion migration test and highlights the strengths and limitations of the test.

The eighth chapter draws together the main findings from this research programme and provides recommendations for further research.

Chapter 2

Chloride transport in concrete

2.1 Introduction

The effect of chloride ions on reinforcing steel has been identified as the main threat to the durability of the reinforced concrete structure (Mehta and Monteiro, 1993). At present the introduction of chlorides into concrete is controlled at the time of mixing using standards, (BS EN 206-1, 2000). Therefore, the predominant source of chloride ions in concrete is the exposure environment. The presence of chloride ions is not particularly detrimental to the concrete itself. However, these may destroy the protective oxide film on the reinforcing steel and, in presence of water and oxygen, corrosion occurs.

The corrosion process involves into two stages viz. the initiation period and the propagation period (Fig. 2.1). During the initiation period the build up of chloride ions occur near the steel. However, the steel remains passive even though the environment surrounding the steel is changing. This ultimately leads to the depassivation of steel and eventually corrosion occurs. Propagation period is considered as the time between the start of corrosion to the time until the performance of the structure can be considered to be acceptable. Therefore, the service life, which is the total time till the structure remains functional, depends on both the initiation and the propagation period (refer Fig. 2.1).

This chapter discusses the effect of various exposure environments on different chloride transport mechanisms and the transport mechanism which dominates in the longer term as far as a structure is concerned. In order to appreciate these topics the structure of concrete needs to be well understood. Therefore, a brief description of the structure of concrete and its main binding material, the hydrated cement paste (hcp) is given next.

2.2 Structure of hardened concrete

Concrete is a heterogeneous material consisting of aggregate particle dispersed in a matrix of cement paste. As the cement paste hydrates, the cement particles react with water to form a cement gel. This gel encapsulates the aggregate particles and forms a cohesive and heterogeneous material, which gains strength as hydration continues. Therefore, a hardened concrete matrix comprises mainly two phases, the aggregate phase and the hydrated cement paste (hcp) phase. If good quality aggregates are used, the structure of the aggregate phase remains unchanged in concrete. However, due to the continued hydration of the cementitious material and the interaction of the hcp with the environment, the structure of the hcp changes with time. Figure 2.2 depicts the structure of a hydrated concrete close to an aggregate. In the figure, a third phase can be seen, which is the interfacial region between the aggregate and the hcp. This is termed as interfacial transition zone (ITZ) and is considered to be weaker during the initial stages of hydration than the other two main phases, (Mehta and Monteiro, 1993). However, Mehta and Monteiro (1993) suggested that with the continued hydration and the deposition of the new reaction products in the ITZ, it may achieve similar properties as that of the hcp with time for concretes containing supplementary cementitious materials such as pulverised fuel ash, ground granulated blast furnace slag and microsilica.

The hcp consists of products of hydration, such as calcium silicate hydrate (C-S-H), calcium hydroxide (CH), unhydrated cement particles and pores of different sizes. The nature and characteristics of each of the hydration products will be affected if any cement replacement materials are present in the concrete. Their influence on the hcp and thus the chloride diffusivity are discussed in section 2.6.2. The hydration of normal Portland cement is briefly described below.

The main compounds of normal Portland cement are tricalcium silicate (C_3S), dicalcium silicate (C_2S), tricalcium aluminate (C_3A) and tetracalcium aluminoferrite (C_4AF). The Bouge compositions of the opc are given in Table 2.1. For simplifying the explanations, the chemical compounds are named with a simple letter representing the corresponding oxide composition (given in brackets), C (CaO), S

(SiO_2), A (Al_2O_3), F (Fe_2O_3), $\bar{S}$ (SO_3) and H (H_2O). The hydration of C_3S and C_2S results in the formation of C-S-H and CH, as shown below.

$$2C_3S + 6H \rightarrow C_3S_2H_3 + 3CH \qquad \text{(Eq. 2.1)}$$

$$2C_2S + 4H \rightarrow C_3S_2H_3 + CH \qquad \text{(Eq. 2.2)}$$

The hydration of C_3A is rapid and produces immediate stiffening of the paste, known as flash set. This rapid reaction is slowed down by the addition of gypsum which reacts with the C_3A (or C_4AF) to form calcium sulpho aluminate or ettringite.

$$C_3A + 26H + 3C\bar{S}H_2 \rightarrow C_6A\bar{S}_3H_{32} \qquad \text{(Eq. 2.3)}$$

gypsum ettringite

As hydration continues for several days, the concentration of sulphates in solution tends to diminish due to the consumption of gypsum. Meanwhile, the aluminate concentration increases due to the renewed hydration of C_3A and C_4AF. This favours the formation of monosulphates.

$$C_6A\bar{S}_3H_{32} + 2C_3A + 4H \rightarrow 3C_4A\bar{S}H_{18} \qquad \text{(Eq. 2.4)}$$

ettringite monosulphate

Monosulphates are regarded as the stable form of aluminate phases and this could be considered as the final product of the hydration of C_3A and C_4AF. However, the presence of ettringite is still found in mature concretes (Mehta and Monteiro, 1993).

The cement components react with various compounds to form a hardened matrix. The change in the volumetric proportions of the cement paste at various stages of the hydration is shown in Fig. 2.3. As cement hydrates, some of the capillary voids will be filled by the hydration products. This disrupts the connectivity of the pores. Majority of the ion transport takes place through the capillary pores (Neville, 1996). Therefore the continuity and torturosity of the capillary pore network or the pore distribution determines the diffusivity (Mehta and Monteiro, 1993).

Neville (1996) represented the on-going hydration of normal Portland cement paste using the volumetric proportions of individual particles (Fig. 2.3). The volume of gel is not sufficient to fill all the voids, thus creating a pore system larger than the gel pores, called capillary pores. The total volume of the capillary pores is termed as the capillary porosity. The total capillary porosity of the cement paste decreases with hydration. They have an approximate size of 1.3μm for cement and, their porosity

could vary with the degree of hydration. In fact the diameter of the capillary pores could be between 10nm to 1000nm (Mehta and Monteiro, 1993).

The formation of hydration product as a function of time is given in Fig. 2.4. The figure depicts the effect of these compounds in reducing the porosity. Besides these compounds certain factors can also affect the pore connectivity, such as pozzolanic reactions, carbonation and chloride binding. In section 2.6.1, the salient features of the chloride binding are discussed. The effect of pozzolanic reactions on the hcp is discussed in section 2.6.2. As the effect of carbonation on the pore structure is considered to be beyond the scope of this work, it is not discussed in this thesis.

2.3 Mechanisms of chloride transport

In concrete, the chloride ions are transported by the capillary pore system, the coarse pore system of the aggregates, the aggregate matrix interface, or the micro cracks present in the cement matrix (Kropp and Hilsdorf, 1995). However, it is the capillary pore network that is primarily responsible for the transport of chloride through concrete (Buenfeld and Newman, 1984). Therefore, the transport of chloride ions through concrete will be mainly influenced by the pore diameter, the pore size distribution and the connectivity between the pores (pore continuity and tortuosity) (McCarter *et al.*, 1992).

The following are the different physical mechanisms responsible for the chloride ion transport through concrete either individually or combined.

2.3.1 Permeation

Permeation of fluid containing chloride ions is relevant only in the cases of structures having a high hydrostatic pressure required to produce ingress (Kropp and Hilsdorf, 1995). Deep water marine structures or the bases of retaining structures are examples where this mechanism becomes relevant.

2.3.2 Capillary absorption

If the surface of a dry concrete is wetted with chloride laden water, the moisture along with the chloride ion is drawn into the dry capillary pores due to capillary

absorption. Therefore, the amount of chloride ions transported depends on the volume of water absorbed and the chloride concentration of the water (Kropp and Hilsdorf, 1995). When the water evaporates the chloride ions are left behind in the pores and, as the process repeats, the chloride concentration in the surface layers increases. As the interior of the concrete retains its moisture content, the capillary absorption is very much limited to the surface layers. However, in most of the structures a mixed mode of transport can be observed, i.e. the build up of chlorides due to the capillary absorption will lead to another form of transport known as diffusion.

2.3.3 Diffusion

The random motion of chloride ions in a saturated pore system under the influence of a concentration gradient is termed as diffusion (Kropp and Hilsdorf, 1995). The chloride ions diffuse towards part of the concrete having a lower chloride concentration (Poulsen, 1990). For a particular material, this can be defined in terms of a diffusion coefficient (Nilsson *et al.*, 1996). The moisture content has a very important role in chloride diffusion as the ions can only diffuse if sufficient moisture is present to provide a continuous liquid path through the pore structure of the concrete (Kropp and Hilsdorf, 1995) (section 2.7.3). This would also mean that if the concrete is relatively dry, the ingress of chloride ions can be due to the ingress of fluid carrying the ions due to the capillary absorption which is governed by the moisture content. Therefore, a mixed mode of chloride transport exists for most exposure conditions, except for concrete structures which are continuously submerged in seawater where diffusion is the sole mechanism, (Kropp and Hilsdorf, 1995).

2.4 Influence of the location of structure on the transport of chlorides

Structures mostly affected by chloride ion ingress and subsequent corrosion can be classified in two major groups, marine structures and traffic structures. The source of chloride ion in these two groups are different, viz., seawater and de-icing salts. A marine structure in this thesis is the term used for structures in contact with sea water directly or to airborne salts for example structures near to or on the coast. Traffic

structures are those which are in contact with de-icing salt, for example bridges and multi-storey car parks. The mechanism of chloride transport in these structures will depend on the location of the structure, the exposure condition and the source of chlorides. Therefore, combinations of these factors are used to identify the exposure classes in BS 8500-1 (2002). The different exposure classes are discussed in the following sections along with the transport mechanisms existing in each case.

2.4.1 Marine structures

The BS 8500-1 (2002) and BS EN 206-1 (2000) classify marine structures into the following three classes:

XS1: This is a semi-wet zone where airborne salts are the predominant source of chloride ions. Wind carries the chloride ion saturated moisture to the structure and therefore the direction of the concrete face will have an effect on the ingress. Windward sides may receive more chlorides than leeward sides, but they are more likely to be washed away by rainwater (Nilsson *et al.*, 1996). The chloride ions are transported into the concrete by means of both capillary absorption and diffusion depending on the moisture condition of the concrete.

XS2: Structures which are permanently submerged are included in this classification. In this case, except the initial absorption when concrete is first exposed to sea water, diffusion is the dominant transport mechanism (Nilsson *et al.*, 1996). Permeation could also exist if sufficient hydrostatic pressure develops (Kropp and Hilsdorf, 1995). The chloride content found in structures in this class is generally high. Nevertheless, in the absence of oxygen, a prerequisite for corrosion, the corrosion process might not occur compared to other classes.

XS3: Structures which undergo continuous wetting and drying are considered here. This includes structures from tidal zone, splash zone and atmospheric zones (see Fig. 2.5). The mechanisms of chloride transport will vary slightly between different zones. In tidal zone, where wetting and drying are continuous, the majority of the concrete remains saturated. Therefore, the predominant mechanism is diffusion and capillary absorption is limited to the outer most layers, provided the surface layer dries out (Nilsson *et al.*, 1996). As oxygen is readily available in this

zone, corrosion might initiate at a lower chloride content compared to structures in XS2 class. In splash zone, however, the chloride ions are either carried by the wind or the waves occasionally. The prolonged drying phase and the intermittent wetting means, the chloride concentration at the surface layers could be higher than the concentration of the sea water (Neville, 1996). Tang and Andersen (2000) suggested that this could be the severest of all the zones.

Even if the outer most layers of the concrete dries out, the interior retains some of the moisture. Therefore, chloride ions will continue to diffuse inward where the concentration is lower (Nilsson *et al.*, 2000). This suggests that after the initial build up of chloride concentration either due to diffusion or capillary absorption, the diffusion becomes the predominant transport mechanism (Bamforth and Chapman-Andrews, 1994).

2.4.2 Traffic structures

The traffic structures are divided into the following classes in BS 8500-1 (2002) and BS EN 206-1 (2000) based on their relative risk of corrosion. The chloride source in all these classes is the de-icing salts.

XD1: This class includes structures or part of structures, exposed occasionally to airborne chlorides. Structures remain in moderately humid environment throughout the exposure period. Therefore, capillary absorption is the main transport mechanism. However, if the interior of the concrete remains humid, this could establish a concentration gradient and subsequently diffusion becomes the main transport mechanism.

XD2: These are the structures which are in direct contact with chloride solution and remain humid through most of the year. Diffusion is the predominant mechanism in these structures.

XD3: This classification includes structures which are subjected to cyclic wetting and drying with water containing de-icing salts. The surface of these structures could be directly exposed to de-icing salts, or by sprays containing de-icing salts, for example walls, abutments and columns within 10m of the carriageway.

In all these classes, the exposure to chlorides is discontinuous as de-icing salts are mostly used in the winter months. Nevertheless, the initial uptake of chloride ions due to the capillary absorption will lead to a build up of high chloride ion concentrations beyond the surface layers. This will lead to a concentration gradient in concrete and chloride ions could diffuse to greater depths. In reality, the chloride ions could be transported towards the reinforcement by diffusion throughout the year. Therefore, similar to most other classes the diffusion can be considered as the predominant mechanism in the longer term.

2.5 Expressing the chloride diffusivity of concrete in terms of diffusion coefficients

Chloride ions enter the concrete by permeation, capillary absorption and diffusion. Permeation can be limited to certain type of structures, while capillary absorption can act either alone or in combination with the diffusion. However, diffusion is considered to be the predominant mechanism in the longer term, which is responsible for the accumulation of chloride ions at the level of reinforcement (Tang, 1995 and Zhang and Gjorv, 1995a). Therefore, for the estimation of service life of structures, the transport of chloride ions by diffusion is generally used as the basis for developing predictive models (Kropp and Hilsdorf, 1995 and Poulsen, 1990).

The following discussion deals with the methods to quantify the chloride diffusivity of concrete. Two types of diffusion are considered here, the steady state diffusion and the non-steady state diffusion.

2.5.1 Steady state diffusion

Steady state diffusion is the one where the rate of transfer of a diffusing substance through a section of unit area is proportional to the concentration gradient measured normal to the section (Page *et al.*, 1981 and Poulsen, 1990). This can be represented by the following equation.

$$J = -D\frac{dc}{dx} \qquad \text{(Eq. 2.5)}$$

where,

J is the ionic flux, mol/m^2.s,

$\frac{dc}{dx}$ is the concentration gradient, mol/m^4,

D is the diffusion coefficient, m^2/s.

This is referred as Fick's 1st law of diffusion. The negative sign indicates that the diffusion is occurring in the direction opposite to the increasing concentration. In order to apply Eq. 2.5 to the chloride transport through concrete, (Andrade, 1993) considered the concrete as an inert substance or a substance with certain binding capacity (see section 2.6.1). That is, any interaction between the diffusing chloride ions and the concrete is considered to be before applying the theory. Also, the interactions of the diffusing species with other ions are ignored (Nilsson *et al.*, 1996).

(Page *et al.*, 1981) applied the Fick's 1st law of diffusion for chloride ions in concrete.

$$J = -D_e \frac{dC_f}{dx} \qquad \text{(Eq. 2.6)}$$

where,

J is the ionic flux, mol/m^2.s,

C_f is the concentration of free chloride ions in pore solution, mol/m^3,

D_e is the effective diffusion coefficient, m^2/s.

In this case, only the gradient of the free chloride ions in the pore solution is effective as a driving force. Therefore, the diffusion coefficient is termed as the effective diffusion coefficient (Kropp and Hilsdorf, 1995 and Nilsson *et al.*, 1996).

The diffusion coefficients obtained from tests using a steady state flow of chloride ions are termed in this thesis as the steady state diffusion coefficient. Details of different test methods, which utilise the steady state flow to determine the coefficient, are discussed in the next Chapter.

2.5.2 Non-steady state diffusion

If the flow of chloride ions per unit volume per time is not constant, the change in concentration can be described by the law of mass conservation (Crank, 1975).

$$\frac{\partial c}{\partial t} = -\frac{\partial}{\partial x}\left(-D\frac{\partial c}{\partial x}\right) \qquad \text{(Eq. 2.7)}$$

This equation is referred to as Fick's 2nd law of diffusion. By considering that the medium is homogeneous and does not change with time (i.e. D is constant) as well as assuming simple boundary conditions, such as the boundary is semi-infinite and one side of the medium is exposed to a solution with constant chloride concentration, the analytical integration of Eq. 2.7 can be obtained (Kropp and Hilsdorf, 1995).

$$C_{(x,t)} = C_s\left[1 - erf\left(\frac{x}{\sqrt{4Dt}}\right)\right] \qquad \text{(Eq. 2.8)}$$

where,

$C_{(x,t)}$ is the chloride concentration at depth x at time t, mol/m^3,

C_s is the surface chloride concentration, mol/m^3,

erf is the error function,

D is the diffusion coefficient, m^2/s.

This equation is referred to as the error function solution to Fick's 2nd law. For non-steady state flow of chlorides in concrete this equation is widely used. The diffusion coefficient is referred to as the non-steady state diffusion coefficient D_{nssd} (or apparent diffusion coefficient D_a). If the spatial distribution of chloride ions in the concrete at any time *t* is known (termed as the chloride profile), the diffusion coefficient can be determined by best fitting the Eq. 2.8 to the data points. Details of different test methods, which utilise the non-steady state flow to determine the coefficient, are discussed in the section 3.2.4.

2.5.3 Relationship between steady and non-steady state diffusion coefficients

The hydrated cement paste can bind a portion of chlorides present in the pore fluid (see section 2.6.1). Therefore, only the rest of the ions are free for further diffusion. The chloride concentration used in Eqs. 2.7 and 2.8 to calculate the apparent diffusion coefficients, is the total chloride content, i.e. the free plus the bound chlorides. This means that the non-steady state diffusion coefficient determined using Fick's 2nd law depends on the chloride binding capacity of the matrix. Therefore, the

non-steady state coefficient can be written in terms of the steady state diffusion coefficient and the binding capacity (Nilsson *et al.*, 1996 and Tang, 1999a).

$$D_{nssd} = \frac{D_{ssd}}{\varepsilon\left(1 + \frac{\partial c_b}{\partial c_f}\right)} \qquad \text{(Eq. 2.9)}$$

where,

The units of D_{nssd} and D_{ssd} are m^2/s,

ε is the volumetric porosity,

$\frac{\partial c_b}{\partial c_f}$ is the chloride binding capacity.

If the binding capacity of a material can be determined, the two coefficients can be related to each other using Eq. 2.9. This suggests that the diffusivity of a material can be expressed using either the steady state diffusion coefficient or the non-steady state diffusion coefficient if the binding capacity is known. Unless otherwise stated, the term diffusivity used in the discussion represents the steady state diffusion coefficient (effective diffusion coefficient). Therefore the discussions mainly focus on two features of the chloride transport, viz. the diffusivity and the binding capacity.

2.6 Characteristics of concrete influencing chloride transport

Different characteristics of concrete which influence the transport of chloride ions through concrete are the water-binder ratio (w/b), the cement content, the type of binder (use of cement replacement materials), the aggregates and the degree of hydration. These factors influence not only the chloride ion diffusion, but also the chloride binding in the hcp.

2.6.1 Chloride binding

Chloride ions are found in concrete either as freely movable (free chloride ions dissolved in pore solution) or chemically or physically bound (bound chloride ions) to the various phases of the cement matrix. The combination of the two types of chlorides is referred to as the total chlorides and is often expressed as follows:

$$C_{total} = C_{free} + C_{bound} \qquad \text{(Eq. 2.10)}$$

The chloride binding reduces the amount of chlorides available in the pore solution (see Fig. 2.6). This in turn reduces the concentration gradient and slows down the transport of chlorides. Therefore, binding allows a higher quantity of total chlorides to be present before corrosion begins. Furthermore, the chloride binding causes modification of the pore structure, which results in blocking of the pores and, hence, a reduction in the transport of chloride ions. In general, it is the free chloride ions in the pore fluid which are considered to be responsible for the corrosion process (Arya *et al.*, 1990). The chloride binding reduces the amount of chlorides present in the pore fluid at the level of reinforcement (see Fig. 2.6).

2.6.1.1 Effect of chloride binding on cement hydrates

As mentioned before, chloride ions can be physically or chemically bound to the various phases within the cement matrix. The different phases in hcp which are responsible for binding chloride ions are discussed below.

Beaudoin *et al.* (1990) studied the interactions of chlorides with the C-S-H gel. He considered that chlorides can be held in C-S-H in three forms: absorbed on the surface of the C-S-H, chlorides in the interlayer space and chlorides that are incorporated in the C-S-H lattice. The first two forms are considered as water removable, i.e. the bond is weaker and is easily removed by the pore fluid. These chlorides are physically bound to the C-S-H gel. Chlorides incorporated in the C-S-H lattice are termed as tightly held. These are considered non-removable by the pore fluid or they are chemically bound in the C-S-H gel. As C_3S and C_2S are responsible for the formation of C-S-H, the total quantity of bound chlorides in the C-S-H depends on the amount of calcium silicates (C_3S and C_2S) present in the binder.

Delagrave *et al.* (1997) suggested that modification of the C-S-H occurs in the presence of chloride ions. The authors considered that the chloride ions can be physically bound to the C-S-H lattice. Suryavanshi *et al.* (1995) compared the scanning electron micrographs of the C-S-H in mortars, one with chlorides added during the mixing and the other without chlorides. In chloride free mortars the C-S-H was fibrous and needle shaped and considerable void space existed between the needles. However, in chloride containing mortars the C-S-H was much denser, with much less void space apparent. However, little published data are available

explaining the actual process by which the C-S-H densifies due to chloride binding, therefore further discussion is difficult.

Monosulphates ($C_4A\bar{S}H_{18}$) formed due to the hydration of cement chemically reacts with chloride ions to form calcium chloroaluminates, $3CaO.Al_2O_3.CaCl_2.10H_2O$. This is also referred to as Friedel's salt (Kropp and Hilsdorf, 1995). Chlorides can also chemically react with monosuplhates to form calcium chloroferrite, $3CaO.Fe_2O_3.CaCl_2.10H_2O$. Therefore, the total quantity of chlorides chemically bound to the hcp will be influenced by the total C_3A and C_4AF content of the binder (Hansson and Berke, 1989).

The capacity of the concrete to bind the chloride ions is termed as the binding capacity, which is often represented as the ratio of free plus the physically bound chlorides, c_f, to the chemically bound chlorides, c_b, ($\delta c_f/\delta c_b$). Nilsson *et al.* (1996) identified the important factors which govern the binding capacity. They are listed in Table 2.2, along with the effect that each factor has on the binding capacity. As this project is on test methods and not on binding capacity, further discussion of these factors are not considered.

2.6.1.2 Effect of chloride binding in opc concrete on the chloride transport

The presence of chlorides, either added at the mixing stage or penetrated into concrete later will lead to an increase in total porosity of the hcp (Kayyali, 1989 and Suryavanshi *et al.*, 1995). However, Suryavanshi *et al.* (1995) suggested that the increase in total porosity is mainly due to an increase in the number of small diameter pores. i.e. those less than 60nm. It is generally considered that chloride ions are transported through pores of diameter greater than 50nm (Hewlett, 1998). Therefore, the reduction in average pore diameter due to the modification of pore structure makes the transport of chloride ions through concrete more difficult.

A possible reason for the smaller pores is the deposition of chloro-complexes, such as Friedel's salt, in pores as mentioned in the previous section. The chloride ions in the chloro-complexes are considered as chemically bound and the deposition of such compounds reduces the pore diameter. As more chloro-complexes can be formed in

the case of binders with higher C_3A content, the chloride diffusivity will be considerably reduced for such binders.

2.6.2 Effect of cement replacement materials

The presence of cement replacement materials in concrete provides significant beneficial effects to the chloride diffusivity of the concrete. As explained in section 2.6.1, the binding of chloride ions, either chemically or physically, would reduce the chloride concentration gradient in the pore fluid. This leads to a reduction in the diffusivity.

From the discussion in section 2.6.1, it is evident that different cement replacement materials with different chemical composition will create varying effects on the binding capacity of a concrete. This could be based on the proportion of chemical compounds (Table 2.4) in the hcp of such concretes to which chloride ions may bind.

2.6.2.1 Pulverised fuel ash (pfa)

In concretes containing pfa as partial cement replacement material, the hydration of the pfa occurs due to the release of calcium hydroxides as a result of the hydration of the opc. The increase in pH due to the release of calcium hydroxide favours the dissolution of the pfa particles. This eventually leads to the formation of more C-A-H and C-S-H. This reaction can be slow, compared to concrete containing only opc. In such cases, the hcp of the pfa containing concrete will be more porous than the concrete containing opc only at early stages of hydration (Kropp and Hilsdorf, 1995). However, with time more reaction products form and occupy the pore spaces, thereby creating a denser hcp than opc concrete. The rate at which pfa particles dissolute depends largely on the fineness of the pfa particles. The specific surface (or fineness) area of commonly used pfa range between 250-600 m^2/kg. Chindaprasirt *et al.* (2007) studied three pfa of fineness 270, 390 and 450 m^2/kg. The authors showed that as fineness of pfa increased the chloride diffusivity decreased.

Nilsson *et al.* (1996) found that pfa was the most effective pozzolan in increasing the binding capacity; the reason attributed for this was the presence of reactive alumina to which chlorides could bind. It means that the higher amount of alumina present in pfa contributes to a higher binding capacity.

The performance of pfa as a binder on chloride diffusivity can be seen in Table 2.3. The replacement of opc with the pfa resulted in a decrease in the diffusion coefficient. Byfors (1987) demonstrated that the beneficial effect of pfa as a cement replacement material could be obtained even at 40%. The results support the findings by Nilsson *et al.* (1996) and, hence, these could be considered to be due to the improved binding capacity provided by the aluminate phase in the pfa. Therefore, the data reported by Page *et al.* (1981) could be considered to be due to the incomplete hydration of the pfa in his research work.

2.6.2.2 Ground granulated blast furnace slag (ggbs)

In concretes containing a blend of opc and ggbs as the binder, the hydration of the ggbs occurs due to the release of calcium hydroxide as a result of the hydration of the opc. The released calcium hydroxide increases the pH of the pore solution which leads to the dissolution of the ggbs particles (aluminosilicate glass) and, thereby, the hydration of the silicates and aluminates in ggbs, forming more C-S-H and C-A-H. The resultant hcp is broadly the same as that formed from the hydration of 100% opc. However, at higher replacement levels (50% ggbs), the hcp will contain less calcium hydroxide and more C-S-H and C-A-H than the opc alone. The additional C-S-H and C-A-H formed are deposited in the available pore spaces, therefore, the density of the hcp increases.

The results reported in Table 2.3 show that concretes containing ggbs have much lower diffusivity than the opc concretes. These trends can be attributed to the dense hcp and to the increased chloride binding and subsequent pore modification of concretes contaning ggbs. Ggbs concretes contain more aluminate content than opc (Table 2.4), therefore more chloride ions can be chemically bound as Friedel's salt. Also, commonly used ggbs has a higher specific surface area ($600m^2/kg$) when compared to opc ($320\ m^2/kg$). Therefore, the ggbs particles are much finer than those of opc. Consequently, more binding sites become active (Nilsson *et al.*, 1996). However, the nature of the chloride binding in ggbs concretes is a topic which needs further investigation. Therefore, the beneficial effect of ggbs in chloride binding is still unclear.

2.6.2.3 Microsilica (ms)

The large amounts of silica present in ms reacts with calcium hydroxide released due to the hydration of the opc particle, to form secondary C-S-H. These secondary C-S-H are formed in the pore space, which results in a very dense and less permeable hcp (Roy, 1989a). This is considered to be the main reason for the lower diffusivity observed in ms concretes.

However, unlike pfa and ggbs, the absence of aluminate phase (see Table 2.4) results in a decrease in the amount of chloride ions which can be bound chemically. As ms contain ultra fine particles it is much more reactive than most other cement replacement materials (Roy, 1989a) and produces a much greater amount of secondary C-S-H. Although, the increased amount of C-S-H could physically bind more chloride ions, this could be released to the pore fluid if the conditions within the concrete change.

Page and Vennesland (1983) studied the binding capacity of ms cement pastes. The authors stated that binding capacity of concretes with ms decreased with increase in ms replacement level. Arya and Xu (1995) reported that at 10% replacement level the use of ms resulted in less chloride binding occurring than in a 100% opc concrete. The results presented in Table 2.3 provide a good comparison of the diffusivity obtained for different concrete specimens. Byfors (1987) showed that the diffusion coefficient of concrete decreased with the inclusion of ms as cement replacement material. Furthermore, with the increase in replacement level (i.e. 0%, 10% and 20% respectively) the diffusivity was reduced considerably, irrespective of the w/b. Therefore, it can be concluded that although the binding is negligible with ms, the pore refinement due to secondary C-S-H leads to a considerable decrease in chloride diffusivity.

2.6.3 Effect of water binder (w/b) ratio

As the w/b increases, the total volume of capillary pores also increases (Neville, 1996). Although most of these pores become filled with the hydration products as cement hydrates, the quantity of empty pores increases with an increase in w/b. These empty pores act as conduits for the passage of chloride ions.

The influence of w/b on the chloride diffusivity of different concretes is shown in Fig. 2.7. Although there is a wide scatter of data, the diffusivity increased with an increase in the w/b.

Atzeni *et al.* (1989) reported that the average pore diameter decreases with a decrease in w/b. As majority of chloride ions are transported through capillary pores of diameter $\geq$ 50nm (Hewlett, 1998), the reduction in the average pore diameter would restrict the amount of chloride ions that can be transported, which would lead to a decrease in diffusivity with a decrease in w/b. In Table 2.3, the effect of w/b on chloride diffusivity for different types of binders can be seen. In each case, the effect of an increase in w/b was to increase the chloride diffusivity, which would suggest that the open porosity resulting from the increased w/b is not completely filled with the hydration products for all binder types. This signifies the need to limit w/b in order to reduce the chloride transport in concretes.

2.6.4 Effect of binder content

The effect of binder content on diffusivity is primarily due to the effect on the binding capacity. Nilsson *et al.* (1996) considered that as the binder content increases a larger volume of reaction products becomes available for binding chlorides.

Furthermore, as the binder content increases, the w/b normally decreases in a concrete, resulting in the effect discussed in the previous section.

2.6.5 Effect of aggregates

The presence of coarse aggregates in concrete can have the following effects:
The aggregate interrupts capillary pore continuity, thereby increasing the tortuosity. As the tortuosity increases the diffusivity decreases (McCarter *et al.*, 1992). Therefore, it can be concluded that an increase in the coarse aggregate content in concrete would decrease the chloride diffusivity.

The ITZ mentioned earlier is more porous than the hcp (Young, 1988). Therefore the diffusivity of this zone can be considered greater than the rest of the hcp. Schiessl and Hardtl, (1994) on their study of different aggregate size and its effect on chloride diffusivity, concluded that a higher specific aggregate surface results in a larger

transition zone, which in turn increases the diffusivity. Therefore, the chloride diffusivity for concretes with large aggregate size could be higher compared to concretes with smaller aggregates.

The porosity of the aggregate could influence the diffusivity of the concrete, but, the effect is considered to be negligible when compared to the porosity of the cement matrix (Nilsson *et al.*, 1996).

The effect of fine aggregate on the chloride diffusivity is generally considered as different to that by the coarse aggregate. An increase in fine aggregate content results in an increase in the ITZ area. As mentioned previously the porosity of the ITZ is higher than the hcp. Therefore, the large ITZ area would result in a faster transport of chloride ions, and, hence, increase the diffusivity.

2.6.6 Effect of curing

The development of a dense hcp depends on a proper curing (Nilsson *et al.*, 1996). The factors affecting the development of the hcp are the curing environment, curing temperature and curing duration. These are discussed in this section.

Page *et al.* (1981) compared the diffusivity of cement paste samples air cured for 60 days and those cured in a saturated in $Ca(OH)_2$ solution for 60 days. The authors found that specimens cured in $Ca(OH)_2$ solution have much lower diffusivity compared to the air cured specimens which highlight the significance of proper moist curing to reduce the diffusivity.

Investigations by Maage *et al.* (1996) found that the diffusivity of concrete specimens which are cured for 2 days was two times higher than those cured for 28 days. This reinforces the need to cure the concrete specimens for a much longer period in order to reduce the chloride diffusivity.

2.7 Other factors influencing the chloride diffusion in concrete

The influence of concrete characteristics on the chloride diffusivity was discussed in the previous section. However, there are other factors which could influence the

diffusivity of chloride. They are the concentration of free chlorides (C_f), the degree of saturation of the concrete, the temperature of the concrete (T) and the maturity of the concrete (M), ((Kropp and Hilsdorf, 1995; Nilsson *et al.*, 1996).

2.7.1 Concentration of free chlorides

Chatterji (1995) investigated the influence of concentration on the chloride diffusivity of concrete and found that the diffusivity of an ion increases with a decrease in the concentration. The following equation was deduced by the author to express the concentration dependency of the ion diffusion.

$$D_C = D_0 - a\sqrt{C} \qquad \text{(Eq. 2.11)}$$

where,

D_c is the diffusion coefficient determined at C, m^2/s,

D_0 is the diffusion coefficient at infinite dilution, m^2/s,

C is the concentration of the free chlorides, mol/m^3,

a is a constant.

The equation suggests that when the concentration is infinitesimal the diffusion coefficient, D_c will equal to the diffusion coefficient at infinite dilution, D_0. As the concentration increases, the D_c becomes smaller than D_0. This favours the conclusion made by Arsenault *et al.* (1995) that the increase in concentration decreases the rate of chloride diffusion.

2.7.2 Chloride cation type

Both sodium chloride (NaCl) and calcium chloride ($CaCl_2$) are used as de-icing agents. Therefore, the transport of chloride ions associated with the effect of different cations on the diffusivity is discussed next.

The diffusion of chloride ions is accompanied by a diffusion of the associated cations. The cations usually move at a slower rate than the anions, (Bockris and Reddy, 1970). This lagging motion of the cations acts as a dragging force on the diffusing chloride ions. Zhang and Gjorv (1996) established the higher dragging force created by the sodium ions compared to the calcium ions was the reason for the higher effective diffusivity of chlorides when the transport of $CaCl_2$ in concrete was studied.

Diffusion coefficients obtained from concrete specimens using different chloride solutions are given in Fig. 2.8. It can be observed from this figure that the diffusion coefficient increases in the order LiCl > NaCl > KCl > $CaCl_2$. (LiCl-lithium chloride, KCl-potasium chloride). Therefore, it can be concluded that the chloride diffusivity in concrete increases on the basis of the associated cation type. For cations with higher dragging force such as lithium, the diffusivity is much lower than that for NaCl and $CaCl_2$. This also confirms the conclusion by Zhang and Gjorv (1996) that the chloride diffusivity is higher for $CaCl_2$ in concrete compared to NaCl.

2.7.3 Degree of saturation

Chloride ions can diffuse through the concrete only, if sufficient moisture concentration provides continuous liquid paths in the capillary pore system. A reduction in the moisture content will cause a reduction in the number of continuous water paths and hence an increase in the diffusion.

Guimaraes and Helene (2002), demonstrated the effect of degree of saturation (S) on the diffusivity using data reproduced in Figs. 2.9 and 2.10. From the work the following observations were made by the authors can be explained.

1. As S decreased from 100% to 85% the diffusivity decreased rapidly. This was considered to be due to the reduction in water layer within pores of diameter ≈ 80nm. The water film in these pores reduced to a thin film adhering to the side of the pore wall.
2. As S decreased from 85% to 70% the reduction of diffusivity was less rapid because the water reduction occurred in smaller pores.
3. When S decreased beyond 75% the thin layer of water film remaining in the large pores also diminished, this further reduced the diffusivity.

Therefore, it can be deduced that the degree of saturation will have a considerable effect on the diffusivity of concrete.

2.7.4 Temperature

Kropp and Hilsdorf (1995) suggested that the diffusion coefficient can be written as a function of the temperature according to the Arrhenius equation.

$$D_T = D_0 e^{-\frac{B}{RT}} \qquad \text{(Eq. 2.12)}$$

where,

D_0, R, B are constants,

T is the absolute temperature of concrete, K,

D_T is the diffusion coefficient at T, m^2/s.

This equation suggests that the diffusion coefficient increases with an increase in temperature of the concrete.

Table 2.5 is a summary of reviewed literature that supports the Arrhenius equation. Page *et al.* (1981) reported the diffusion coefficient of cement pastes determined at different temperatures (see Table 2.5). The data show that irrespective of the w/b the diffusivity increased with the increase in temperature. The results reported by Goto and Roy (1981) confirmed that the diffusion coefficient is a function of the temperature and, hence, will increase with the increase in temperature.

2.7.5 Maturity of concrete

As concrete matures, capillary porosity decreases with the progression of the hydration reaction. The diffusivity will be higher for concretes at an early age compared to a mature concrete (Kropp and Hilsdorf, 1995). Table 2.6 provides a summary of the diffusion coefficients (non-steady state diffusion coefficient), determined from a marine structure exposed to varying exposure condition for a period of 7 years. The results suggested that for concretes in tidal region the diffusion coefficient stabilised within 1 year of exposure, while for splash and atmospheric zone, the reduction continued up to 7 years. The carbonation of the concrete in these two zones could have resulted in the reduction of the diffusion coefficient observed in Table 2.6.

2.8 Concluding remarks

In this chapter, it was established that the chloride transport in concrete in the long term depends primarily on its diffusivity, which can be characterised using either steady state or non-steady state measurements. Numerous factors affect the chloride diffusivity, some of which are related to the characteristics of the concrete and others

are influenced by the conditions of the concrete during the time of measurements. Therefore, in order to determine the chloride diffusivity, both in laboratories and on site, the following measures should be taken:

1. The specimens are sufficiently cured and fully saturated prior to carrying out the diffusion tests.
2. The tests are carried out at a constant temperature.
3. The chloride concentrations used are the same for each test.

In addition, care should be taken for any other factor which could affect the measurements.

Table 2.1 Main compounds of Portland cement (Neville, 1996)

Name of compound	Oxide composition	Abbreviation
Tricalcium silicate	$3CaO.SiO_2$	C_3S
Dicalcium silicate	$2CaO.SiO_2$	C_2S
Tricalcium aluminate	$3CaO.Al_2O_3$	C_3A
Tetracalcium aluminoferrite	$4CaO.Al_2O_3.Fe_2O_3$	C_4AF

Table 2.2 Factors affecting chloride binding (Nilsson *et al.*, 1996)

Factor	Increase(↑) or decrease(↓) of factor	Effect on chloride binding capacity	Remarks
Carbonation of binder	↑	↓↓↓↓↓	Cl^- binding ≈ zero in carbonated concrete
Temperature	↑	↓↓	
pH (or hydroxide concentration)	↓	↑	
Relative humidity	↓	↓	
Soluble sulphates	↑	↓	
Aluminate phase in cement	↑	↑↑	
Ferrite phase in cement	↑	↑	Ferrites phase is considered less effective as compared to aluminates phase, therefore binding may be less effective
Mineral admixture with reactive aluminium (fly ash, slag, etc.)	↑	↑↑	3 effects: A) more reactive aluminate phase B) lower pH in pore solution C) pozzolanic reaction, increases the C-S-H gel
Microsilica	↑	↑↑↓	3 effects: A) ms increases binding at given pH B) ms decreases pH C) ms increases the amount of C-S-H gel

Table 2.3 The effect of w/b and type of binder on the diffusion coefficient

Reference	Type of cement	w/b	Diffusion coefficient ($x10^{-12}$ m^2/s)
Page *et al*. (1981)	100% opc	0.5	4.47
	70% opc + 30% pfa	0.5	14.70
	35% opc + 65% ggbs	0.5	0.41
Decter *et al*. (1989)	100% opc	0.5	4.51
	60% opc + 40% ggbs	0.5	1.51
	50% opc + 50% ggbs	0.5	1.02
	35% opc + 65% ggbs	0.5	0.17
Byfors (1987)	100% opc	0.4	1.80
	100% opc	0.5	6.80
	100% opc	0.6	18.70
	90% opc + 10% ms	0.4	1.80
	90% opc + 10% ms	0.5	2.40
	90% opc + 10% ms	0.6	9.90
	80% opc + 20% ms	0.4	0.32
	80% opc + 20% ms	0.5	0.59
	80% opc + 20% ms	0.6	3.10
	85% opc + 15% pfa	0.4	0.63
	85% opc + 15% pfa	0.5	3.20
	85% opc + 15% pfa	0.6	2.60
	60% opc + 40% pfa	0.4	0.08
	60% opc + 40% pfa	0.5	0.13
	60% opc + 40% pfa	0.6	1.70

Table 2.4 A comparison of different cementitious materials (Newman and Choo, 2003)

Material	CaO	Al_2O_3	Fe_2O_3	SiO_2
Normal Portland cement	65%	5%	3.5%	20%
Ground granulated blast furnace slag	40%	11%	0.3%	38%
Pulverised fuel ash	3%	28%	10.4%	50%
Microsilica	0.2%	0.7%	1.2%	92%

Table 2.5 The effect of temperature on the effective diffusion coefficient of cement paste (Kropp and Hilsdorf, 1995)

Reference	**w/b**	**Temperature (°C)**	**Curing**	**Diffusion coefficient ($x10^{-12}$ m^2/s)**	**Type of mix**
Page *et al.* (1981)	0.4	7	60 day moist curing	1.1	Cement paste
		25		2.6	
		44		8.4	
	0.5	7		2.1	
		25		4.5	
		44		18.4	
	0.6	7		5.2	
		25		12.3	
		44		31.8	
Goto and Roy (1981)	0.4	35	4 weeks at 60°C	2.7	Cement paste
		45		3.7	
		60		9.2	

Table 2.6 The effect of exposure duration (maturity) on the diffusivity of concrete (Nanukuttan *et al.*, 2005)

Exposure zone	Exposure duration (years)	Diffusivity ($x10^{-12}m^2/s$)
Tidal low level	1	3.77
	2	3.35
	3	2.77
	4.67	3.65
	7	3.13
Tidal high level	1	1.75
	2	2.66
	3	2.23
	4.67	2.03
	7	0.41
Splash zone	1	5.41
	2	1.28
	3	0.99
	4.67	0.82
	7	0.28
Atmospheric zone	1	-
	2	1.30
	3	0.62
	4.67	0.32
	7	2.21

Note: diffusivity determined using chloride profiles from w/b 0.40 opc concrete piers.

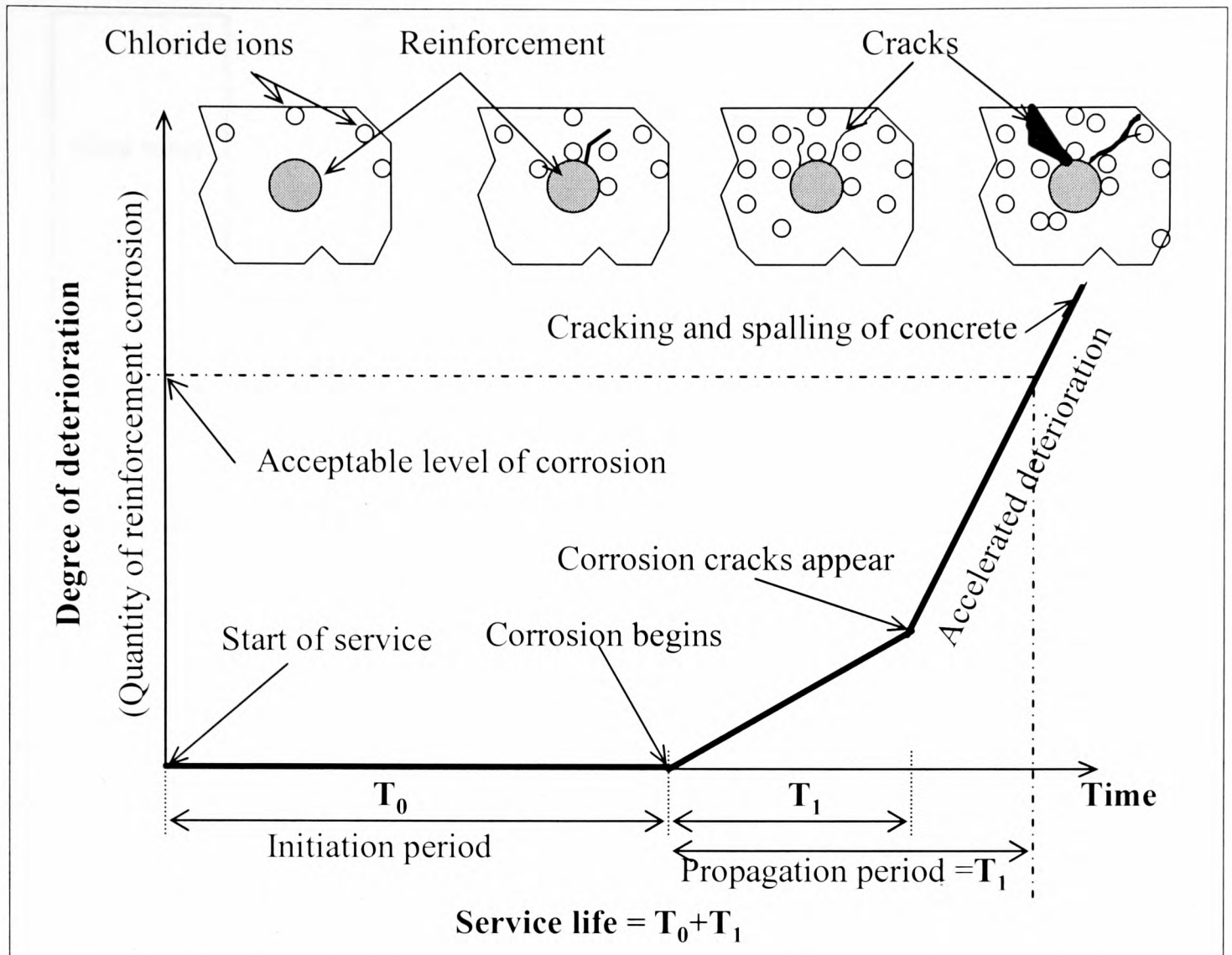

Figure 2.1 Progress of chloride-induced deterioration (Yamamoto *et al.*, 1995)

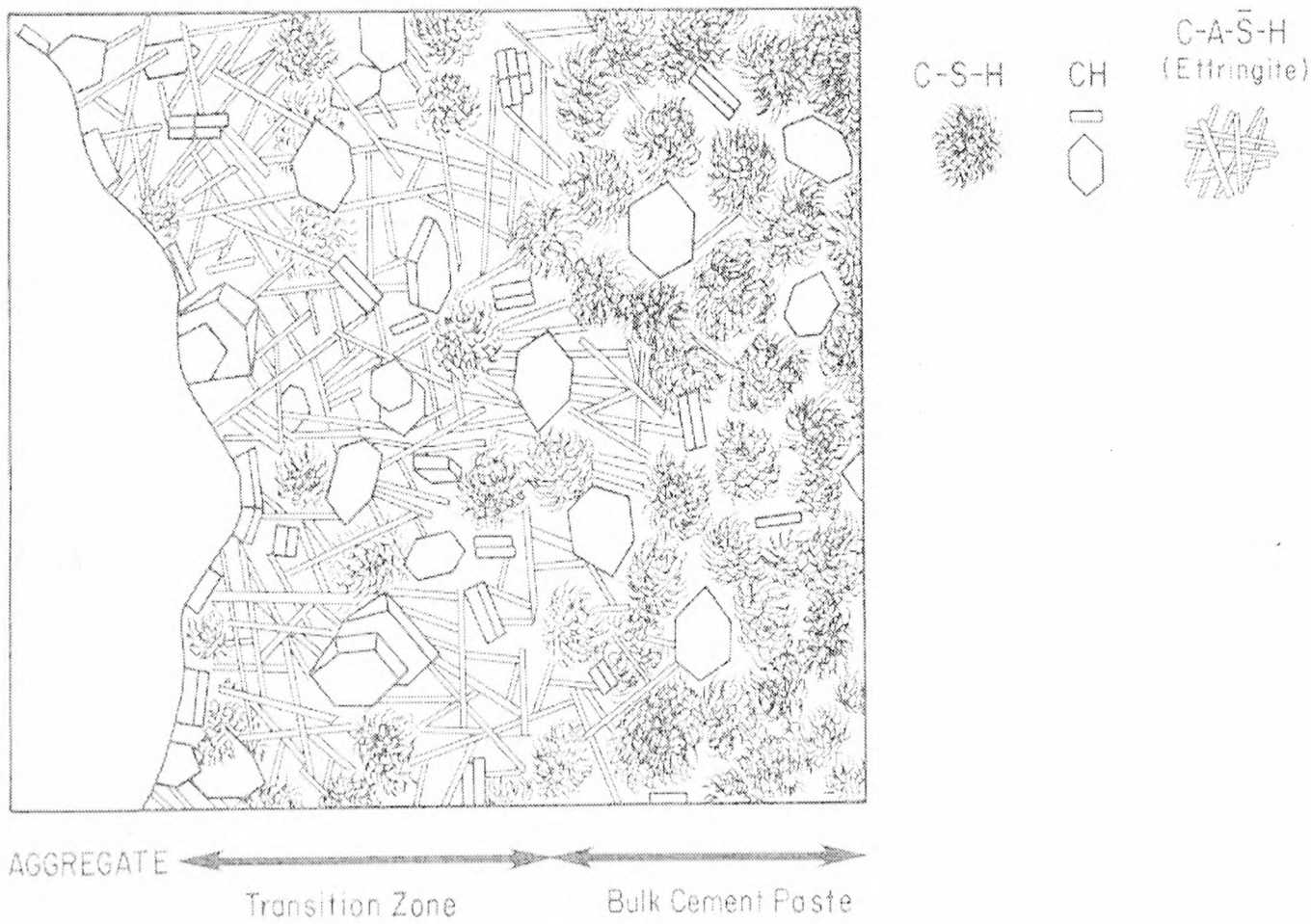

Figure 2.2 The structure of hardened concrete (Mehta and Monteiro, 1993)

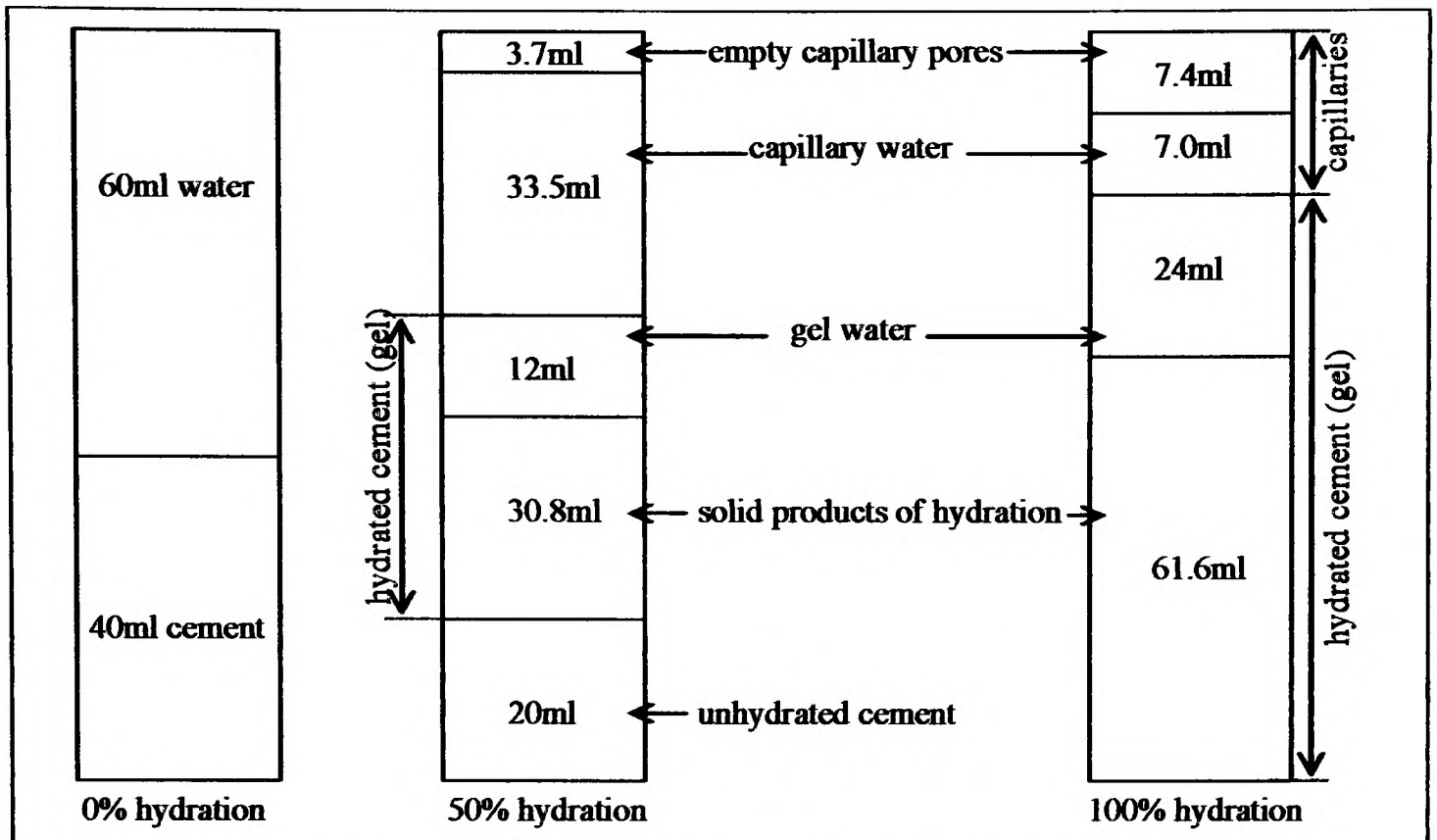

Figure 2.3 Diagrammatic representation of the volumetric proportions of cement paste at various stages of hydration for w/b of 1.25 (Neville, 1996)

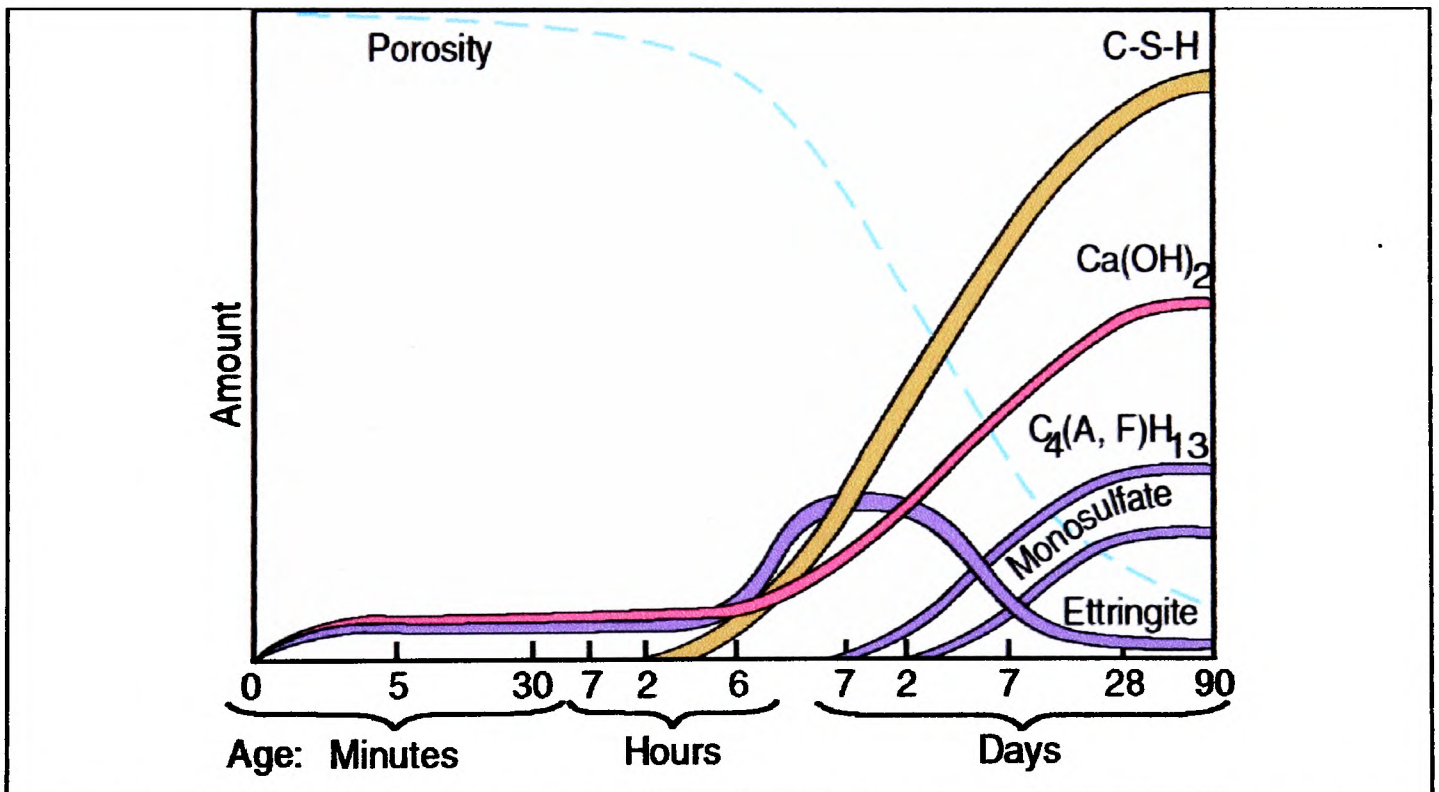

Figure 2.4 The products of hydration represented as a function of time (Kosmatka *et al.*, 2002)

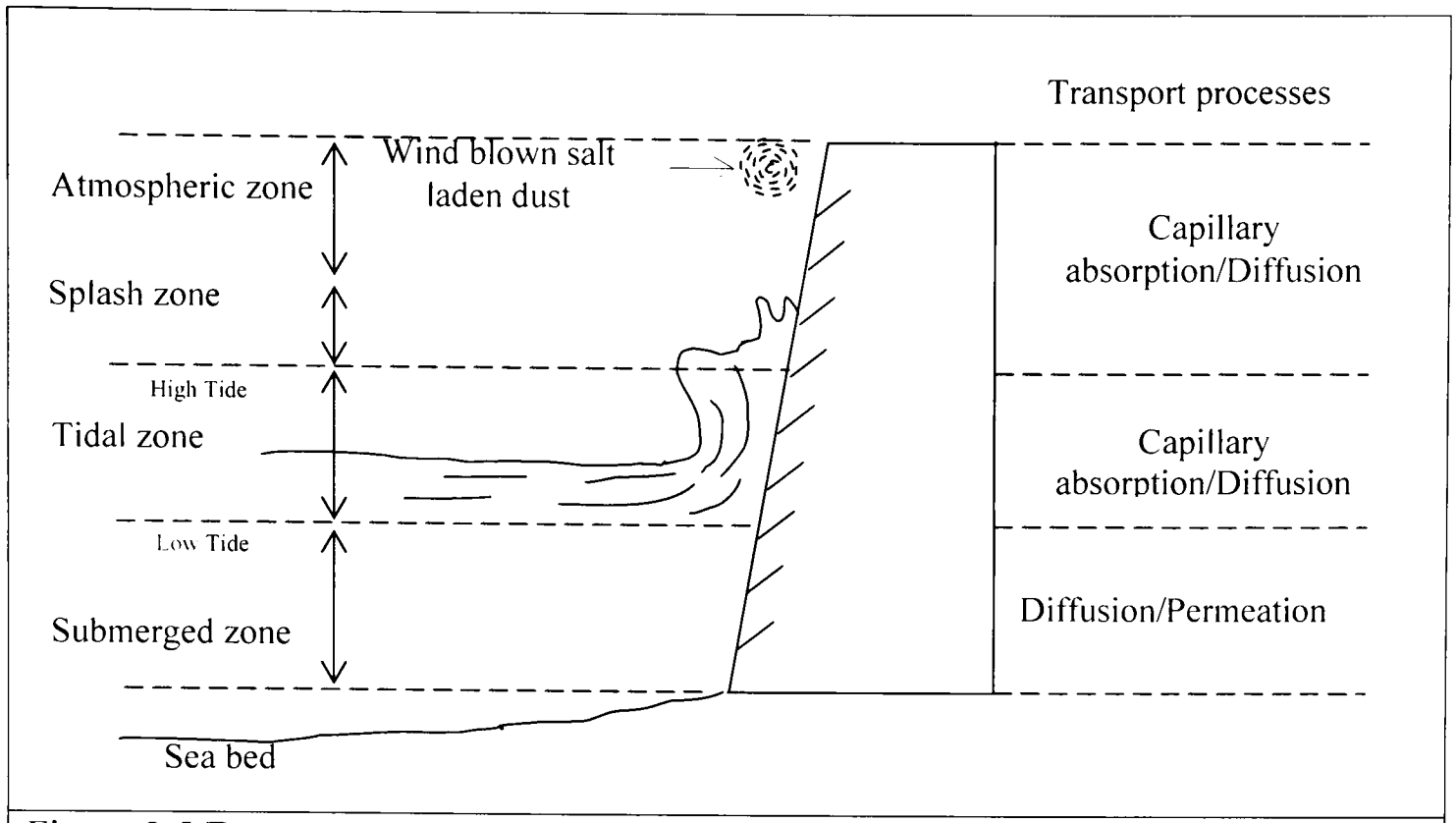

Figure 2.5 Exposure zones for a marine structure and the possible transport processes

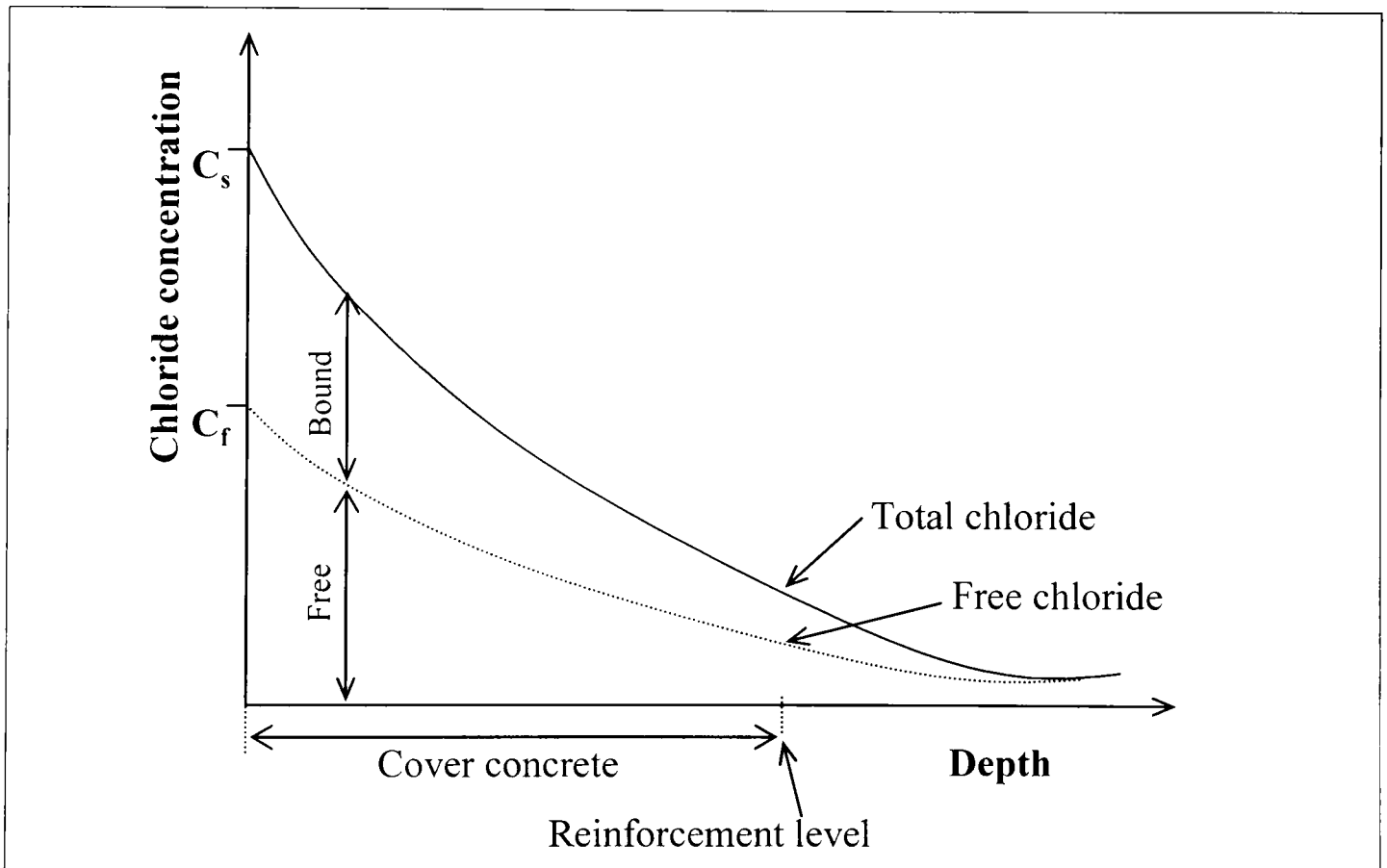

Figure 2.6 Typical profiles of free and bound chlorides (Nilsson *et al.*, 1996)

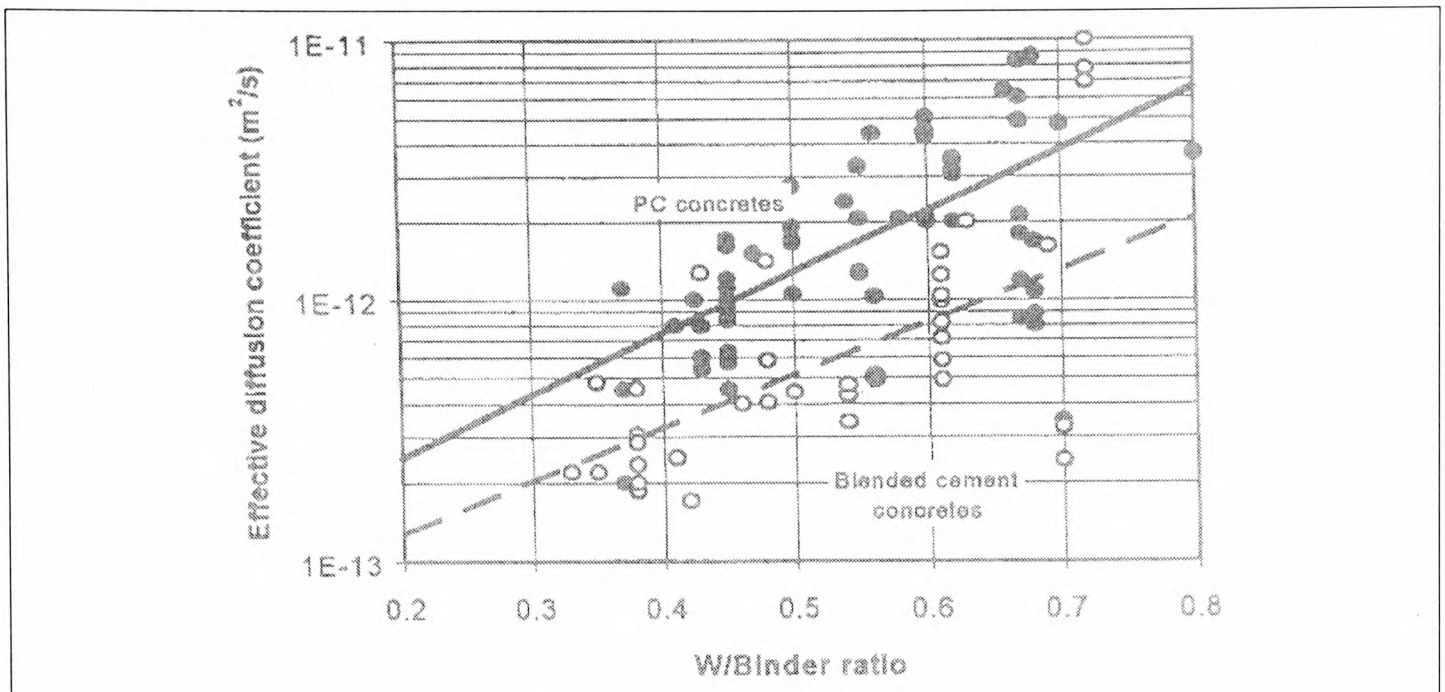

Figure 2.7 The effect of w/b on the diffusion coefficient (Bamforth *et al.*, 1997)

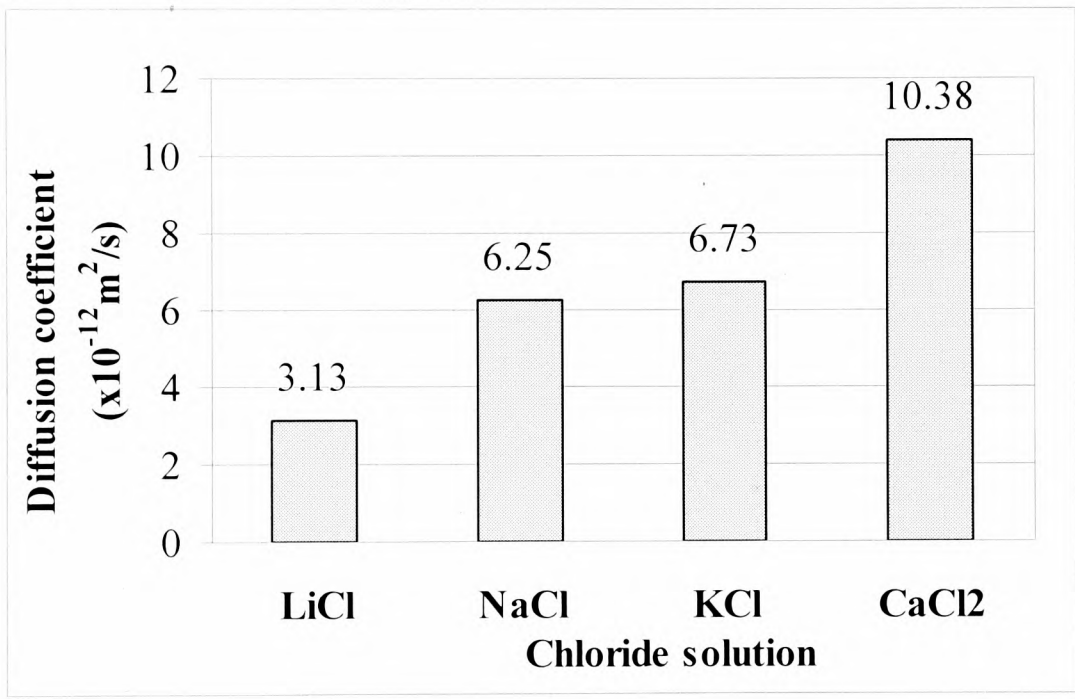

Figure 2.8 The effect of the type of cations associated with chlorides on the diffusion coefficient (Zhang and Gjorv, 1995b)

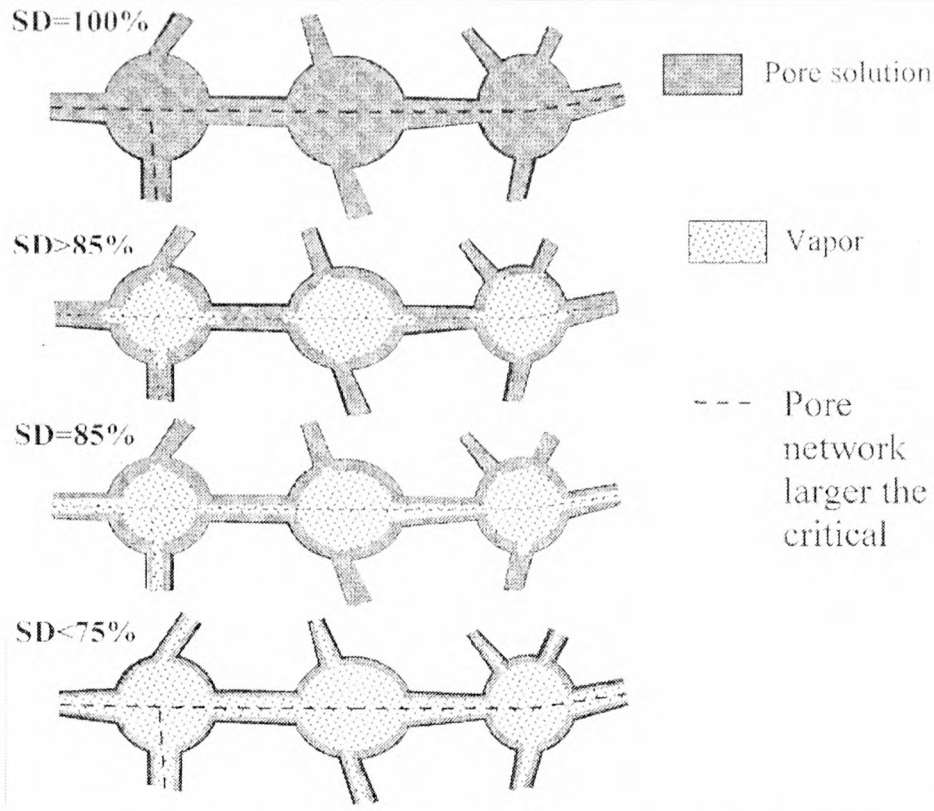

Note: SD = degree of saturation; Pores of diameter >50nm considered critical and are indicated by dotted line

Figure 2.9 Diagrammatic representation of the pore network in hcp at different moisture contents (Guimaraes and Helene, 2002)

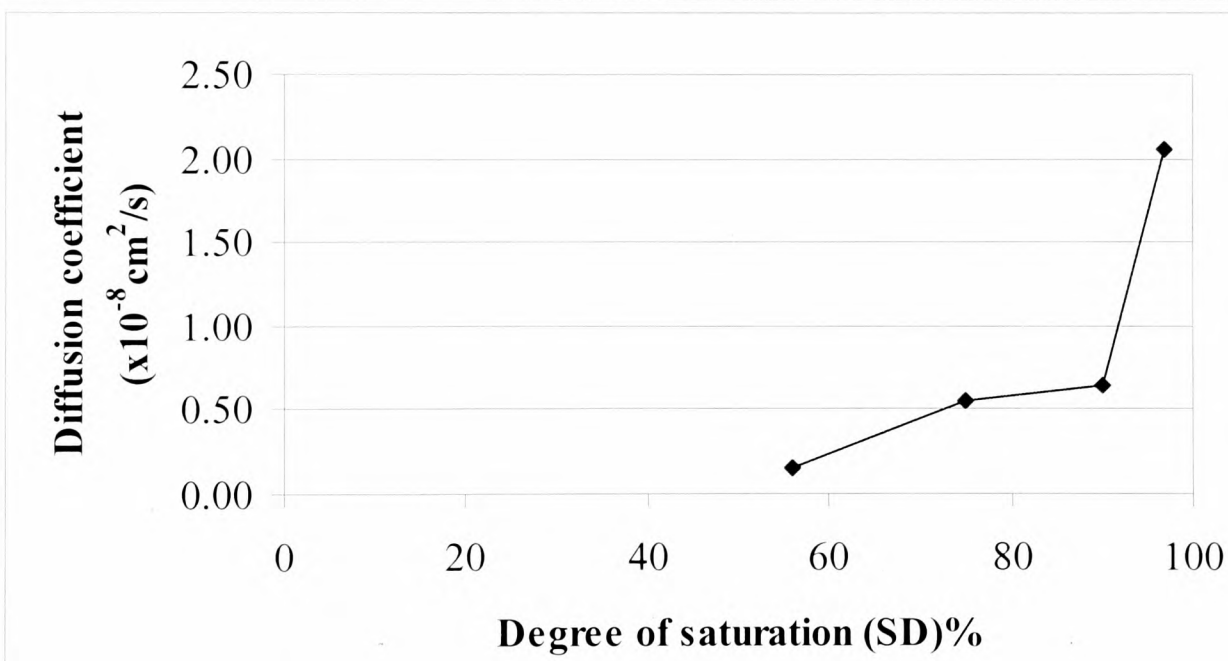

Figure 2.10 The effect of degree of saturation on the diffusion coefficient (Guimaraes and Helene, 2002)

Chapter 3

Determination of chloride transport resistance of concrete

3.1 Introduction

In this chapter, a review of different test methods used for determining the chloride transport resistance of concrete is presented. These test methods can be classified as diffusion based tests, migration based tests and indirect methods. Furthermore, advantages and disadvantages of each of the test with respect to their effectiveness of the measured parameter, the test duration, etc. are also discussed.

The results obtained from each of the test are different, such as diffusion coefficient, migration coefficient, resistivity, etc., and these are reported as 'test parameters'. The term 'test variables' refer to all the different factors of the test protocol such as salt solution concentration, voltage, etc.

3.2 Diffusion based test methods

These are the tests, which determine the chloride diffusivity of concrete by diffusing chlorides through the saturated capillary pores. There are two types of diffusion based tests. These are the steady state diffusion test and the non-steady state diffusion test. In the steady state diffusion test the rate of flow of chloride ions through an unit area of concrete is considered to be constant, whereas in the non-steady state the rate of flow varies. The theoretical consideration used in obtaining diffusion coefficients from these tests has already been described in section 2.5. The different test methods that make use of the principle of diffusion are described in the following sections.

3.2.1 Steady state diffusion tests

The diffusion coefficient obtained from a steady state diffusion test is termed as the effective diffusion coefficient, D_e or D_{ssd}. A typical test arrangement is shown in Fig. 3.1, which can be described as follows. A concrete disc is placed in between two cells, containing a chloride source solution (upstream) and a chloride-free solution (downstream). At the start of the test, the upstream solution has a particular chloride concentration and the downstream has no chlorides (normally de-ionised water). Due to the difference in chloride concentration on either side of the concrete test specimen (i.e. a concentration gradient), the chloride ions diffuse through the concrete disc from the upstream cell to the downstream cell. The chloride flux is continuously monitored by measuring the change in chloride concentration at the downstream cell. A typical chloride concentration-time graph obtained from a steady state diffusion test is shown in Fig. 3.2. The figure shows that the flow can be classified into transition period and steady state period, which is indicated by the highlighted straight-line portion. This straight-line portion of the graph indicates a steady flow of chloride ions across the specimen, i.e, the rate of flow of chlorides through the specimen is constant. Therefore, the steady flux of chlorides through the specimen per unit area (J) can be obtained. This flux (J) is used to calculate the effective diffusion coefficient, using Fick's 1st law of diffusion (Eq. 3.1) (Page *et al.*, 1981).

$$D_e = -J\frac{L}{C} \qquad \text{(Eq. 3.1)}$$

and,

$$J = \frac{dc}{dt}\frac{V}{A} \qquad \text{(Eq. 3.2)}$$

where,

D_e is the effective diffusion coefficient, m^2/s,

J is the steady state flux of chloride ions, mol/m^2s,

$\frac{dc}{dt}$ is the rate of flow of chlorides, mol/m^3s,

t is the time, s,

V is the volume of downstream cell, m^3,

A is the area of concrete specimen exposed to the solution, m^2,

L is the thickness of the concrete specimen, m,

C is the chloride concentration of the upstream cell, mol/m^3.

It is important that the concentration of the chloride source solution is maintained in order to achieve and maintain the steady state conditions (Andrade, 1993).

3.2.2 Observations from the literature

The principle of this test and the theory of calculating a diffusion coefficient are well established. A summary of the different steady state diffusion tests reviewed are presented in Table 3.1. The time required to achieve a steady state condition in most of the cases was weeks or months, depending on the quality of the material (concrete, mortar or cement paste) and the thickness of the specimen (Kropp and Hilsdorf, 1995 and Nilsson *et al.*, 1996). The thickness of the test specimens was generally influenced by the material being tested (see Table 3.1). When cement paste samples were used, the thickness of the test specimens was relatively small. Page *et al.* (1981) and MacDonald and Northwood (1995) used cement paste discs of 50 mm in diameter and 3 mm thickness. Hansson and Berke (1989) used cement paste discs of 45 mm diameter and 3 mm thickness. Buenfeld (1984), in his investigations of cement mortars, used test specimens of 76 mm diameter and 7 mm thickness.

When concrete was tested, the thickness of the specimens was larger than that for cement paste and mortar. A factor controlling this increase in thickness was the maximum aggregate size. Young (1988) suggested that as the porosity of the aggregate-paste interface is higher than the bulk paste, aggregate particles spanning the thickness of the specimen may give unrealistic results.

Dhir *et al.* (1990) used concrete specimens of 100 mm diameter and 25 mm thickness. The maximum aggregate size was 20 mm. Sugiyama *et al.* (1996) considered that the thickness of the test specimen should be larger than the maximum size of aggregate Therefore, Sugiyama *et al.* (1996) used concrete specimens of 100 mm diameter and 50 mm thickness where the maximum aggregate size was 20 mm. Nilsson *et al.* (1996) considered that the test specimen should be three times the maximum aggregate size so as to eliminate the effect of the transition zone and to make the sample representative of the bulk material.

The very long test period used for the diffusion cell test would induce leaching of hydroxyl and alkali ions from the test sample (Nilsson *et al.*, 1996). It is for this reason that saturated $Ca(OH)_2$ has been used in both solutions of the diffusion cell test (Page *et al.*, 1981; Dhir *et al.*, 1990). Hansson and Berke (1989) used a half-saturated $Ca(OH)_2$ solution. Although no explanation was given for this, it was probably deemed that this was sufficient to prevent leaching. Sugiyama *et al.* (1996) did not use $Ca(OH)_2$ in the test, but instead used sodium hydroxide (NaOH).

The concentration of chloride solution used varied between researchers. Buenfeld (1984) used sea water and Sugiyama *et al.* (1996) used a 3% NaCl solution (both approximately 0.5 M). Page *et al.* (1981), Hansson and Berke (1989) and MacDonald and Northwood (1995) used a 1 M NaCl solution. In tests by Dhir *et al.* (1990), the source solution was 5 M NaCl. A direct comparison of these variations was difficult due to different sample type and thickness of the specimens used.

3.2.3 Remarks on the steady state diffusion tests

The following factors should be considered in assessing the chloride diffusivity of concrete by this method.

1. Thickness of the test sample should be small enough to obtain adequate data within an acceptable test duration. However, it should be sufficiently large to limit the aggregate-paste interface influencing the test result.
2. Samples should be tested in a saturated state so that diffusion is the only mechanism of transport.
3. As the test runs for a long duration in order to prevent leaching of hydroxyl ions from the material, the solutions on both cells are to be saturated with $Ca(OH)_2$.
4. As the test progresses, more and more chloride ions diffuse through the concrete, thus decreasing the chloride concentration of the source solution. To avoid this affecting the test result, the source solution has to be either replaced or replenished at regular intervals.

3.2.4 Non-steady state diffusion tests

In case of the non-steady state diffusion test, a thicker concrete sample is exposed to the chloride salt solution for a certain duration (a typical set-up is shown in Fig. 3.3).

The ingress of chloride is measured by analysing the chloride concentration of the dust samples collected from various depths. The chloride concentration-depth graph thus obtained is termed as the chloride concentration profile (see Fig. 3.4). This profile can be used to calculate the non-steady state diffusion coefficient (or apparent diffusion coefficient) using the error function solution of Fick's 2nd law of diffusion (Eq. 3.3).

The value of surface chloride concentration, C_s, and that of the non-steady state diffusion coefficient, D_{nssd} are determined by fitting Eq. 3.3 to the measured chloride profile by means of a non-linear regression analysis (NT BUILD 443, 1995; Poulsen, 1990).

$$C_{(x,t)} = C_s + (C_s - C_i)erf\left(\frac{x}{\sqrt{4tD_{nssd}}}\right) \qquad \text{(Eq. 3.3)}$$

where,

$C_{(x,t)}$ is the chloride profile, i.e., the chloride concentration of the concrete at depth, x (m), from the exposed surface at time, t (s), since the chloride exposure started,

C_i is the initial chloride concentration of the concrete (chloride concentration of the reference specimen, which is kept in ideal conditions), mol/m^3,

C_s is the chloride concentration of the concrete surface, mol/m^3,

D_{nssd} is the apparent chloride diffusion coefficient, m^2/s,

erf is the error function, found in mathematical handbooks.

Based on the test set-up the non-steady state diffusion tests can be classified into ponding and immersion tests. A summary of the different versions of these tests found in the literature is given in Table 3.2. In addition to these methods, sometimes the chloride profile from a concrete structure in service is used to determine a non-steady state diffusivity, D_a, which is also described in this section due to the similarities of this method with those in Table 3.2.

3.2.4.1 Ponding tests

One-dimensional diffusion of chloride into concrete can be achieved in two ways: by continuous (or intermittent) ponding of a chloride solution on the concrete surface or by sealing all surfaces except one and immersing the sample in a chloride solution.

Page *et al.* (1991) used concrete slabs of size 300 x 200 x 100 mm with a 25 mm dyke cast into the upper surface as shown in Fig. 3.5. The sides were coated with an epoxy paint to prevent any movement of chlorides laterally during the ponding test. Both the top and the bottom surfaces were not coated with the epoxy paint because the top surface allowed the penetration of chlorides during the test and the bottom surface allowed air to escape when the chloride laden water penetrated from the opposite (top) surface. The slabs were ponded with 1litre of a 5% NaCl solution, which was replaced weekly to maintain the concentration of the chloride solution. The exposure period used was 6, 12 and 24 months. After the exposure period, the slab was broken into small cubes and these were crushed to obtain the dust concrete sample. The concrete dust was analysed for its chloride concentration and the data obtained was plotted against corresponding depth from which the concrete dust was obtained. This is termed as chloride profile and the non-steady state diffusion coefficient was determined from such profiles using the method described earlier.

3.2.4.2 Immersion tests

Sergi *et al.* (1992) immersed cement paste cylinders in a salt solution, after masking with paraffin wax all surfaces except the exposure surface. They were kept in a sealed container and filled with 5 litres of 1M NaCl solution saturated with $Ca(OH)_2$. The volume of the solution was large enough for any change in concentration due to the specimen uptake to be considered negligible. Therefore the change in the chloride concentration during the test was considered negligible. The cylinders were exposed for a period of 100 days, and chloride concentration profiles as well as the corresponding non-steady state diffusion coefficients were obtained as described earlier.

Three standard test procedures are available for the based on non-steady state diffusion test by immersion, which are NT BUILD 443 (1995), BS EN 13396 (2004), and ASTM C 1556 (2004).

In BS EN 13396 (2004), the chloride ingress is represented by the change in chloride concentration at a number of specific depths from the exposure surface at different exposure durations. Three concrete cylinders of 100mm diameter and 60mm thickness are immersed in a 3% NaCl solution for 28, 90 and 180days respectively.

Concrete dust samples are collected from 2mm, 6mm and 10mm depth from the exposed surface of each cylinder after the respective test duration. The chloride concentrations at these depths are used as a tool to compare the diffusivity of different concretes. The main disadvantage of this procedure is that the results obtained can only be used to compare the performance of different concretes. It does not provide a diffusivity value.

The temperature of the exposure is the only difference between the prEN 13396 (2002) method (as suggested by the Chlortest project) and the BS EN 13396 (2004), the former suggest 40°C, whereas, the latter suggests a temperature of 20°C.

Both the ASTM C 1556 (2004) and NT BUILD 443 (1995) both measures the bulk diffusivity of concrete in a similar manner. The test set-up required for both the tests are also similar, therefore only one is described in the following review The test protocol for NT BUILD 443 (1995) is described in Chapter 4 section 4.3.4.1 in detail, however, the following paragraphs give the salient feature of this test. The test arrangement of this test is shown in Fig. 3.3.

A concrete sample of 60mm thickness and at least 75mm diameter is saturated using $Ca(OH)_2$ solution. The saturation with the $Ca(OH)_2$ solution should prevent any binding or adherence of chloride ions to the pores in concrete (Nilsson *et al.*, 1996). This should also prevent any capillary absorption effects when the specimen is exposed to chloride ions. After allowing all faces except the exposed face of the sample to dry at room temperature, the test specimen is coated with an epoxy paint or polyurethane on all sides except the exposure face. Then the sample is reintroduced to the $Ca(OH)_2$ solution to keep it saturated.

The saturated concrete samples are then exposed to a salt solution containing 165g per litre of NaCl. The exposure duration is 35days (exposure can be longer for testing a good quality of concrete). The salt solution needs to be replaced every 5 weeks, should the test duration be longer. At the end of the exposure, the chloride dust samples are obtained by milling layers concrete parallel to the exposure face. Andrews, (1999) in his review concluded that grinding of the sample will provide

undisturbed sample in a controlled manner over a small depth. The dry samples collected from each depth interval are analysed for the acid soluble chloride content in accordance with NT BUILD 208 (1984). They are plotted against the corresponding depth to obtain the chloride profiles. The non-steady state migration coefficient is calculated from the chloride profile as discussed earlier.

In comparison with other test methods, the NT BUILD 443 have a well defined procedure for carrying out the test, and the test duration is 35 days except for low permeability concretes. In addition, the NT BUILD 443 provides a recommendation for the sampling depths upon which the concrete dust samples need to be collected.

3.2.4.3 Chloride profiles from site

The concrete dusts are collected from various depths perpendicular to the concrete surface. The chloride analysis of the dusts can be done in accordance with any of the standards such as NT BUILD 208 (1984) and BS 1881-124 (1988). The chloride concentrations of the dust samples collected from the respective depths are plotted against the corresponding depth to obtain a chloride profile. A non-steady state diffusion coefficient and the surface chloride concentration are obtained from the non-linear curve fitting of the chloride profile as described earlier.

The chloride ions have to penetrate into the concrete in order to establish a chloride profile. Therefore, this test cannot give any results for new concretes. This means that measures to improve the quality of the concrete cannot be introduced until the chloride concentration inside the concrete builds up. The error associated with the curve fitting could also lead to misinterpretation of the results obtained from concrete structures exposed to non-severe conditions or for a very short duration of exposure (Nanukuttan *et al.*, 2005). In such cases the chloride profiles are rarely developed and most data points show zero chloride concentration.

As the concrete is exposed to different environments, any generalisation of the test parameter is incomplete without describing the corresponding environmental factors. The degree of saturation of the concrete, the concentration of the salt solution and the temperature of the exposure environment will all influence the rate of chloride ingress. Therefore, the test parameter is influenced by many such factors.

3.2.5 Remarks on the non-steady state diffusion tests

The main drawbacks of the non-steady state diffusion test are the accuracy of the chloride concentration of the dust sample, the long test duration and the cost of carrying out the test. The chloride concentration of the concrete dust samples could vary largely due to the dust collection method used. If the sample is collected over a large aggregate, the corresponding chloride concentration will be very low. As a profile grinder uses a larger cross section of concrete to obtain the dust sample, the corresponding results can be considered representative compared to the dust collected by a conventional rotary hammer drill.

In general, assessing the chloride diffusivity of concrete using non-steady state diffusion techniques involves the following aspects:

1. The transport of chlorides into concrete in a non-steady state diffusion test more closely resembles to that of the real site exposure.
2. Thickness of the test specimen should be sufficiently large enough to allow deeper penetration of chlorides in case of the specimens with higher w/b.
3. Specimen needs to be saturated with $Ca(OH)_2$ solution to avoid the binding of chloride ions and to prevent capillary absorption influencing the transport of chlorides.
4. The minimum test duration is five weeks and for denser samples, such as those made with microsilica and ground granulated blast furnace slag, the test duration could be longer.
5. For long duration tests, there is a need to replenish the chloride source solution.

3.3 Migration based test methods

The determination of the chloride diffusivity of concrete from diffusion based tests requires long test duration (McGrath and Hooton, 1996). Therefore, researchers attempted accelerating the movement of chloride ions into (or through) concrete by using an electrical potential (Andrade, 1993 and Whiting, 1981). This process is termed as electrochemical migration and in the following sections the application of electrochemical migration in testing concrete diffusivity is described. The methods developed based on this theory are explained at the end of this section.

3.3.1 The concept of electrical conduction through concrete

Whittington *et al.* (1981) investigated the ability of concrete to conduct an electric current and found that a high percentage of the electric current is conducted through the paste. The authors concluded that concrete can be considered as a composite of non-conductive particles in a conductive cement paste matrix. Buenfeld and Newman (1987) observed that moist concrete behaves as a conductor, whereas dry concrete is a reasonably good insulator. This implied that the electric current is conducted through the concrete by electrolytic means, i.e. by the ions in the pore solution, and the electronic conduction through the solid paste matrix is negligible. The transfer of ions during this process is termed generally as ion migration. Therefore, tests which make use of the applied potential to promote the movement of ions are called ion migration tests or simply migration tests.

3.3.1.1 Electrochemical migration

The phenomenon that occurs in concrete, when it is placed in a diffusion cell and an electric field is applied, has been described by various researchers (Andrade, 1993; Tang and Nilsson, 1992b; Tong and Gjorv, 2001; Zhang and Buenfeld, 1994). The electric field is applied across the concrete specimen by connecting the negative terminal of the power supply to the electrode (cathode) in the cell containing the chloride source solution (catholyte) and the positive terminal to the electrode (anode) placed in the cell containing the neutral solution (anolyte) (see Fig. 3.6). The processes that occur when an electrical field is applied have been described by Andrade (1993) and are illustrated in Fig. 3.6. The main processes are the migration of ions and the electrode reactions.

Migration of ions

All the ions present in the aqueous phase contribute to the flow of current through the cell (Andrade, 1993; Castellote *et al.*, 2000). The ions move towards the electrode of opposite sign. The relative movement (migration) of ions in the electrolyte under the action of an electric field depends on their transference number. This is defined by 'the proportion of current carried by a particular ion in relation to the current carried by the rest of the ions' (Bockris and Reddy, 1970).

Electrode reactions

At the electrode surfaces, the electrochemical reactions must take place. This is the only way in which the flow of current is shifted from electrons (in metals) to ions (in electrolytes). The reactions which occur are described below, based on Andrade (1993) and Castellote *et al.* (2000).

1. Metal dissolution – generates cations at the anolyte, if the anode is an oxidisable metal. In the case of iron the process will be:

$$Fe \rightarrow Fe^{2+} + 2e^{-} \quad \text{(Eq. 3.4)}$$

$$Fe^{2+} \rightarrow Fe^{3+} + e^{-} \quad \text{(Eq. 3.5)}$$

Further,

$$Fe^{2+} + 2H_2 0 \rightarrow Fe(OH)_2 \downarrow + 2H^{+} \quad \text{(Eq. 3.6)}$$

$$Fe^{3+} + 3H_2 0 \rightarrow Fe(OH)_3 \downarrow + 3H^{+} \quad \text{(Eq. 3.7)}$$

2. Evolution of gases – due to the electrolysis of water, in both anolyte and catholyte, generating O_2 and H_2. The reactions occurring are:

$$\text{Anode: } H_2 0 \rightarrow \frac{1}{2} O_2 \uparrow + 2H^{+} + 2e^{-} \quad \text{(Eq. 3.8)}$$

$$\text{Cathode: } 2H_2 0 + 2e^{-} \rightarrow H_2 \uparrow + 2OH^{-} \quad \text{(Eq. 3.9)}$$

3. If the electrodes are not corrodible, other reactions can occur, apart from water electrolysis. Chlorine gas is evolved from the migrating chloride ions,

$$2Cl^{-} \rightarrow Cl_2 + 2e^{-} \quad \text{(Eq. 3.10)}$$

There is also the oxygen reduction at the cathode.

$$\frac{1}{2} O_2 + H_2 O + 2e^{-} \rightarrow 2OH^{-} \quad \text{(Eq. 3.11)}$$

All these reactions tend to maintain the total electro-neutrality of the whole arrangement, where the quantity of positive charge flowing is equal in magnitude and opposite in sign to the quantity of negative charge flowing (Andrade, 1993; Bockris and Reddy, 1970).

3.3.1.2 Theoretical background (after Bockris and Reddy, 1970)

Conduction (migration) refers to the drift of ions under an electric field, whereby an ion would attain a net terminal velocity, termed the drift velocity (v_d). The drift velocity attained under a unit electric field is the mobility (u) of an ion. The total ionic flux (J_c) can be determined by multiplying the drift velocity of the individual ions by the ionic concentration:

$$J_c = cuE_f \qquad \text{(Eq. 3.12)}$$

$$i.e., \qquad J_c = cv_d \qquad \text{(Eq. 3.13)}$$

where,

J_c is the ionic flux by conduction, mol/m^{2}s,

u is the mobility of ions, m^2/Vs,

c is the ionic concentration, mol/m^3,

E_f is the electric field, V/m,

v_d is the drift velocity, m/s.

The ionic flux (J_c) due to conduction is also equal to the current density divided by the charge of 1 mole of z-valent ions:

$$J_c = \frac{i}{zF} \qquad \text{(Eq. 3.14)}$$

where,

i is the current density, A/m^2,

z is the valency of ions, eq/mol,

F is the Faraday's constant, coulombs/eq.

Einstein relation

Einstein developed a relationship between the diffusivity and ionic mobility by reversing the electric field in a solution with a concentration gradient so that conduction and diffusion cancelled each other out:

$$D = u\frac{RT}{zF} \qquad \text{(Eq. 3.15)}$$

where,

D is the ion diffusivity, m^2/s,

R is the universal gas constant, J/K.mol,

T is the absolute temperature, K,

u is the mobility of ions, m^2/Vs,

z is the valency of ions, eq/mol,

F is the Faraday's constant, coulombs/eq.

The Nernst-Planck equation

In an electrolytic system where both the concentration gradient and the electrical field (E_f) coexist, the total driving force on the ions arises from the total potential, the sum of the chemical potential and the electrical potential. Thus, the flux J is obtained as:

$$J = -\frac{Dc}{RT} zFE_f - D\frac{dc}{dx} - cV_e \qquad \text{(Eq. 3.16)}$$

where,

J is the total ionic flux, mol/m^{2}s,

$\frac{dc}{dx}$ is the concentration gradient, mol/m^4.

V_e is the velocity of solution, m/s.

Equation 3.16 is known as the Nernst-Planck equation, where the terms on the right side can be expressed by the three components of the total flux: the conduction flux (J_c), the diffusion flux (J_D) and convective flux respectively. Thus, Eq. 3.16 shows that under the action of both chemical and electrical driving forces, the ionic movement is the combination of both diffusion and migration. For a pure migration process, therefore,

$$J = J_c = -\frac{Dc}{RT} zFE_f \qquad \text{(Eq. 3.17)}$$

where the unit is given before (c.f. Eqs. 3.12 to 3.16)

The above formulae (Eqs. 3.16 and 3.17) are based on ideal solutions where ions behave independently of each other, but they provide the theoretical background for determining the chloride diffusivity in concrete using migration based tests. Both the Einstein relation (Eq. 3.15) and the Nernst-Planck (Eq. 3.17) relate the diffusivity to the direct transport parameters of the ions, i.e. the mobility or the flux. Therefore, the chloride diffusivity can be obtained from the measurement of the flux of the chloride ions.

The various tests developed based on the principle of electrochemical migration are described in the following sections. The tests are categorised as steady state migration tests and non-steady state migration tests.

3.3.2 Steady state migration tests

The test set-up used in this type is similar to that in the steady state diffusion test method, described in section 3.2.1. The principal difference is that an electric potential is applied across the specimen as the driving force in the steady state migration test (Fig. 3.7). The chloride concentration of the anolyte (downstream cell) is monitored and plotted against time. A typical concentration-time graph obtained from a steady state migration test is presented in Fig. 3.8. The flow can be considered to occur in three stages, viz. non-steady state, steady state and attenuate state. In a steady state migration test, a migration coefficient is calculated based on the steady flow of chloride ions through a unit cross section of the material (concrete, mortar or cement paste). As the steady flow of chloride ions to the anolyte is observed (represented by the straight line portion with slope $\frac{dc}{dt}$ as shown in Fig. 3.8), it is assumed that there is a constant flow of chloride ions through a unit section of the material. This allows the use of Nernst-Planck equation to calculate the steady state migration coefficient, D_{mig} or D_{ssm}. The method of calculating the migration coefficient is explained later in the section.

Given below is a summary of the different tests based on the principle described above Details of the test methods are summarised in Table 3.3.

3.3.2.1 Variations in test set-up and protocol

Potential difference test

This test was developed by Dhir *et al.* (1990); the test set-up is shown in Fig. 3.9. Concrete discs of 100mm diameter and 25mm thickness (vacuum saturated with water) was attached to the diffusion cell as shown in the figure. The catholyte used was a 5M NaCl solution, with a stainless steel sheet as the cathode, and the anolyte solution was de-ionised water, with a graphite anode. A potential difference of 10V was applied as the driving force. The chloride gain in the anolyte was monitored by using a chloride ion selective electrode (ise), and a diffusion coefficient was calculated using Fick's 1st law of diffusion as given below:

$$J = -D_{PD}\frac{(c_1 - c_2)}{L} \qquad \text{(Eq. 3.18)}$$

where,

J is the flux of chloride ions, mol/m^2s,

D_{PD} is the diffusion index, m^2/s,

c_1-c_2 is the difference in chloride concentration between the two sides of the specimen, mol/cm^3,

L is the thickness of the specimen, cm.

Results by Dhir *et al.* (1990) showed a reasonably good relationship between the proposed test and the steady state diffusion test. However, the test attracted the following criticisms:

1. Tang and Nilsson (1993) considered that the theoretical relationship used in Eq. 3.18 was incorrect, meaning that only a diffusion index is obtained instead of a coefficient of chloride diffusion.
2. Streicher and Alexander (1994) considered that the use of the 1st law of diffusion in an applied potential test is incorrect, as the application of a potential difference would cause an ionic flux, even if the concentration gradient was zero. Also, during the electrochemical process in migration test, hydrogen gas is evolved at cathode due to water electrolysis. In the arrangement used by Dhir *et al.* (1990), the evolved hydrogen gas would be trapped between the cathode and the concrete surface, thereby sealing the concrete surface and reducing the effective flow area.

Accelerated chloride ion diffusion (ACID) test

The ACID test was developed by El-Belbol (1990) and Zhang and Buenfeld (1994). The cell arrangement was as shown in Fig. 3.10. A 100mm diameter mortar disc of 50mm thickness was placed in a perspex box, between a 0.5M NaCl catholyte and a 0.3M NaOH anolyte. A potential difference of 40V was applied between two graphite electrodes placed in the cell as shown in Fig. 3.10. The chloride concentration in the anolyte was measured using a chloride ion selective electrode.

The chloride diffusivity was defined by the parameters T_o, which is the time taken for the chloride ions to penetrate the full thickness of the specimen, and g, which is the rate of chloride accumulation in the anolyte. However, the major criticism was that the measured parameters T_o and g are strongly dependent on the test variables used

(Gjorv and Sakai, 1995), i.e., the voltage, the temperature and the concentration of the catholyte will influence the observed rate of chloride penetration. However, T_o and g do not account for any of the above mentioned factors. Therefore, they can only be used to compare the diffusivity of different concrete mixes.

Steady state chloride migration tests

This test protocol was first proposed by Andrade and Sanjuan (1994) and further modified or customised by McGrath and Hooton (1996); Sugiyama *et al.* (1996); Zang and Gjorv (1995). Although a summary of the different versions of this test protocol was presented in Table 3.3, some salient features and differences are highlighted below.

The test initially developed by Andrade and Sanjuan (1994) was further modified by Castellote *et al.* (2001) and has since been considered in the RILEM committee TMC-168 Round Robin Test programme and Chlortest (Chlortest, 2006) Round Robin Test programme. The test set-up and the protocol developed by Andrade and Sanjuan (1994) are highlighted first along with the modifications made by other researchers. The modifications proposed by Castellote *et al.* (2001) are given at the end of this section.

The test set-up used by Andrade and Sanjuan (1994) is illustrated in Fig. 3.11. A similar set-up was used by other researcher who developed the steady state chloride migration tests. Andrade and Sanjuan (1994) considered that any arrangement in which two compartments are separated by a concrete specimen could be used for carrying out the steady state migration test. All researchers used a 0.5M NaCl source solution. However, McGrath and Hooton (1996) added a 0.3M NaOH to the chloride source solution. For the anolyte, Andrade and Sanjuan (1994) used distilled water, whereas other researchers used a NaOH solution with the strength varying between 0.3M and 0.5M. The use of NaOH is presumed to have the following benefits. The presence of NaOH improves the conductivity of the anolyte and this will reduce the potential lost across the anolyte. For an applied voltage as low as 12V, this loss in potential across the anolyte can be significant (McGrath and Hooton, 1996). The pH of the anolyte solution decreases during a steady state migration test. This will result in chloride ions escaping from the anolyte as chlorine gas. Sugiyama *et al.* (1996)

considered that by adding NaOH, the pH of the anolyte can be maintained between 11 and 13, and this prevents the chlorine gas formation. This is further discussed at the end of this section.

The choice of electrodes was different in each case. Andrade and Sanjuan (1994) used steel rods as both the anode and the cathode. Zhang and Gjorv (1995a) and McGrath and Hooton (1996) used stainless steel mesh electrodes in both chambers. Sugiyama *et al.* (1996) used a steel cathode and a graphite anode similar to that employed by Dhir *et al.* (1990).

As the effect of the variations in the test set-up on the migration based tests is discussed in detail at the end of this section no comments are made here.

Method of calculating the migration coefficient

The coefficients obtained from the migration tests are termed as migration coefficients, which can be obtained using the formula given by Eq. 3.17 (described in section 3.3.1.2) The Nernst-Planck equation is further discussed here, as this is directly relevant to the research reported in this thesis.

Nernst-Planck equation

The migration coefficient can be calculated using the Nernst-Planck equation (Eq. 3.16), by making the following assumptions (after Andrade, 1993).

1. Both the diffusion and the convection component in Eq. 3.16 are considered to be negligible in comparison to migration.
2. The concentration of chlorides in the catholyte is much higher than that in the anolyte. That is, the chloride concentration of the catholyte should be high and should remain relatively constant throughout the test duration. Meanwhile, the chloride concentration of the anolyte should be zero or relatively insignificant compared to the catholyte.
3. The electrical potential across the concrete disc follows a linear decay.

By considering these assumptions, the Nernst-Planck equation can be modified in the following way:

$$J = -\frac{Dc}{RT} zF \frac{E}{L} \quad \text{(Eq. 3.19)}$$

or

$$D = -\frac{JRTL}{zFcE} \quad \text{(Eq. 3.20)}$$

and,

$$J = \frac{dc}{dt} \frac{V}{A} \quad \text{(Eq. 3.21)}$$

where,

D is the migration coefficient, m^2/s,

$\frac{dc}{dt}$ is the slope of the straight line portion of steady state flow, mol/m^3s,

V is the volume of the anolyte, m^3,

A is the area of the specimen, m^2,

R is the gas constant, 8.31 J/K.mol,

T is the absolute temperature, K,

L is the thickness of the disc specimen, m,

z is the valency of chloride ions, -1,

F is Faraday's constant, $9.65x10^4$ c/mol,

C is the concentration of chloride source solution, mol/m^3,

E is the electrical potential applied between the anode and cathode, V.

INSA steady state chloride migration test

For a similar arrangement as the one developed by Andrade and Sanjuan (1994), Truc *et al.* (2000) showed that the migration coefficient can be determined by measuring the chloride loss at the catholyte. He considered that during the steady state in a steady state migration test the chloride loss with time in the catholyte is equal to the chloride gain in the anolyte. Therefore, the migration coefficient can be found using the following equation.

$$D_{up} = \frac{1}{C_{up}} \frac{RTJ_{up}}{FE} \quad \text{(Eq. 3.22)}$$

and,

$$J_{up} = \frac{(C_{up1} - C_{up2})V}{At} \quad \text{(Eq. 3.23)}$$

where,

D_{up} is the migration coefficient (based on catholyte measurements), m^2/s,

C_{up1}-C_{up2} is the change in chloride concentration in the catholyte, mol/m^3,

t is the duration between C_{up1} and C_{up2}, s,

V is the volume of the catholyte, m^3,

A is the surface area of the specimen, m^2,

C_{up} is the average concentration in the catholyte, mol/m^3,

R is the Universal gas constant, 8.31 J/K.mol,

T is the absolute temperature, K,

F is Faraday's constant, 9.65x10^4 c/mol,

E is the electrical potential applied between the anode and the cathode, V.

Truc *et al.* (2000) established that the migration coefficient, D_{up} obtained from the upstream measurements correlates with the D_{mig} or D_{ssm} obtained from downstream measurements (Eq. 3.20).

IETcc steady state migration test

Based on the test method developed by Andrade and Sanjuan (1994), Castellote *et al.* (2001) proposed a change in protocol to determine the chloride diffusivity by measuring the conductivity of the anolyte. A schematic diagram of the test arrangement is presented in Fig. 3.12. The catholyte used was 1M NaCl with black steel circular disc as cathode. The anolyte solution was de-ionised water and the anode was made of black steel. A potential difference of 12V was applied as the driving force. However, the actual potential difference across the specimen was measured and this was used in the calculation of the migration coefficient (Eq. 3.26).

Unlike the predecessors, Castellote *et al.* (2001) used conductivity of the anolyte to identify the steady state. Castellote *et al.* (2001) identified an empirical relationship between the conductivity and the chloride concentration of the anolyte (Eq. 3.24). This relationship was used to obtain a equivalent chloride concentration from the conductivity measurements and further to calculate the steady rate of chloride flux, i.e., the slope of the straight-line portion of the concentration-time graph ($\frac{dc}{dt}$).

$$Cl^- = 11.45(\lambda_{25}) - 1.71 \qquad \text{(Eq. 3.24)}$$

and,

$$\lambda_{25} = \lambda_{Tc} + 0.02(25 - T_c)\lambda_{Tc} \quad \text{(Eq. 3.25)}$$

where,

cl^- is the concentration of the anolyte, mmol/l,

λ_{25} is the conductivity of the anolyte at 25°C, mS/cm,

λ_{Tc} is the conductivity of the anolyte at temperature T_c, mS/cm,

T_c is the temperature, °C,

The following equation was used to calculate the migration coefficient:

$$D = -\frac{JRTL}{zFC\gamma\Delta\phi} \quad \text{(Eq. 3.26)}$$

where, all parameters as defined for Eq. 3.20, except γ and $\Delta\Phi$,

γ is the activity coefficient, 0.657,

$\Delta\Phi$ is the actual electrical potential measured across the specimen, V.

Permit ion migration test

This is a site based chloride migration test developed by Andrews (1999). This test is based on the principle of steady state migration of chloride ions through concrete. Due to the importance of the information regarding this test, it is considered ideal to discuss the details of this test separately towards the end of this chapter (see section 3.5).

3.3.2.2 Effect of test variables on migration based test methods

A review of the effect of different test variables (see Table 3.3) such as applied voltage, the concentration of the catholyte, the type of electrodes and the type of anolyte solution on the migration based test are presented next.

Applied voltage on migration tests

The objective of applying a potential difference across the specimen is to accelerate the transport of chlorides through the concrete, i.e., to reduce the test duration. As can be seen from Table 3.3 many researchers have attempted different voltages in order to reduce the test duration, but the voltage cannot be too high, as it will result in the excessive heating of the specimen and, which in turn would lead to the temperature induced transport of the chloride ions (Andrade, 1993).

El-Belbol (1990) investigated the effect of test voltage on the temperature rise by varying it between 10 and 60V and concluded that an effective test voltage is 40V when considering the temperature rise and the test duration. The test duration was approximately 90 hours. However, Andrade and Sanjuan (1994) and McGrath and Hooton (1996) found that a lower voltage of 12-15V is sufficient to accelerate the transport process without resulting in appreciable heating of the solution.

Based on the above discussion, it can be concluded that the test voltage in the steady state migration test should be selected such that the temperature generated is not high enough to influence the transport of chloride ions. Therefore, the author of this thesis considers the use of two test voltage viz. 12V and 60V for concretes with very low resistance and high resistance respectively.

Effect of the potential drop in the electrolytes on the migration parameters

In the migration set-up, the actual potential difference across the specimen might be lower than the applied voltage between the electrodes. This is due to the potential drop across the electrode-electrolyte interface and across the solutions. McGrath and Hooton (1996) suggested that this drop in potential could cause a discrepancy in the value of the migration coefficient, if the applied voltage was used instead of the actual potential difference.

Streicher and Alexander (1995) confirmed that the potential drop across the electrolytes was small. However, in their test set-up the electrolytes were concentrated NaCl solution. To this effect, Prince and Gagne (2001) studied the effect of concentration of the anolyte on the potential drop and found that as the concentration of the anolyte increased the potential drop decreased. This suggests that the potential drop could be influenced by the concentration of ions in the electrolyte (catholyte and anolyte).

The drop in potential at the electrode is termed as the polarisation resistance (Bockris and Reddy, 1970). This is due to the cathodic and anodic reaction at the electrodes (Zhang and Buenfeld, 1994). The total potential drop was estimated to be 17% by Sugiyama *et al.* (1996) when the test voltage was 15V. Therefore, they

factored the applied voltage by a constant (0.83) and used this potential difference in the calculation of the migration coefficients. A similar factor was found by McGrath and Hooton (1996). They estimated that the potential across the specimen were 85% of the applied voltage 12V. The set-up used in both tests was comparable.

Investigations by McGrath and Hooton (1996) revealed that the total potential drop remained constant despite the increase in applied voltage. This was further substantiated by estimating the error associated with the migration coefficient calculated using the applied voltage and the actual potential difference across the specimen. The author found that the percentage error in the migration coefficient decreased with an increase in applied voltage.

In all of the tests considered, the electric field is applied using electrodes kept at a distance from the test specimen. This means that the actual potential across the specimen will be predominantly influenced by the electrical conductivity of the electrolytes. Therefore, by keeping the electrodes closer to the test specimen this reduction in potential can be avoided. However, the drop in potential due to the electrode-electrolyte interface would still have an effect on the actual potential difference.

Effect of concentration of the catholyte on migration tests

Bockris and Reddy (1970) states that the ion-ion interaction can be described as the formation of an oppositely charged ionic cloud surrounding the central (chloride) ion of interest according to Deybe-Hückel theory. This ionic cloud lowers the electric potential of the chloride ion, and thereby retards the drift velocity.

Besides, the cathode will attract the cations and the anode will attract the anions. This opposing flow of ions causes friction in the system, thus further reducing the flow (Tang, 1999a). As concluded by Prince and Gagne (2001) a direct comparison of the different migration set-ups used by different researchers could be difficult, as the actual electrochemical process in all the cases are different. Tang (1999a) attempted to obtain an intrinsic migration coefficient, taking into account of the frictional force and the ionic cloud. Although the initial findings were interesting, the author suggested that more results would be needed to validate the theory experimentally.

Gilleece (1996) studied the effect of different NaCl solutions (catholyte) on the steady state migration test by keeping water as the anolyte solution. He found that the chloride migration index (at both 10V and 30V) decreased with increase in catholyte concentration from 0.5M to 3M. Theoretical concepts provided by Andrade and Sanjuan (1994); Castellote *et al.* (2001); Tang (1999b) are considered below to explain this reduction in chloride migration index.

Andrade and Sanjuan (1994) introduced a term called the activity coefficient, γ, which is the measure of the chemical-potential change arising from ion-ion interactions. This was applied to the Nernst-Planck equation (Eq. 3.26) previously introduced by Castellote *et al.* (2001). For a 1M NaCl solution the value of the 0.657 was used for γ. Both Andrade and Sanjuan (1994) and Castellote *et al.* (2001) considered that by introducing a term to account for the ion-ion interaction in concrete, the resulting migration coefficient would be independent of the concentration of the catholyte solution. Tang (1999b) plotted the value of γ for chloride concentration up to 5M NaCl (see Fig. 3.13; for a reference temperature 25°C).

Figure 3.13 shows that the value of γ decreases with the increase in chloride concentration up to 0.5M and then increases with the increase in chloride concentration up to 5M. This means that the ion-ion interaction increases with the increase in catholyte concentration from 0.5M to 5M. This suggests that the migration index evaluated using a 3M NaCl solution as catholyte would be low compared to the migration index evaluated using 0.5M NaCl solution. This explains the observations made by Gilleece (1996).

Electrodes and anolytes on migration tests

The general approach in the migration test is to use a neutral solution that prevents chlorine gas evolution or use a sacrificial anode which dissolves and retains the chloride ions in solution. However, some variations to this general approach can be seen in literature.

Sugiyama *et al.* (1996) considered that by maintaining the pH of the anolyte between 11 and 13, the chlorine gas evolution could be prevented. Therefore, Sugiyama *et al.* (1996) considered that any electrode material could be used as anode. However, the high alkalinity could influence the conductivity measurements in tests similar to the modified steady state migration test. Therefore, an anode material which promotes its active dissolution should be used for such tests. Andrade and Sanjuan (1994) suggested that a combination of mild steel as anode and de-ionised water as anolyte could prevent the chlorine gas formation.

Zhang and Buenfeld (1994) observed that when the applied voltage was 30V, 'significant chlorine gas evolution did not occur, provided the pH of the anolyte was not allowed to fall too low'. However, the limits of the pH for which the evolution of chlorine gas occurred were not given. Therefore, the most suitable way of ensuring no chlorine gas was evolved would be to promote an active dissolution of the anode. Andrews (1999) in his *in situ* migration test considered using a sacrificial anode as the best option compared to a pH controlled anolyte. The author of this thesis considers that the use of highly alkaline anolyte would influence the conductivity measurements, as observed by Castellote *et al.* (2001). Therefore, from a practical point of view mild steel anode was considered the best anode material, along with de-ionised water as the anolyte.

3.3.3 Non-steady state migration tests

A typical test set-up used in this type is shown in Fig. 3.14. The principal difference is that an electric potential is applied across the specimen as the driving force. In a steady state migration test, the flow can be considered to occur in three stages, viz. non-steady state, steady state and attenuate state. For the non-steady state migration test, the test is stopped while the flow is in non-steady state and the specimen is split open and the depth to which chloride ions penetrated is measured by spraying silver nitrate solution. A modified Nernst-Planck equation was used to calculate the non-steady state migration coefficient (denoted by D_{CTH} or D_{nssm}) using the penetration depth. Two test methods are reviewed in this section, viz. the CTH method and the NT BUILD 492 (1999). The variations in the test set-up and test protocol for those are given next.

3.3.3.1 The CTH method

The CTH method was proposed by Tang and Nilsson (1992b). A typical experimental arrangement is presented in Fig. 3.14. A potential gradient of 30V is applied across the two faces of the specimen by two stainless steel electrodes, for a specified time. The temperature of the anolyte and the electric current are both monitored during the testing. Using the initial current, the time required for the testing is found out, this is typically about 8, 24 or 48 hours depending on the concrete quality (Nilsson *et al.*, 1996). After testing, the cylinders are split opened along the length. The two fractured surfaces are sprayed with a 0.1N $AgNO_3$ solution, to detect the depth to which chlorides penetrated. A modified Nernst-Planck equation is used to determine the migration coefficient from the penetration depth, X_d. A modified Nernst-Planck equation is used to determine the migration coefficient from the penetration depth, X_d.

$$D_{CTH} = \frac{RT}{zFE}\frac{X_d}{t} \qquad \text{(Eq. 3.27)}$$

where,

D_{CTH} is the migration coefficient of concrete, m^2/s,

X_d is the depth of chloride penetration, m,

t is the test duration, s,

R is the Universal gas constant, 8.31 J/K.mol,

T is the absolute temperature, K,

z is the valency of chloride ions, -1,

F is the Faradays Constant, 9.65×10^4 c/mol,

E is the electrical potential applied, V.

According to Zhang and Gjorv (1998), the CTH method has a sound theoretical basis and this test can determine the non-steady state migration coefficient in relatively short time and with moderate effort.

However, the method does have some sources of error. In order to calculate the migration coefficient, Tang and Nilsson (1992b) has to assume that the electric field is constant through out the specimen. However, the electric field will differ between the two sides of the chloride front (where, the chloride front is the collective movement of the chloride ions). Therefore, the electric field is a function of distance

and time and not a constant as assumed by Tang and Nilsson (1992b). The time of testing should be selected appropriately in order to obtain an appropriate penetration depth and for concrete of unknown quality this may be difficult to control (Zhang and Gjorv, 1998). This was further highlighted by Stanish *et al.* (2000), who suggested that the presence of calcium nitrate ions, which is more ionically mobile, would reduce the potential gradient acting on the chloride ions, thereby reducing the movement of the chloride front.

These criticisms were addressed in the Nordic standard NT BUILD 492 (1999) derived from the CTH test method, which was recommended by the Chlortest (2006) consortium as a reliable and repeatable test method to determine chloride diffusivity of concrete. The changes to the test method in NT BUILD 492 (1999) are discussed below.

3.3.3.2 Nordic Standard (NT BUILD 492)

A test set-up similar to the CTH test method is used in this test. The chloride concentration of the catholyte was increased from 0.5M NaCl to 1.8M. It is considered that the increased chloride concentration would promote chloride binding, thereby making the test comparable to the natural diffusion test (Castellote *et al.*, 2001). The anolyte solution was changed to 0.3M NaOH in de-ionised water, increased pH of the anolyte would prevent the pH of the anolyte dropping drastically during the migration test (El-Belbol, 1990). The voltage to be applied and the duration of test were selected based on the initial current. Therefore, a reasonably acceptable depth of penetration can be achieved. The guideline for selecting the voltage and the test duration is given in the standard (which is described in detail in Chapter 4 Table 4.8. The migration coefficient, D_{nssm} can be calculated using the following modified equation:

$$D_{nssm} = \frac{RT}{zFE} \frac{\left(X_d - \alpha\sqrt{X_d}\right)}{t} \qquad \text{(Eq. 3.28)}$$

where,

$$E = \frac{U - 2}{L} \qquad \text{(Eq. 3.29)}$$

$$\alpha = 2\sqrt{\frac{RT}{zFE}} erf^{-1}\left(1 - \frac{2c_d}{c_o}\right) \qquad \text{(Eq. 3.30)}$$

In the above equations,

D_{nssm} is the (non-steady state) migration coefficient of concrete, m^2/s,

t is the test duration, s,

E and α are given in Eqs. 3.29 and 3.30 respectively,

U is the voltage applied, V,

L is the thickness of the specimen, m,

erf^{-1} is the inverse of the error function,

c_d is considered as the chloride concentration at colour change, (~0.07N),

c_o is the chloride concentration of the catholyte, (1.8M),

Other parameters are as defined earlier for Eq. 3.27.

3.3.4 Migration coefficients as a measure of diffusivity

Dhir *et al.* (1990) found a good correlation between the diffusion index, D_{PD} from their potential difference test and the diffusion coefficient, D_e, obtained from the steady state diffusion test. The author concluded that the two parameters correlated well and using the relationship, the corresponding D_e values could be estimated with 95% confidence from the D_{PD}. Andrade and Sanjuan (1994) reported a good correlation between the migration coefficient, D_{mig}, and the steady state diffusion coefficient, D_e, although details of the relationship was not presented. Sugiyama *et al.* (1996) reported that both D_{mig} and D_e was very similar (see Fig. 3.15. This may be because Sugiyama *et al.* (1996) measured the actual potential across the specimen to calculate the value of D_{mig}, whereas Andrade and Sanjuan (1994) used the potential across the electrodes, which could underestimate the migration coefficient of the concrete.

Tang and Nilsson (1992b) observed a good correlation between the D_{CTH} and the non-steady state diffusion coefficient. A similar finding was reported by Baroghel-Bouny *et al.* (2002), who presented the correlation between the two parameters from different non-steady state diffusion tests and NT BUILD 492 test for a range of concrete mixes (see Fig. 3.16). Therefore, it can be concluded that the NT BUILD 492 can determine the corresponding non-steady state diffusion coefficient in a more rapid manner.

Discussion on the effect of test set-ups on the relationship between diffusion and migration coefficient

Figure 3.13 shows that the difference in the value of γ between chloride concentrations 0.5M NaCl and 2M NaCl at 25°C is negligible. This means that the ionic interaction of catholytes in this range is similar. However, Zhang and Gjorv (1996) reported that the activity coefficient for a given concentration decreases with the increase in temperature. This would mean that different activity coefficients need to be used for a catholyte of a given chloride concentration, depending on the temperature of the solution.

Tang (1999b) showed that the influence of the ionic interaction on the difference between the diffusion and the migration coefficient is similar for the given concentration range (i.e. 0.5M NaCl and 2M NaCl). However, the author concluded that this influence is negligible compared to the other effects such as the frictional force (i.e. due to the counter-electric fields created by the ions flowing in the either direction in a migration test), the chloride cation type, etc. The data from Prince and Gagne (2001) can be used here to highlight that the different test set-ups will have different frictional force. Therefore, a direct comparison between the diffusion and migration coefficient is only applicable if the test set-up used in both cases are similar.

From the above discussions, it can be concluded that the relationship between the diffusion and migration coefficients can be different for different test methods used. Therefore, it is considered that the use of an activity coefficient alone will not make the resulting migration coefficient comparable to the diffusivity of concrete, and hence, the use of activity coefficient is not considered in this thesis.

3.4 Indirect measure of ionic transport resistance

The tests discussed in this section are based on the measurement of electric current through concrete in a saturated condition. As concrete is a porous material, and often with well developed pore network, the pores are filled with highly conductive pore fluid. The ability of harmful ions to penetrate through this pore system can be characterised by the ability of the pore system to conduct electricity (Andrade, 1993). The test methods based on the principle of conduction of concrete are termed

conduction tests. Five conduction tests are discussed here, viz. the rapid chloride permeability test (ASTM C1202, 1997), the chloride conduction test by Streicher and Alexander (1995), the bulk (electrical) resistivity test (Andrade, 2006; Chlortest, 2006), the Wenner four probe resistivity test by Millard *et al.* (1990) and the electrode array by Mc Carter *et al.* (1995). A review of the test details along with the effectiveness of the measured parameter are discussed in the following sections.

3.4.1 Rapid Chloride Permeability Test (RCPT or AASHTO T 277-93)

This test was developed by Whiting (1981) and the test set-up is similar to that shown in Fig. 3.17. It consists of placing a water saturated 50mm thick concrete disc of 100mm diameter between two acrylic cells. One of the cell contains 3% NaCl solution and the other contains 0.3M NaOH solution. A 60V is applied across the test specimen through the copper mesh electrodes in both cells. The voltage was applied for a period of 6 hours and the current passed is recorded at every 30 minutes. The charge passed in coulombs during the test duration of 6 hours is determined by integrating the area under the current versus time graph. ASTM C 1202 (1997) gives a classification of chloride ion penetrability of concrete based on this coulomb value (see Table 3.4)

This test has been widely used because of the short test duration and its simple procedure. Nevertheless, there have been numerous criticisms of this technique:

1. The charge passed is related to all ions transported through concrete not just chloride ions. Therefore, the test accounts for the total current and not that corresponding to the chloride flux (Andrade, 1993). The conductivity of the pore solution is influenced by the concentration of ions in the pore solution and the concentration of these ions can vary between cement types (Page and Vennesland, 1983).
2. The test only provides an index and no theoretical relationship exists whereby the results obtained could be used to determine the chloride diffusivity (Stanish *et al.*, 2000).
3. The high voltage used (60V) induces heat, which in turn, changes the rate of flow of ions (Andrade, 1993).

Misra *et al.* (1994) studied the effect of test voltage on RCPT and found that the charge passed at different voltages increased with the increase in test voltage. Therefore, they suggested that the RCPT test can be carried out at different voltages and the relative charge passed at 60V can be obtained from the relationship presented in Fig. 3.18.

3.4.2 Chloride conduction test

Following the criticisms received for the ASTM C1202, Streicher and Alexander (1995), developed a Chloride Conduction Test. The test incorporates the following characteristics:

- A sound theoretical background.
- Yields a diffusion coefficient.
- Independent of the pore solution conductivity.
- More rapid than the ASTM C1202 (1997).

The cell arrangement used for the test is shown in Fig. 3.19. The apparatus consisted of two 500ml cells kept apart by the specimen. The thickness of the specimen was generally 10mm for mortar 25mm for concrete, and the diameter was 68mm in both cases. Prior to testing the specimens were dried, then vacuum saturated with 5M NaCl solution for 5 hours and left in the solution for an additional 18 hours. Both cells were filled with a 5M NaCl solution. An electric field of 10V was applied between a carbon anode and a stainless steel cathode. Two copper/copper sulphate half cells and a voltmeter were used to measure the potential difference between the solutions on either side of the specimen accurately. Two plastic tubes led from the half cells to the concrete surface were used to measure accurately the potential across the specimen. An ammeter was included to record the current flowing through the system. The current measured was shown to be independent of the conductivity of the cell solutions. This current was used to calculate the conductivity of the specimen:

$$\sigma = \frac{I}{v}\frac{L}{A} \qquad \text{(Eq. 3.31)}$$

where,

σ is the conductivity of the specimen, mS/cm,

I is the electric current, mA,

v is the potential difference across the specimen, V,

L is the thickness of the specimen, cm,

A is the cross-sectional area of the specimen, cm^2.

Streicher and Alexander (1995) considered a material constant, q, which is the ratio of the diffusivity of an ion in a porous material to that of the same ion alone in the pore solution. This constant (q) has been found to be equal to the ratio of the mobility (conductivity) of an ion in the porous material to that of the same ion in the pore solution of the same material (Garboczi and Bentz, 1992). Therefore, the value of conductivity obtained has been related to the diffusivity of the concrete:

$$q = \frac{D}{D_o} = \frac{\sigma}{\sigma_o} \qquad \text{(Eq. 3.32)}$$

where,

q is a constant of the porous material,

D is the diffusivity of ion through the porous material, m^2/s,

D_o is the diffusivity of ion through the pore solution, m^2/s,

σ is the conductivity of the porous material, mS/cm,

σ_o is the conductivity of the pore solution, mS/cm.

Streicher and Alexander (1995) observed that the conductivity of pore solution, σ_o, was similar to that of the 5M NaCl saturating solution. Therefore, from the conductivity (σ) value determined by Eq. 3.31, the diffusivity ratio (D/D_o) was obtained. This ratio was then multiplied by the diffusivity of chloride ions in the pore solution (D_o) to obtain the chloride diffusivity of the porous medium (D).

The D value obtained from the conduction test was compared to the steady state migration coefficient, D_{mig} by Johnson *et al.* (1996). The authors concluded that the D value from the conduction test was comparable to the D_{mig} from the steady state migration test.

However, this test method does have some limitations as described by Zhang and Gjorv (1998).

1. In electrolytic solutions, both the diffusivity and conductivity are concentration dependent due to ionic interaction. However, they vary with the concentration differently.
2. Since the chloride diffusivity is a function of concentration and natural concentrations as high as 5M are uncommon, the diffusivity obtained may be beyond a realistic range of diffusivities. The results obtained will probably reflect information about the general permeability of the concrete rather than the chloride diffusivity.

3.4.3 Bulk resistivity test

Polder (1995) and Andrade *et al.* (2000) established that the bulk resistivity of concrete can be used to determine the diffusivity. Figure 3.20 shows the arrangement proposed by Andrade (2006). A saturated concrete specimen was placed between two solid electrodes. By passing an alternating current the resistance of the specimen was found at a reference temperature. Resistivity of the specimen was determined using the dimensions of the specimen.

$$\rho = R_e \frac{A}{L} \qquad \text{(Eq. 3.33)}$$

where,

ρ is the bulk resistivity of the concrete specimen, ohm.m,

R_e is the resistance of the specimen, ohm,

A is the cross sectional area of the specimen, m^2,

L is the thickness of the specimen, m.

A classification of different concretes based on the resistivity values (see Table 3.5) was given by Polder (2001) on behalf of the findings from the RILEM TC-154 Technical committee recommendations.

In saturated concrete, the resistivity is a function of the volume of pores, the pore connectivity, type of cement and the maturity of the concrete (Andrade *et al.*, 2000; Whittington *et al.*, 1981). Andrade *et al.* (2000) found the following empirical relationship between the diffusivity and the resistivity of the concrete:

$$D_{ssm} = \frac{120}{\rho} \qquad \text{(Eq. 3.34)}$$

where,

D_{ssm} is the steady state migration coefficient (if 1M NaCl solution is used as catholyte), m^2/s,

ρ is bulk resistivity of the concrete specimen, ohm.m.

Andrade (2006) reported that for a catholyte concentration of 0.5M NaCl, the relationship was similar to the one presented in Eq. 3.34, but the constant term increased from 120 to 230.

Andrade *et al.* (2000) highlighted that the diffusivity calculated using Eq. 3.34 does not take into account the binding capacity of the material. Both Andrade *et al.* (2000) and Polder (1995) showed that the product of the resistivity and diffusivity were more or less constant. However, Polder (1995) concluded that the product between the diffusivity and resistivity varied between mixes when the diffusivity was obtained from the chloride profiles, i.e., in non-steady state condition. According to Tang (1999a) the diffusivity from the non-steady state test is influenced by the binding capacity of the material and, therefore, the difference in binding capacity of the different mixes used by Polder (1995) could be the reason for the above observation.

Nevertheless, it can be concluded that bulk resistivity is by far the easiest and the fastest method for determining the resistance to chloride transport.

3.4.4 Embedded electrodes

McCarter *et al.* (1995) developed an electrode array system with miniature multi-electrodes to monitor the advance of a chloride front in concrete. A typical array system by McCarter *et al.* (1995) is presented in Fig. 3.21.

The probe consisted of 10 stainless steel electrode pairs, 1.5mm in diameter, mounted on a perspex slab. The 5mm tip of the electrodes was exposed while the rest was sleeved. All the electrodes were kept 5mm apart in both vertical and horizontal directions and each pair was staggered to minimise the interference caused by the aggregates on the resistivity measurements. The electrode array is placed on the cover zone while casting concrete in a structure.

The electrode system was able to provide information on the short and the long term depth-related variation of the resistivity of the concrete subjected to different environments. McCarter *et al.* (1996) showed that the resistivity measurements from embedded electrodes could be used to monitor the ingress of water and chlorides into concrete. That is, instead of using the resistivity measurements to determine the diffusivity, the authors suggested to use resistivity changes as a monitoring technique. As the electrode pairs are placed at varying depths from the exposure face of a concrete, the resistivity of the concrete at different depth can be obtained, which enables the determination of an advancing chloride front.

3.4.5 Wenner four probe resistivity test

The Wenner four probe resistivity test determines the near-surface resistivity of a material using a four probe array of electrodes (see Fig. 3.22) (Millard *et al.*, 1990). The technique consists of passing a constant magnitude alternating current between the two outer electrodes and measuring the potential difference across the two inner electrodes. The resistivity of the material is given by:

$$\rho_{Wenner} = 2\pi a\left(\frac{v}{I}\right) \qquad \text{(Eq. 3.35)}$$

where,

ρ_{Wenner} is the Wenner probe surface resistivity, (10) ohm.m,

a is the spacing of the probes, m,

v is the potential difference measured across the electrodes, V,

I is the applied current, A.

The test method however has the following disadvantages:

1. The contact between the electrodes and the surface is often the main source of error. To ensure the flow of current from the electrode to the concrete, a highly conductive gel is applied to the tip of the electrode. If this gel is not applied correctly, this can lead to inaccurate result.
2. In order to determine the diffusivity of concrete using the resistivity it is necessary to saturate the concrete (Nilsson *et al.*, 1996). Again, the criticisms applicable to the conductivity tests apply here as well. The conductivity of the pore solution should be known in order to determine the diffusivity of

concrete (Nilsson *et al.*, 1996). However, Polder (2001) have shown that a rough estimation of the diffusivity of the concrete is possible with the help of the resistivity values.

3.5 Permit ion migration test

Andrews, (1999) developed an *in situ* chloride ion migration test to determine the chloride diffusivity of concrete *in situ*. This test was later named as the Permit ion migration test and the test apparatus was called the Permit (Basheer *et al.*, 2005). As mentioned earlier in section 3.3.2, this test was developed based on the principle of steady state chloride migration tests. In any steady state chloride migration test, the concrete specimen separates the catholyte and anolyte (see Fig. 3.7). The chloride ions from the catholyte move towards the anolyte through the specimen in presence of an electric field. However, in Permit, instead of having two cells containing the anolyte and the catholyte kept on either side of the concrete specimen, both the cells are concentrically kept on the concrete surface itself (Fig. 3.23). Therefore, the ions migrate from the inner cell containing the catholyte through the specimen to the anolyte in the outer cell. The amount of chloride ions at the anolyte (initially de-ionised water) is monitored regularly and a concentration-time graph is plotted. The straight-line portion, which is similar to that of the steady state diffusion test (Fig. 3.2), is used to calculate the *in situ* migration coefficient, $D_{in\ situ}$, using a modified Nernst – Planck equation, described in the next section.

3.5.1 Test set-up and test protocol

A typical test arrangement of the Permit ion migration test is shown in Fig. 3.24. The Permit body consists of two cylinders of different diameters (see Fig. 3.23), concentrically placed on the concrete surface. The cylinder with the smaller diameter, the inner cell, contains a 0.55M NaCl solution (catholyte). The annular region between the two cylinders, the outer cell, contains de-ionised water (anolyte). The inner cell contains a circular stainless steel cathode, while the outer cell contains an annular mild steel anode.

A potential difference of 60V is applied across the electrodes. This creates an axi-symmetric flow of ions from the inner cell to the outer cell, through the cover

concrete. The chloride concentration in the outer cell (anolyte) is continually monitored using a chloride ion selective electrode. During the course of the test, data as shown in Fig. 3.25 are obtained by considering assumptions as that described in section 3.3.2 (Andrade, 1993; Bockris and Reddy, 1970), the slope of the straight-line portion is used to calculate the *in situ* migration coefficient, $D_{in\ situ}$, as described below.

Calculation of $D_{in\ situ}$

The Nernst-Planck equation similar to the one used by Andrade and Sanjuan (1994) (section 3.3.2.1) termed as modified Nernst-Planck equation, was used to calculate the *in situ* migration coefficient.

$$D_{in\ situ} = -\left(\frac{dc}{dt}T\right)\left(\frac{R}{zF}\right)\left(V\frac{L}{A}\right)\left(\frac{1}{CE}\right) \qquad \text{(Eq. 3.36)}$$

where,

$D_{in\ situ}$ is the *in situ* migration coefficient, m^2/s,

$\frac{dc}{dt}$ is the rate of change of concentration in the anolyte at the steady state conditon, $mol/m^3.s$,

T is the absolute temperature (average during the steady state), K,

R is the universal gas constant, 8.31 J/K.mol,

z is the valency of the ions, -1 for chlorides,

F is Faraday's constant, $9.65x10^4$ c/mol,

V is the volume of the anolyte, $7.25x10^{-4}\ m^3$,

A is the average area through which the flow takes place, ($6x10^{-3}$ see section 3.5.2) m^2,

L is the flow length, ($2.72x10^{-2}$ see section 3.5.2) m,

C is the concentration of ion source solution, $0.55x10^{-3}\ mol/m^3$,

E is the electrical potential applied between the anode and the cathode, V.

3.5.2 Obtaining parameters of the flow path to calculate $D_{in\ situ}$

Andrews (1999) considered that the total flow of chloride ions takes place through the tapered region, as illustrated in Fig. 3.26. He considered that the average area, A of flow as $6x10^{-3}\ m^2$, which is the average of the area of the inner cell and the outer cell. In order to evaluate the *in situ* migration coefficient, an effective length, L, was

required. Integrating the flow of chloride ions through the tapered section and using the geometry of the cells given in Fig. 3.26. Andrews (1999) was able to obtain an equation for the flow length as given below:

$$LQ_{cl^-} = D\frac{\alpha C}{T}(E_1 - E_2)(A_2 - A_1)\left[Log\left(\frac{A_2}{A_1}\right)\right]^{-1} \qquad \text{(Eq. 3.37)}$$

and,

$$Q_{cl^-} = V\frac{dc}{dt} \qquad \text{(Eq. 3.38)}$$

L is the average flow length, m,

Q_{Cl^-} is the total flow of chloride ions through the concrete, mol/s,

V is the volume of the anolyte, m^3,

$\frac{dc}{dt}$ is the slope of the straight – line portion of the concentration – time graph, mol/m^3.s

D is the migration coefficient, m^2/s,

$\alpha = \frac{|z|F}{R}$, where all are constants as defined for Eq. 3.36, mol.K/m^3.V,

C is the concentration of the catholyte, mol/m^3,

T is the average temperature during the steady state, K,

(E_2-E_1) is the potential difference, V,

A_1 is the area of inner cell, m^2,

A_2 is the area of outer cell, m^2.

According to Andrews (1999), in Eq. 3.37, the variables E_1, E_2, A_1 and A_2 are known. The value of α is constant and C is unique for a specific test. The rest of the variables is estimated from a test. However, the migration coefficient D is estimated from a steady state migration test, which was considered to be equivalent to the $D_{in\ situ}$.

The flow lengths estimated for three different opc mixes using the above equation were comparable and hence an average value of 0.272m was used as the average flow length. The flow length was also determined using a finite element model and an average flow length of 0.05m was obtained. As the experimental value of flow length (L = 0.0272m) was repeatable for three different concrete mixes, the author

concluded that this value of the average flow length should be used in calculating the *in situ* migration coefficient. That is the average flow path dimensions in Permit ion migration test are L = 0.0272m and A = 60 x 10^{-4} m^2.

3.5.3 Finite element modelling of the flow path

Discussion on the flow path

Andrews (1999) considered that the flow of chloride ions through the concrete under an electrical potential is analogous to the flow of electrical current through a material with a given conductivity under an electrical potential. The Permit ion migration test being a typical potential problem, the distribution of the potential is governed by Poisson's equation. Therefore, a finite element package was used to solve the Poisson's equation using the heat transfer facility in a finite element software, ABAQUS. As the flow of chloride ions in the Permit ion migration test is axi-symmetric, only the region (AEFJ in Fig. 3.23) was modelled (Fig. 3.27). The following assumptions were used for the modelling:

- Concrete is a homogeneous and isotropic material.
- The conductivity of the concrete in the model was considered as 1S/cm.
- A potential difference of 30V was selected to fit the experimental part of the theory. Therefore, the boundary conditions of Fig. 3.27 were set as AB having zero potential and CD having a potential of 30V. The boundary DEFJ was considered to be impermeable.

The flow of electrical current was determined using the model. The equi-potential lines are closely spaced close to the concrete surface, where the distance between the prescribed potential was small, whereas they are more widely spaced deeper in the concrete. The flow of current will be largest when the equipotential lines are closely spaced.

Further study by Basheer *et al.* (2005) on the Permit ion migration test identified that the rate at which chloride ions are transported through the concrete specimen is different at different depths. A finite element model showing the axi-symmetric flow of chloride ions between the cells in the Permit ion migration test is shown in Fig. 3.28. This figure shows that a greater quantity of flow occurs through the surface layers compared to the interior. Basheer *et al.* (2005) reported that about 90%

of the flow took place through the initial 15mm depth from the test surface. After the completion of the test, the chloride concentration at the centre of the test was found to be constant up to a depth of 30mm. Fig. 3.28 also suggests that the outward flow of chloride ions from the inner cell into the concrete could be greater than the inward flow into the outer cell from the concrete. This means some ions are penetrating deeper into the concrete specimen.

3.5.4 Selection of optimum test variables

Electrodes

Andrews (1999) studied the effect of different anode materials on the *in situ* migration coefficient and the following conclusions were made:

1. Graphite was not a suitable material for the anode as chlorine gas evolved during the test at high voltages (30V and 60V), resulting in relatively low migration coefficients.
2. For both mild steel and cast iron anodes, the time to steady state flow of chlorides and, thus, the test duration were similar. The *in situ* migration coefficient obtained in both cases were comparable. Both materials produced similar but easily removable deposition of corrosion products on the concrete surface.

Therefore, the material chosen for the anode was mild steel. Stainless steel was considered the best material for cathode.

Concentration of the catholyte

Andrews (1999) studied the effect of the catholyte concentration on both the time to reach steady state and the chloride flux measured in the anolyte. Figure 3.29 shows the chloride concentration in the anolyte versus time plot, for three different catholyte concentrations, tested at 60V. This figure shows that the change in chloride concentration of the catholyte did not increase the time to reach steady state, suggesting that the test duration will not be influenced much by the change in the concentration of the catholyte. However, the figure also indicates that the amount of chloride ions arriving at the anolyte increases with an increase in the catholyte concentration. This means that there was an increase in chloride ions being transported through the concrete pores at the higher catholyte concentrations, and therefore, more chlorides left in the concrete at the completion of the test. From a

consideration of the minimum damage to the structure under test, Andrews (1999) concluded that the lowest concentration of 0.55M should be used.

The *in situ* as well as the steady state migration coefficients calculated for the three chloride concentrations decreased with the increase in the catholyte concentration. This was similar to the findings reported in section 3.3.2.2. The variation of the *in situ* migration coefficient, $D_{in\ situ}$ with the chloride concentration of the catholyte is shown in Fig. 3.30. This variation in the $D_{in\ situ}$ can be accounted by considering the activity coefficients corresponding to the appropriate catholyte concentration. The activity coefficient decrease with the increase in chloride concentration from 0.5 to 3M (see Fig. 3.13). Therefore, by dividing the activity coefficient with the corresponding $D_{in\ situ}$ (as specified by Castellote *et al.* (2001) in Eq. 3.26), the resulting value might be comparable for all the catholyte concentrations studied.

Applied voltage

Andrews (1999) studied the effect of voltage on the chloride ion flow to the anolyte as well as the *in situ* migration coefficient. The concentration versus time graph obtained for the three test voltages studied are shown in Fig. 3.31. This figure shows that the time to reach steady state increased with the increase in the applied voltage. However, this did not affect the *in situ* migration coefficient obtained (shown in Fig. 3.32). The *in situ* migration coefficient remained the same irrespective of the applied voltage, suggesting the possibility of conducting the test at any voltage between 10V and 60V. However, the author commented that increasing voltage had increased the temperature of the anolyte, but decreased the test duration. Therefore, from a practical consideration of completing the test within a day, the author concluded that 60V is the optimum applied voltage in order to obtain the chloride diffusivity on site.

3.5.5 Effectiveness of $D_{in\ situ}$

Andrews (1999) reported the results obtained from the Permit ion migration test for a range of opc concretes. The author found that the *in situ* migration coefficient, ($D_{in\ situ}$) correlated well with the results obtained from both the steady state diffusion test (D_e) (Fig. 3.34) and the steady state migration test, D_{ssm} (Fig. 3.33). A good relationship was obtained between the $D_{in\ situ}$ and the D_{ssm}

(R^2=0.95). Similarly, a good relationship was obtained between the $D_{in\ situ}$ and the D_e (Fig. 3.34) (R^2=0.92). Figure 3.34 shows that the $D_{in\ situ}$ values are lower compared to the corresponding D_e. However, this difference can be accounted by using the activity coefficient suggested by Andrade and Sanjuan (1994) in $D_{in\ situ}$, similar to the discussions in section 3.3.2.2.

Andrews (1999) also reported a relationship between the *in situ* migration coefficient and the non-steady state diffusion coefficient (apparent diffusion coefficient) obtained from a non-steady state diffusion test (see Fig. 3.35). The coefficient of determination of the power relationship was R^2=0.79, which was considered lower than the previous two. Therefore, the author concluded that the *in situ* migration coefficient obtained from the Permit ion migration test is as effective as the results from the other steady state test methods. Advantage of this test over the other tests that he highlighted was that the *in situ* migration coefficient can be measured at any stage of the structure in service using the Permit ion migration test.

3.5.6 Limitations of the Permit ion migration test

As discussed earlier, differences in conductivity of the concrete could influence the flow path of chloride ions in Permit ion migration test. Andrews (1999) tested only opc concretes to obtain the value of L as 0.0272m. Therefore, the effect the conductivity of concrete has on the flow paths need to be investigated further. This would also necessitate determining the value of L/A for calculating the $D_{in\ situ}$ for concretes containing supplementary cementitious materials.

In the test protocol developed by Andrews (1999), the chloride ion concentration of the anolyte was measured using an ion selective electrodes (ise). Although the ise requires constant calibration and special care especially on site, a number of data points can be obtained without depleting the anolyte. Therefore, Andrews (1999) considered that compared to the conventional chloride measurement of taking liquid anolyte samples, this is advantageous. However, the measurement still requires a skilled technician throughout the test duration. For very dense concretes, this test duration can be more than 10 hours. Therefore, a simpler method such as measuring the conductivity of the anolyte, needs to be considered instead of using the ise.

In the Permit ion migration test by Andrews (1999), measurements such as the chloride concentration, the current and the temperature are measured manually. This will not only increase the expense of carrying out a test, but also increases the experimental error. Therefore, the Permit ion migration test requires a new test procedure that can be carried out automatically.

The *in situ* migration coefficient correlated with results from other established test methods. However, the validation was only done for opc concrete mixes. As discussed in section 2.6.2, the presence of supplementary cementitious materials influences the chloride ion transport through concrete. The influence of the supplementary cementitious materials on the *in situ* migration coefficient needs to be established.

Therefore, it is considered that the Permit ion migration test protocol have to be revised to account for the aforementioned limitations and the new test protocol need to be validated against the results from other established test methods for a range of concretes containing supplementary cementitious materials. In addition, the test procedure should be automated and made user-friendly, in order to make the test usable on site.

3.6 Concluding remarks

A summary of the different test methods and the effectiveness of the reported test parameter in determining the chloride penetration resistance of concrete are given in this chapter. From this discussion the following conclusions can be drawn:

1. Steady state diffusion and non-steady state diffusion tests have sound theoretical bases and are generally considered to be the most accurate means of determining the chloride diffusivity of concrete. However, both the tests require very long test duration, which prevents an immediate assessment of concrete quality on site. Nevertheless, the method of transport of chloride ions in the non-steady state diffusion tests is considered to resemble to the site conditions.
2. Steady state migration tests, where a migration coefficient is determined, have a sound theoretical basis and are found to correlate well with the long-term steady state diffusion tests. However, it was evident that the test

variables have an influence on the reported test parameters and hence, the resulting migration coefficients are functions of the test variables in addition to the chloride transport resistance of concrete being tested.

3. The non-steady state migration test NT BUILD 492 (1999), has a sound theoretical basis and the resulting parameter, was comparable with that of the non-steady state diffusion tests.
4. The indirect tests measure the chloride transport resistance of concrete in a more rapid manner compared to the other tests. However, the resulting parameter can be inaccurate if the influence of the pore solution conductivity is not known. The effect of pore solution on the resulting parameter can be eliminated by replacing the pore solution by a highly conductive solution. However, the resulting parameter will depend on the ion-ion interaction of the conductive solution used, and in this case, it may give unrealistic value. Nevertheless, the indirect tests are very rapid and hence the usability of this test to classify concrete based on the chloride transport resistance need to be studied further.
5. It was identified that the Permit ion migration test can be used to obtain the chloride penetration resistance of concrete on site by using the principle of steady state migration. The influence of the different test variables on the measured parameter was studied and the optimum test variables were obtained. However, it is considered that the test requires a new test protocol by which the resulting migration coefficient can be measured in a more reliable and user-friendly manner.
6. The *in situ* migration coefficient from the Permit ion migration test correlated well with results from other commonly used test methods for a range of opc mixes. As the use of supplementary cementitious materials in concrete is now a common practice, it is necessary to establish a relationship between the *in situ* migration coefficient and the test results from other common test methods for a range of concretes containing supplementary cementitious materials in addition to mixes with only opc.

The review of different test methods highlights the need to identify reliable and rapid test methods for determining the chloride penetration resistance of concrete. In order to exploit further the usefulness of the Permit ion migration test, it would be necessary to modify the test protocol and to establish the validity of this new

test protocol with the other reliable test methods. Furthermore, the measurement procedure in the Permit ion migration test needs to be automated to make the instrument more user-friendly for site applications.

Table 3.1 Summary of steady state diffusion test

Reference	Test set-up	Core specimen	Compartment solutions		Determination of chloride content
			upstream	downstream	
Page *et al.* (1981)	Diffusion cell	Cement paste 50mm diameter 3mm thickness	1M NaCl in saturated $Ca(OH)_2$ solution	Saturated $Ca(OH)_2$ solution	100 ml aliquots extracted for spectrophotometric analysis
Buenfeld (1984)	Diffusion cell	Mortar sample 76mm diameter 7mm thickness	Sea water	Saturated $Ca(OH)_2$ solution	Ion selective electrode
Hansson and Berke (1989)	Sample glued to one half of the diffusion cell, placed in a bath of chloride solution	Cement paste 45mm diameter 3mm thickness	1M NaCl in saturated $Ca(OH)_2$ solution	50% saturated $Ca(OH)_2$ solution	Ion selective electrode
Dhir *et al.* (1990)	Sample clamped and sealed with silicone to one half of the diffusion cell, placed in a bath of chloride solution	Concrete, 20mm maximum aggregate 100mm diameter 25mm thickness	5M NaCl in saturated $Ca(OH)_2$ solution	50% saturated $Ca(OH)_2$ solution	Ion selective electrode
MacDonald and Northwood (1995)	Diffusion cell, stirrers in both cells	Cement paste 50mm diameter 3mm thickness	1M NaCl solution	Distilled water	Ion selective electrode
Sugiyama *et al.* (1996)	Diffusion cell	Concrete, 20mm maximum aggregate 100mm diameter 50mm thickness	3 % NaCl solution	0.3N NaOH solution	5 ml samples extracted for auto-titration analysis

Table 3.2 Summary of non-steady state diffusion tests

Reference	Test set-up and specimen preparation	Duration	Exposure solution	Determination of chloride content (dry concrete dust sample)
Page *et al.* (1991) Ponding test	Continuous exposure/Intermittent wetting/Wetting and drying 25mm deep pond on top of 300x200x100mm concrete slab	6,12 and 24 months	5% NaCl (~1M NaCl)	Spectrophotometric technique (Acid soluble chloride content)
Sergi *et al.* (1992) Immersion test	Continuous exposure of 49mm diameter and 65mm thick cylindrical concrete specimen Covered in paraffin wax except the exposure surface	100 days	1M NaCl in saturated $Ca(OH)_2$ solution	Spectrophotometric technique (Acid soluble chloride content)
NT BUILD 443 (1995) Immersion test	Continuously immersing a cylindrical concrete specimen 100mm diameter x 60mm thick The curved face and the bottom of the cylinder coated with epoxy paint (or polyurethane) to restrict chloride ingress.	≥35days	Aqueous solution of 165g/L of NaCl (~2.8M NaCl)	Acid soluble chloride content (Volhard's Titration) (NT BUILD 208, 1984)
BS EN 13396 (2004) (closely related to prEN-13396-1 (2002)) Immersion test	Continuous exposure of concrete cylinders ≥100mm diameter ≥60mm thickness (ingress from the sides are not prevented)	28days, 90 days and 180 days	3% NaCl solution kept at 40°C (~0.5M NaCl)	Potentiometric titration technique (Acid soluble chloride content) (Concrete samples are taken from an area having 60mm diameter from the centre of the specimen)
ASTM C 1556 (2004) Immersion test	Same as NT BUILD 443 (1995)	≥35days	2.8M NaCl	Acid soluble chlorides (similar to Volhard's Method) (ASTM C 1152, 1990)

Table 3.3 Steady state migration tests

Reference	Test set-up	Specimen: discs of different dimension	Electrolytes		Voltage (V) DC	Electrodes	Measured parameter
			Catholyte	Anolyte			
Potential Difference Test Dhir *et al.* (1990)	Diffusion cell placed in a bath of chloride solution [Figure 3.9]	Concrete 100 mm diameter 25mm thickness 20mm max aggregate	5M NaCl solution	Distilled water	10	Graphite anode Stainless steel cathode	Potential Difference Index, from Fick's 1st law of diffusion. [Eq. 3.18]
Andrade and Sanjuán (1994)	Split cell [Figure 3.11]	Concrete disc 75mm diameter 5mm thick Max aggregate 12mm	0.5M NaCl solution	Distilled water	12	Both electrodes Steel rods	Migration coefficient using Nernst-Plank equation [Eq. 3.20]
ACID test(El-Belbol and Buenfeld, 1989; Zhang and Buenfeld, 1994)	Split cell [Figure 3.10]	Mortar 10mm diameter, 50mm thickness	0.5M NaCl solution	0.3M NaOH solution	40	Both electrodes graphite	Time to steady state T_o Chloride flux, g
Zhang and Gjorv (1995a)	Split cell [similar to Figure 3.11]	Concrete 100mm diameter 50mm thickness Max aggregate 16mm	0.5M NaCl solution	0.5M NaOH solution	12	Both electrodes stainless steel mesh	Migration coefficient using Einstein relation
Sugiyama *et al.* (1996)	Split cell [similar to Figure 3.11]	Concrete 100mm diameter 50mm thick Max aggregate 20mm	0.5M NaCl solution	0.3M NaOH solution	15	Steel cathode Graphite anode	Migration coefficient using Nernst-Plank equation. Similar to [Eq. 3.20]
McGrath and Hooton (1996)	Split cell [similar to Figure 3.11]	Concrete 10mm diameter 30mm thickness Max aggregate 10mm	0.5M NaCl + 0.3M NaOH solution	0.3M NaOH solution	6-30	Both electrodes stainless steel mesh	Migration coefficient using Nernst-Plank equation. Similar to [Eq. 3.20]
Truc *et al.* (2000)	Split cell [similar to Figure 3.11]	Concrete discs 110mm diameter 30mm thickness Max aggregate 14mm	0.56M NaCl 0.025M NaOH + 0.083M KOH solution	0.025M NaOH + 0.083M KOH solution	12	Not mentioned	Different version of Nernst-Planck equation [Eq. 3.22]
Proposed by (Castellote *et al.*, 2001)	Split cell [Figure 3.12]	Concrete disc 15-20mm thickness Max aggregate size not specified	1M NaCl solution	Distilled water	12	Both electrodes Steel rods	Migration coefficient using Nernst-Plank equation [Eq. 3.26]

Table 3.4 Classification of concrete according to ASTM C1202 (1997)

Coulombs	Permeability Class	Typical of
>4000	High	w/c > 0.5
4000-2000	Moderate	w/c 0.4-0.5
2000-1000	Low	w/c < 0.4
1000-100	Very Low	Latex modified concrete
<100	Negligible	Polymer concrete

Table 3.5 Reference values at 20°C for the electrical resistivity of dense aggregate concrete of mature structures

Environment	Concrete resistivity (ohm.m)	
	Normal Portland cement	Blast furnace slag cement (>65% ggbs) or pulverised fuel ash (>25% pfa) or silica fume (>5% ms)
Very wet, submerged, splash zone, fog room	50-200	300-1000
Outside, exposed	100-400	500-2000
Outside, sheltered, coated, hydrophobised (not carbonated) 20°C 80% RH	200-500	1000-4000
Outside, sheltered, coated, hydrophobised carbonated	1000 and higher	2000-6000 and higher
Indoor climate (carbonated) 20°C 50% RH	3000 and higher	4000-10000 and higher

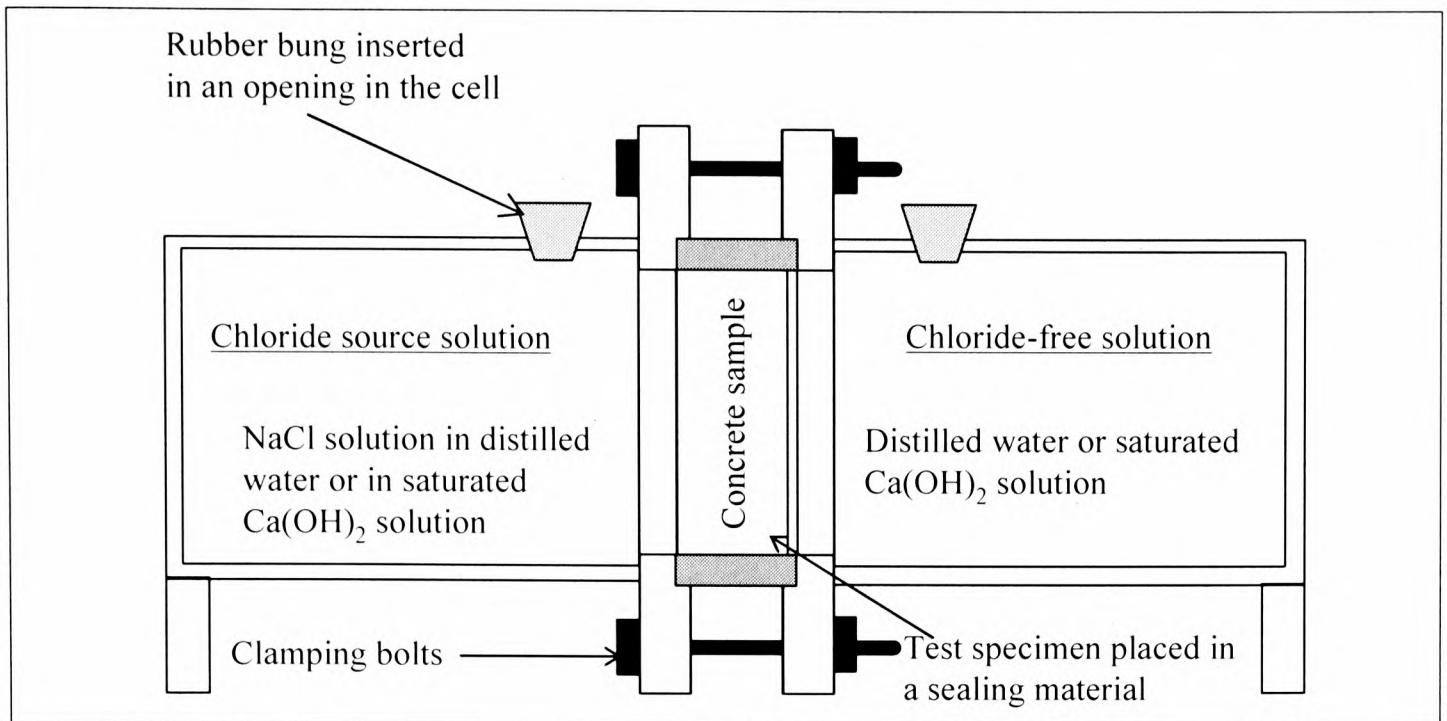

Figure 3.1 Schematic representation of the steady state diffusion test

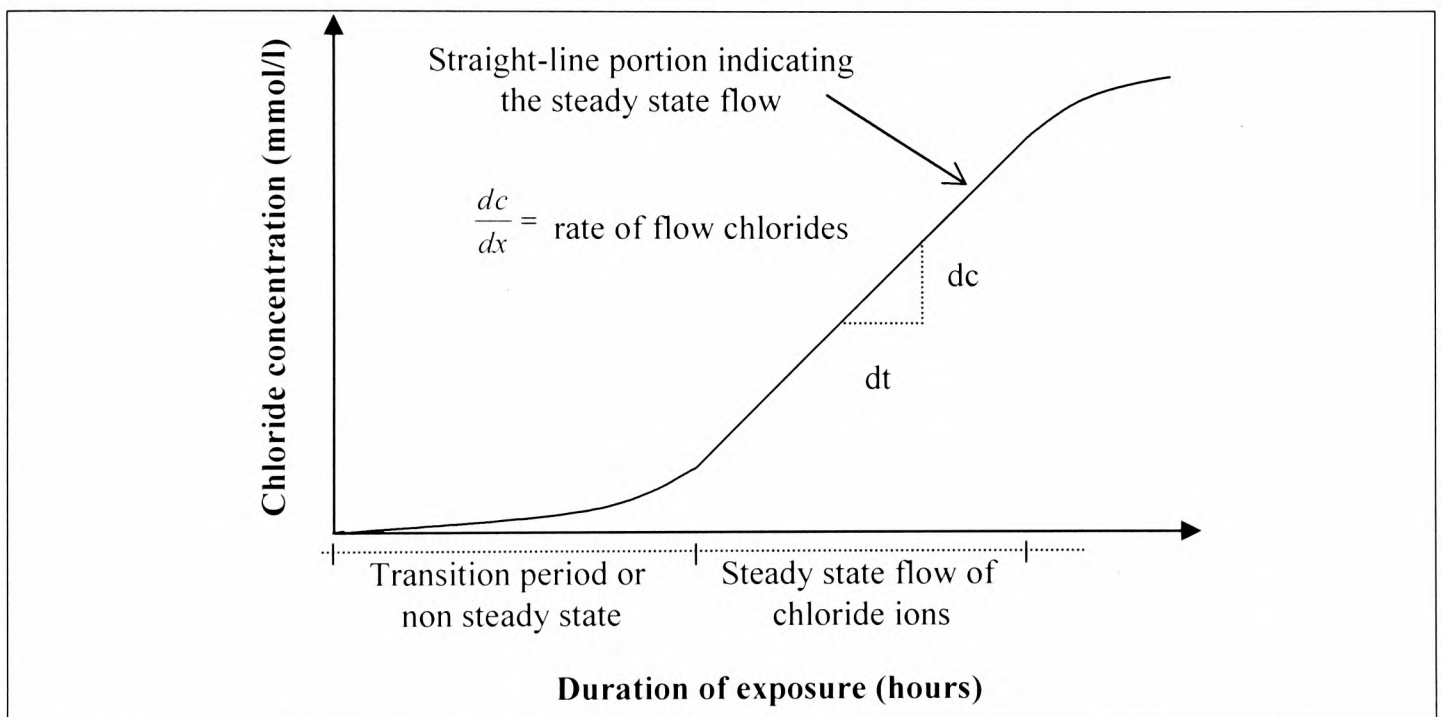

Figure 3.2 Typical concentration – time graph from a steady state diffusion test

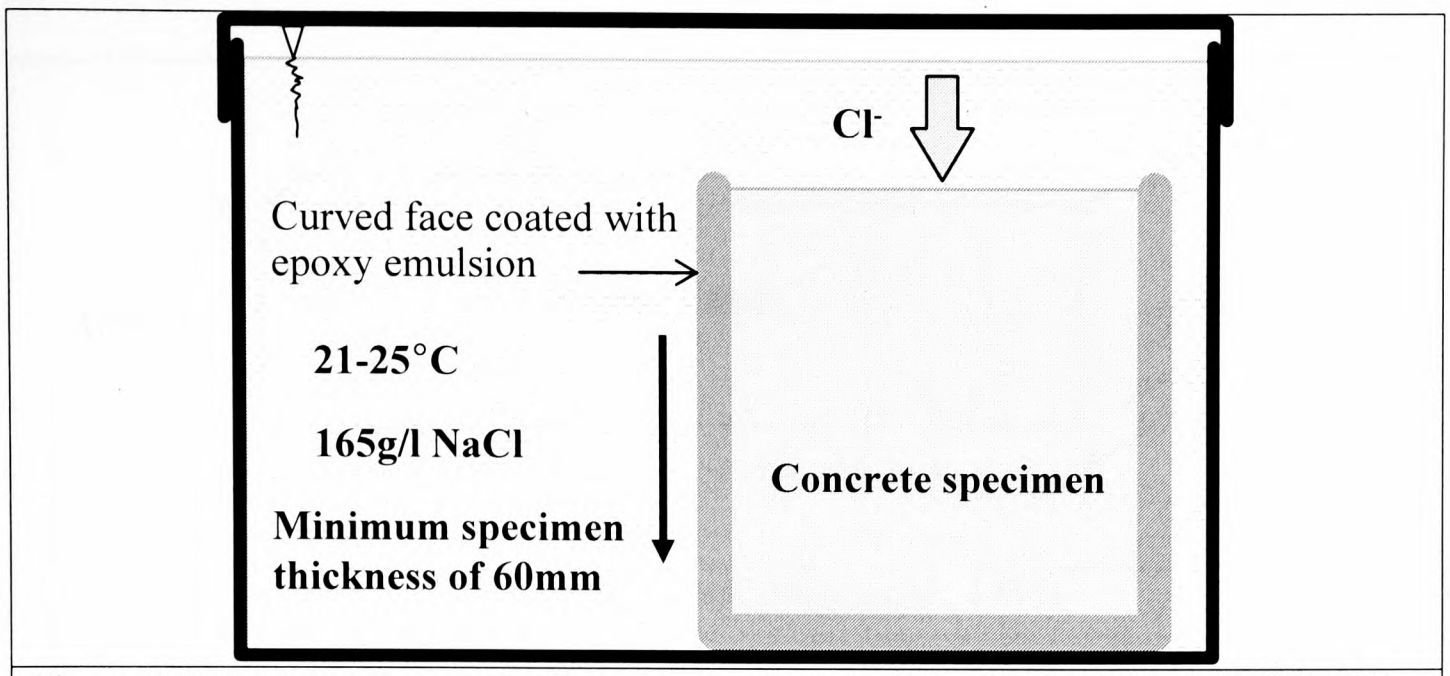

Figure 3.3 A typical set-up for the non-steady state diffusion test (NT BUILD 443, 1995)

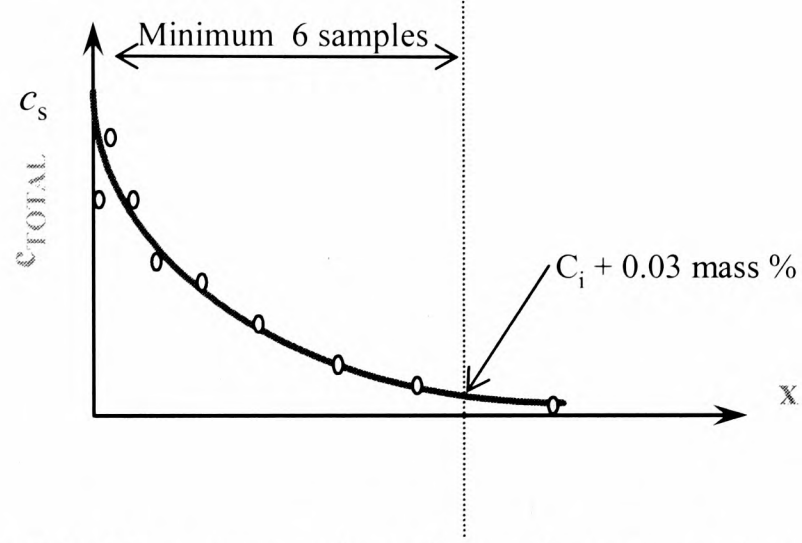

Note: C_i is the chloride concentration of the reference specimen which is not exposed to chlorides

Figure 3.4 Typical chloride concentration profile from a non-steady diffusion test

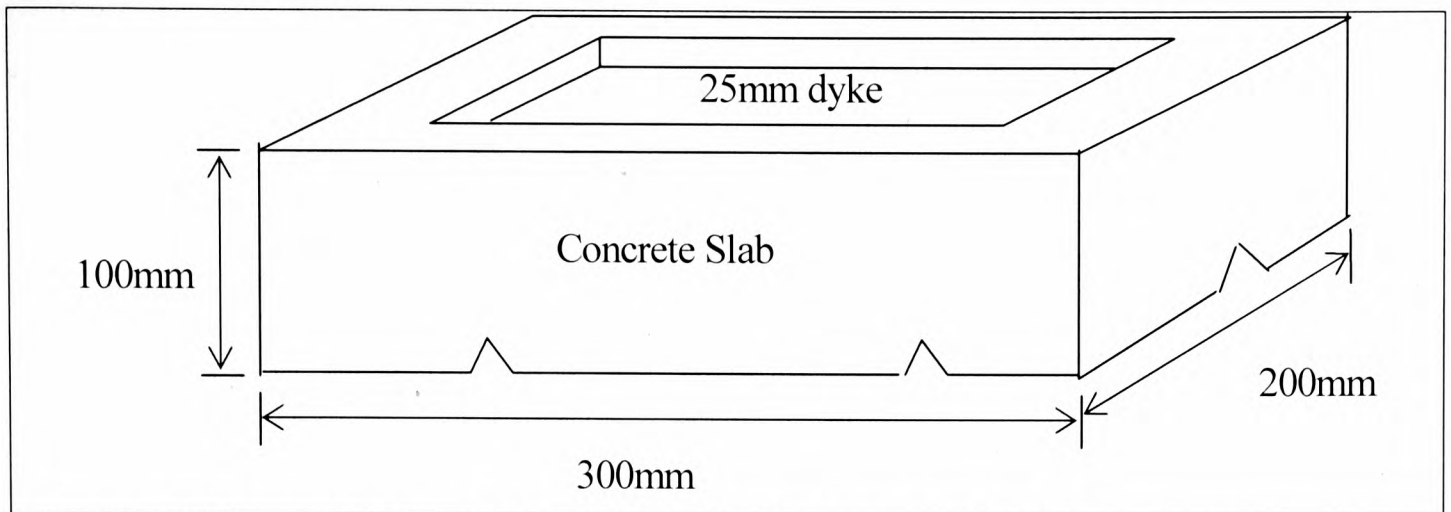

Figure 3.5 Concrete slabs for ponding tests (Page *et al.*, 1991)

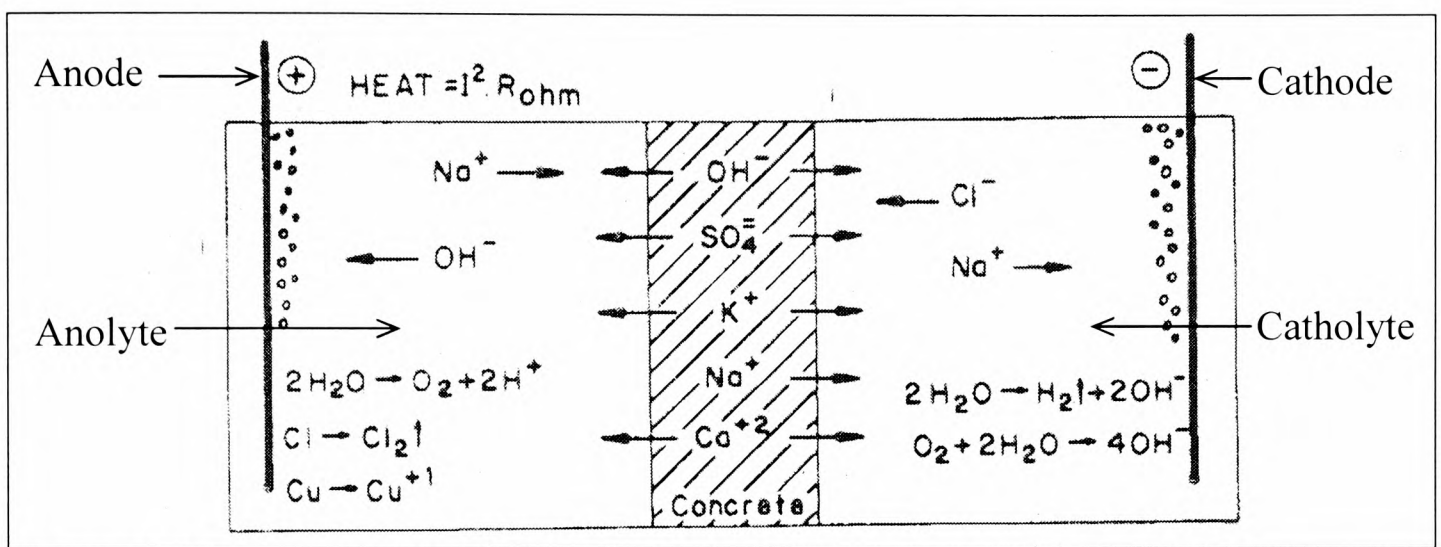

Figure 3.6 Electrochemical processes in a migration test (Andrade, 1993)

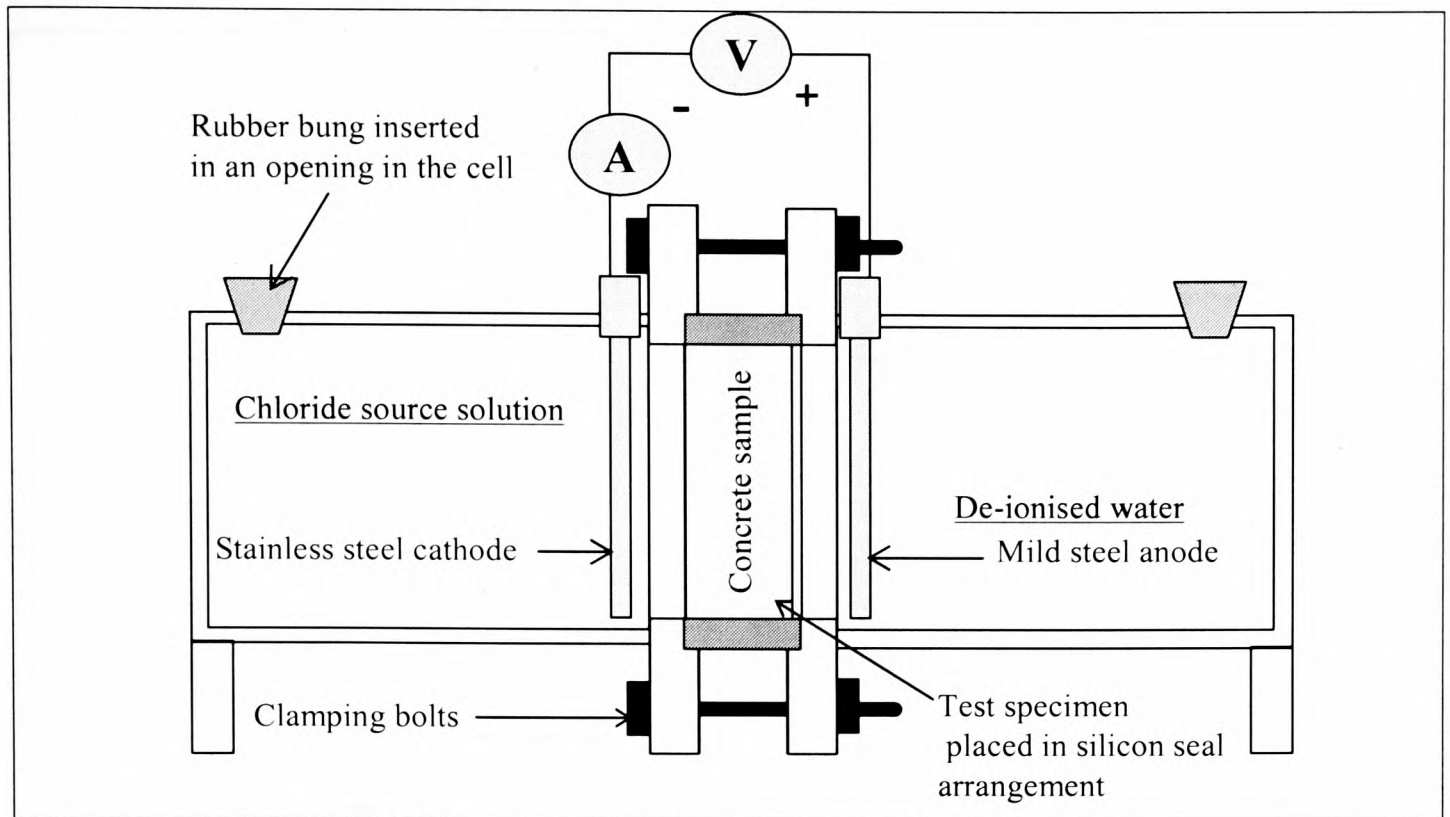

Figure 3.7 A typical test set-up for the steady state migration test

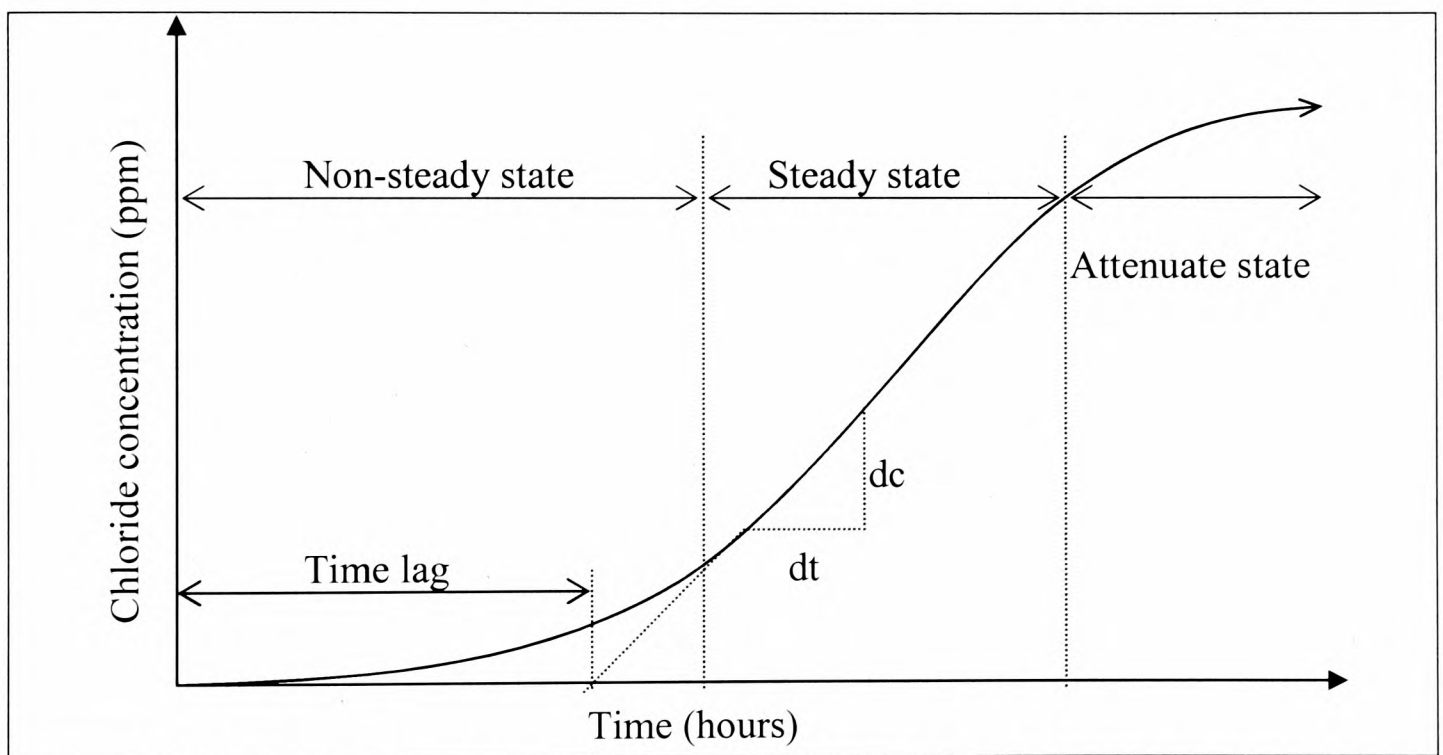

Figure 3.8 Typical concentration time plot from a steady state migration test

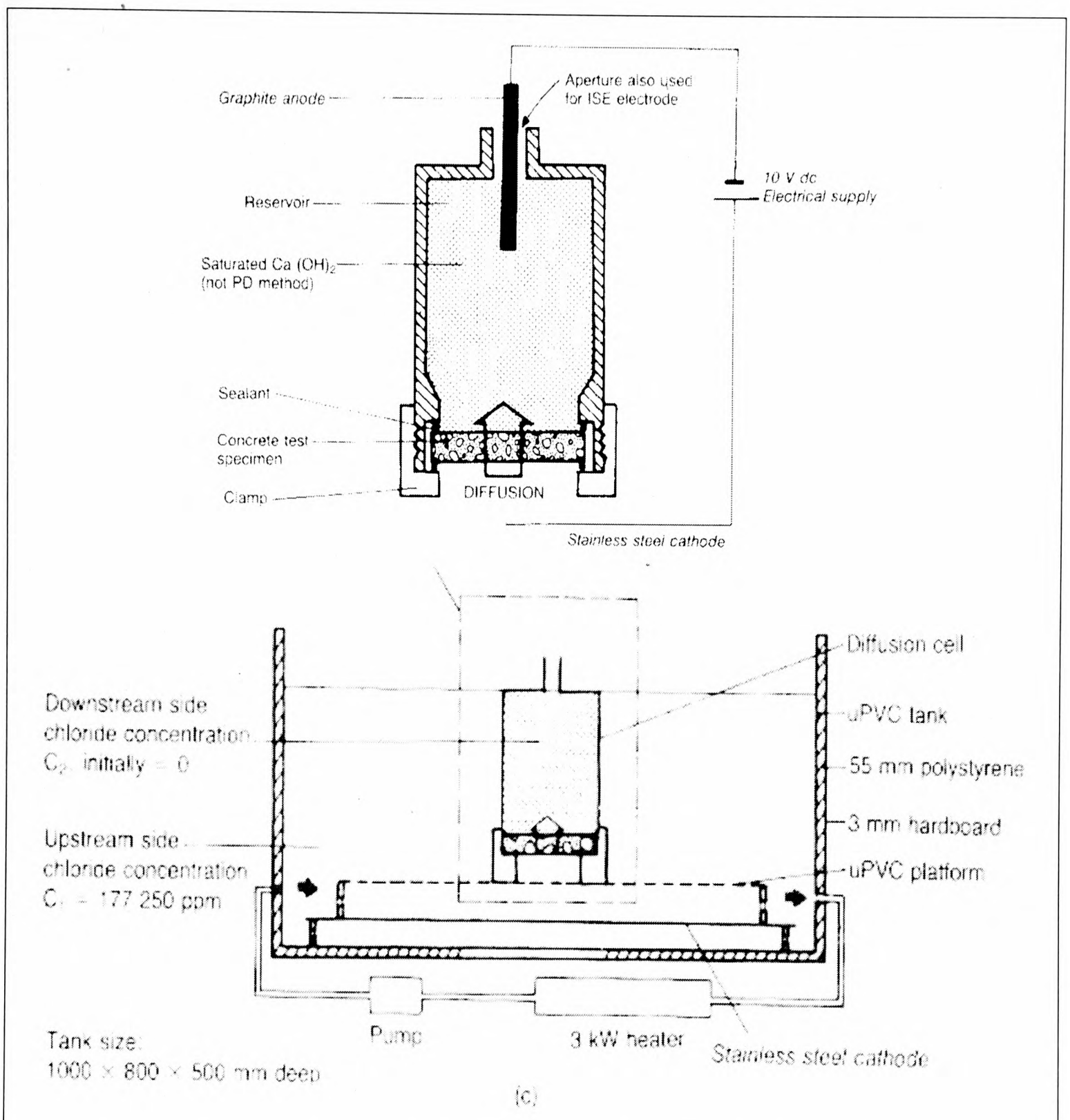

Figure 3.9 Potential difference test arrangement used by Dhir *et al.*, (1990)

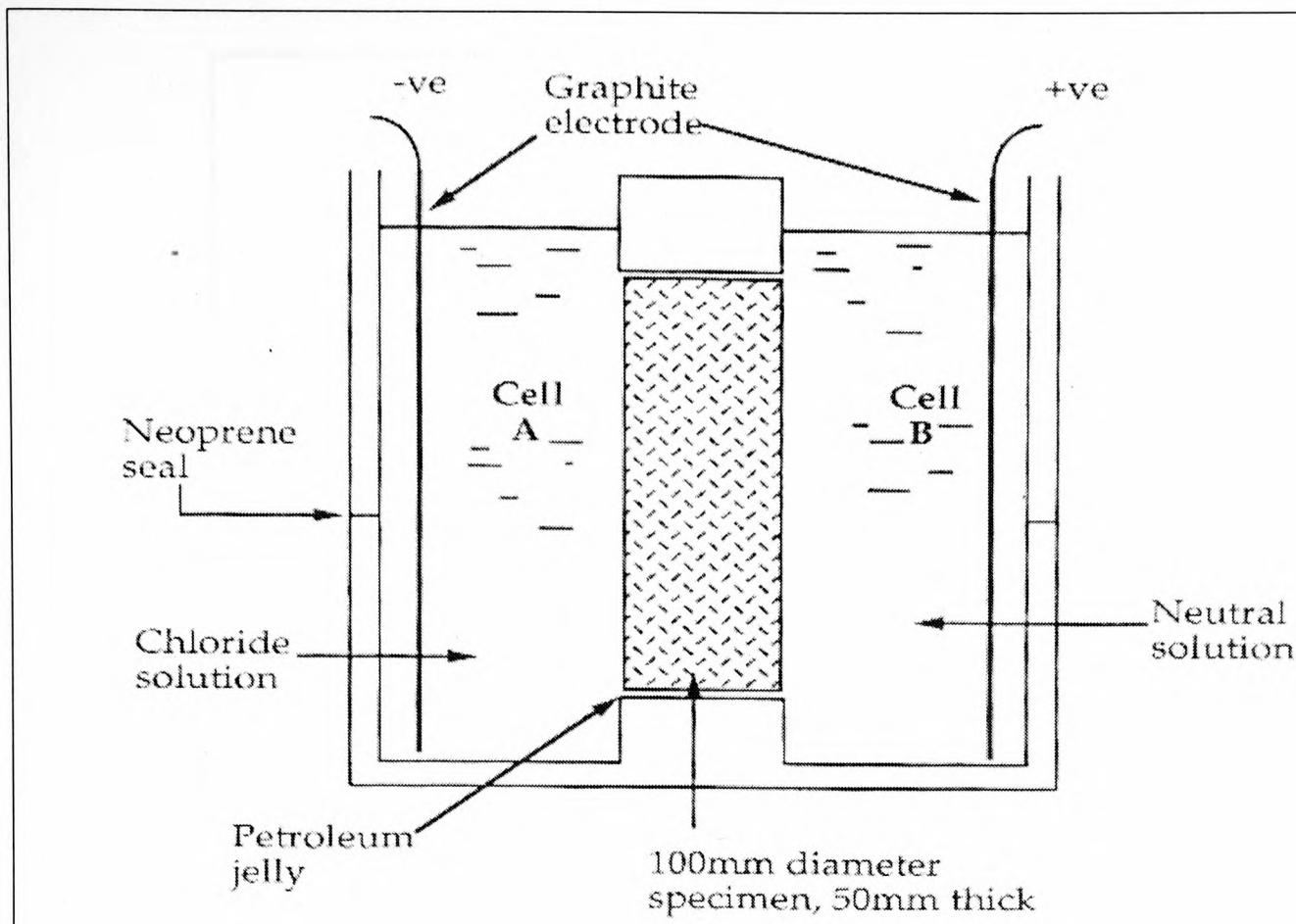

Figure 3.10 Schematic diagram showing the ACID test cell arrangement used by Zhang and Buenfeld (1994)

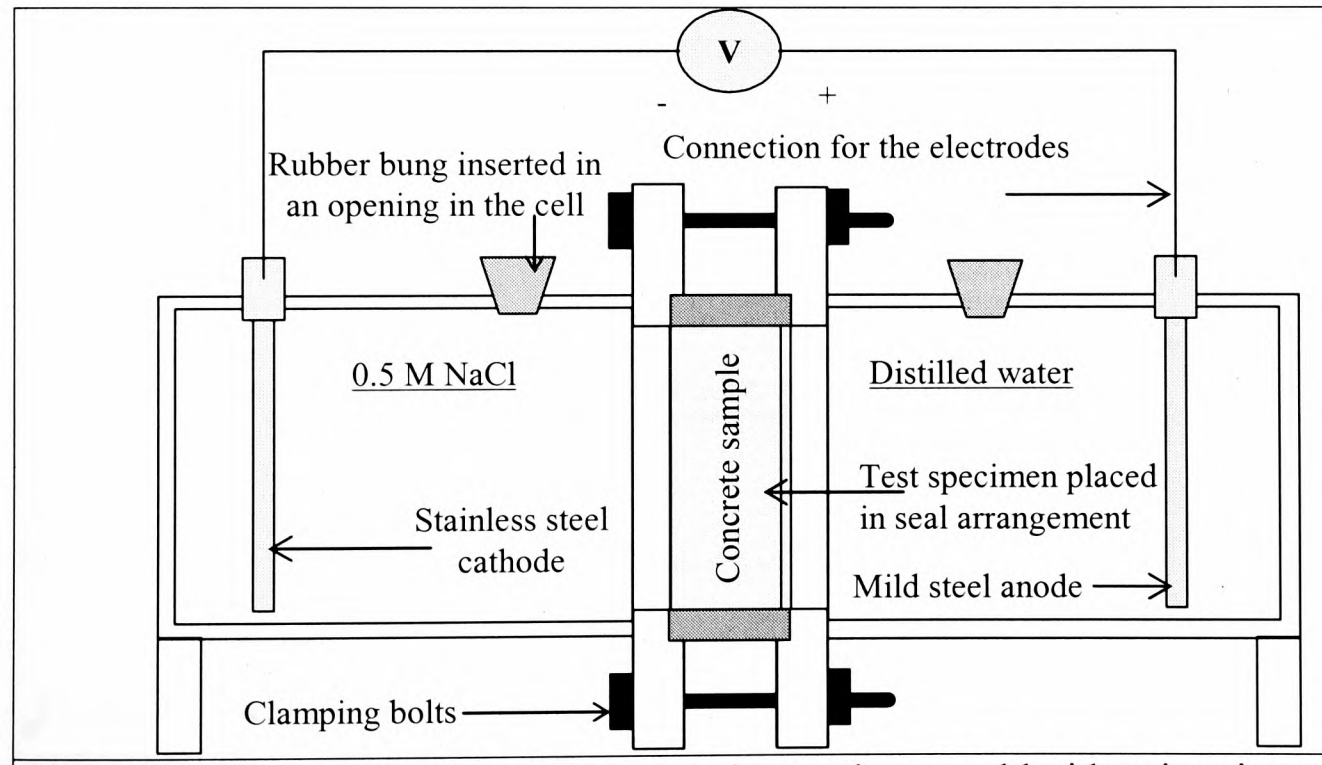

Figure 3.11 Schematic diagram showing the steady state chloride migration test by Andrade and Sanjuan, (1994)

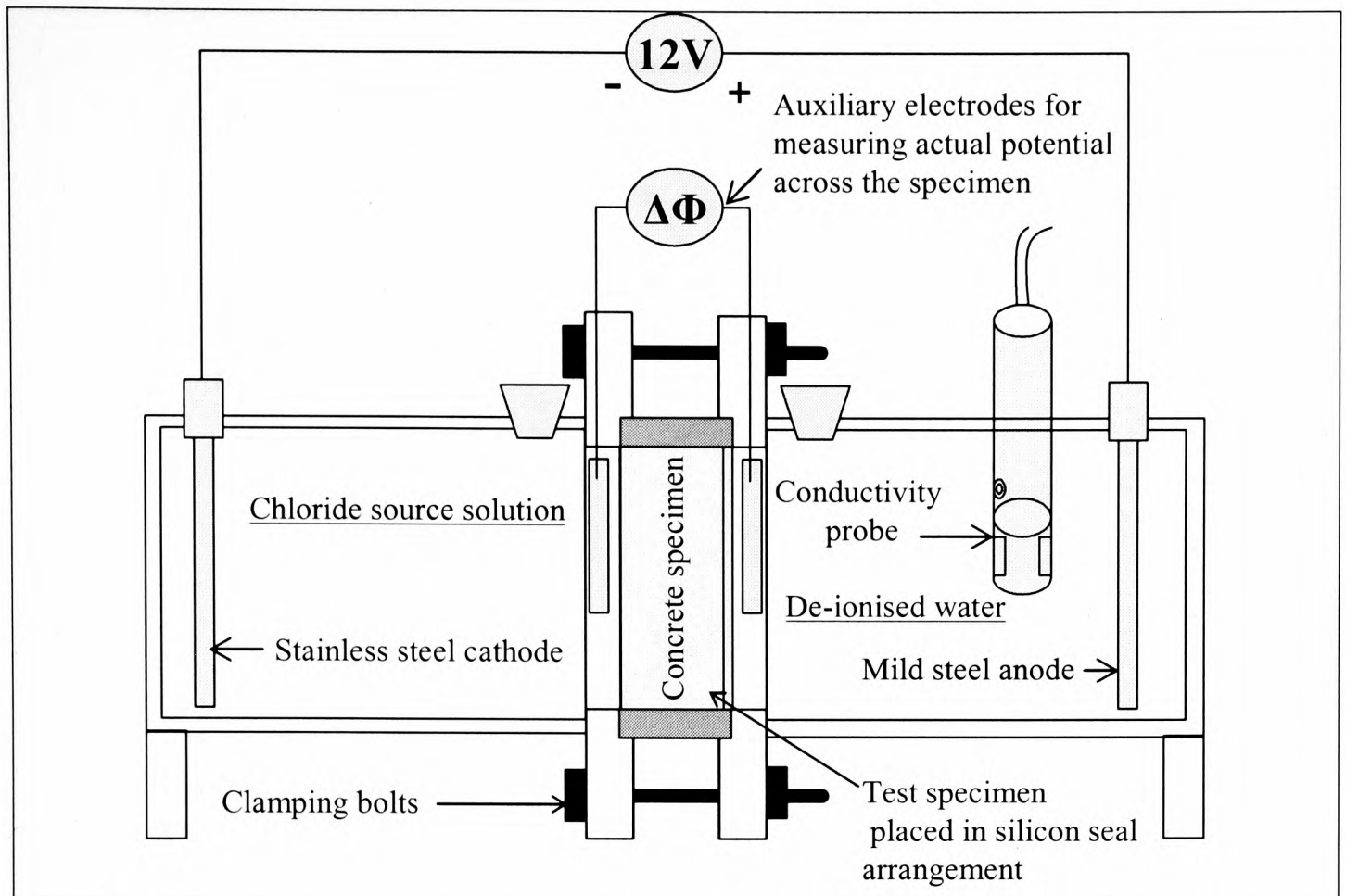

Figure 3.12 Modified steady state chloride migration test proposed by Castellote *et al.* (2006) (as included in Chlortest (2006))

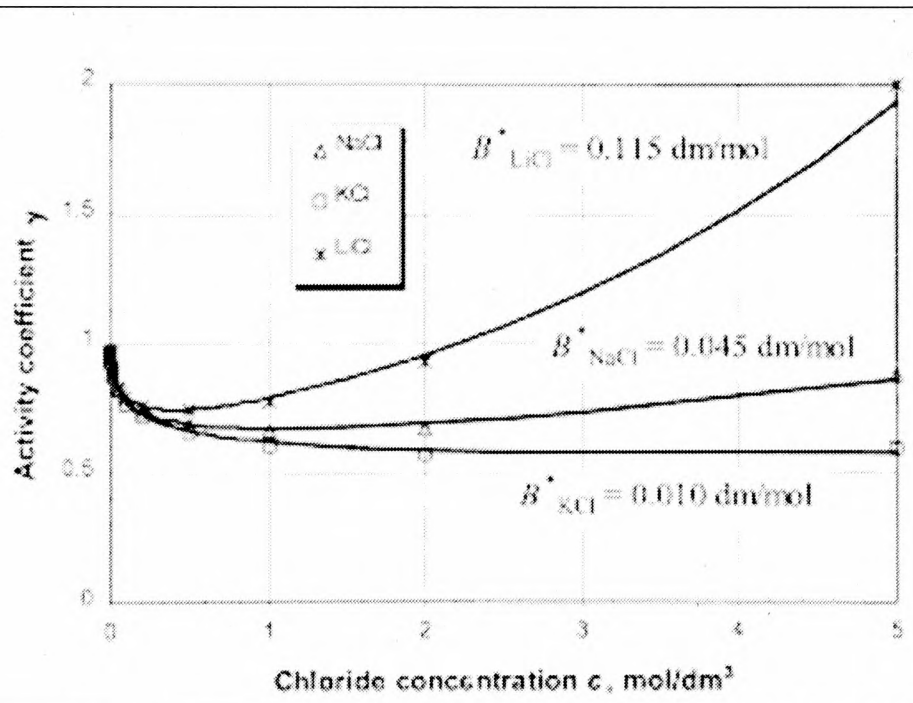

Figure 3.13 Relationship between the activity coefficient and the chloride concentration of catholyte (Tang, 1999b)

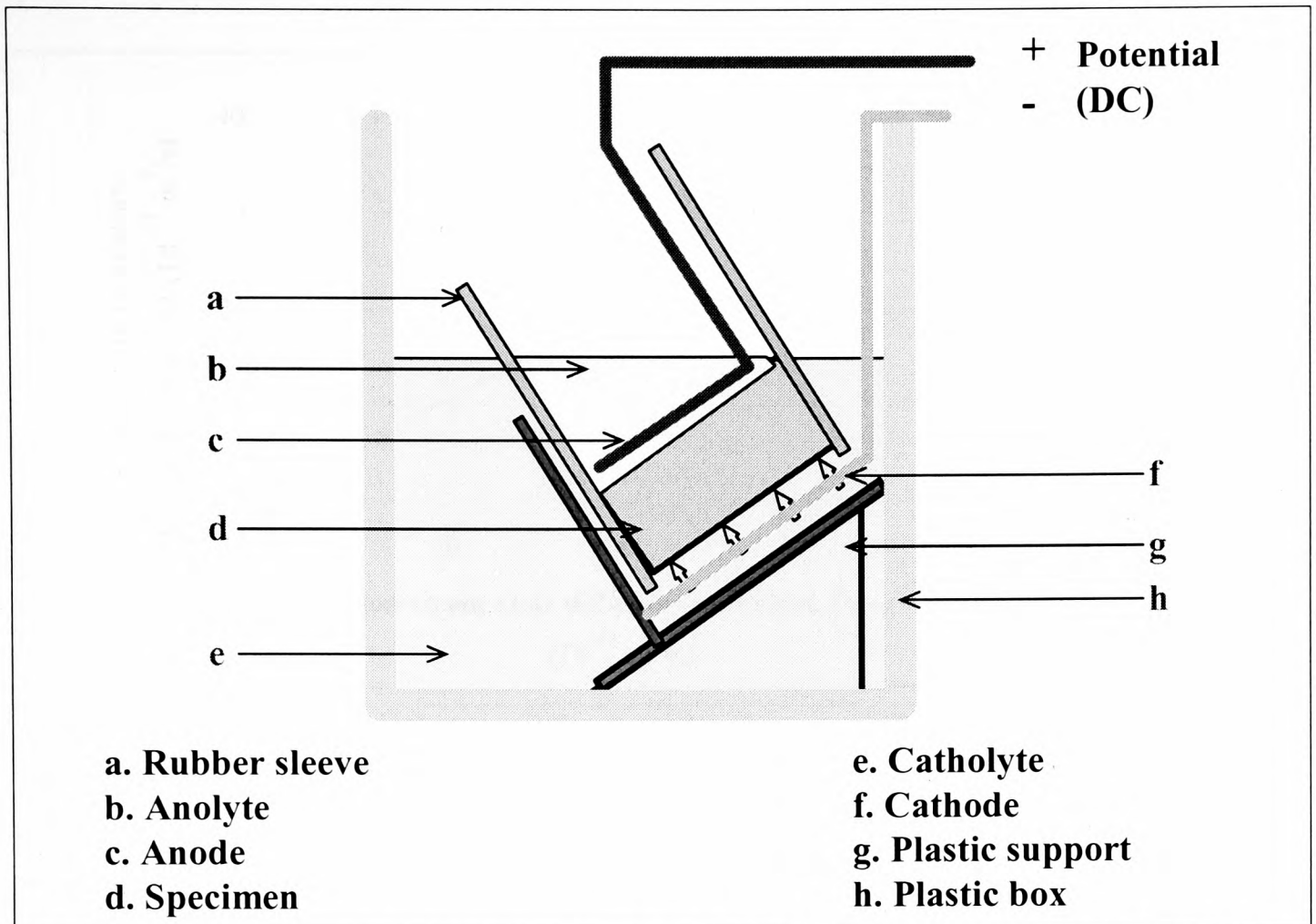

Figure 3.14 A typical test arrangement for the CTH test (Tang and Nilsson, 1992b)

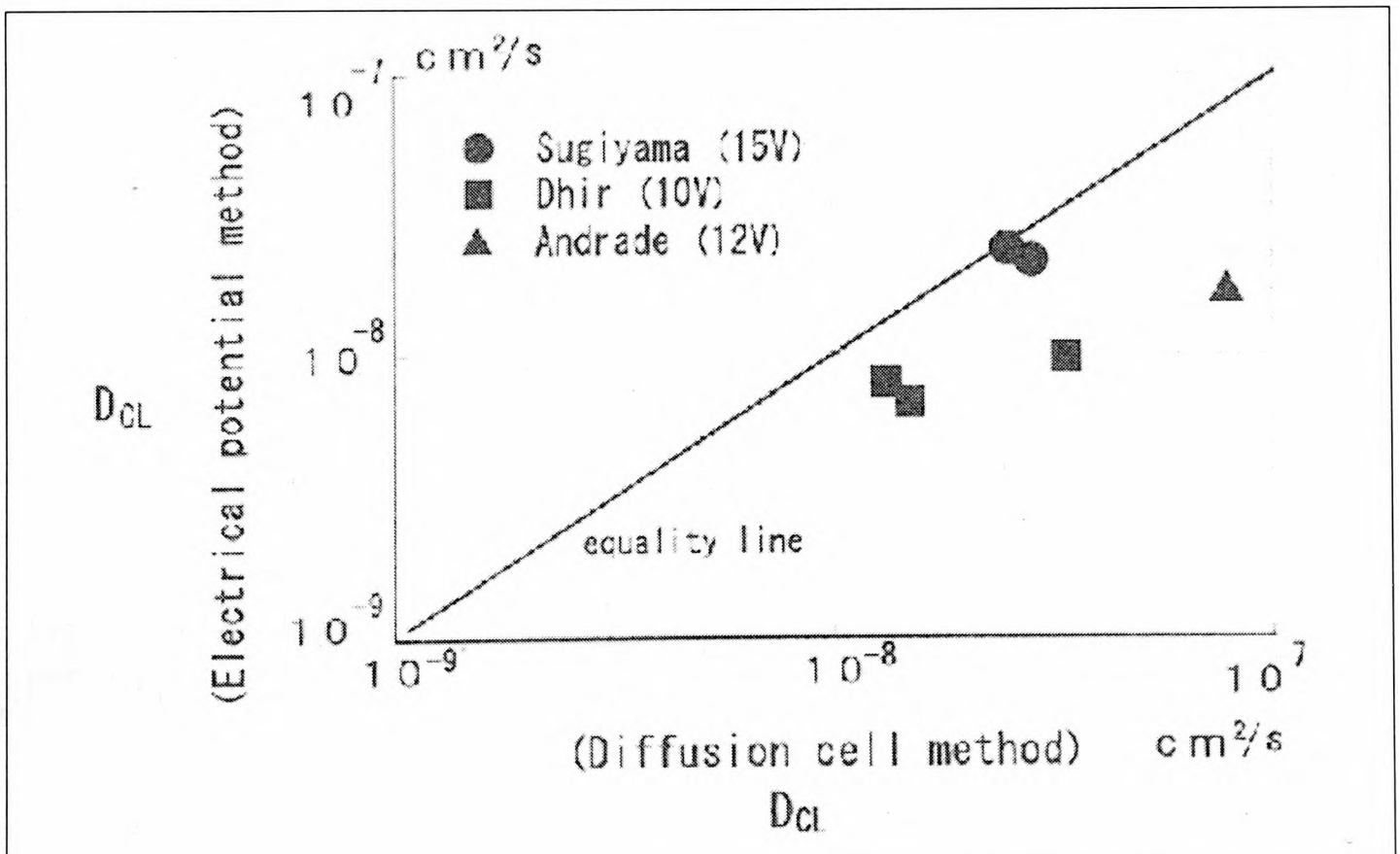

Figure 3.15 Comparison of the steady state migration coefficient and steady state diffusion coefficient (Andrews, 1999)

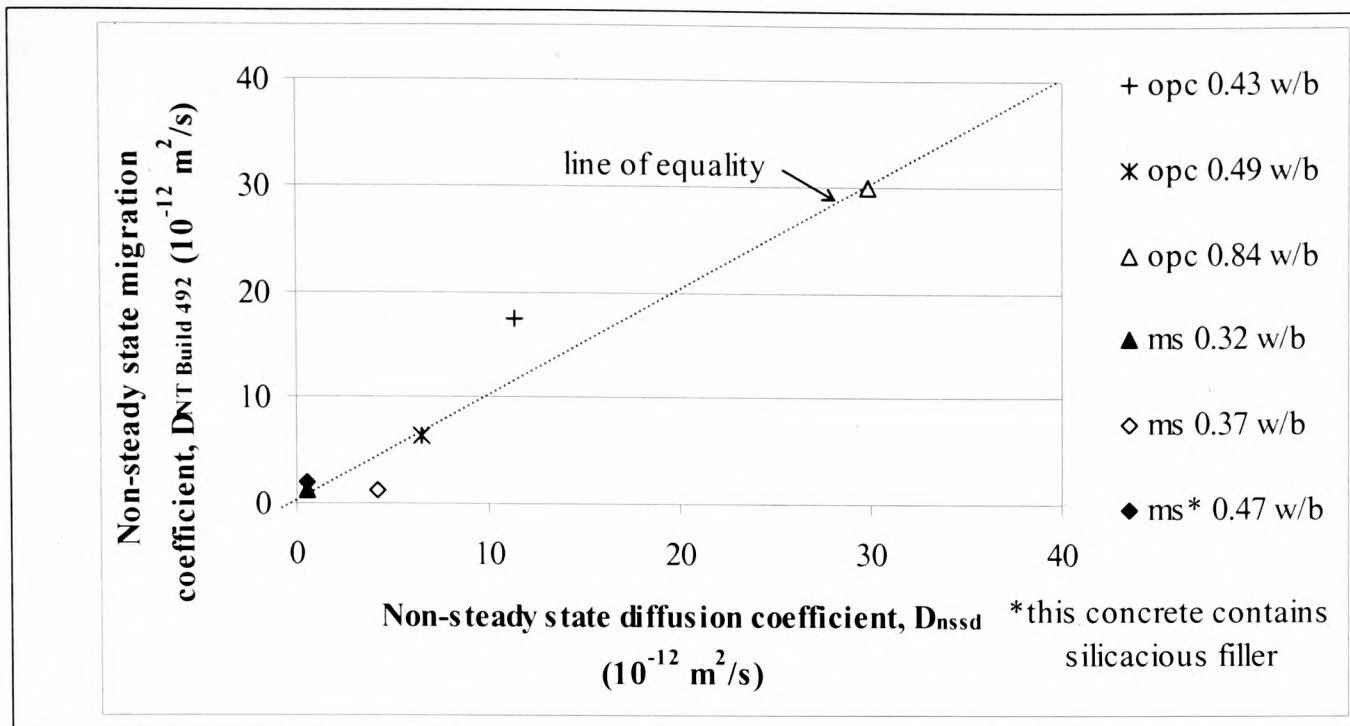

Figure 3.16 Relationship between the non-steady state diffusion coefficient and the non-steady state migration coefficient (NT BUILD 492) (Baroghel-Bouny *et al.*, 2002)

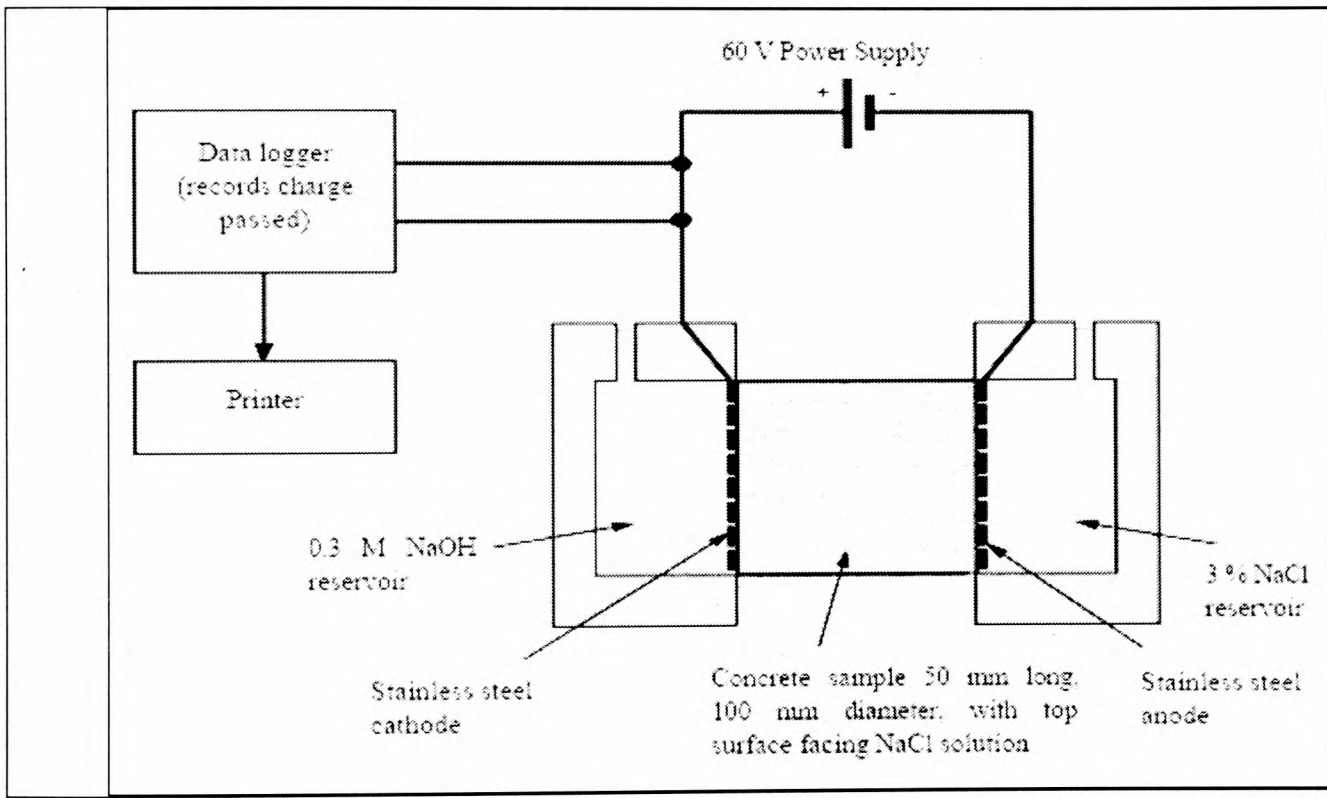

Figure 3.17 Schematic diagram showing the test arrangement for the rapid chloride permeability test (RCPT)(similar to Whiting (1981))

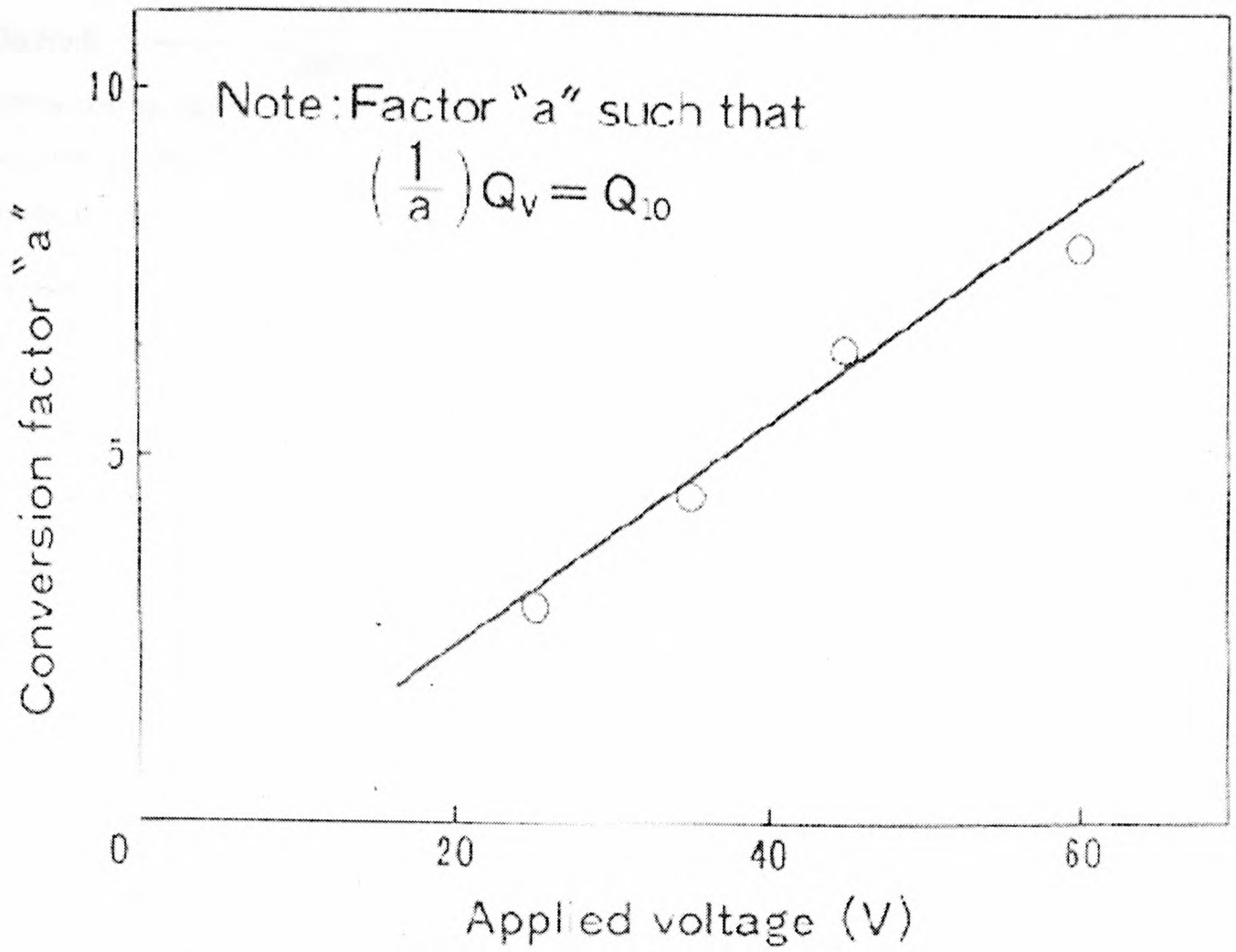

Note: This relationship is used to estimate the charge passed at a reference voltage (60V) using the charge passed at a lower test voltage (10V)

Figure 3.18 Relationship between the conversion factor and the applied voltage

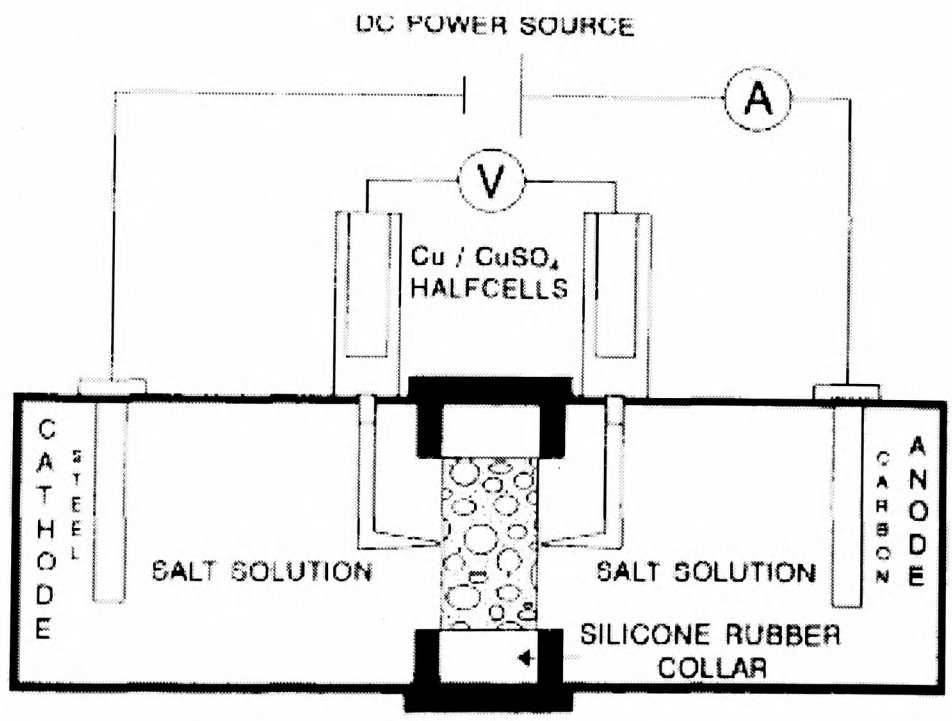

Figure 3.19 Schematic diagram showing the test arrangement for the chloride conduction test (Streicher and Alexander, 1995)

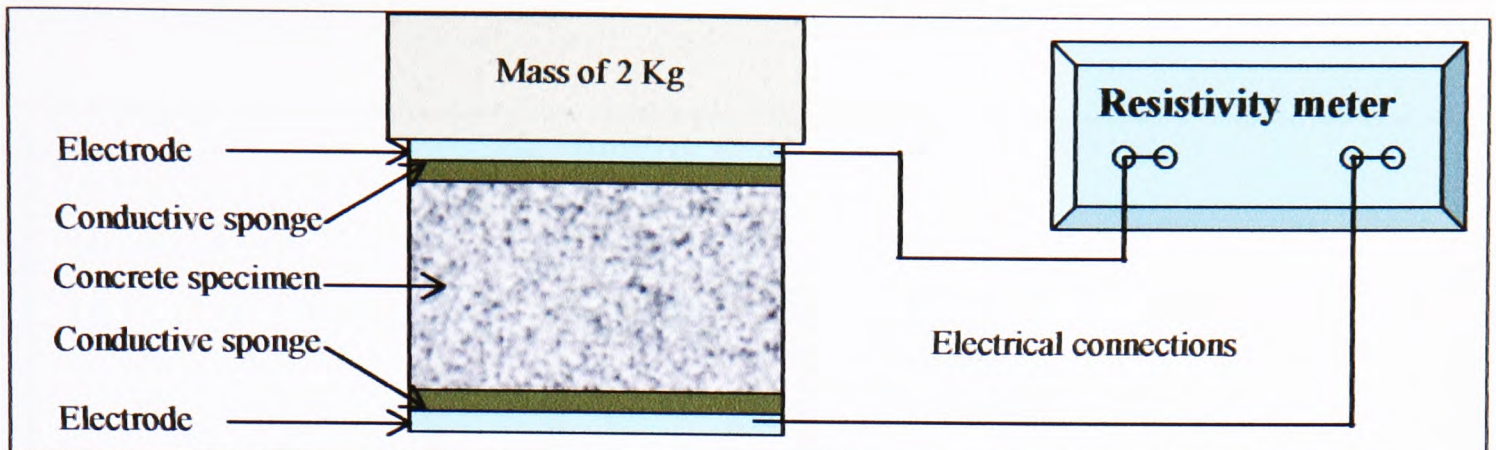

Figure 3.20 Schematic diagram showing the test arrangement for bulk resistivity test proposed by Andrade (2006) (as included in Chlortest (2006))

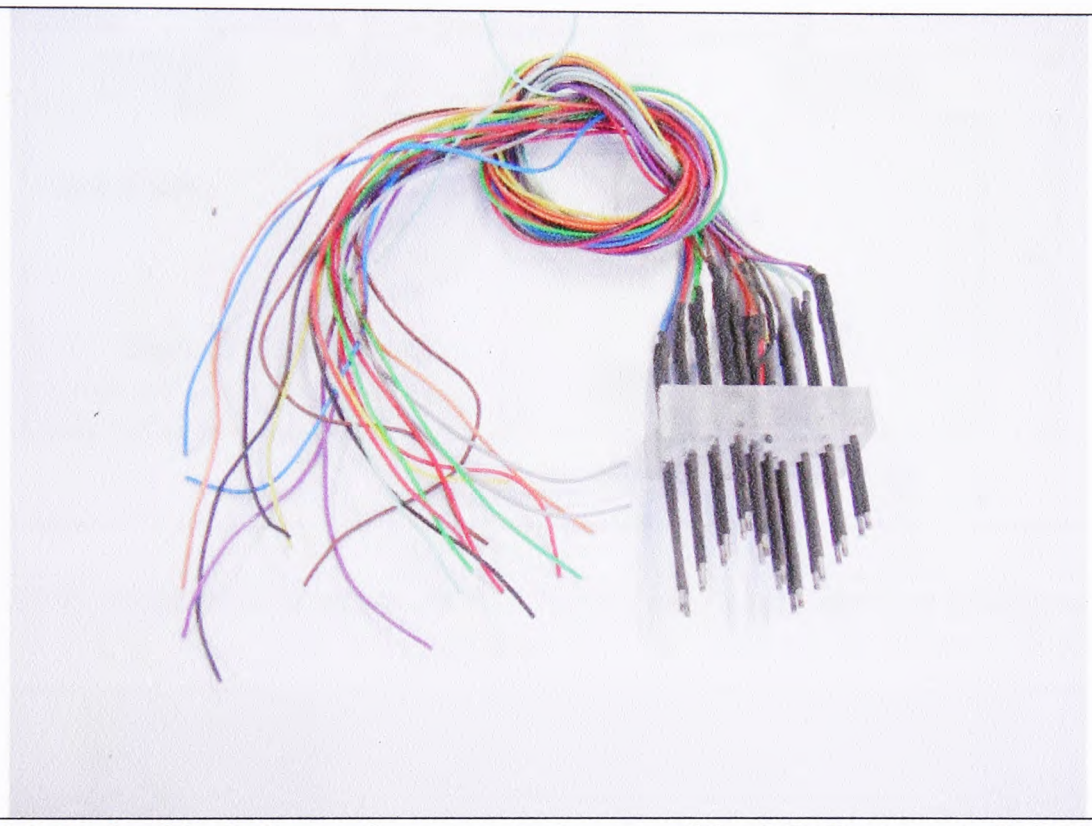

Figure 3.21 Embedded electrode array system used by McCarter *et al.* (1995)

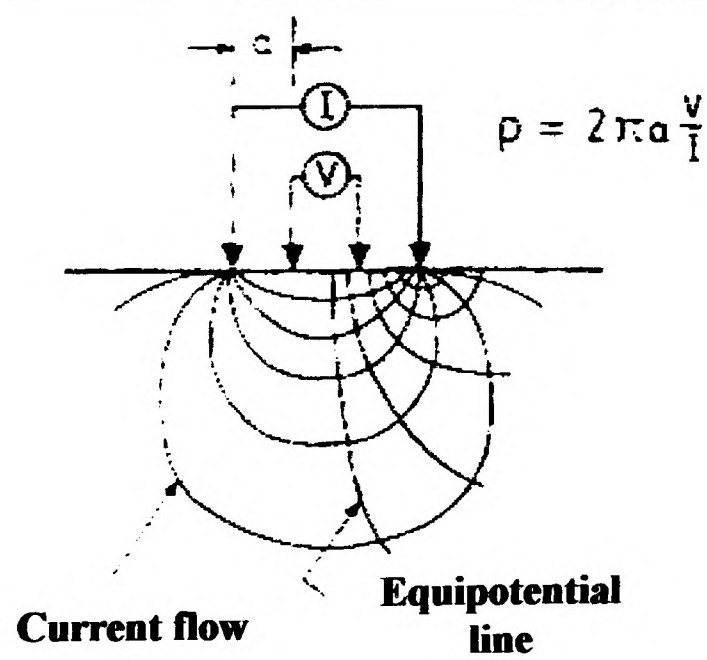

Figure 3.22 Schematic diagram of the Wenner probe resistivity test (Millard *et al.*, 1990)

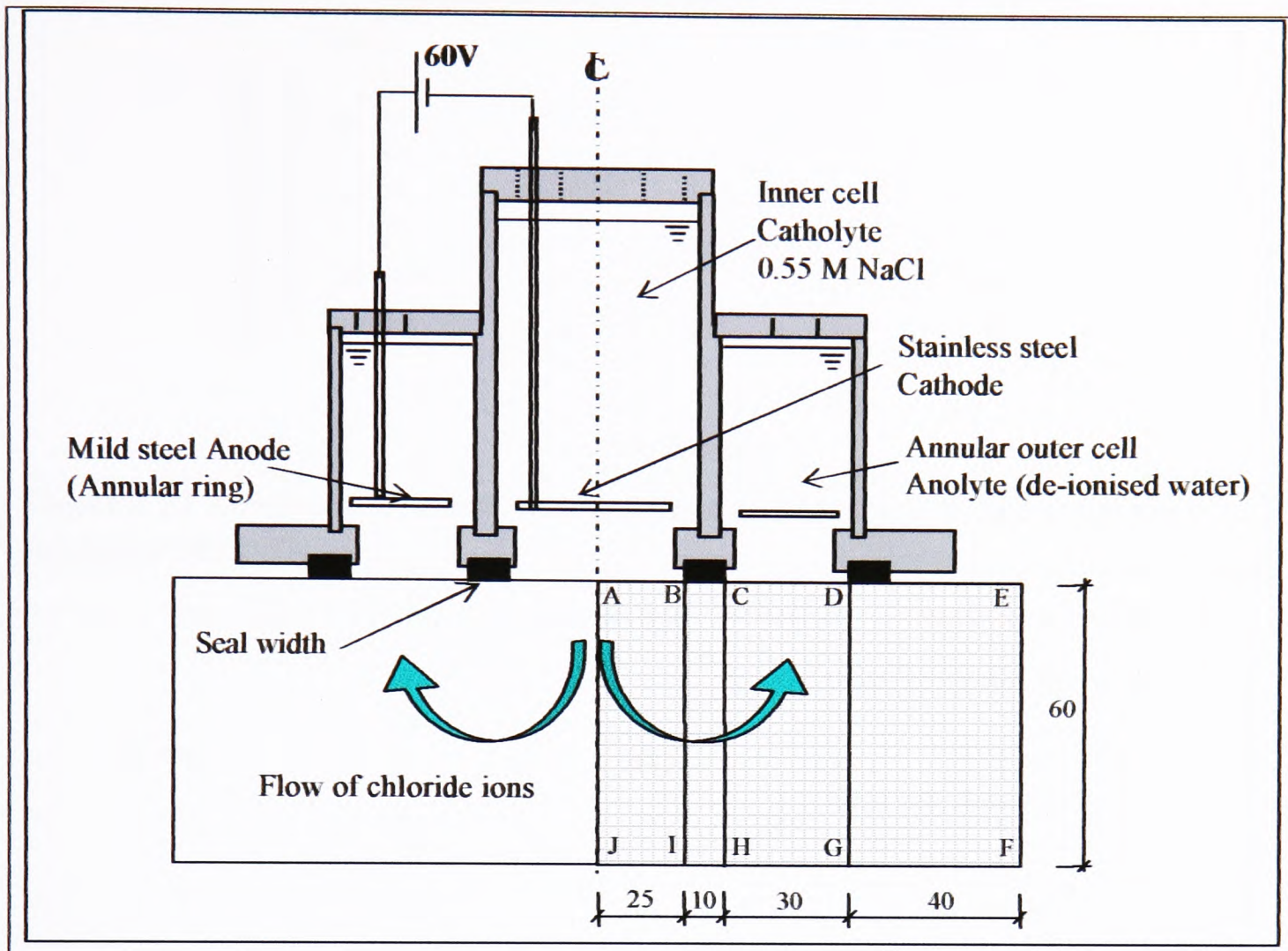

Figure 3.23 A schematic diagram of the Permit ion migration test (Andrews, 1999)

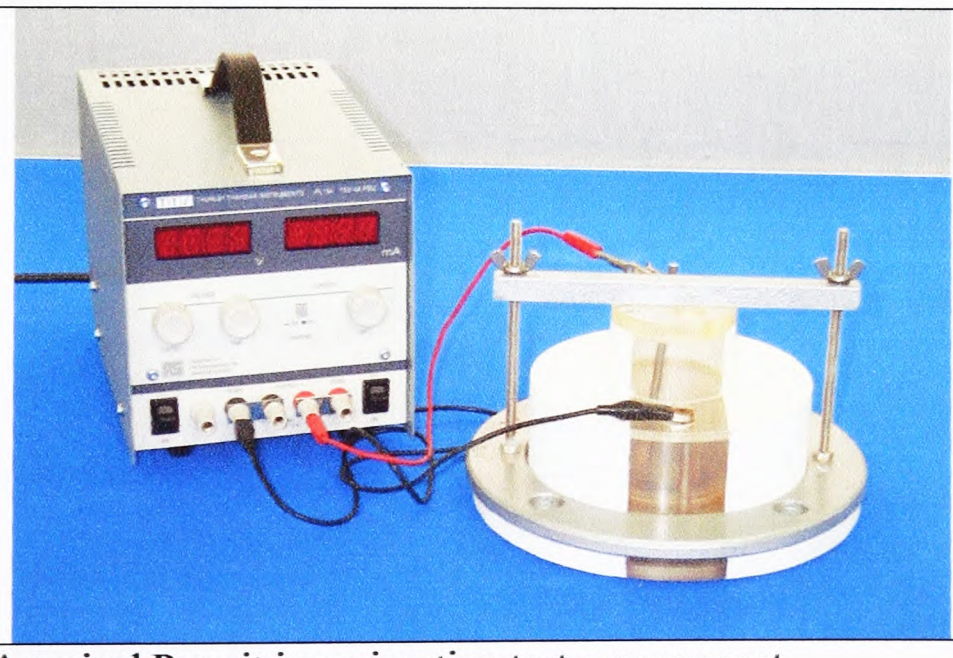

Figure 3.24 A typical Permit ion migration test arrangement

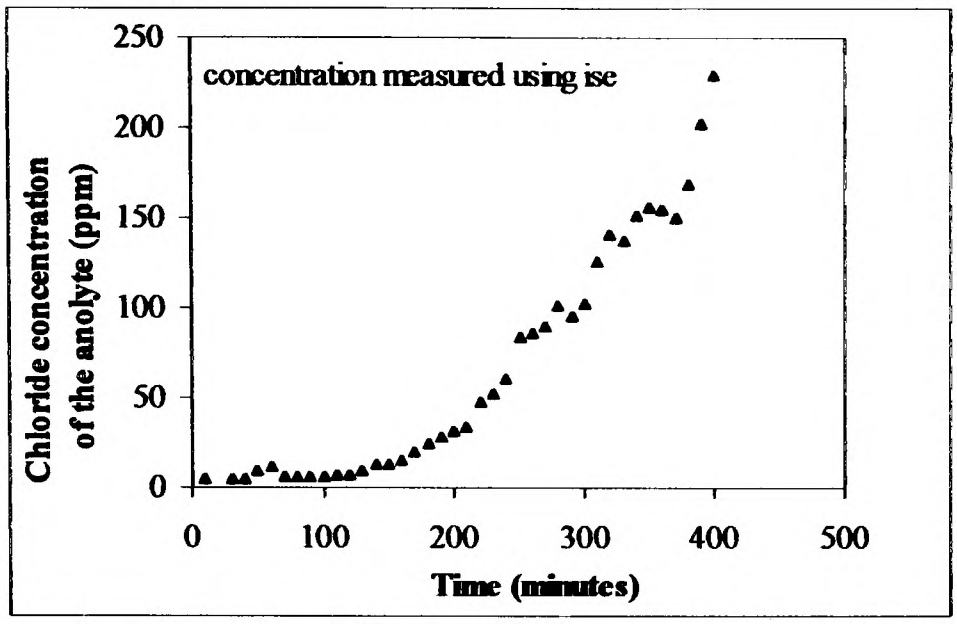

Figure 3.25 A typical concentration versus time plot obtained in the Permit ion migration test

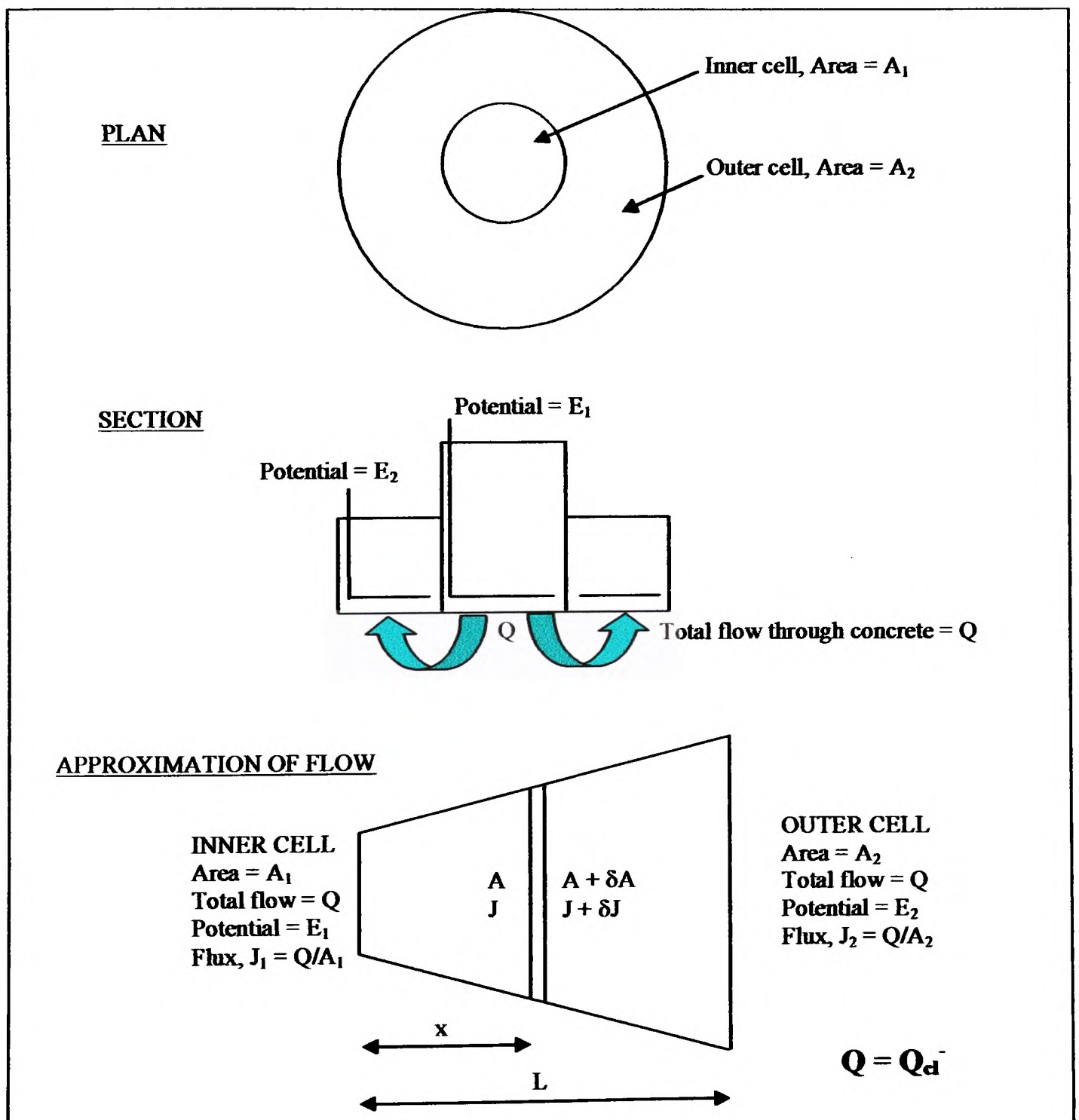

Figure 3.26 Approximation of flow of chloride ions through concrete in the Permit ion migration test (Andrews, 1999)

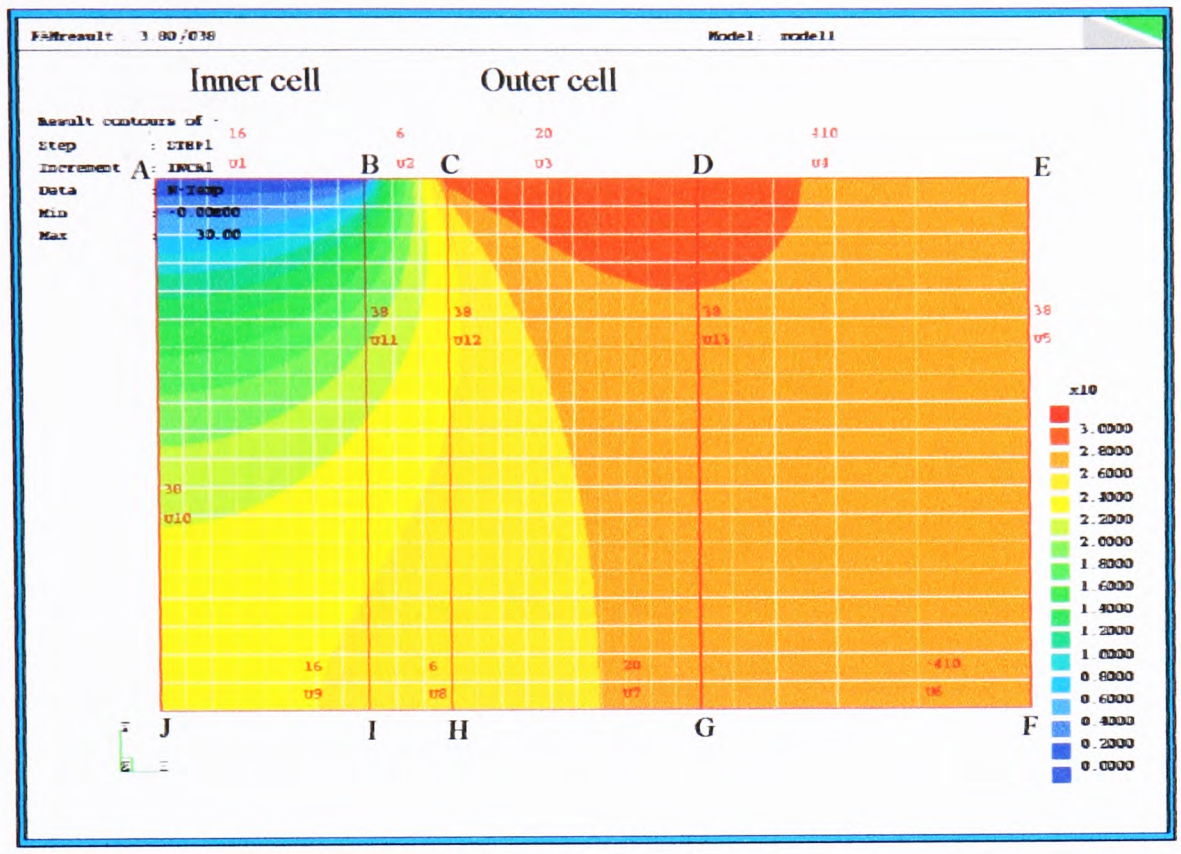

Figure 3.27 Contour plot of the variation of electrical potential through concrete in Permit ion migration test (Andrews, 1999) (refer Figure 3.23 for details of ABCDGHIJ)

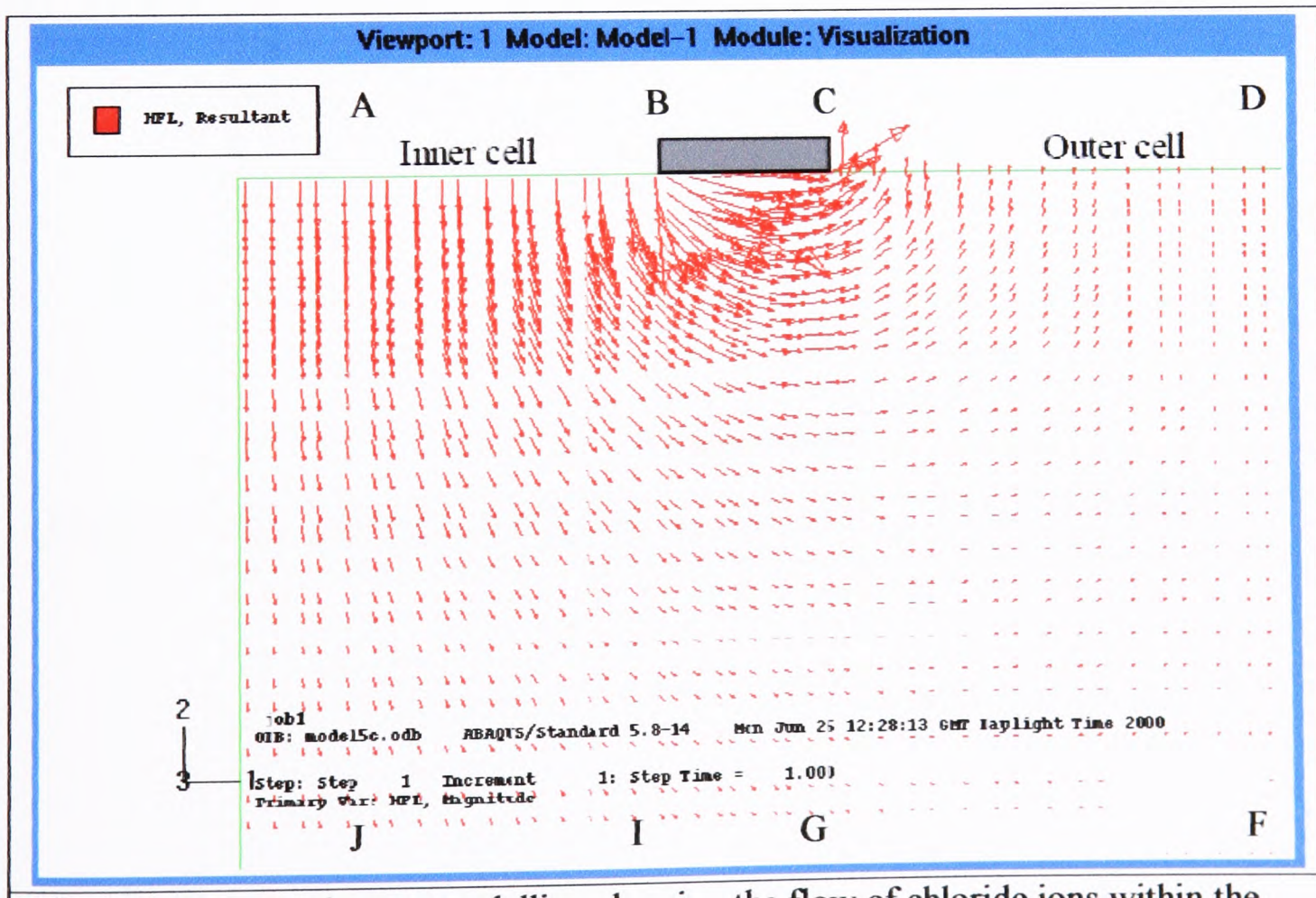

Figure 3.28 Finite element modelling showing the flow of chloride ions within the concrete specimen in the Permit ion migration test (Andrews, 1999) (refer Figure 3.23 for details of ABCDGHIJ)

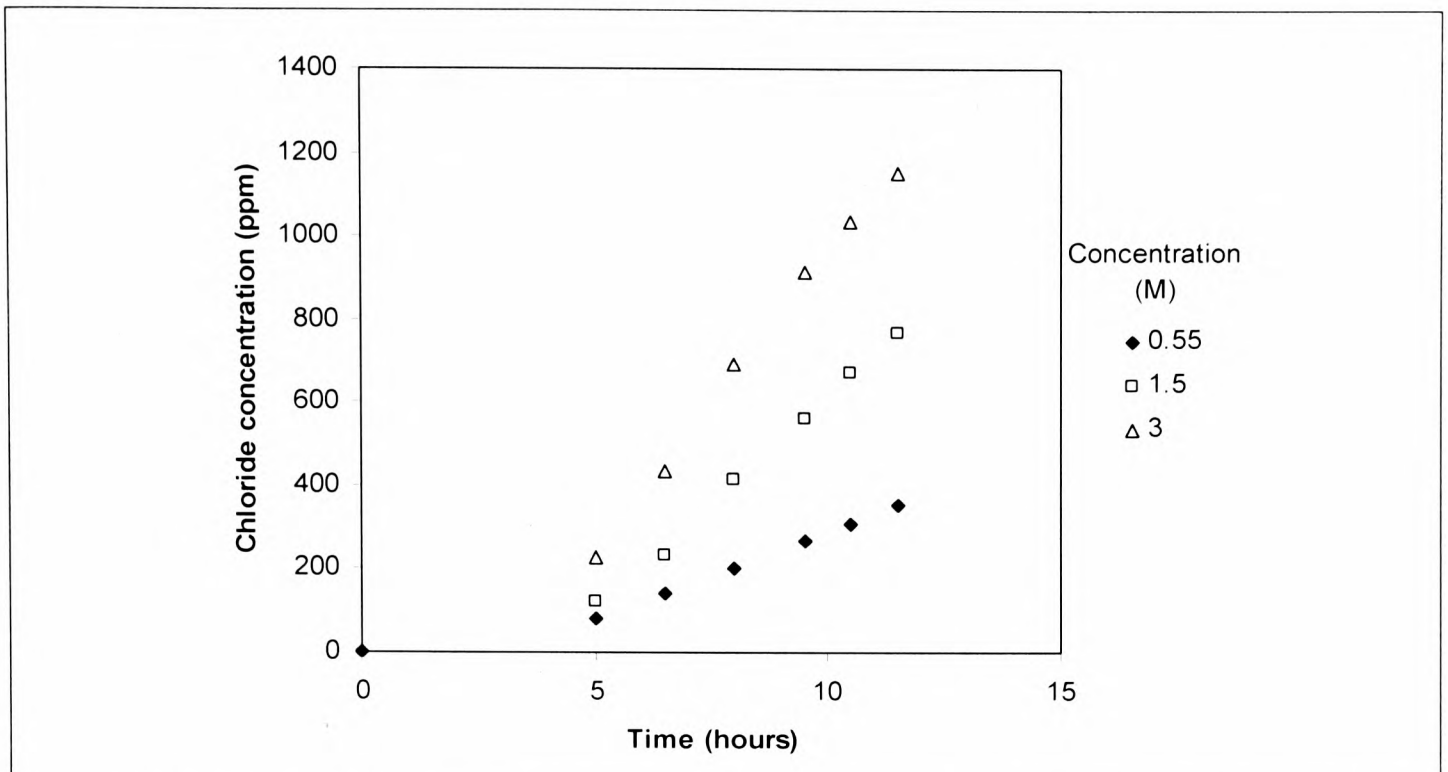

Figure 3.29 The effect of catholyte concentration on chloride ions arriving at the anolyte in the Permit ion migration test (Andrews, 1999)

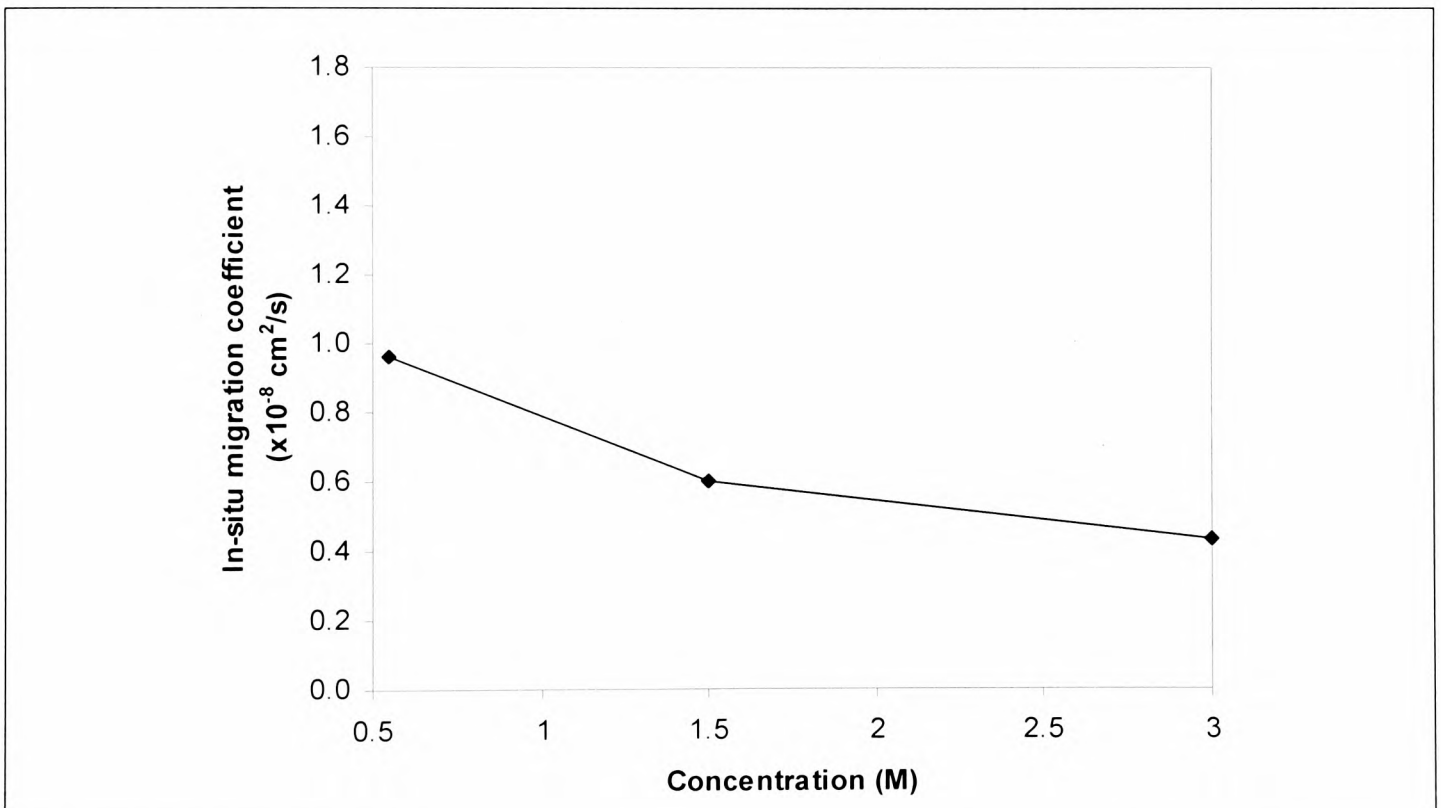

Figure 3.30 The effect of catholyte concentration on $D_{in\ situ}$ (Andrews, 1999)

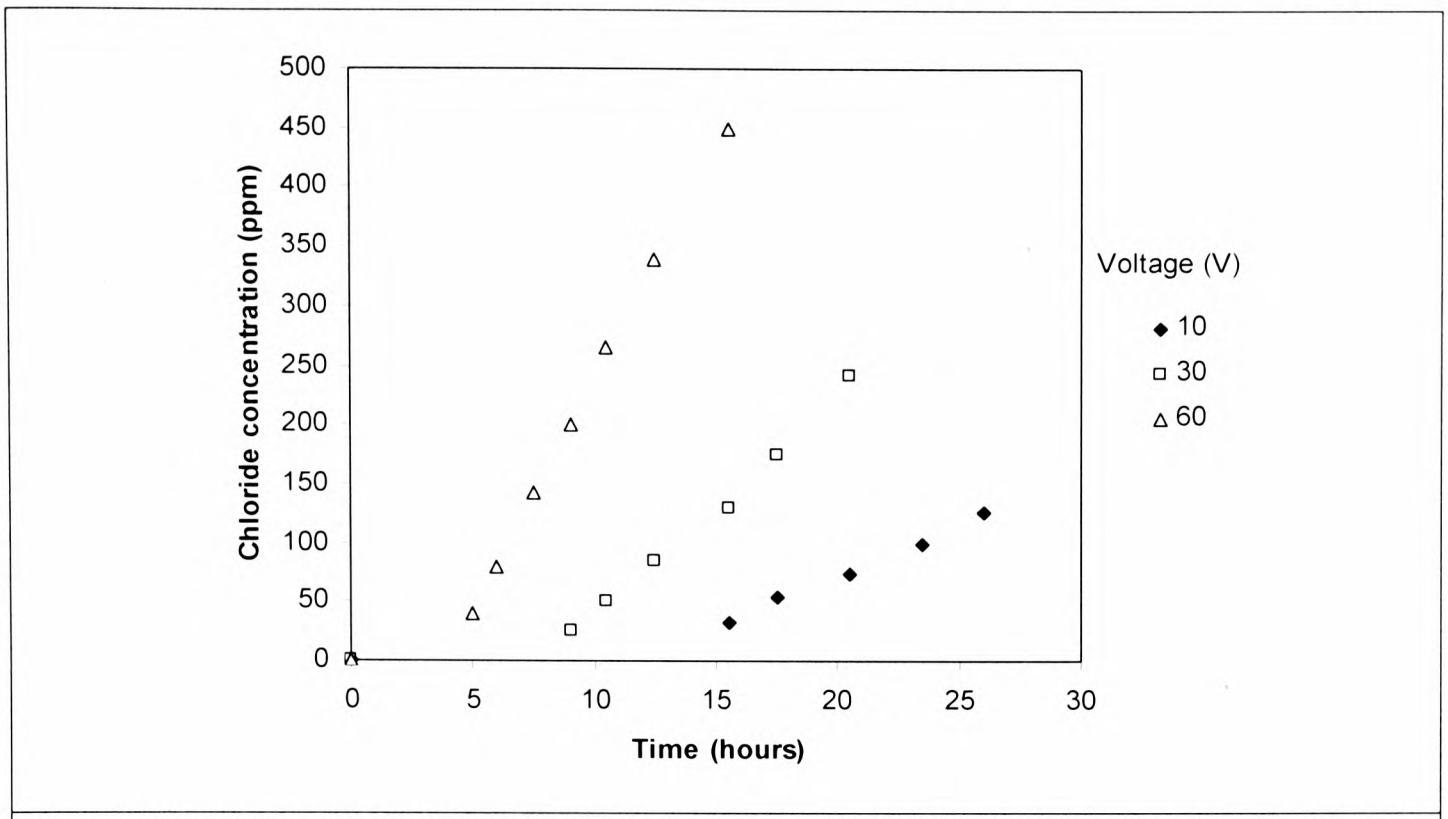

Figure 3.31 The effect of the applied voltage on the chloride ions arriving at the anolyte in the Permit ion migration test (Andrews, 1999)

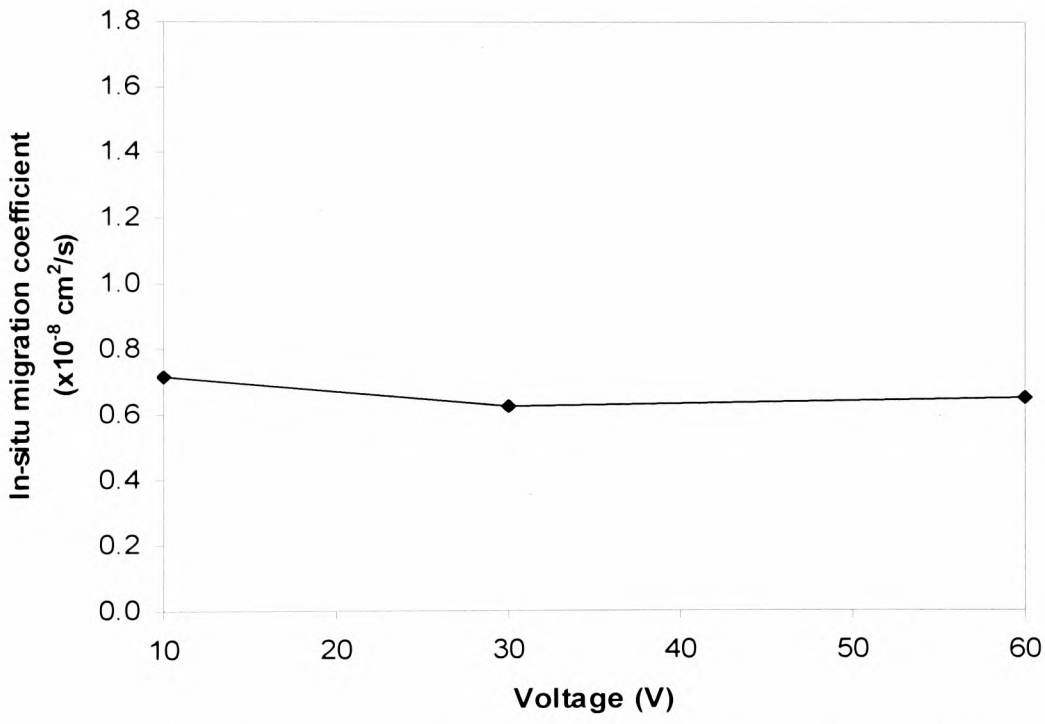

Figure 3.32 The effect of the applied voltage on $D_{in\ situ}$ (Andrews, 1999)

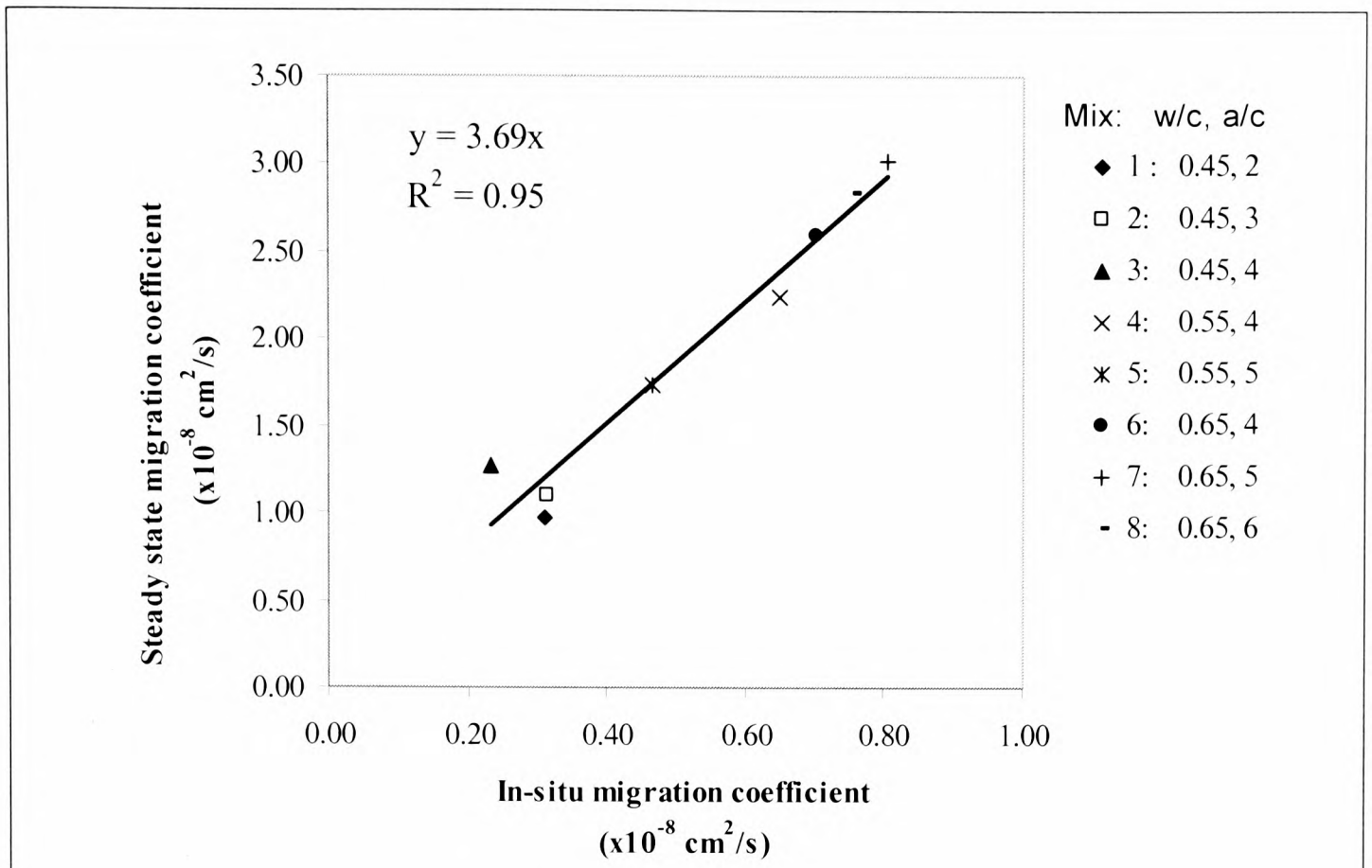

Figure 3.33 Relationship between D_{mig} (from a conventional steady state migration test) and $D_{in\ situ}$ (Andrews, 1999)

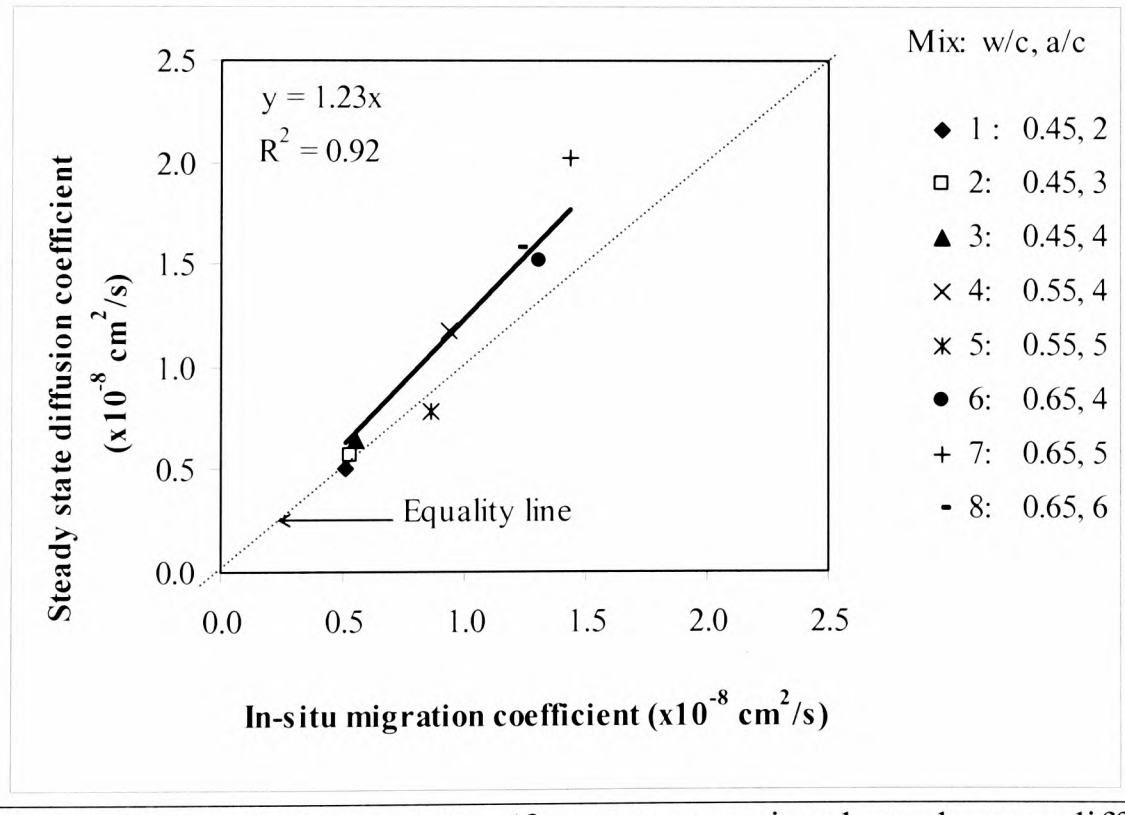

Figure 3.34 Relationship between D_e (from a conventional steady state diffusion test) and $D_{in\ situ}$ (Andrews, 1999)

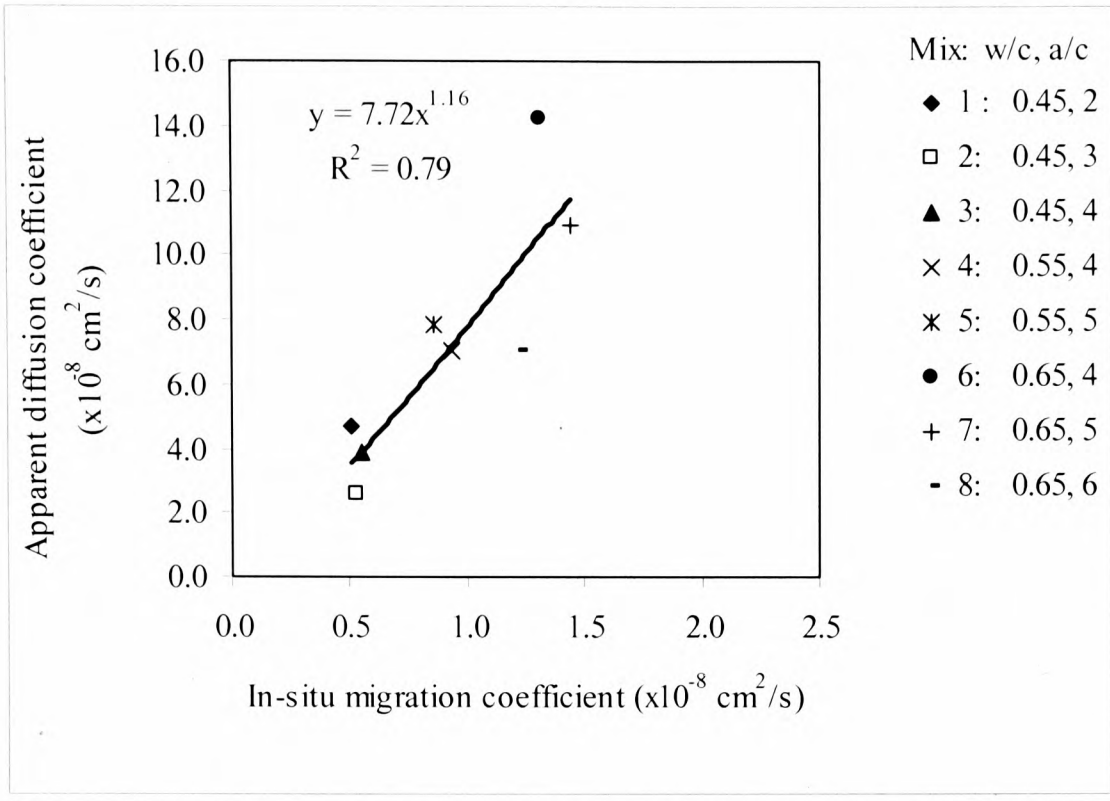

Figure 3.35 Relationship between D_{nssd} (from a conventional non-steady state diffusion test) and $D_{in\ situ}$ (Andrews, 1999).

Chapter 4

Experimental Programme

4.1 Introduction

This chapter describes the experimental programme used in achieving the objectives mentioned in Chapter 1. Details of the materials used, the methods adopted in preparing the test specimens and the different test procedure are discussed.

4.2 Programme of investigation

The experimental programme consisted of two main experiments: the experimental evaluation of chloride diffusivity test methods (Evaluation programme) and the experimental validation of the new test protocol for Permit ion migration test (Validation programme). The former was used to identify reliable laboratory based rapid (short-term) test methods for determining the chloride diffusivity of concrete. This was done in collaboration with a European Round Robin Test Programme, Chlortest, the details of which are given in section 4.3.1. This experimental programme (Evaluation programme) was also used in part to propose a new test protocol for the Permit. The findings from this experimental programme are presented and discussed in Chapter 5, while the results from the validation programme based on Permit are presented and discussed in Chapter 6.

A summary of the experimental programme is presented diagrammatically in Fig. 4.1.

4.3 European RRT Programme: Chlortest (Evaluation Programme)

4.3.1 Introduction and objectives

The European Round Robin Test Programme which was called 'Chlortest', studied the different aspects of the resistance of concrete to chloride ingress. Part of the objectives of this thesis, viz. *to identify reliable laboratory based test methods for assessing the chloride diffusivity of concrete*, was fulfilled by participating in the Chlortest RRT.

The following were the objectives of the Chlortest programme:

(i) To evaluate the performance of different laboratory based test methods and thereby to propose reliable test methods, with sound theoretical basis, technical feasibility and measurement precision.

(ii) To collect on site performance data of reinforced concrete structures in terms of chloride ingress and reinforcement corrosion.

(iii) To verify the performance of laboratory tests by comparing with the data collected on site performance, using different models, including scientific, empirical and probabilistic approaches.

(iv) To recommend the practical use of the laboratory performance tests and the interpretation of the test results.

The details of the test programme and the findings have been published in the final technical report of the Chlortest programme, Chlortest, (2006). For the evaluation of the performance of different laboratory based test methods, the following six methods were selected:

- Immersion tests
  1. pr EN 13396-1: 2002, Measurement of Chloride Ion Ingress by Diffusion of Repair Mortar (BS EN 13396, 2004)
  2. NT BUILD 443: 95, Concrete, Hardened: Accelerated Chloride Penetration (NT BUILD 443, 1995)

- Migration tests
  3. NT BUILD 492: 99, Concrete, Mortar and Cement Based Repair Materials: Chloride Migration Coefficient from Non-steady State Migration Experiments (NT BUILD 492, 1999)
  4. INSA Steady-state migration test (Truc *et al.*, 2000)
  5. IETcc Steady-state migration test (Castellote *et al.*, 2001)
- Indirect test
  6. Electrical resistivity (Andrade, 2006; Chlortest, 2006)

The evaluation was performed in two stages. Initially the performance of all the six test methods was compared, for which four concrete mixes were used. On the basis of the results of this investigation, significant shortcomings were identified for some methods and, hence, only four methods were selected for the second stage of the performance evaluation. Six mixes were used for this stage and the tests selected were 2, 3, 5 and 6 from the above list. A description of these four test methods are given in section 4.3.4. The results obtained from both stages for the four test methods are presented and discussed in Chapter 5. Due to the shortcomings as stated earlier, the results from stage 1 for the test methods 1 and 4 are not discussed. The details of the ten mixes are given next.

4.3.2 Materials used and mix details

The concrete mixes used in this evaluation study were manufactured in different countries across Europe. Ten concrete mixes were used in this evaluation (Table 4.1). These were cast with materials available locally to the respective countries. Therefore, it was possible to compare the performance of each test with a greater variety of concretes.

Four normal (ordinary) Portland cement (opc) concretes and six concretes with cement replacement materials such as pulverized fuel ash (pfa), microsilica (ms) and ground granulated blast-furnace slag (ggbs) were used. The details of the type of binder, the mix proportions, the type of superplasticiser and the w/b used in all mixes along with their country of origin are presented in Table 4.1. The concretes mainly differed by the water-binder ratio (w/b). The mixes are designated by the w/b and the

binder type; for example 0.45 ms is the concrete mix with microsilica partially replacing opc and it has a w/b of 0.45. The aggregate-binder ratio (a/b) used in most concretes was between 4 and 4.4, but for 0.45 pfa and 0.45 ggbs an a/b of 5.4 was used. Further details of the mixes can be obtained from Chlortest (Chlortest, 2006).

The cements used conformed to BS EN 197-1 (2000). The types of cement used are listed in Table 4.1. The percentage of supplementary cementitious materials present in each type of cement is given in Table 4.1. As the test specimens were manufactured by Readymix companies from four different countries, further details of the mixes, such as properties of aggregates, procedure used for casting the concrete, curing etc. were not supplied to the research consortium. Efforts to obtain these details were in vain and, hence, these details could not be included in this thesis.

4.3.3 Description of test specimens (casting and curing)

All the concrete specimens were cast in the form of slabs by the Readymix suppliers. The 0.35 opc, 0.42 opc, 0.50 opc, 0.40 ms, 0.42 ms, 0.42 ggbs and 0.45 ggbs mixes were cast as slabs of size 1200×800×200mm and cured by placing the slabs (with the mould) under moist condition for four weeks. The slabs were stored for another 5 months, during which there was no control of the storage condition. After this concrete cores of 100mm diameter were cut. This method of casting slabs and then cutting cores, instead of casting the concrete in a cylindrical mould was considered to give a more representative specimen of the bulk concrete, by preventing the preferential orientation of the aggregate close to the mould surfaces. The cores were wrapped in wet paper and transported to each participating laboratory in sealed plastic bags.

The exact detail of casting or curing of the 0.45 opc, 0.42 pfa and 0.45 pfa mixes were not available. However, casting slabs and then extracting cores were considered to be a standard practice by all the participating countries. Therefore, all the concrete cores received at Queen's University Belfast were extracted from slabs.

The concrete specimens required for each type of tests were sliced from the concrete cores, as illustrated in Fig. 4.2. The test protocols for the different tests carried out in the Evaluation Programme are discussed below.

4.3.4 Test methods

4.3.4.1 Non-steady state diffusion test

The non-steady state diffusion test was carried out according to NT BUILD 443 (1995) Using this test protocol, which is described in the following sub-sections, a non-steady state diffusion coefficient and the surface chloride concentration were obtained. In addition, a 'penetration parameter' was also obtained based on the non-steady state diffusion coefficient.

Preparation of test specimens

As shown in Fig. 4.2, the specimen used in this test was a concrete disc of 100mm diameter and 60mm length, which was obtained from the bottom of the concrete core described in section 4.3.3. Three such replicate specimens were used for this test. The test specimens were immersed in saturated $Ca(OH)_2$ solution in a covered desiccator. The desiccator was stored in a room maintained at 23°C (±1°C) and it was filled with the solution up to the top to eliminate the possibility of the specimens getting carbonated. After 24 hours of immersion, the specimens were taken out from the desiccator and allowed the surface to dry out by exposing them in the lab at 23°C (±1°C). The specimens were weighed and returned to the desiccator. The mass of specimen was determined again after 24 hours of immersion in a similar manner. The specimens were left in the $Ca(OH)_2$ solution until the change in mass of the surface dry specimen was less than 0.1 percentage between two consecutive days. Once the mass was constant, all the faces except the test face (i.e. the saw cut face, see Fig. 4.2) of the surface-dried specimens were coated with an epoxy emulsion twice, with the second coat applied when the first coat was dry. When the epoxy coating was hardened, the specimens were returned to the desiccator and immersed in the $Ca(OH)_2$ solution until the mass stabilised.

Test set-up

A schematic diagram and the photograph of the test arrangement are presented in Figs. 4.4 and 4.5 respectively. The liquid in the tank was 2.8M chloride solution (165g/litre NaCl) as per the protocol for the NT BUILD 443 (1995). The test specimen saturated by $Ca(OH)_2$ as described in the previous section was introduced in the solution in surface-dry condition. The test arrangement was kept in a room maintained at temperature 23°C (±1°C) for a period of 35 days. The solution was stirred occasionally to prevent the formation of salt scales at the top surface of the solution. The container was closed tightly to prevent any evaporation of water during the immersion of the test specimens in salt solution and thereby to ensure a constant concentration of the salt solution throughout the test duration.

Profile grinding and the chloride analysis

After 35 days of exposure, the test specimens were taken out of the exposure liquid and the chloride profiles were determined. For this, concrete dust samples were collected from different depths from the exposure face by grinding using a commercially available profile grinder, Germann Instruments (see Fig. 4.6), and analysed for the chloride content as described below.

Profile grinding

The profile grinding consisted of milling concrete dust in layers parallel to the exposed surface. The grinding was performed within a 75mm diameter circular area located centrally within the 100mm diameter cylindrical specimen, thereby avoiding the risk of edge effects and disturbances from the coating.

At least ten layers were ground from each specimen. The thickness of the layer was adjusted according to the expected chloride profile so that a minimum of 6 points in the chloride profile (chloride content versus depth graph) lie between the exposed surface and the depth with a chloride content of at least C_i+ 0.03 mass percentage of the material, where Ci is the chloride content of the reference specimen (see Fig. 4.2) in mass percentage of the material. The recommended profiling depth intervals for opc concrete with different w/b according to NT BUILD 443 (1995) are presented in Table 4.7. For concretes with cement replacement materials the depth interval was taken from Table 4.7, but the value used for each w/b was that for the opc concrete

with the nearest lower w/b. For example, the recommended profiling depth for opc concrete with w/b 0.40 w/b is up to 20mm. So for pfa concrete with w/b 0.40 the profile depth is that of opc concrete with w/b 0.35, i.e., up to 16mm and, hence the depth intervals for this case could be used for 0.40 w/b pfa concrete with w/b 0.40.

A minimum of 5g of dry concrete was ground from each layer. The depth below the exposed surface was measured using a Vernier callipers at four random locations and an average was calculated. This depth was used to plot the chloride profiles. In all cases, the outermost 1mm layer was ground off from the exposed face and this layer was excluded from plotting the chloride profile.

Chloride analysis

Principle of the analysis: The chloride content of the concrete dust collected from various depths was measured using Volhard's back titration method (NT BUILD 208, 1996). This method was recommended by the RILEM Technical Committee TC 178-TMC, with minor amendments. The procedure detailed below is based on the recommendation of the RILEM TC 178-TMC.

In this method a back titration with ammonium thiocyanate is used to determine the concentration of chloride ions in the solution. Firstly, the concrete dust samples were digested with concentrated nitric acid and heated to extract the chloride ions. Then excess silver nitrate (when compared to the expected chloride content of the sample) was added so that all chloride ions present in the solution would react to give silver chloride.

$$Ag^{+}_{(aq)} + Cl^{-}_{(aq)} \rightarrow AgCl_{(s)} \qquad \text{(Eq. 4.1)}$$

The indicator ammonium iron (III) sulphate was then added and the solution was titrated with ammonium thiocyanate solution. The titrate remained pale yellow as the unreacted silver ions react with the thiocyanate ions to form silver thiocyanate precipitate.

$$Ag^{+}_{(aq)} + SCN^{-}_{(aq)} \rightarrow AgSCN_{(s)} \qquad \text{(Eq. 4.2)}$$

When all the silver ions had reacted as in Eq. 4.2, the slightest excess of thiocyanate would result in its reaction reacts with Fe^{3+} to form ferrous thiocyanate, which is a

dark red compound and the change of the colour of the solution from pale yellow to dark red brown is the end point.

$$Fe^{3+}{}_{(aq)} + SCN^{-}{}_{(aq)} \rightarrow \left[FeSCN\right]^{2+}{}_{(aq)} \qquad \text{(Eq. 4.3)}$$

The titration was first run with no concrete sample to find the end point, i.e., the amount of thiocyanate required to balance the silver nitrate solution. Then the test was run with concrete sample with chlorides. The difference in volume of thiocyanate consumed to produce the colour change was used in calculating the amount of chlorides present in the concrete dust.

The procedure used for the acid extraction and the subsequent analysis:

1. 1 gram of the dust sample was weighed in a 250 ml glass beaker.
2. 50 ml of concentrated nitric acid (obtained by mixing 1 portion of nitric acid (60% by weight; specific gravity 1370 kg/m^3) with 2 portions of de-ionised water, i.e. 1+2) was added and the glass beaker was covered with watch glass till the effervescence ceased.
3. The suspension was boiled for a minute using a hot plate while agitating the suspension continuously using a magnetic stirrer.
4. 5 ml of 0.05M silver nitrate was added carefully by means of a pipette and the suspension was boiled again for another minute.
5. The suspension was filtered through a filter paper, previously washed with dilute nitric acid solution, receiving the filtrate in a 500 ml filtration flask.
6. The final volume of the filtrate was made up to 200 ml by washing the glass beaker, the agitator and the filter paper with dilute nitric acid (obtained by mixing 1 portion of nitric acid (60% by weight; specific gravity 1370 kg/m^3) with 100 portions of de-ionised water, i.e. 1+100).
7. The filtrate was allowed to cool to room temperature 23°C (± 2°C).
8. 20 drops of the indicator solution (ammonium iron (III) sulphate) were added.
9. The filtrate was titrated against 0.05M Ammonium thiocyanate from the burette while the solution was stirred vigorously using a magnetic stirrer. The titration was stopped when a drop of thiocyanate solution produced a slight red colour, which did not disappear with agitation. The volume of thiocyanate required was accurately measured, i.e., V_1.

10. A blank test, with no concrete dust, was run using the procedure as described above and the volume of thiocyanate spent was found, i.e., V_2.

The chloride content of concrete as percentage chlorides relative to the mass of concrete (mass %) was calculated using the following equation (NT BUILD 208, 1996):

$$\%Cl = \frac{3.5453\left(V_{Ag} M_{Ag} (V_2 - V_1)\right)}{m V_2} \qquad \text{(Eq. 4.4)}$$

where,

V_{Ag} is the volume of silver nitrate added, ml,

M_{Ag} is the molarity of the silver nitrate solution, moles,

V_1 is the volume of ammonium thiocyanate used for testing dust sample, ml,

V_2 is the volume of ammonium thiocyanate used for the blank test, ml,

m is the mass of the dust sample (1 grams).

Chloride profiles and diffusion parameters

The chloride content obtained for each layer was plotted against the corresponding depth to obtain the chloride profiles for each case, as shown in Fig. 4.7.

The values of the diffusion parameters D_{nssd}, C_s and K_{cr} , were determined by fitting Eq. 4.5 to the measured chloride profile by means of a non-linear regression analysis in accordance with the method of least squares. According to NT BUILD 443 (1995), the chloride content $C_{(x,t)}$ is given by the following equation.

$$C_{(x,t)} = C_s - (C_s - C_i) erf\left(\frac{x}{\sqrt{4 D_{nssd} t}}\right) \qquad \text{(Eq. 4.5)}$$

where,

$C_{(x,t)}$ is the chloride content, mass % by that of concrete, i.e., the chloride concentration of the concrete at depth, x (m), from the exposed surface, at the exposure time, t (s);

C_i is the initial chloride concentration of the concrete, mass % by that of concrete, (measured from the reference sample (see Fig. 4.2), non chloride contaminated specimen kept in an ideal sealed condition);

C_s is the chloride concentration of the concrete surface, mass % by that of concrete;

D_{nssd} is the non-steady state diffusion coefficient, m^2/s, erf is the error function as defined in Eq. 4.6, (NT BUILD 443, 1995).

$$erf\ Z = \frac{2}{\sqrt{\pi}} \int_0^z \exp(-u^2)du \qquad \text{(Eq. 4.6)}$$

The solver function in Excel Spreadsheet Application (Microsoft office XP 2002) was used for the non-linear curve fitting.

The penetration parameter, K_{cr} ($m/\sqrt{s}$), was calculated using the values of C_i, C_s, D_{nssd} and C_r (reference chloride concentration taken as 0.05 mass % by that of concrete) in Eq. 4.7 (NT BUILD 443, 1995).

$$K_{cr} = 2\sqrt{D_{nssd}}\, erf^{-1}\left(\frac{C_s - C_r}{C_s - C_i}\right) \qquad \text{(Eq. 4.7)}$$

The parameters, D_{nssd}, C_s and K_{cr} were obtained for all the mixes, which are discussed in Chapter 5.

4.3.4.2 Non-steady state migration test

The non-steady state migration test was carried out according to NT BUILD 492 (1999) to determine the non-steady state migration coefficient D_{nssm}. A two cell arrangement was used similar to that used by Andrade and Sanjuan (1994). The schematic diagram and photograph of the arrangement are shown in Figs. 4.8 and 4.9 respectively.

Preparation of test specimens

The test specimen for the non-steady state migration test was a concrete disc of 100mm diameter and 50mm thickness, as shown in Fig. 4.2. This was obtained by slicing the concrete core as described in section 4.3.3. The location of test specimen and the test face are also shown in Fig. 4.2. Three such replicate specimens were used in this test. The exact thickness of the specimens was measured using the Vernier callipers.

The concrete disc specimens were vacuum saturated prior to the test. The following procedure was used for attaining the vacuum saturation:

1. The surface dry disc specimens was kept in a desiccator such that their two parallel faces (saw cut faces) were exposed, i.e. they sat on their curved face.
2. The pressure inside the desiccator was reduced to 40mm of Hg. The vacuum was maintained for a period of 3 hours.
3. With the vacuum pump still running, saturated $Ca(OH)_2$ solution was introduced into the desiccator until the specimens were submerged in the solution.
4. The vacuum was maintained for 1 hour before allowing air to re-enter the container.
5. The specimens were kept in the solution for 20 hours before removing them for testing.

Test set-up

Catholyte and Anolyte

The catholyte used was 10% NaCl (by mass) solution, i.e., 100g of NaCl in 900g of water (tap water) which is approximately equal to 2M. The anolyte solution was 0.3M NaOH i.e., 12g of NaOH dissolved in 1 litre of de-ionised water. Both the solutions were stored in room temperature 23°C (± 2°C) prior to testing. On average each perspex cell contained 1300 cm^3 of (respective) electrolyte.

Cell arrangement

The schematic diagram of the cell arrangement and the method used to seal the concrete disc are presented in Figs. 4.8 and 4.10 respectively. The perspex cells were cleaned and the electrodes (circular stainless steel cathode of 100mm diameter 3mm thickness and circular mild steel anode of the same dimensions) were placed in the appropriate cells. The concrete specimen was placed inside a silicon annular ring, with a hard nylon ring outside the silicon ring (sealing arrangement shown in Fig. 4.10). The specimen was then placed between the cells such that the mould finished face was exposed to the cell containing the stainless steel cathode, and pressure was applied with the help of three clamping bolts. The silicon ring was deeper (60mm) than the concrete specimen (50mm), so that once the perspex cells were brought together by means of the clamping bolts, the pressure on the silicon ring would force the silica to expand laterally (i.e. in a direction opposite to that of the applied pressure), thereby providing a good seal between the specimen, the hard

nylon ring and the perspex cells. The hard nylon ring outside the silicon ring stopped the silicon ring from expanding outwards, thereby increasing the seal on the concrete surface.

Once the clamping bolts were tightened, the adequacy of the seal of the cell arrangement was checked. The seal between the cells and the concrete specimen was checked by admitting de-ionised water into one cell and waiting for few minutes to check if there was any flow between the cells or between the cell and the concrete specimen. Once the water tightness of the seal was verified, the electrolytes were introduced into the cells; i.e. sodium chloride solution into the cell with the cathode and sodium hydroxide solution into the cell with the anode. The negative terminal of the power supply was connected to the stainless steel cathode and positive to the mild steel anode.

Procedure for carrying out the measurements

A constant DC voltage of 30V was applied between the cathode and the anode, and the initial current through the specimen was recorded. Based on this initial current, the recommended test voltage as well as the test duration were selected from Table 4.8. The 30V was changed to the recommended test voltage and the new current was measured along with the temperature of the electrolytes. At the end of the test (depending on the test duration), the current and the temperature of the electrolytes were again measured. Then the concrete disc specimen was removed from the cell arrangement and the surfaces were cleaned with tap water. The disc was split along the length into two halves and the half section which has a regular broken surface was used for the depth of chloride penetration measurement. A 0.1M silver nitrate solution was sprayed on to the selected half and waited till the silver nitrate reacted with chlorides to give a white silver chloride precipitation on the surface. The depth up to which the white silver chloride precipitate was found is considered as the chloride penetration depth. At least eight such penetration depth measurements were taken perpendicular to the exposed surface using the Vernier callipers after avoiding the outer 10mm width from the curved edge of the specimen. An average depth of the chloride penetration (average of the eight measurements) was calculated, which was used in the calculation of the non-steady state migration coefficient, D_{nssm} (Eq. 4.8), as described below.

Calculation of the non-steady state migration coefficient

The non-steady state migration coefficient, D_{nssm}, (m^2/s) was calculated using the following equation in accordance with NT BUILD 492 (1999):

$$D_{nssm} = -\frac{RT}{zFE}\frac{X_d - \alpha\sqrt{X_d}}{t} \qquad \text{(Eq. 4.8)}$$

where,

$$E = \frac{U-2}{L} \qquad \text{(Eq. 4.9)}$$

$$\alpha = 2\sqrt{\frac{RT}{zFE}}erf^{-1}\left(1 - \frac{2C_d}{C_0}\right) \qquad \text{(Eq. 4.10)}$$

R is the universal gas constant, R = 8.314 J/K.mol;

T is the average values of initial and final temperatures in the anolyte solution, °K;

z is the absolute value of ions valence for chloride, z=-1;

F is Faraday constant, F = 9.648 x 10^{-4} J/V.mol;

E is the linear decay of voltage, V/m;

U is the applied voltage, V;

L is the thickness of the specimen, m;

X_d is the average value of the chloride penetration depths, m;

α is defined by Eq. 4.10, with no units;

t is the test duration, seconds;

erf^{-1} is the inverse of the error function;

C_d is the minimum chloride concentration, at which the colour changes from white to colourless, $C_d \approx 0.07M$;

C_0 is the chloride concentration in the catholyte solution, $C_0 \approx 2M$.

By substituting for C_d and C_o in Eq. 4.10 and simplifying Eq. 4.8, the following simplified equation can be obtained (NT BUILD 492, 1999).

$$D_{nssm} = \frac{0.0239TL}{(U-2)t}\left(X_d - 0.0238\sqrt{\frac{TLX_d}{U-2}}\right) \qquad \text{(Eq. 4.11)}$$

The results from this test are discussed in Chapter 5.

4.3.4.3 Steady state migration test

The steady state migration test was carried out in accordance with the test protocol proposed by Castellote *et al.* (2001) to obtain the steady state migration coefficient D_{ssm}. The schematic diagram of the cell arrangement is shown in Fig. 4.11 and the test set-up for three replicate tests is shown in Fig. 4.12.

Preparation of test specimens

The test specimen for the steady state migration test was a concrete disc of 100mm diameter and 20mm thickness, as shown in Fig. 4.2. This was obtained by slicing the concrete core as described in section 4.3.3. The location of test specimen and the test face are also shown in Fig. 4.2. Three such replicate specimens are used in this test. The exact thickness of the specimens was measured using the Vernier callipers.

The concrete disc specimens were vacuum saturated prior to the test. The following procedure was used for attaining the vacuum saturation (according to ASTM C1202, 1997):

1. The surface dry disc specimens were kept in a desiccator such that their two parallel faces (saw cut faces) were exposed, i.e. they sat on their curved face.
2. The pressure inside the desiccator was reduced to 1mm of Hg and the vacuum was maintained for a period of 3 hours.
3. With the vacuum pump still running, de-ionised solution was introduced into the desiccator until the specimens were submerged in the solution.
4. The vacuum was maintained for 1 hour, by running the vacuum pump if necessary, before allowing air to re-enter the container.
5. The specimens were kept in the solution for 18 hours before removing them for testing.

Test set-up

Catholyte and Anolyte

The catholyte used was 1M NaCl (by mass) solution, i.e., 58.44g of NaCl in 1litre of de-ionised water. The anolyte solution was de-ionised water. Both solutions were stored in room temperature prior to testing 23°C (±1°C). The quantity of the electrolyte in each cell was measured; on average each perspex cell contained 1300 ml of the (respective) electrolyte.

Cell arrangement

The cell arrangement was similar to that for the non-steady state migration test described in section 4.3.4.2. However, the electrodes, i.e., the anode and the cathode, were kept at a distance away from the concrete specimen (see Fig. 4.11). As a result of this arrangement of electrodes for applying voltage, it was expected that there would be some potential drop within the anolyte and the catholyte, which meant that the actual voltage across the concrete disc would be less than that of the applied voltage. Therefore, two auxiliary electrodes made of stainless steel (30mmx20mmx2mm) were placed close to the test specimen just prior to taking measurements, which enabled the measurement of the potential across the concrete disc.

The depth of the silicon ring and the nylon outer ring that went around the concrete disc was 30mm and 20mm respectively because the concrete disc was only 20mm thick. The concrete disc was kept in the silicon seal arrangement (similar to that shown in Fig. 4.10). The cell containing the cathode (the circular stainless steel disc) was attached to the test face (as shown in Fig. 4.2) and the cell with anode (the circular mild steel disc) was attached to the opposite side. The clamping bolts were tightened and the water tightness between the cells and the concrete disc were checked as described in section 4.3.4.2. Once the water tightness of the seal was verified, the sodium chloride solution was introduced into the cell containing the cathode and the de-ionised water into the cell containing the anode. The negative terminal of the power supply lead was connected to the stainless steel cathode and positive to the mild steel anode. A potential difference of 12 V DC was applied through the electrodes and the following measurements were taken regularly throughout the test duration until the test was completed.

Procedure for carrying out the measurements

1. Conductivity of the anolyte using a standard platinum conductivity probe and a Jenway conductivity meter (see Fig. 4.13). While measuring the conductivity, the voltage across the electrodes was discontinued.
2. Temperature of the anolyte using a Digitron digital thermometer.

3. The actual potential difference across the concrete specimen using the two auxiliary electrodes connected to an ammeter. The auxiliary electrodes were introduced just at the time of measurements and they were removed immediately after the measurements. These auxiliary electrodes were placed on either faces of the test specimen to measure the voltage acting across the specimen.

The flow of chloride ions through the concrete has mainly three stages as shown in Fig. 4.14:

1. Non-steady flow (time lag), during which chloride ions have not reached the anolyte.
2. Steady flow (steady state), during which chloride ions arrive at the anolyte at a steady rate.
3. Attenuate, in which the flow of chloride ions gradually ceases.

The measurements 1-3 were repeated at least once in every 12 hours during non-steady flow and once in every 4 hours during the steady flow. During the steady state flow, 5ml of the anolyte was removed and its chloride content was analysed using a Potentiometric titration (described below), the data from which was used to obtain a relationship between the conductivity and the chloride concentration of the anolyte. Although this relationship was not used in the calculation of the steady state migration coefficient, the results were used to refine the test protocol for Permit ion migration test (see section 5.2.5).

Potentiometric titration

RILEM Technical Committee TC 178-TMC found this method to estimate the chloride concentration of samples more accurate than other normally used methods. This method of determining the chloride concentration of liquid involves titration of a measured volume of the unknown solution against a known concentration of silver nitrate (0.02M). The silver in silver nitrate combines with the chlorides to form silver chloride (Eq. 4.1) until all the chloride ions are consumed. The negative potential generated by the chloride ions get balanced as all the chloride ions combine with silver ions. Therefore, when there is no more chloride ions to react the potential becomes more positive. This sudden change in potential can therefore be used to

identify the end point. The chloride ions can then be calculated using stoichiometry calculations for the reaction of silver nitrate with the chloride (Titrino 768, Instruction Manual, Metrohm, Ireland):

$$Cl^- = \frac{35.453(M_{Ag}V_{Ag})}{m} \qquad \text{(Eq. 4.12)}$$

where,

Cl^- is the chloride concentration, ppm;

M_{Ag} is the molarity of silver nitrate solution, mmol/l;

V_{Ag} is the volume of silver nitrate solution required to balance chloride ions, ml;

m is the volume of the sample (liquid of unknown concentration), litres.

A commercially available Potentiometric Titrator (Metrohm Titrino 768) was used for the analysis (see Fig. 4.15). The instrument was assembled and the procedure given below was followed in order to carry out the potentiometric titration.

1. The sample taken out (5ml) from the anolyte was placed in a 120ml glass beaker.
2. 60ml de-ionised water was added to the glass beaker to dispense the anolyte sample, and it was kept in the automatic sample changer unit of the Titrator (Fig. 4.15).
3. The volume of sample and the molarity of silver nitrate were entered in the control unit memory using the key board provided.
4. The burette was pre-adjusted to deliver 1µl of $AgNO_3$ per minute, which was inserted into the solution along with the stirrer and the electrode for measuring the potential.
5. Once the test was started, the solution in the beaker was continuously stirred and potential measurements were taken using the electrode.
6. The end point was identified by the Titrator (based on the principle outlined earlier in this section) and from the knowledge of the volume of silver nitrate solution used to reach the end point, the chloride content was reported by the instrument, using Eq. 4.12.

Termination of the test and processing of the data

The exposure was stopped when the flow reached the 'attenuate' stage and the following calculations were performed.

The conductivity measurements were converted to chloride concentration by using an empirical relationship given by Castellote *et al.* (2001) (Eq. 4.13):

$$Cl^- = -1.71 + 11.45(\lambda_{25}) \qquad \text{(Eq. 4.13)}$$

Where,

Cl^- is the chloride concentration, mmol/l,

λ_{25} is the equivalent conductivity at 25°C (refer Eq.3.25), mS/cm,

The concentration (from Eq. 4.13) versus time graph was plotted. The slope of the straight-line portion of the graph, i.e. the slope of concentration versus time graph at steady state, $\frac{dc}{dt}$, was obtained. This was used to calculate the steady state migration coefficient, D_{ssm}, as discussed in the next section.

Calculation of the steady state migration coefficient

The steady state migration coefficient, D_{ssm}, was calculated using the modified Nernst-Planck equation (Castellote *et al.*, 2001):

$$D_{ssm} = -\frac{J_{Cl}RTL}{zFC\gamma\Delta\Phi} \qquad \text{(Eq. 4.14)}$$

and,

$$J_{Cl} = (\frac{dc}{dt})\frac{V}{S} \qquad \text{(Eq. 4.15)}$$

where,

D_{ssm} is the steady state migration coefficient, m^2/s,

J_{Cl} is the flux of chlorides through the specimen during the steady state, $mol/m^2.s$,

$\frac{dc}{dt}$ is the slope of the concentration-time graph at the steady state, $mol/ m^3.s$,

V is the volume of the anolyte, m^3,

S is the surface area of the concrete specimen, m^2,

R is the universal gas constant, R = 8.31 J/K.mol,

T is the absolute temperature (average during steady state), °K,

L is the thickness of the concrete specimen, m,

z is the valency of the ions, -1 for chlorides,

F is Faraday constant, $F = 9.65 \times 10^4$ J/V.mol,

C is the concentration of ion source solution, $C = 1x10^{-3}$ mol/m^3,

γ is the activity coefficient of the catholyte solution, $\gamma = 0.657$,

$\Delta\Phi$ is the average potential difference measured across the specimen during the steady state period, V.

4.3.4.4 Electrical resistivity test (Bulk resistivity)

The test set-up for measuring the bulk resistivity of the concrete specimen is shown in Fig. 4.19. The cylindrical saturated concrete specimen (same specimen described in section 4.3.4.2) was placed between two solid stainless steel electrodes. The contact between the electrode and the specimen was achieved by means of a wet conductive sponge made of carbon foam. An LCR Databridge (Potentiostat) was used to measure the resistance.

Procedure for carrying out the test

The resistance of the concrete specimen with sponges (R_{c+sp}) was measured first and the resistance of the sponges (R_{sp}) was measured afterwards. The difference between the two values is the resistance of the concrete specimen (R_c), which was used to calculate the bulk resistivity using Eq. 4.16. The contact between the electrodes and the concrete specimen was ensured by applying a 1 kg mass on top of the electrode arrangement in Fig. 4.19. The measurements were made at room temperature i.e., 23°C (±2°C).

Calculation of bulk resistivity

The bulk electrical resistivity, ρ_{bulk}, was calculated using the following equation (Andrade, 2006; Chlortest, 2006):

$$\rho_{bulk} = \frac{R_c A}{L} \qquad \text{(Eq. 4.16)}$$

and,

$$R_c = R_{c+sp} - R_{sp} \qquad \text{(Eq. 4.17)}$$

where,

ρ_{bulk} is the resistivity of the concrete specimen, ohm.m,

R_c is the resistance of the concrete specimen, ohm,

R_{c+sp} is the resistance of the concrete specimen plus sponges, ohm,

R_{sp} is the resistance of the sponges, ohm,

A is the area of the concrete specimen, m^2,

L is the length of the concrete specimen, m.

The results obtained from this test are discussed in Chapter 5.

4.4 Validation Programme

4.4.1 Introduction

The test methods used in the Validation Programme were:

- Migration tests
    1. NT BUILD 492: 99, Concrete, Mortar and Cement Based Repair Materials: Chloride Migration Coefficient from Non-steady State Migration Experiments (NT BUILD 492, 1999)
    2. Steady state migration test (Castellote *et al.*, 2001)
    3. Permit ion migration test (Andrews, 1999)
- Indirect tests
    4. Wenner four probe resistivity test (Millard *et al.*, 1990)
    5. Electrical resistivity (Andrade, 2006; Chlortest, 2006)

Eight mixes were used in this experimental programme. Four of them were manufactured to resemble the mixes used in the previous testing programme (Evaluation Programme) and were tested at an age of 28 days. Remaining four mixes were tested at the age of 56 days. The details of the materials used as well as the mixes are presented in Table 4.2. Although the concrete specimens used in this experiment programme were cast in the laboratory in accordance with the relevant BS Standards, there existed differences in the source of aggregates and the properties of the binder between the pervious experimental programme and this. Therefore, the details of the materials used are presented in the next section

4.4.2 Materials used and mix details

4.4.2.1 Type of binders

Three cementitious materials were used in addition to normal Portland cement in this experimental programme. They were pulverised fuel ash (pfa), microsilica (ms) and ground granulated blast-furnace slag (ggbs). The chemical composition of all the binders are presented in Table 4.4 and the their physical properties are given in Table 4.5.

Normal Portland Cement (opc)

The normal Portland cement used in this study was manufactured by Blue Circle in Cookstown, Northern Ireland and conformed to BS EN 197-1 (2000) CEM 1 4.25 N.

Pulverised Fuel Ash (pfa)

The pulverised fuel ash used was obtained from Kilroot Power Station and was supplied by Conexpo (N.I.) Ltd. The pfa conformed to BS 3892: Part 1 (1997).

Ground Granulated Blast-furnace Slag (ggbs)

The ground granulated blast-furnace slag was supplied by Civil and Marine Slag Cement Ltd. from their outlet based in the Belfast Harbour Estate. The ggbs was manufactured according to BS 6699 (1992).

Microsilica (ms)

The microsilica was supplied by Larsen in Northern Ireland. The ms conformed to BS EN 13263-1 (2005) Silica fume for concrete.

4.4.2.2 Aggregates

The aggregates used in this work were sourced locally in Northern Ireland. The fine aggregate used was medium graded sand (BS 882, 1992) and the coarse aggregate used was crushed basalt with a maximum size of 6mm and 10mm (BS EN 882, 1992). The aggregates were oven dried and allowed to cool to room temperature before the use. The 1 hr moisture absorption of the dry aggregates and their specific gravity in saturated surface dry condition were determined (Table 4.6). As the

aggregates were in an oven dry state, the water required to achieve the saturated surface dry state was added during mixing, in addition to the mix water.

4.4.2.3 Water

Tap water from the mains supply in Queen's University Belfast was used for manufacturing all concrete mixes. Therefore, it conformed to the UK Standards for mixing water BS EN 1008, (2002).

4.4.2.4 Superplasticiser

A naphthalene-Formaldehyde based superplasticiser supplied by Larsen, branded as Chemcrete S725, was used in all the mixes. It contained 50% water, which was considered to be part of the mixing water. The superplasticiser was added to the mixing water in accordance with the manufacturer's guidelines. The amount of superplasticiser used varied for different mixes, the quantities (percentage by mass of the cement) of which are shown in Table 4.2.

4.4.2.5 Mix proportioning

As mentioned earlier, the first four mixes (0.45 opc, 0.45 pfa. 0.40 ms and 0.45 ggbs) given in Table 4.2 were manufactured to resemble the mixes used in the Evaluation Programme. Therefore, the percentage of cement replacement, the w/b, the a/b, the fine aggregate/coarse aggregate (fa/ca) of the mixes were the same as that of the corresponding mixes in the Evaluation Programme. Due to the non-practicability of obtaining the same type of cement, superplasticiser and aggregates used for the mixes in the Evaluation Programme, the materials described in sections 4.4.2.1 to 4.4.2.4 were used instead. The coarse aggregate of maximum size 10mm was used in case of these four mixes. As the specific gravity of the materials were different compared to those used in Evaluation Programme, the yield equation was used to recalculate the mass of each constituent required (as described in the following section) using the proportions listed above (i.e. w/b, a/b, fa/ca etc.). The mass of the different constituents in these mixes is given in Table 4.2.

The method of mix proportioning using yield equation involves calculating the mass of each constituent required to yield $1m^3$ of concrete. The specific gravity of each material must be known to use this method. An excel spreadsheet was used for this

purpose (see Fig. 4.16). The mix proportions were entered on to the spreadsheet in terms of w/b, a/b, fa/ca and percentage of opc plus cement replacement materials as the case may be (as shown on Fig. 4.16). The spreadsheet was then used to calculate the required mass of each constituent to produce $1m^3$.

The mix proportions for the other four mixes (0.52 opc, 0.52 pfa, 0.52 ggbs and 0.52 ms) were selected based on the work carried out by Gilleece (1996). By using proportions of mixes similar to those used by Gilleece (1996), the intention was to compare the diffusion parameters obtained from these two sets. The yield equation (as described before) was used to calculate the mass of the different constituent materials. The mass of the different constituent materials are given in Table 4.2.

4.4.3 Manufacturing of concrete

The mix constituents were batched by mass and then mixed in a pan mixer (see Fig. 4.3) in accordance with BS 1881: 125 (1988). The test specimens (see section 4.4.4) for each mix were prepared from the same batch in order to ensure uniformity in quality. The mixing procedure is summarised as follows:

1. The mixer pan and paddles were moistened with a damp cloth.
2. Half the coarse aggregate, all the fine aggregate, and then the rest of the coarse aggregate were added to the mixer pan, in that order and spread evenly over the pan surface.
3. The aggregates were then mixed for 30 seconds.
4. Half of the total volume of water (i.e. mixing water plus that required for 1 hour absorption by aggregates) was added within the next 15 seconds.
5. The mixing continued for another 3 minutes after which the machine was stopped and the contents of the pan covered for 15 minutes to enable the aggregates to absorb the water.
6. After the 15 minutes absorption period the cementitious material was added and spread in an even layer over the aggregate.
7. The mixer was started again and allowed to run for 30 seconds.
8. The mixer was then stopped and any material adhering to the paddles and sides of the pan were scrapped into the pan.

9. The mixer was started again and the remaining water, mixed with the superplasticiser, was added over the next 30 seconds.
10. Mixing continued for a further 3 minutes after the last of the materials had been added.

4.4.4 Description of test specimens

4.4.4.1 Casting of test specimens

The moulds (rectangular boxes made of treated plywood see Fig. 4.2) used for casting the concrete were different for different tests conducted in the experimental programme. For both the steady state and the non-steady state migration tests, 100mm diameter concrete discs were used. The bulk resistivity was also measured using 100mm diameter concrete discs. These discs were cut from cores extracted from slabs of size 300x300x60mm. In case of both the Permit ion migration test and the Wenner four probe resistivity test, slabs of size 250x250x60mm were tested. That is, two sets of slabs were cast using each type of concrete. Figure 4.3 shows the rectangular mould used to cast one type of slabs. The type of mould used for the second type of slabs was also similar to the one shown in this figure.

The leakage of mix water and cement paste was prevented by sealing the mould joints by silicon sealant. All the moulds were coated with mould release oil one hour before casting. The concrete was added to the moulds in three equal layers and compacted using a vibrating table (Fig. 4.3). Each layer was vibrated until air bubbles stopped appearing at the concrete surface. The top face of the material was then finished off using a steel float. For each mix three 100mm sized cubes were also cast in the above manner.

4.4.4.2 Curing of test specimens

As water is required for the hydration of cement, a proper curing can be achieved either by immersing the concrete in water or by preventing the loss of water from the concrete. The temperature controlled water baths available in the laboratory continuously circulate water and, hence, this could result in leaching soluble hydrates from the surface layers. So a curing regime that would retain the water in the concrete was adopted for this experiment programme.

After casting, the moulds were covered with polythene sheet to reduce the loss of moisture by surface evaporation. After 24 hours the test specimens were removed from the moulds and then placed in a water bath at 20°C (±1°C) for 3 days. They were then removed from the water bath, sealed in polythene sheets and placed in a constant temperature room at 20°C (±1°C), 55% (±1 %) relative humidity, where they remained until they were ready for testing at the age of 28 or 56 days. The procedure of specimen preparation for each experiment was the same up to this point However, the conditioning of the specimens required for different tests were different and, hence, they are discussed in the sections describing the tests.

4.4.5 Standard tests for workability and compressive strength

The workability of fresh concrete was measured in terms of slump and air content immediately after manufacturing the concrete for each mix. The slump test was carried out on fresh concrete mixes in accordance with BS EN 12350-2 (2000), while, the air content was measured according to BS EN 12350-7 (2000), using the pressure gauge method.

The compressive strength of all the concrete was determined by crushing 3 cubes of 100mm size at an age of 28 days. The testing was carried out according to BS EN 12390-3 (2002). The average values of these properties are reported in Table 4.3.

4.4.6 Test methods

The following tests methods were used in the Validation Programme.

4.4.6.1 Non-steady state migration test

The non-steady state migration test was carried out according to NT BUILD 492 (1999) to obtain the non-steady state migration coefficient D_{nssm}. The test set-up, the procedure for carrying out the test and the method of calculating the D_{nssm} were similar to those described in section 4.3.4.2. However, in the Validation Programme, the concrete specimens were obtained from slabs as described in section 4.4.4.1. The procedure for obtaining the specimens is described in the following section:

Three 100mm diameter cores were cut from each of the three (300x300x60mm) slabs described in section 4.4.4.1. One core from each slab (i.e. 3 in total) was used for the

non-steady state migration test. The specimen for the non-steady state migration test was obtained by slicing off a 10mm thick concrete from the trowel finished face. The exact thickness of the specimen was then measured using Vernier callipers.

The above specimens were saturated and tested to determine the non-steady state migration coefficient using the procedure described in section 4.3.4.2.

4.4.6.2 Steady state migration test

The steady state migration test was carried out in accordance with the test protocol used by Andrews (1999) to obtain the steady state migration coefficient D_{1Dssm}. The cell arrangement was similar to that used in section 4.3.4.3. The schematic diagram is shown in Fig. 4.17.

Preparation of test specimens

Three 100mm diameter cores were cut from each of the three (300x300x60mm) slabs described in section 4.4.4.1. One core from each slab (i.e. 3 in total) was used for the steady state migration test. The specimen for the steady state migration test was obtained by slicing a disk of required thickness (i.e. 30mm for the first four mixes in Table 4.2 and 20mm for the rest) from the mould finished face (mould finished face was considered as the test face). The reason for selecting different thickness for the test specimen is discussed below.

For completing the test within an acceptable test duration, the thickness of the test specimen may be limited to 20-30mm, which would require the maximum size of aggregate to be one third of the size of the test specimen in order to eliminate the preferential flow along the interfacial transition zone (Nilsson *et al.*, 1996). Therefore, in case of the mixes with 10mm aggregates (first four mixes in Table 4.2), the minimum thickness of the test specimen was considered as 30mm and for mixes with 6mm aggregates (the last four mixes in Table 4.2) it was taken as 20mm.

The exact thickness of the specimen was then measured using the Vernier callipers. The test specimens were saturated using the procedure described in section 4.3.4.3.

Test set-up

Catholyte and Anolyte

The catholyte used was 0.55M NaCl (by mass) solution, i.e., 32.14g of NaCl in 1litre of de-ionised water. The anolyte solution was de-ionised water. Both solutions were stored in room temperature prior to testing 23°C (±1°C). The quantity of the electrolyte in each cell was measured; on average each perspex cell contained 1300 ml of the (respective) electrolyte.

Cell arrangement

The cell arrangement was similar to that for the steady state migration test described in section 4.3.4.3. Except, the electrodes, i.e., the anode and the cathode, were kept closer to the concrete specimen (see Fig. 4.17). Therefore, the potential drop in the electrolytes was considered negligible. The concrete specimen was kept in place using the silicon seal arrangement and the water tightness of the seal was checked as described in section 4.3.4.3. Once the water tightness of the seal was verified, the sodium chloride solution was introduced into the cell containing the circular stainless steel disc (cathode) and the de-ionised water into the cell containing the circular mild steel disc (anode). The negative terminal of the power supply lead was connected to the stainless steel cathode and positive to the mild steel anode. Potential difference of 60 or 12 V DC was applied through the electrodes depending on the resistivity of the concrete. The following measurements were taken regularly throughout the test duration until the test was completed.

Procedure for carrying out the measurements

1. The current flowing between the electrodes using an Ammeter.
2. Conductivity of the anolyte using a stainless steel conductivity probe and a Jenway conductivity meter (see Fig. 4.13). While measuring the conductivity, the voltage across the electrodes was discontinued.
3. Temperature of the anolyte using a Digitron digital thermometer.

These measurements were repeated once in every 6 hours during non-steady flow and more frequent (i.e. at least every two hrs) during steady state flow.

Processing of the data

The conductivity measurements obtained from the test were first corrected for temperature using Eq. 4.18 (Castellote *et al.*, 2001):

$$\lambda_{25} = \lambda_T + 0.02(25 - T_C)\lambda_T \qquad \text{(Eq. 4.18)}$$

where,

λ_{25} is the conductivity at 25°C, mS/cm,

λ_T is the conductivity of the anolyte at T_C°C, mS/cm,

T_C is the temperature of anolyte at the measured time, °C.

Then the conductivity versus time graph was plot. This graph was used to identify the different stages of flow as described in section 4.3.4.3. The conductivity measurements were used only to identify the onset of the steady state in this case compared to the steady state migration test described in the Evaluation Programme (section 4.3.4.3), were the conductivity was converted to chloride concentration and used for calculating D_{1Dssm}.

As the flow reached the steady state (see Fig. 4.14), four to five liquid samples (5ml) were removed from the anolyte at a regular interval of 30 minutes. The chloride content was analysed using a Potentiometric titration (described in section 4.3.4.3), the data from which was used to plot the concentration versus time graph. The slope of the straight-line portion of the graph, i.e. the slope of concentration versus time graph at steady state, $\frac{dc}{dt}$, was obtained. This was used to calculate the steady state migration coefficient, D_{1Dssm}, as discussed in the next section. The current was plotted against time and the charge passed also was estimated from the area under the current versus time graph.

Calculation of the steady state migration coefficient

A modified Nernst-Planck equation was used to calculate the steady state migration coefficient D_{1Dssm} (Andrews, 1999).

$$D_{1Dssm} = -\left(\frac{dc}{dt}\frac{V}{A}\right)\left(\frac{RTL}{zFCE}\right) \qquad \text{(Eq. 4.19)}$$

where,

D_{1Dssm} is the steady state migration coefficient, m^2/s,

$\frac{dc}{dt}$ is the rate of change of concentration in the anolyte, $mol/m^3.s$,

V is the volume of the anolyte solution, m^3,

A is the surface area of the test specimen, m^2,

R is the universal gas constant, R = 8.31 J/K.mol,

L is the thickness of the concrete specimen, m,

T is the absolute temperature (average during steady state), K,

z is the valency of the ions, z = -1 for chlorides,

F is Faradays constant, $F = 9.65x10^4$ J/V.mol,

C is the concentration of ion source solution, $C = 0.55x10^{-3}$ mol/m^3,

E is the electrical potential applied between the electrodes, E = 60 or 12 V.

The results from this test are discussed in Chapter 6.

4.4.6.3 Permit ion migration test

The *in situ* migration coefficient, $D_{in\ situ}$, was obtained by testing the concrete specimens (slabs described in 4.4.4.1) with the Permit ion migration test. The instrument was developed at Queen's University Belfast to measure the chloride migration coefficient of concrete on site, without removing cores from the structure (Andrews, 1999, Basheer *et al.*, 2005 and Nanukuttan *et al.*, 2006). The schematic diagram of the Permit is shown in Fig. 4.20 and the test set-up of the Permit ion migration test is shown in Fig. 4.21.

The test specimen (250x250x60mm concrete slab) was saturated with de-ionised water 48 hours prior to the test.

Test set-up

Catholyte and Anolyte

The catholyte used was a 0.55M NaCl solution, i.e., 32.14g of NaCl in 1 litre of de-ionised water. The anolyte solution was de-ionised water. Both the solutions were stored in room temperature at 23°C (±1°C) prior to testing.

Permit

The Permit consisted of two cells, which were made by placing two thin walled (<5mm) cylindrical tubes of different diameters concentrically (see Fig. 4.20). The cell with the smaller diameter, the inner cell, contained 425ml of catholyte and the annular region between the two cylinders, the outer cell, contained 725ml of anolyte. A circular stainless steel cathode was placed in the inner cell and an annular shaped mild steel anode was placed in the outer cell.

The Permit was fixed to the saturated concrete specimen (on the mould finished face) using the three clamping bolts (see Fig. 4.21). The rubber rings at the bottom of the cells provided the seal between the inner cell and the outer cell as well as preventing any leakage from the outer cell when the Permit was attached to the test specimen. Once the Permit was fixed on the test surface, the water tightness of the seals were checked by introducing de-ionised water to the inner cell first and then to the outer cell in succession, and each time the leakage if any was checked. The de-ionised water from both cells were then removed and the electrolytes were introduced. The negative of the power lead was connected to the cathode and the positive lead to the anode. A potential difference of 60V was applied between the electrodes.

Procedure for carrying out the measurements and processing of the data

The procedure for carrying out the measurement was the same as described in section 4.4.6.2 for steady state migration test. The data was also process as described in the section 4.4.6.2.

Calculation of *in situ* migration coefficient

A modified Nernst-Planck equation was used to calculate the *in situ* migration coefficient (Nanukuttan *et al.*, 2006).

$$D_{in\ situ} = -\left(\frac{dc}{dt}T\right)\left(\frac{R}{zFCE}\right)\left(V\frac{L}{A}\right) \qquad \text{(Eq. 4.20)}$$

Where,

$D_{in\ situ}$ is the migration coefficient, m^2/s,

$\frac{dc}{dt}$ is the steady rate of change of concentration in the anolyte, mol/m^3.s,

T is the absolute temperature (average during steady state), K,

R is the universal gas constant, R = 8.31 J/K.mol,

z is the valency of the ions, z = -1 for chlorides,

F is Faradays constant, F = 9.65x10^4 J/V.mol,

C is the concentration of the catholyte, C = 0.55x10^{-3} mol/m^3,

E is the electrical potential applied between the anode and the cathode, E = 60V,

V is the volume of anolyte, V = 7.25x10^{-4} m^3,

L/A is the ratio of the flow length to the flow area (see section 6.3), L/A = 3.76 m^{-1}.

The results are discussed in Chapter 6.

4.4.6.4 Electrical resistivity test (Wenner resistivity)

The electrical resistivity of the concrete was measured using the Wenner four probe resistivity meter (Resistivity Meter Mark II from C.N.S. Electronics Ltd, England). The test set-up used for measuring the electrical resistivity (termed as Wenner resistivity) is shown in Fig. 4.18.

The Wenner probe resistivity test was conducted on concrete slabs described in section 4.4.6.3 prior to testing the slabs with Permit ion migration test.

The Wenner four probe resistivity meter uses four cylindrical electrical probes arranged in a straight line and kept at a constant distance of 5cm between each. The outer two probes apply an alternating current through the concrete and the inner two electrodes are used to measure the potential difference between them. The probes are connected to a control unit, which displays the resistivity, resistance and current. The contact between the concrete specimen and the probes was obtained by using wet wooden pegs at the bottom of each probe. The probes were held firmly against the concrete surface to ensure good contact between the probes and the concrete surface. The measurements were made at room temperature 23°C (±1°C).

Calculation of the Wenner resistivity

The Wenner resistivity ρ_{Wenner} was calculated using the semi-empirical formula given in Eq. 4.21 (Millard *et at.*, 1990).

$$\rho_{Wenner} = 2\pi a \frac{V}{I} \qquad \text{(Eq. 4.21)}$$

where,

ρ_{Wenner} is the resistivity of the concrete specimen in k.ohm.cm,

a is the spacing between the electrodes, 5cm,

V is the potential difference between the inner two electrodes, V,

I is the current, mA.

The ρ_{Wenner} obtained from the control unit of the Wenner four probe resistivity meter was converted to ohm.m as all the other resistivity measurements presented in the discussion are in ohm.m. The results from this test are discussed in Chapter 6.

4.4.6.5 Electrical resistivity test (Bulk resistivity)

Electrical resistivity test described in section 4.3.4.4 was carried out to determine the bulk resistivity of concrete specimens in the Validation Programme. The cylindrical concrete specimens (same specimens as that described in section 4.4.6.1) were used for this test. The procedure for carrying out the measurement and the calculation of the ρ_{bulk} were the same as section 4.3.4.4. The results from this test are discussed in Chapter 6.

Table 4.1 Details of mixes used in the evaluation programme (Quantities reported in kg/m^3)

Mix designation	**opc 0.35**	**opc 0.42**	**opc 0.45**	**opc 0.50**	**ms 0.40**	**ms 0.42**	**pfa 0.42**	**pfa 0.45**	**ggbs 0.42**	**ggbs 0.45**
Country of Origin	Sweden		Spain	Sweden			Norway	Portugal	Netherlands	
Cement type (BS EN 197-1, 2000)	CEM I 42.5 N		CEM I-42.5 N	CEM I 42.5 N			(18% PFA) CEM II/A-V 42.5 R	(39% PFA) CEM IV B 32.5R	(~70% Slag) CEM III B 42.5 LH HS	
Cement content	450	420	400	400	399	389.5	410	340	410	350
Microsilica					21	20.5				
Water	157.5	176.4	180	200	168	172.2	172.2	153	172.2	157.5
Fine Aggregate (Min size 75μm)	904 (~8mm)	926 (~8mm)	742 (≤6mm)	920 (~8mm)	842.5 (~8mm)	897 (~8mm)	901 (~8mm)	62 (~2mm) 603 (2-4mm)	901 (~8mm)	70 (≤1mm) 790 (1-4mm)
Coarse Aggregate	904 (10-5mm)	855 (10-5mm)	1030 (6-16mm)	816 (10-5mm)	842.5 (8-16mm)	897 (10-15mm)	901 (10-15mm)	619 (4-12mm) 555 (12-25mm)	901 (10-5mm)	1040 (4-16mm)
Superplasticiser % of cement	CemFlux Bro 1.0	CemFlux Bro 0.5	Melcret 222 4.8	-	Cementa 92M 3.4	CemFlux Bro 0.5	CemFlux Bro 0.5	Rheobuild 1000 4.1	CemFlux Bro 0.5	Cretoplast 3.9
water binder (w/b)	**0.35**	**0.42**	**0.45**	**0.5**	**0.4**	**0.42**	**0.42**	**0.45**	**0.42**	**0.45**
Age at test (years)	~0.5	~0.5	~1.0	~0.5	>1.0	~0.5	~0.5	<1.0	~0.5	<1.0

Note: CemFlux Bro is polycarboxylether based superplasticiser

Melcret 222 and Rheobuild 1000 are both napthalene based superplasticisers

Cretoplast is manufactured by Cugla (Netherlands), this is a water reducing superplasticiser

Cementa 92M is melamine formaldehyde based superplasticiser

Table 4.2 Details of mixes used in the Validation Programme

Mix reference	w/b	a/b	fa/ca	Mass of the ingredients kg/m^3						Superplasticiser (% by mass of cement)
				Water	Portland cement	Cement replacements	10mm ca	6mm ca	fa	
0.45 opc	0.45	4.43	0.72	180.0	400.0	0	1030.0		742.0	
0.45 pfa	0.45	5.41	0.57	153.0	207.4	132.6 (pfa)	1174.0		665.0	3.4
0.40 ms	0.40	4.01	1.00	168.0	399.0	21.0 (ms)	842.5		842.5	3.4
0.45 ggbs	0.45	5.43	0.83	157.5	84.0	266.0 (ggbs)	1040.0		860.0	4.5
0.52 opc	0.52	4.65	0.55	208.0	399.9	0		1199.7	659.9	0.9
0.52 pfa	0.52	4.65	0.55	204.0	274.6	117.7 (pfa)		1176.7	647.2	0.9
0.52 ms	0.52	4.65	0.55	206.8	357.9	39.8 (ms)		1193.0	656.1	0.9
0.52 ggbs	0.52	4.65	0.55	206.7	198.8	198.8 (ggbs)		1192.7	656.0	0.9

Note: w/b - water to binder ratio
fa - fine aggregate
ca - coarse aggregate
a/b - total aggregate to binder ratio
fa/ca - fine aggregate to coarse aggregate ratio

Table 4.3 Slump, air content and compressive strength of the mixes used in the Validation Programme

Mix reference	Slump (mm)	Air content (%)	28-day compressive strength (N/mm^2)
0.45 opc	55	2.4	34.5
0.45 pfa	70	2.0	28.0
0.40 ms	28	2.8	35.5
0.45 ggbs	100	2.4	39.6
0.52 opc	5	2.9	21.0
0.52 pfa	5	2.7	13.0
0.52 ms	6	2.9	37.0
0.52 ggbs	6	2.4	21.0

Table 4.4 Chemical composition

	opc	pfa	ggbs	ms
CaO	64.49	2.38	41.21	0.3
SiO_2	19.92	59.18	35.18	92
Al_2O_3	6.06	22.8	13.96	0.7
Fe_2O_3	2.77	8.8	0.25	1.2
MgO	1.72	1.39	8.18	0.2
SO_3	3.16	0.27	0.1	0.3
K_2O	0.79	2.81	0.42	1.8
Na_2O	0.14	0.74		1.5
Cl^-	0.007	< 0.01		
Mn_2O_4		0.08	0.55	
P_2O_5		0.394		
TiO_2		1.15	0.57	
MnO			0.49	
Loss of ignition	*0.94*	*6.7**	*0.64**	*2*

Note: Loss of ignition with * sign means that the chemical composition given in Table 4.4 are balanced to 100% by the manufacturer

Table 4.5 Physical properties

	opc	pfa	ggbs	ms
Specific gravity	3.18	2.52	2.91	2.1
Specific surface area (m^2/kg)	322	340	600	20000

Table 4.6 Aggregate absorption and relative density

Type of aggregate	Specific gravity in saturated surface dry condition	Water absorption (1 hour)
Fine aggregate	2.72	2.3
Coarse aggregate 6mm	2.85	1.8
Coarse aggregate 10mm	2.90	1.1

Table 4.7 Recommended depths (millimetre) for profile grinding for opc mixes (NT BUILD 443, 1995)

w/b	0.25	0.3	0.35	0.4	0.5	0.6	0.7
Depth **1**	0~1	0~1	0~1	0~1	0~1	0~1	0~1
Depth **2**	1~2	1~2	1~2	1~3	1~3	1~3	1~5
Depth **3**	2~3	2~3	2~3	3~5	3~5	3~6	5~10
Depth **4**	3~4	3~4	3~5	5~7	5~8	6~10	10~15
Depth **5**	4~5	4~6	5~7	7~10	8~12	10~15	15~20
Depth **6**	5~6	6~8	7~9	10~13	12~16	15~20	20~25
Depth **7**	6~8	8~10	9~12	13~16	16~20	20~25	25~30
Depth **8**	8~10	10~12	12~16	16~20	20~25	25~30	30~35

Note: w/b is the water to binder ratio.

The profile depths are for opc mixes only.

Table 4.8 Recommended test voltage and test duration (NT BUILD 492, 1999)

Initial current *I* with 30V(mA)	Voltage to be applied (after adjustment) (V)	Possible new initial current *Io* (mA)	Test duration t (hour)
$Io < 5$	60	$Io < 10$	96
$5 \leq Io < 10$	60	$10 \leq Io < 20$	48
$10 \leq Io < 15$	60	$20 \leq Io < 30$	24
$15 \leq Io < 20$	50	$25 \leq Io < 35$	24
$20 \leq Io < 30$	40	$25 \leq Io < 40$	24
$30 \leq Io < 40$	35	$35 \leq Io < 50$	24
$40 \leq Io < 60$	30	$40 \leq Io < 60$	24
$60 \leq Io < 90$	25	$50 \leq Io < 75$	24
$90 \leq Io < 120$	20	$60 \leq Io < 80$	24
$120 \leq Io < 180$	15	$60 \leq Io < 90$	24
$180 \leq Io < 360$	10	$60 \leq Io < 120$	24
$Io \geq 360$	10	$Io \geq 120$	6

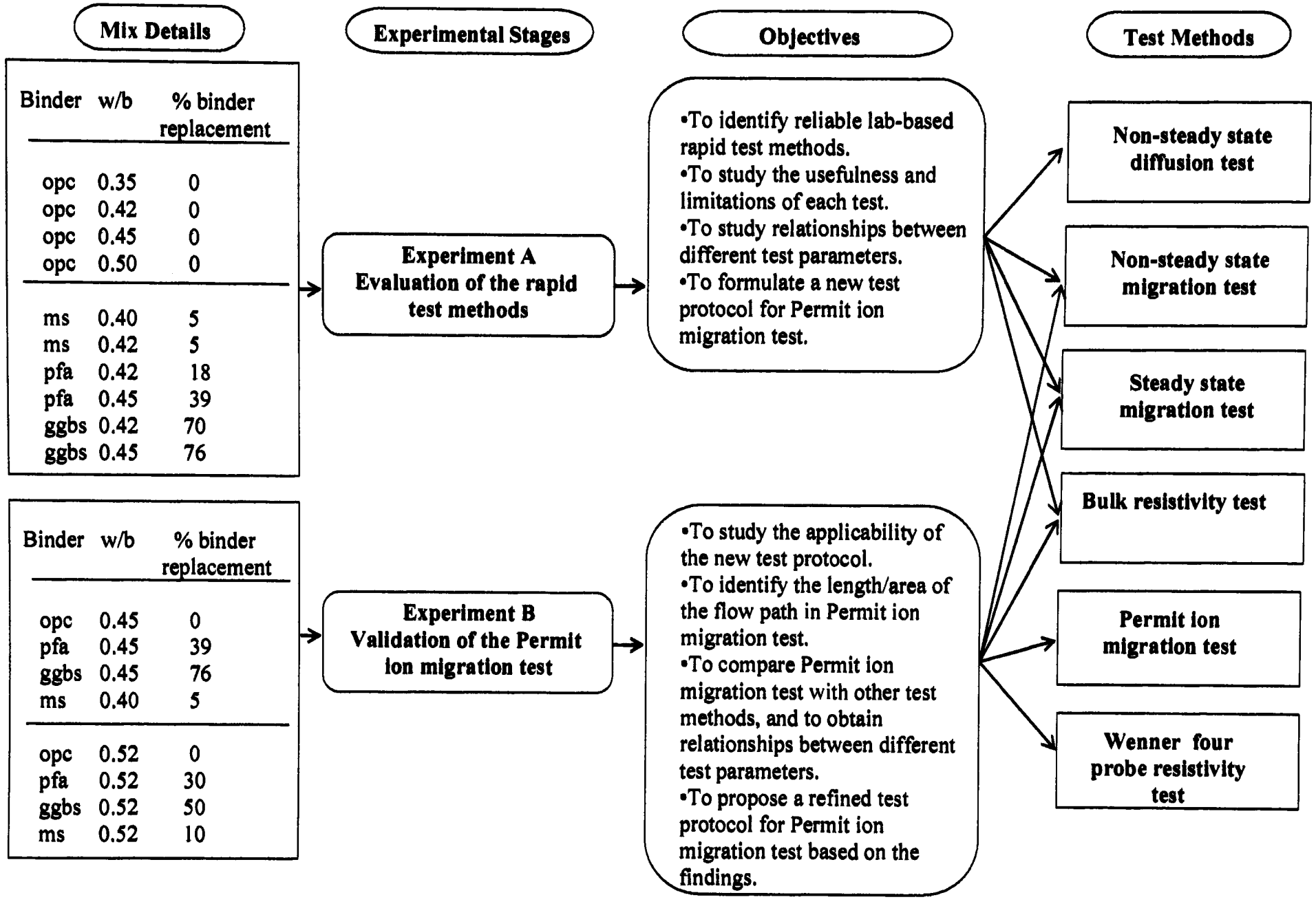

4.1 Flowchart of the experimental programme

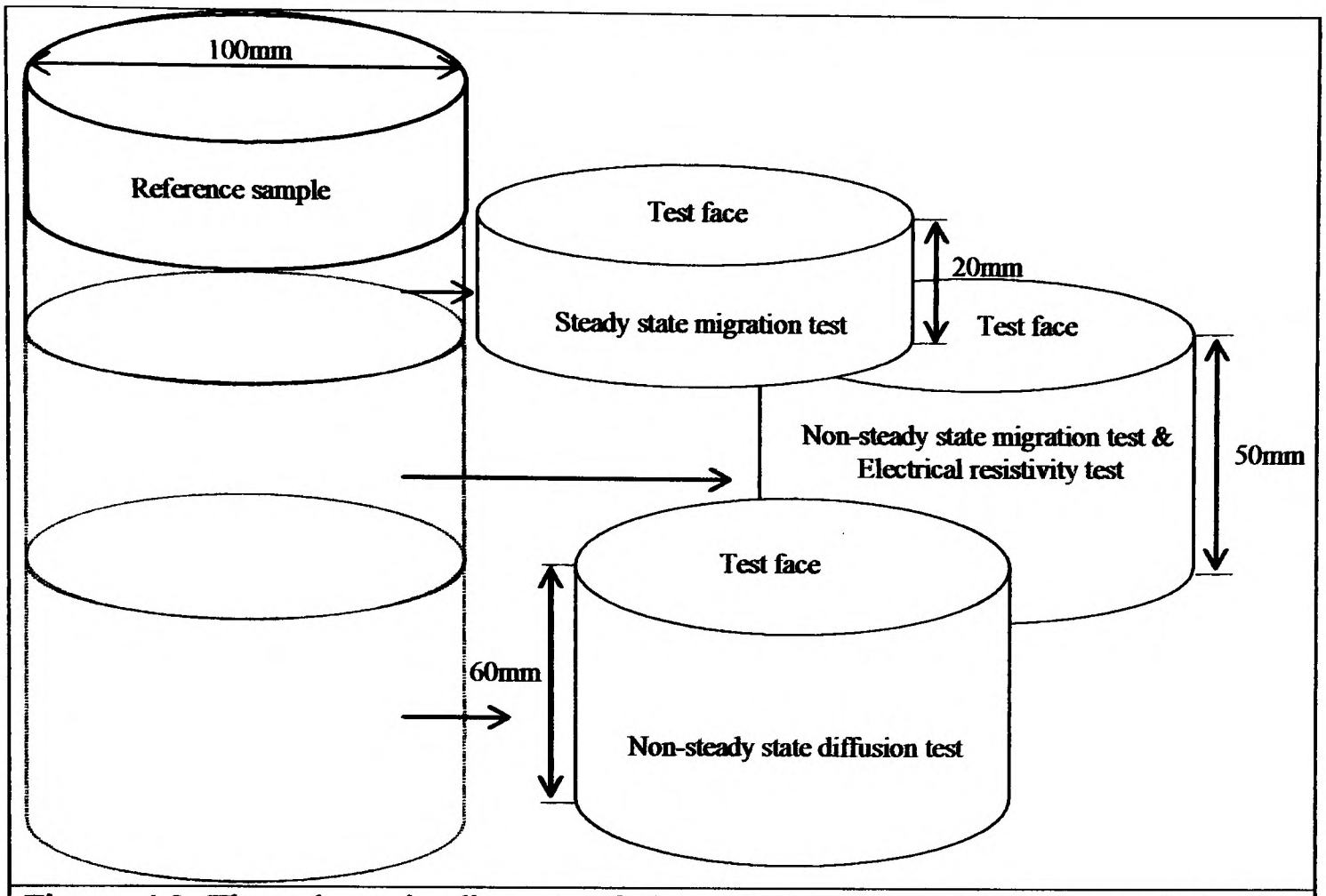

Figure 4.2 The schematic diagram of the cylindrical concrete core used for the Evaluation Programme showing the positions where the test specimens were cut

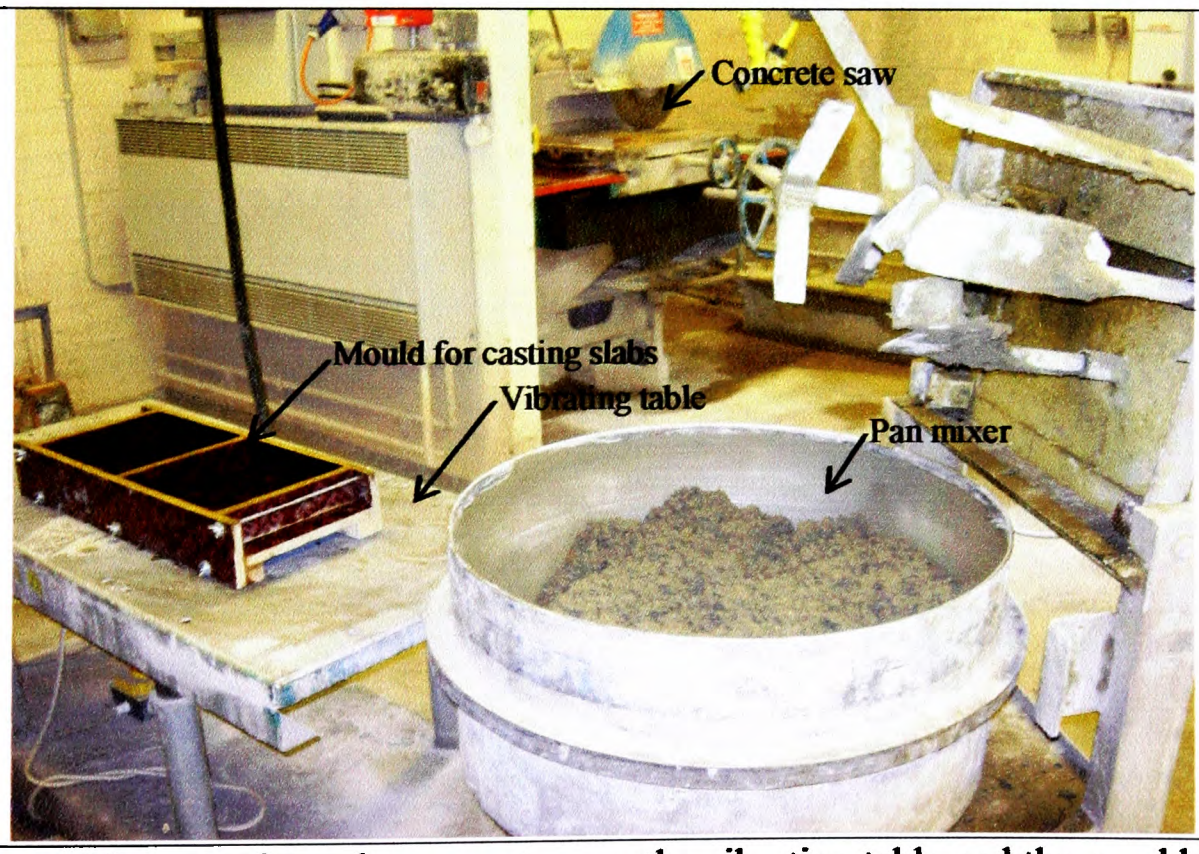

Figure 4.3 The pan mixer, the concrete saw, the vibrating table and the mould used

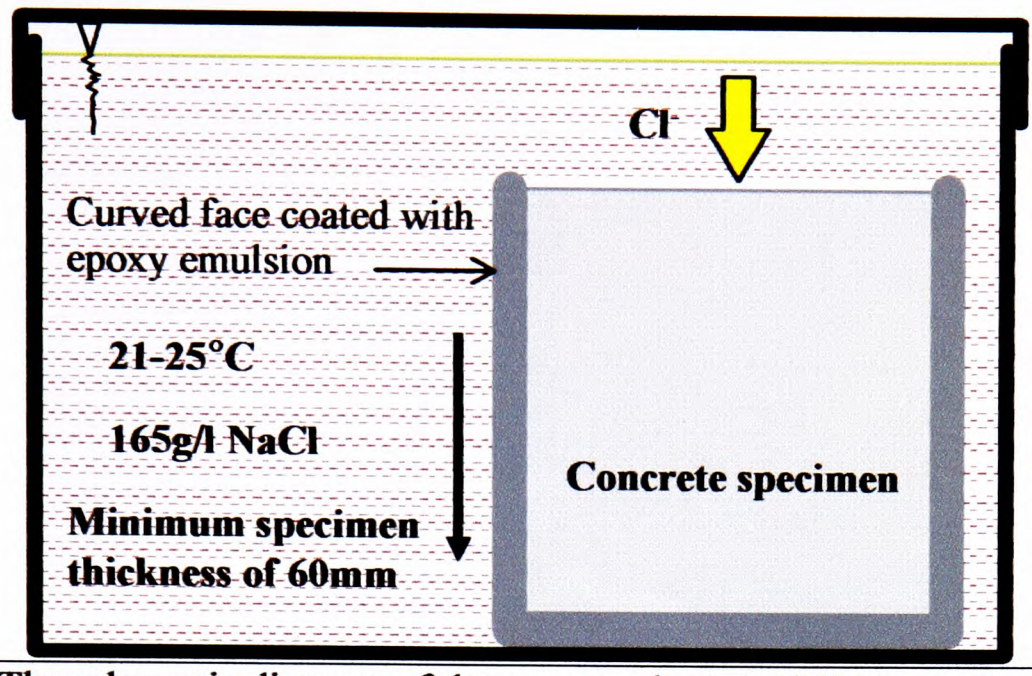

Figure 4.4 The schematic diagram of the non-steady state diffusion test

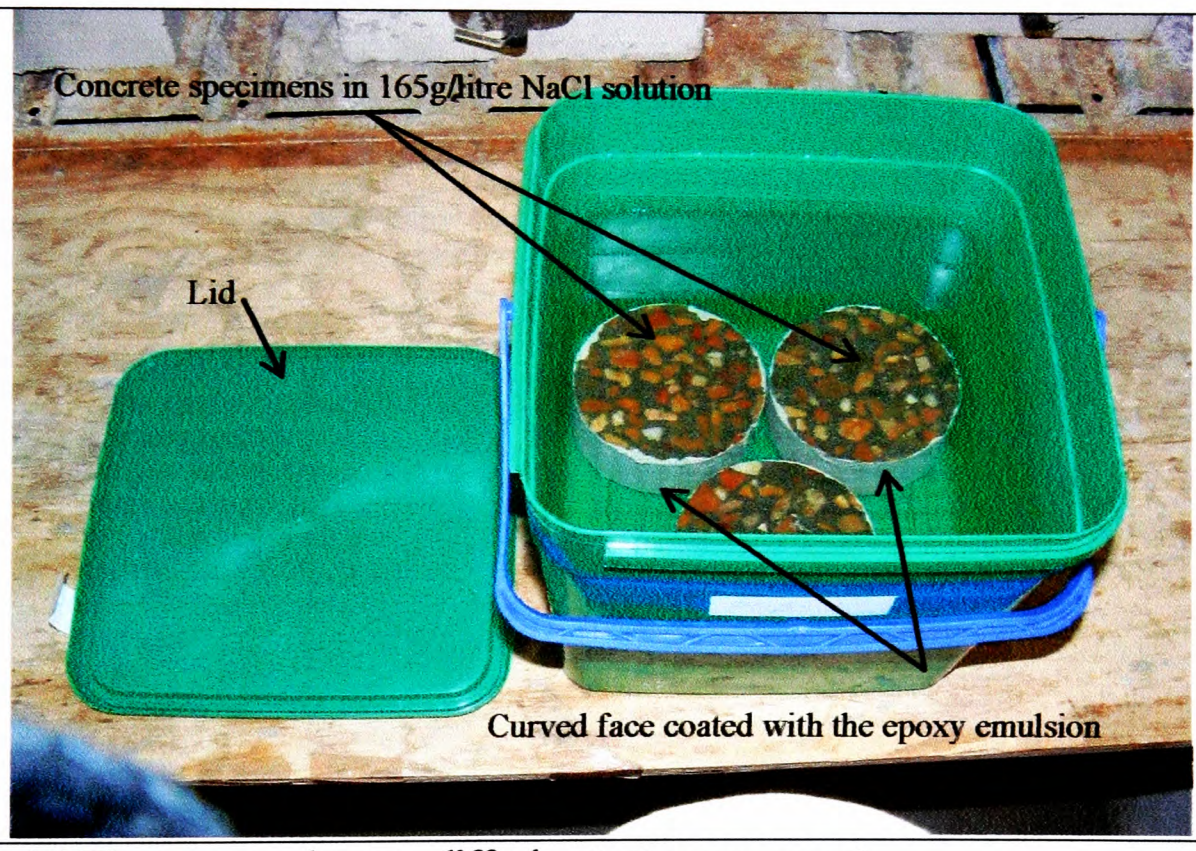

Figure 4.5 The non-steady state diffusion test arrangement

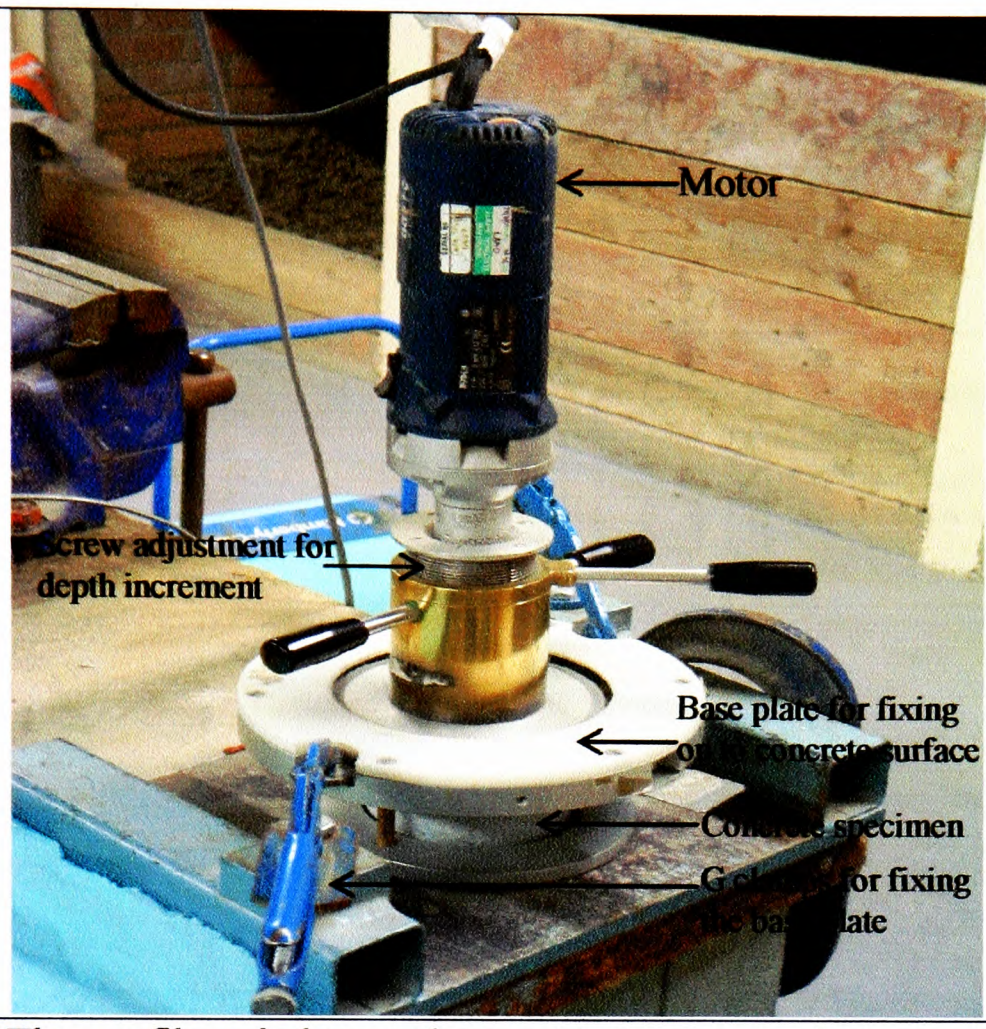

Figure 4.6 The profile grinder used to extract concrete dust samples (Germann Instruments)

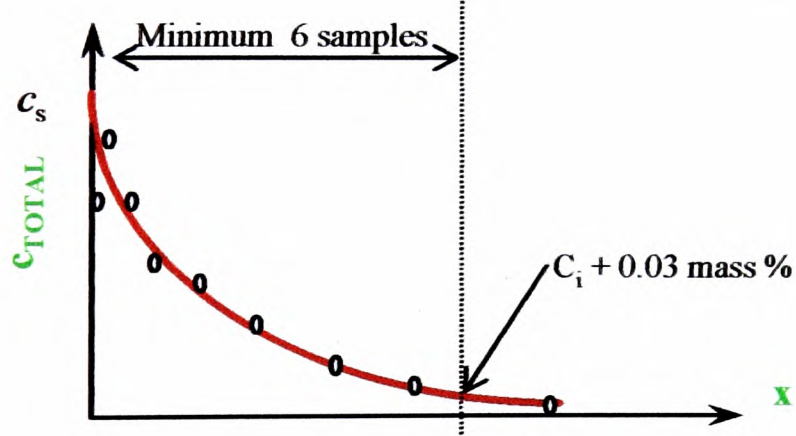

Figure 4.7 Typical chloride concentration profile from a non-steady state diffusion test

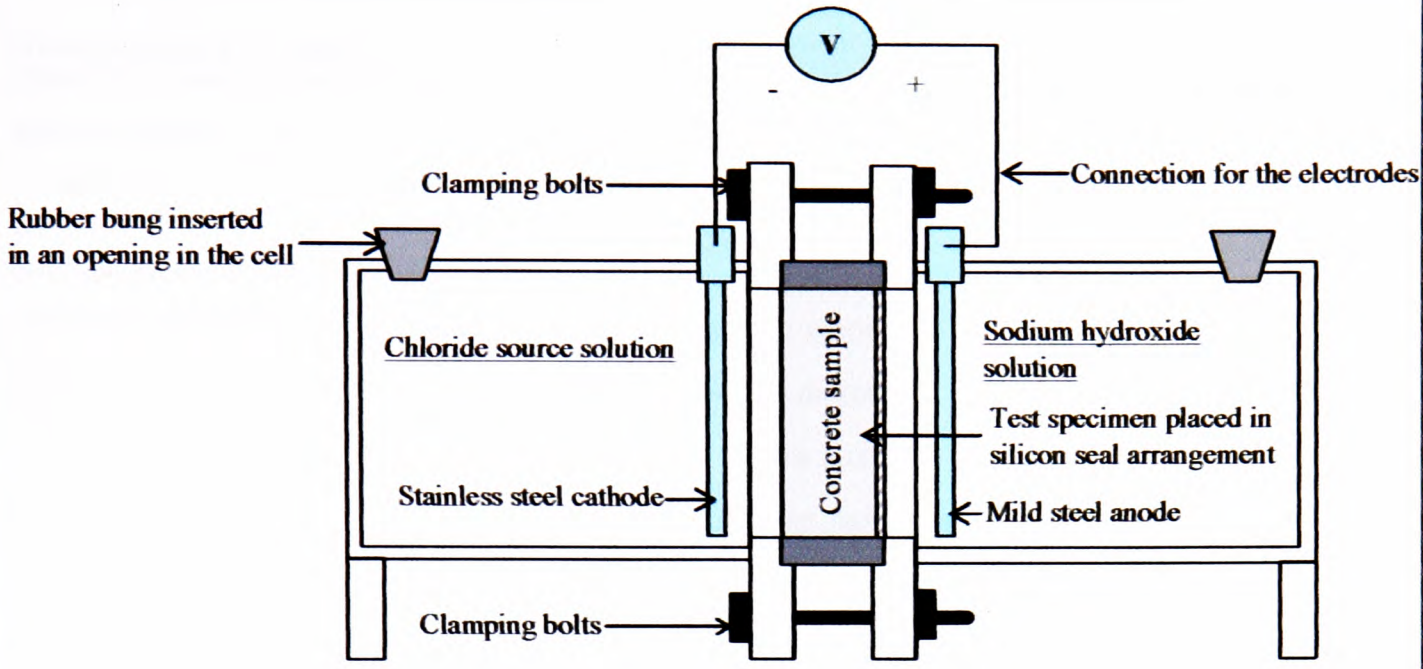

Figure 4.8 The schematic diagram of the non-steady state migration test

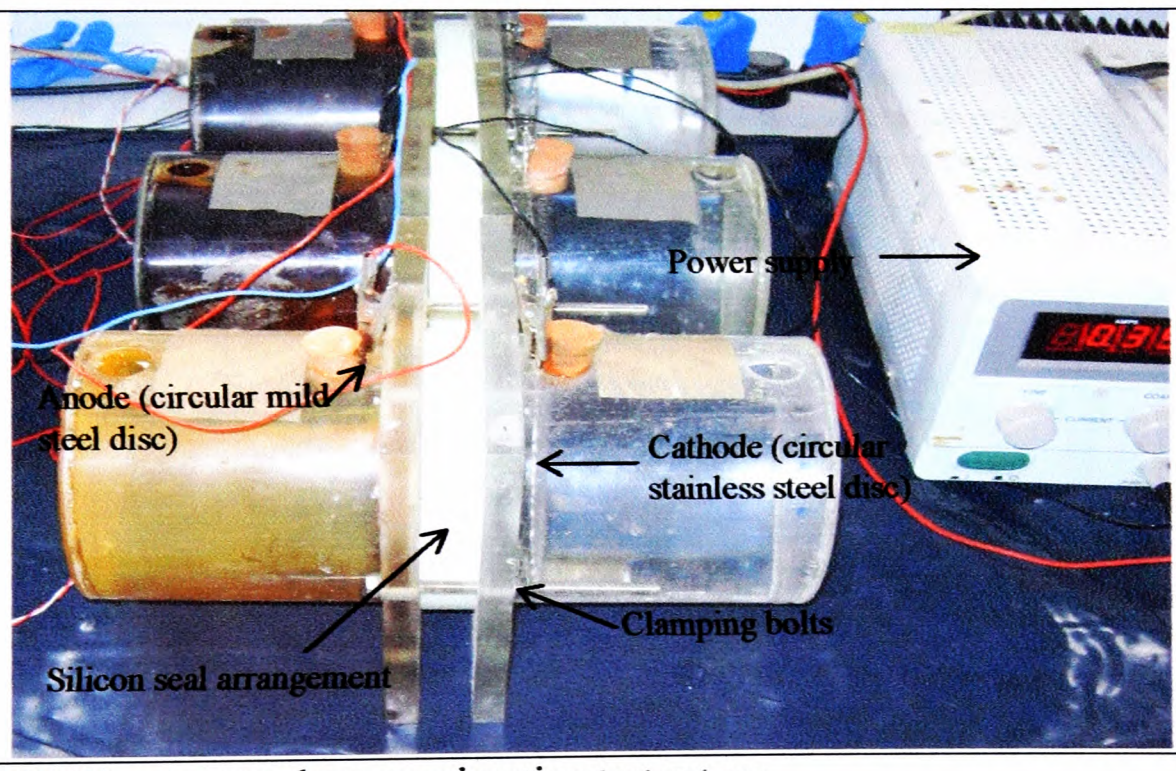

Figure 4.9 The non-steady state migration test set-up

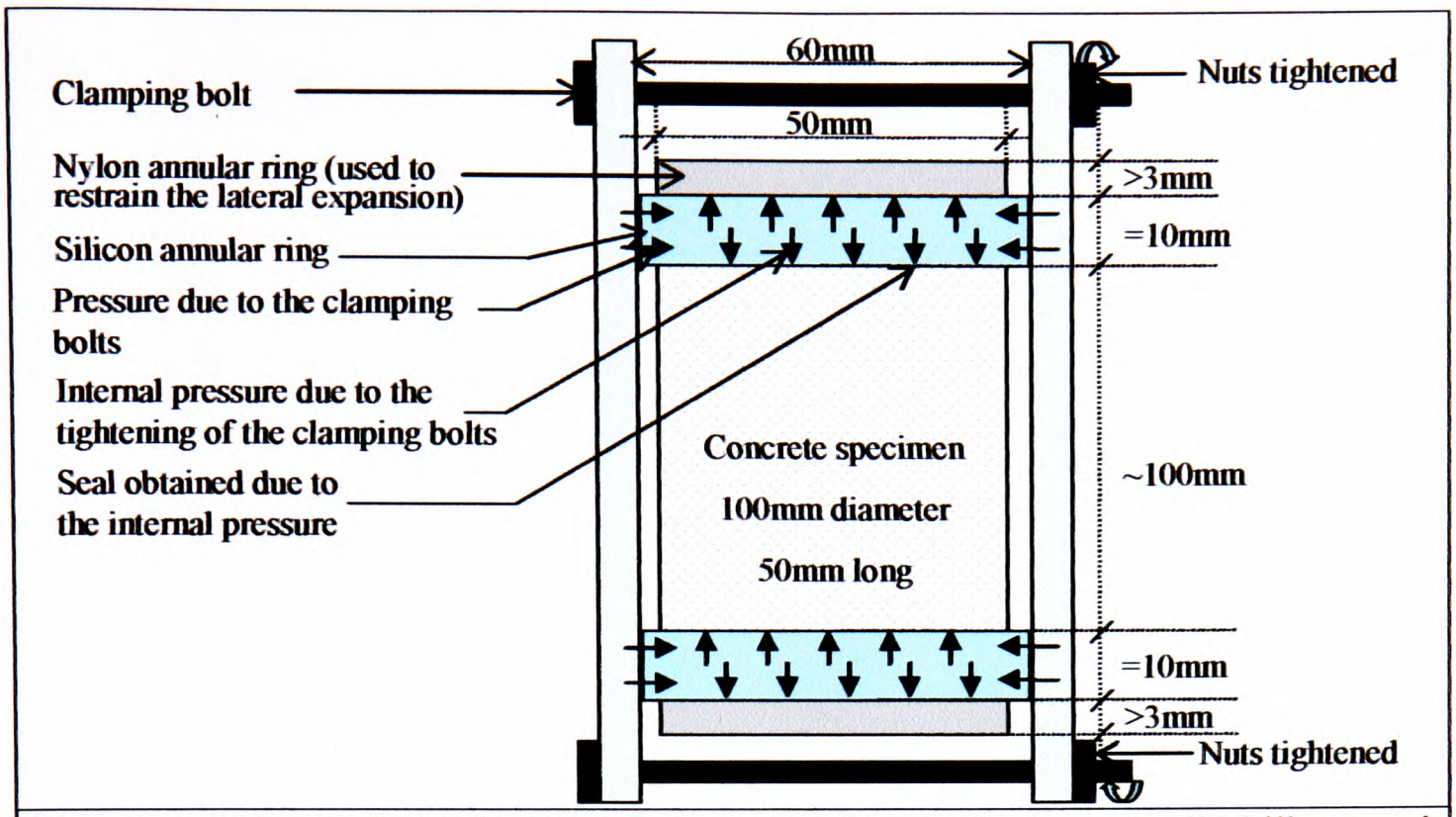

Figure 4.10 The method of sealing the concrete disc within the test cells (silicon seal arrangement, see Figure 4.7 and 4.8)

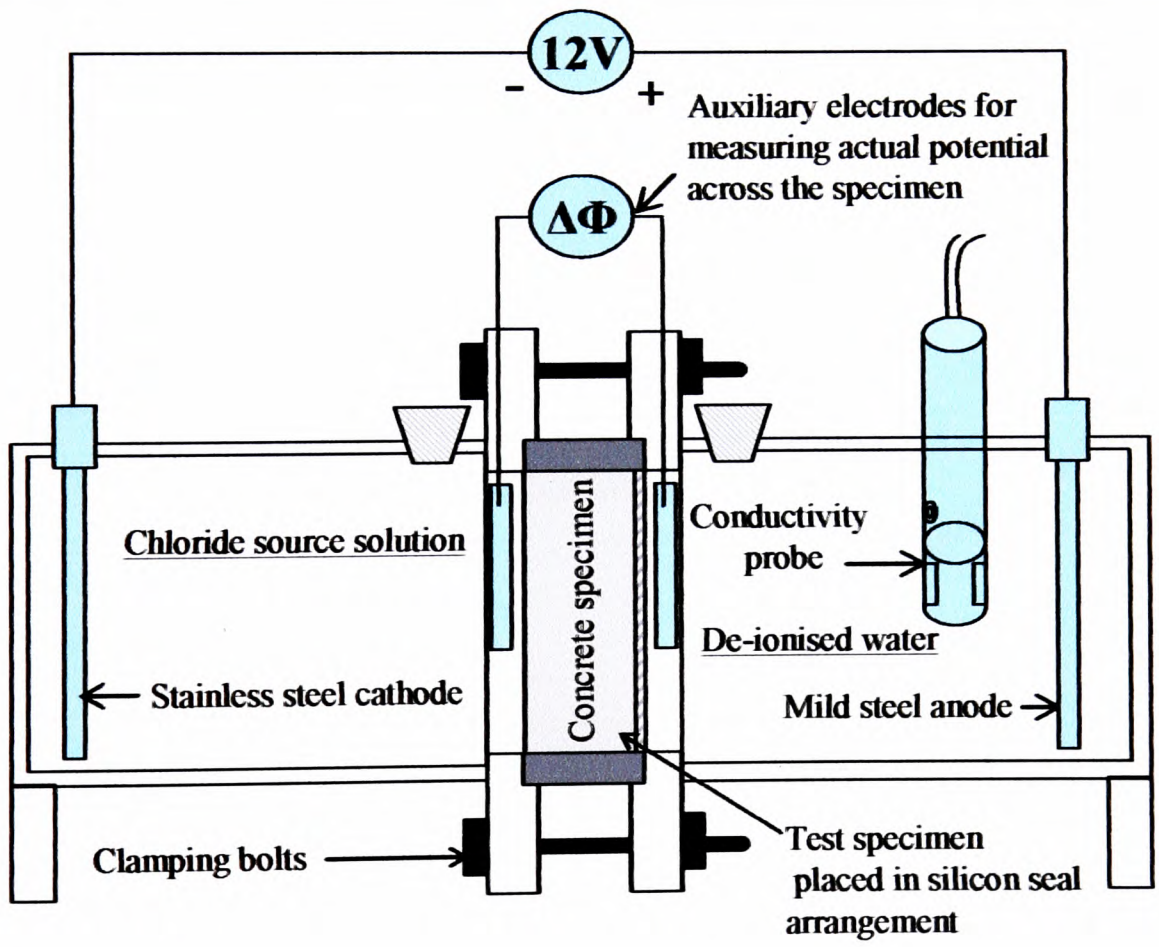

Figure 4.11 A schematic representation of the steady state migration test used in Evaluation Programme

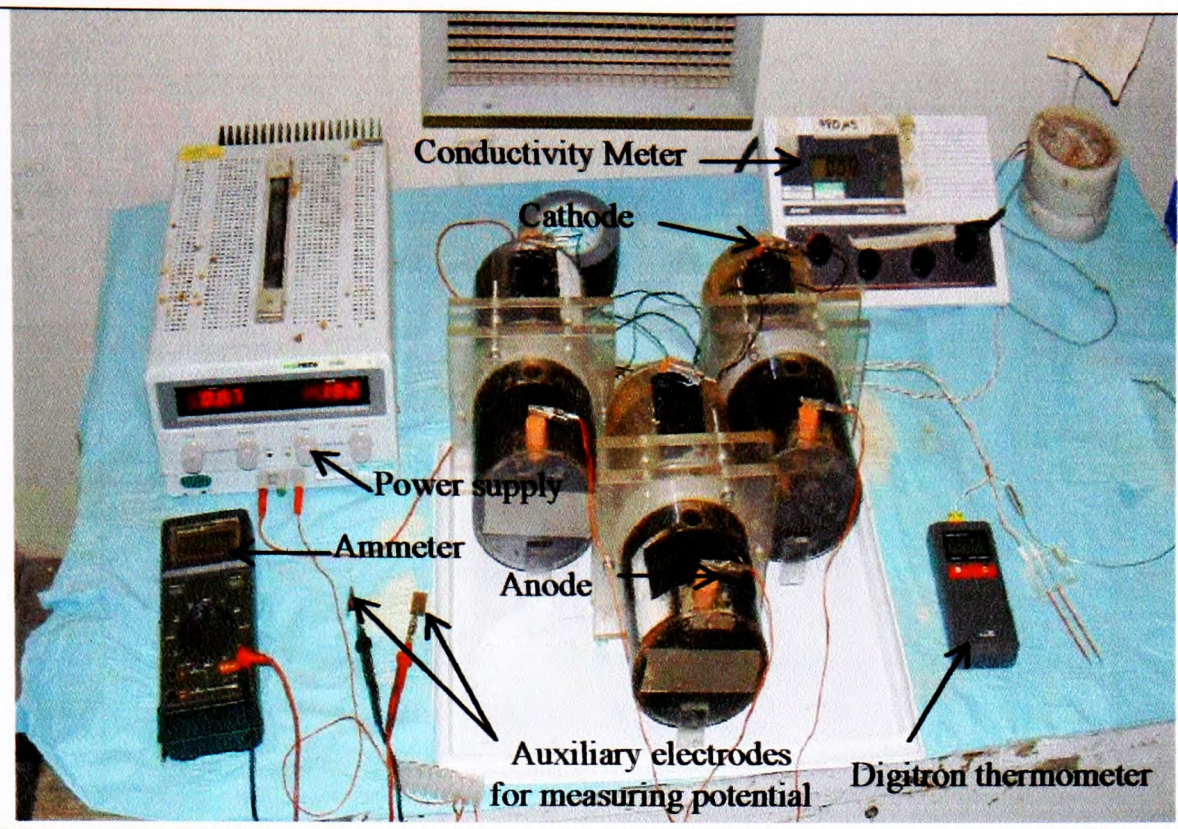

Figure 4.12 The steady state migration test set-up (The test apparatus is similar to the one shown in Figure 4.8. However, the electrodes are kept furthest from the specimen, and hence, temporary electrodes are used to measure the actual potential)

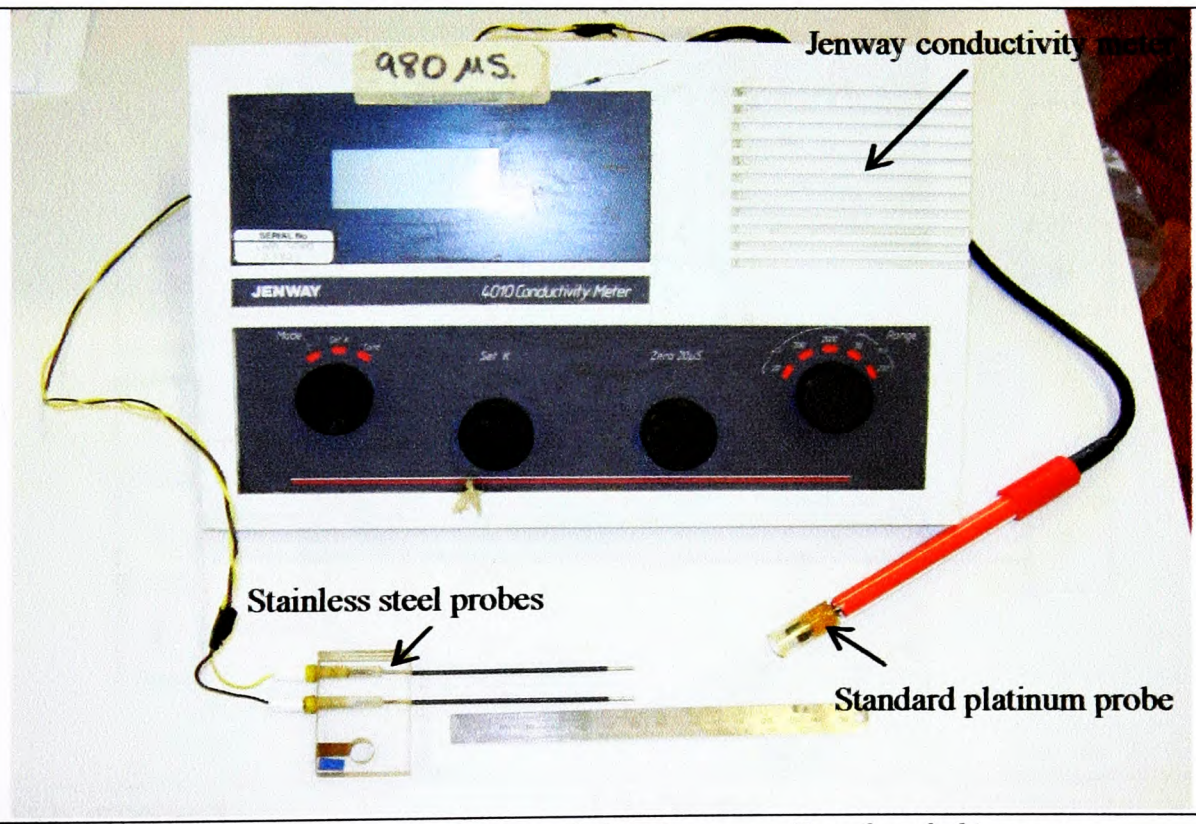

Figure 4.13 The conductivity probes and the Jenway Conductivity meter
Note: Platinum probe used in the Evaluation Programme and stainless steel probes used in the Validation Programme

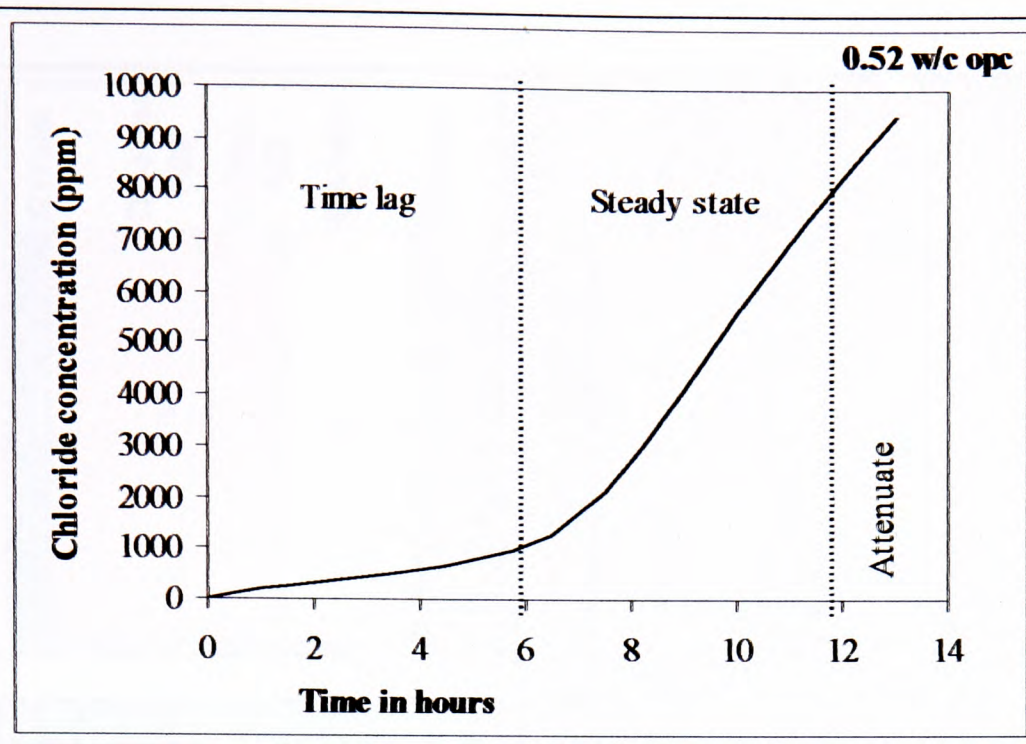

Figure 4.14 A typical concentration versus time plot from a steady state migration test

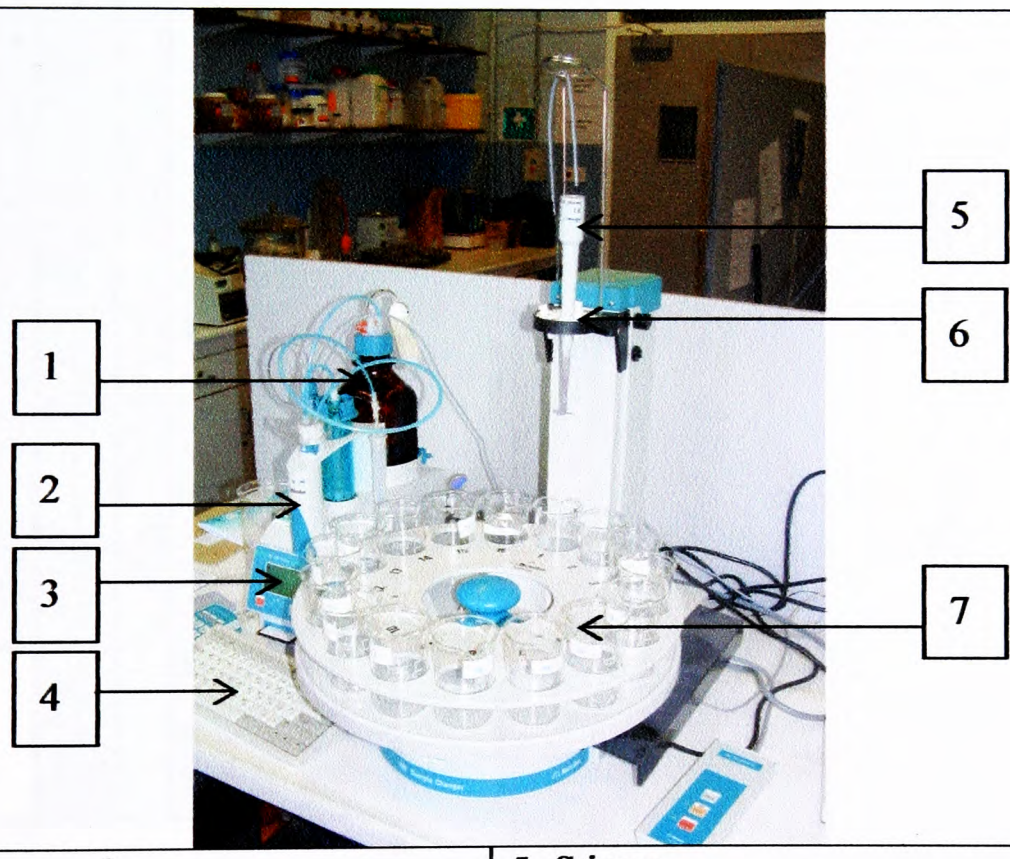

1: $AgNO_3$ reservoir	5: Stirrer
2: Electronic $AgNO_3$ dispenser	6: Vertical stand for electrode and Burette for dispensing $AgNO_3$
3: Control unit display	7: Automatic sample changer
4: Keyboard	

Figure 4.15 The Metrohm potentiometric titration device used for chloride analysis

Yield Equation: Mass of Constituents to yield $1m^3$ Concrete

INPUT DATA

RATIOS

Water/Binder	0.52
Aggregate/Binder	4.65
Fine Agg/Course Agg	0.55

Material	Specific Gravity
Fine Aggregate	2720
Course Aggregate	2900
Water	1000
Binder	3180
Binder Replacement	Microsilica
%	10
Super Plastisicer %	1

RESULTS

	Binder	Additive	Fine Agg	Course Agg	Water
Mass (Kg)	357.39	39.71	655.22	1191.31	206.49
Ratio	0.9	0.1	1.65	3.00	0.52
	10%	Microsilica	1.0%	3.971	S.P.

Specific Gravity of Various Additives

P.F.A.	2520
G.G.B.S.	2910
Metakaolin	2520
Microsilica	2200

Print Screen

DIAGRAMMATIC

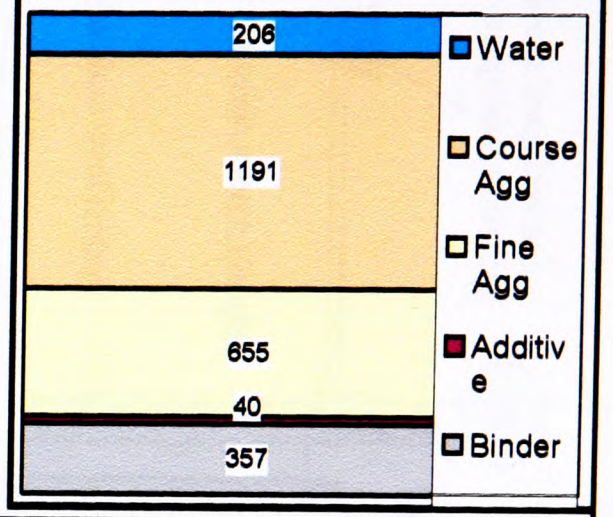

Calculations

$$Vol_{Binder} + Vol_{Additive} + Vol_{Fine\ Agg} + Vol_{Course\ Agg} + Vol_{Water} + Vol_{Super\ plast.} + Vol_{air} = 1m^3_{Concrete}$$

$$\frac{Mass_{Binder}}{S.G._{Binder}} + \frac{Mass_{Additive}}{S.G._{Additive}} + \frac{Mass_{Fine\ Agg}}{S.G._{Fine\ Agg}} + \frac{Mass_{Course\ Agg}}{S.G._{Course\ Agg}} + \frac{Mass_{Water}}{S.G._{Water}} + \frac{Mass_{Super\ Plast.}}{S.G._{Water}} + Vol_{air} = 1m^3_{Concrete}$$

$$Mass_{Binder}\left\{\frac{0.9}{3180} + \frac{0.1}{2200} + \frac{1.65}{2720} + \frac{3.00}{2900} + \frac{0.515}{1000} + \frac{0.01}{1180}\right\} + 0.01 = 1$$

$$Mass_{Binder}\{0.0002830 + 0.0000455 + 0.00060662 + 0.00103448 + 0.000515 + 0.0000085\} + 0.01 = 1$$

$$Mass_{Binder} = 397.1$$

Figure 4.16 Spreadsheet used for obtaining the mix proportions in the Validation Programme

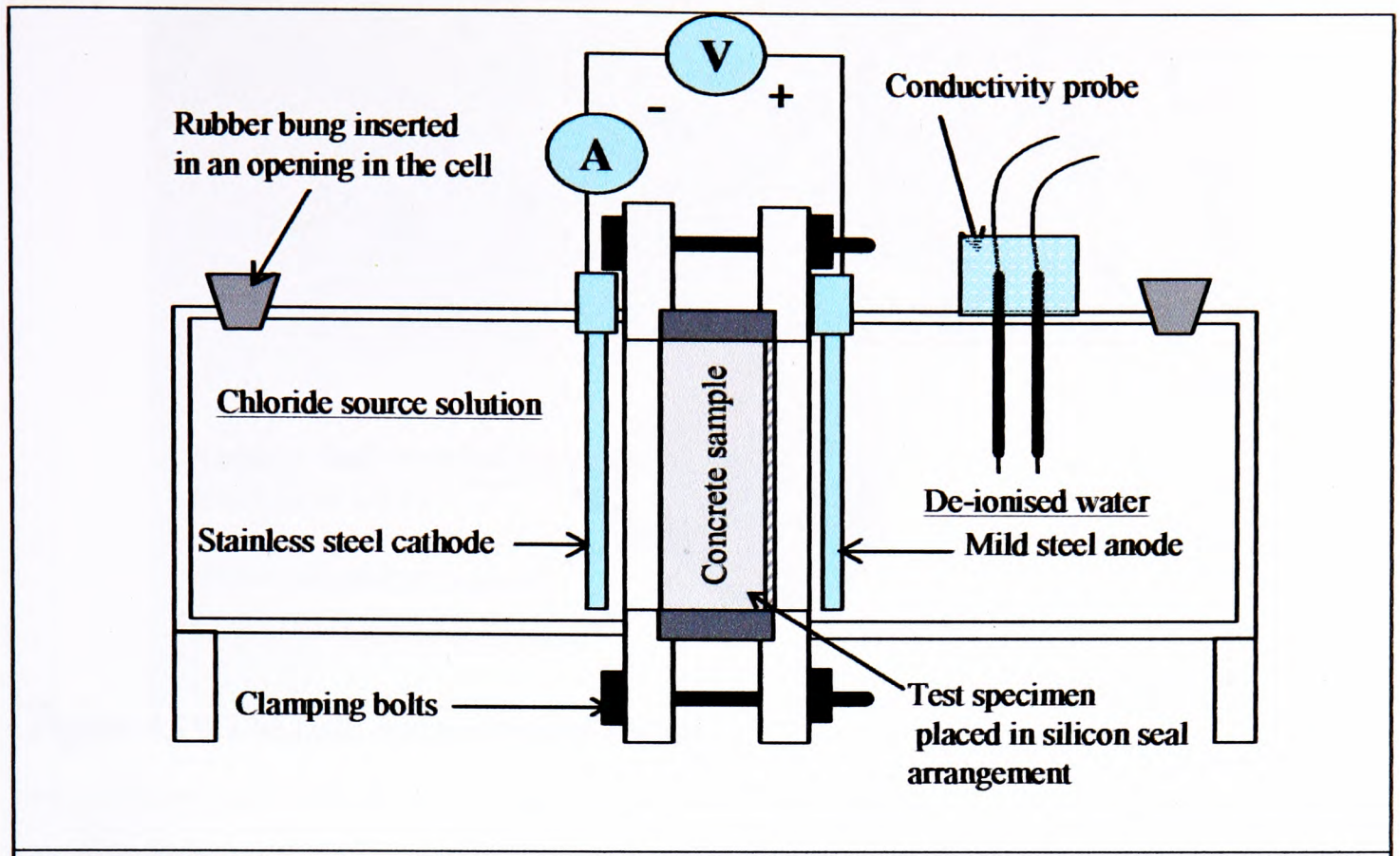

Figure 4.17 The schematic representation of the steady state migration test used in the Validation Programme

Figure 4.18 Wenner four probe resistivity test set-up

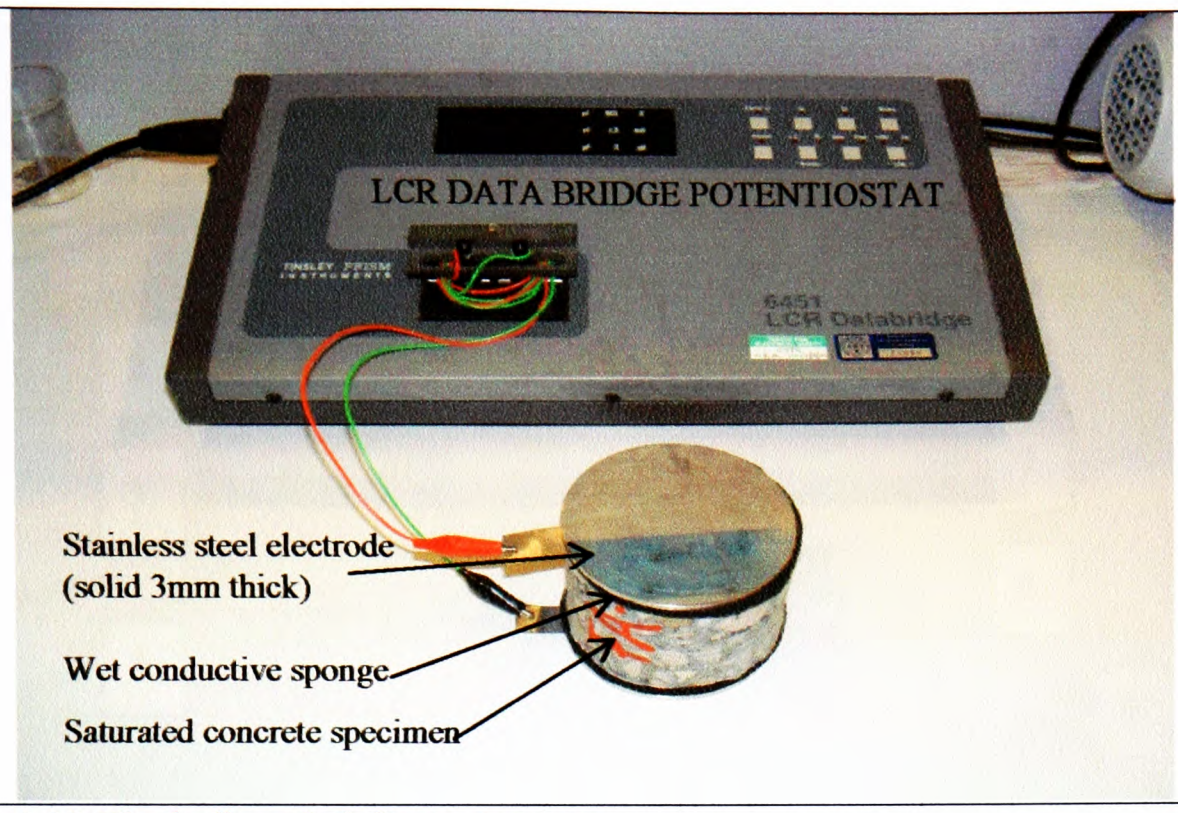

Figure 4.19 The bulk resistivity test set-up

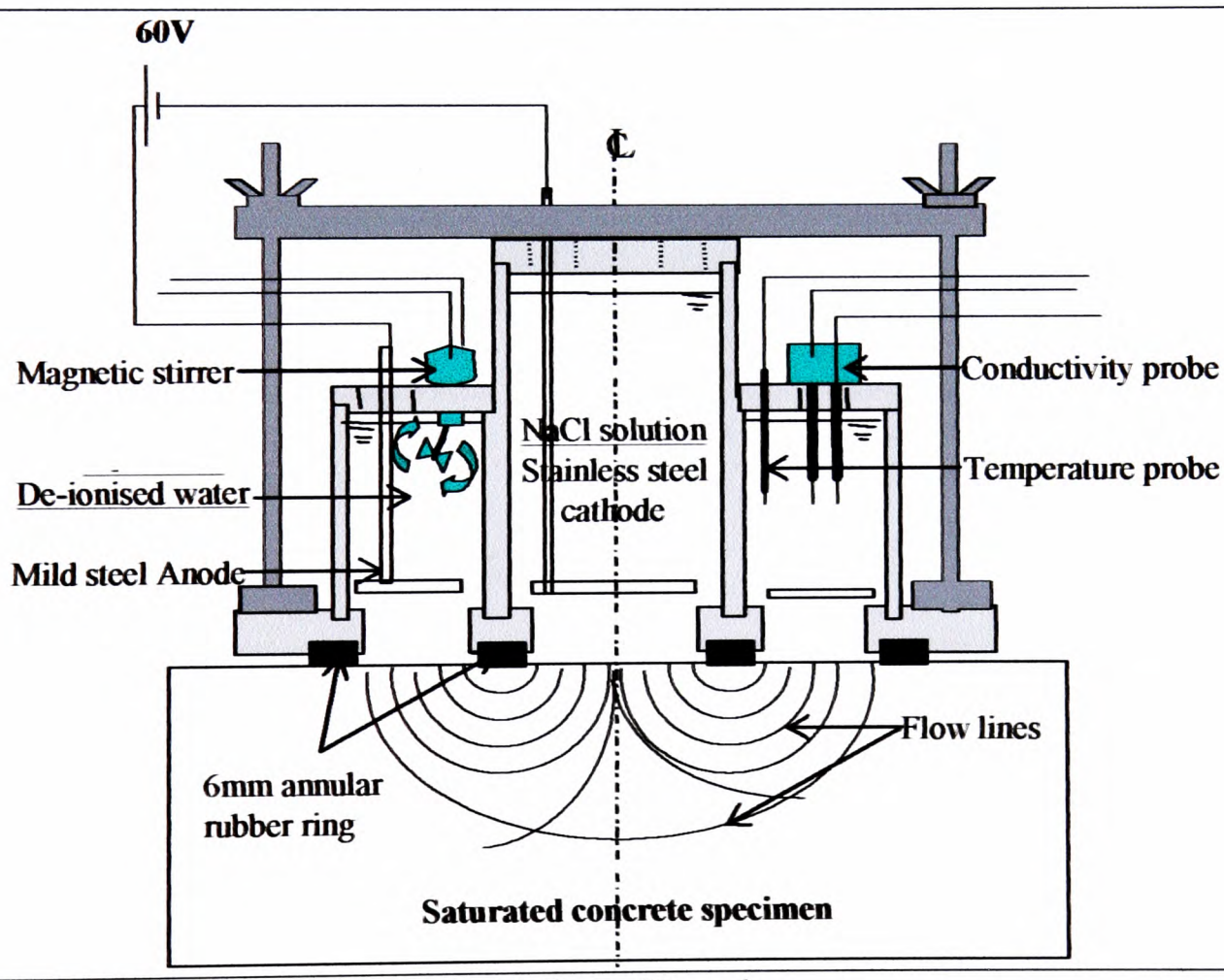

Figure 4.20 The schematic representation of Permit

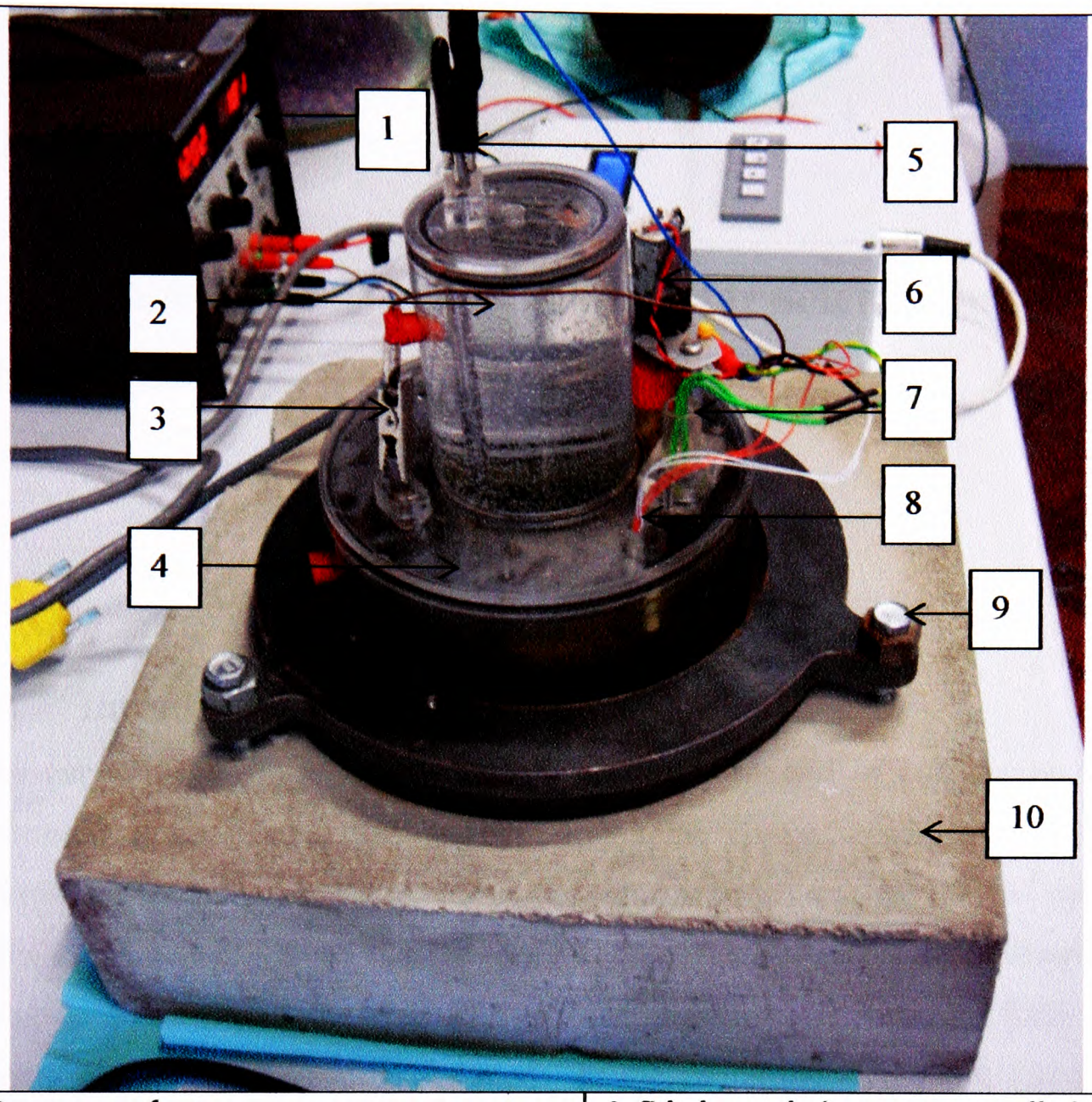

1: Power supply	6: Stirring unit (motor + propeller)
2: Inner cell (containing catholyte)	7: Conductivity probe
3: Connection to Anode	8: Temperature sensor
4: Outer cell (containing anolyte)	9: Clamping bolts
5: Connection to cathode	10: Saturated concrete specimen

Figure 4.21 The Permit ion migration test set-up

Chapter 5

An evaluation of rapid test methods for determining the chloride diffusivity

5.1 Introduction

The experimental programme was designed and executed in conjunction with a European Round Robin Test (RRT) Programme entitled 'Chlortest'. As stated previously in section 4.3.1, the Chlortest consortium comprised 17 EU members whose main task was to identify and propose test protocols for evaluating the chloride diffusivity of concrete. Although the primary objective of the RRT was to identify reliable lab based test methods for measuring the chloride diffusivity, the participation by Queen's University Belfast in the RRT provided an opportunity to carry out a detailed investigation of various test methods so as to arrive at relationships between various test parameters listed in section 5.1.2 and to propose a new protocol for the Permit ion migration test.

5.1.1 Objectives of the experimental programme

The main objectives of the experimental programme were:

1. To identify reliable and repeatable rapid test methods for measuring the chloride diffusivity and to compare the test parameters from each test so as to investigate their interdependence.
2. To explore the potential use of the rapid chloride transport tests for assessing the chloride ion diffusivity and to establish the limitations of each test.

Besides these objectives, the evaluation programme was used to develop a new testing protocol for the Permit ion migration test.

5.1.2 Test parameters and layout of experiments

Six test methods were selected in the first round of the evaluation programme by the Chlortest partners, but only four were considered for the detailed study due to their shortcomings, as stated in 4.3.1. These are: (i) non-steady state diffusion test (described in section 4.3.4.1), (ii) non-steady state migration test (described in section 4.3.4.2), (iii) steady state migration test (described in section 4.3.4.3) and (iv) electrical resistivity test (described in 4.3.4.4). Essentially the primary reasons for choosing them for the detailed study were that they were commonly used by the various research establishments across Europe and they had a theoretically sound test protocol.

The layout of the experiment is graphically presented in Fig. 5.1. Test parameters calculated from each of the tests are highlighted below.

Following parameters were obtained from curve fitting of the chloride profiles obtained from a non-steady state diffusion test:

- A non-steady state diffusion coefficient, D_{nssd}. (This is traditionally called the apparent diffusion coefficient, D_a.)
- A surface chloride concentration, C_s, by extrapolating the profile back to the y-axis.
- A penetration parameter, K_{cr}, using Eq. 4.7.

The method of calculating these parameters has already been discussed in section 4.3.4.1.

A non-steady state migration coefficient, D_{nssm}, was obtained from the depth to which the chloride front penetrated in a non-steady state migration test (as described in section 4.3.4.2). As the samples were saturated with $Ca(OH)_2$ solution, the electrical resistivity of the sample, ρ_{bulk}, was determined using a bridge potentiostat prior to mounting the samples to carry out the non-steady state migration test.

In the case of the steady state migration test (see section 4.3.4.3), a steady state migration coefficient, D_{ssm}, was obtained once a constant flow of chlorides across the samples was observed. This is sometimes designated by D_{mig}.

5.1.3 Mix variables

Ten concrete mixes commonly used in the EU countries represented by the Chlortest partners were selected for this investigation (see Table 4.1 in Chapter 4 for details of the mixes). This provided an excellent opportunity to study the performance of each test method on a good variety of concrete mixes. Amongst them, four concrete mixes containing normal Portland cement (opc) were used in the investigation to identify the effect of water-binder ratio on chloride diffusivity. The water-binder ratios (w/b) selected for the investigation were 0.35, 0.42, 0.45 and 0.50. The other six mixes contained cement replacement materials to substitute for the opc, viz. microsilica (ms) at 5% by weight of opc, pulverised fuel ash (pfa) at 18% and 39% by weight of opc and ground granulated blast furnace slag (ggbs) at 70% by weight of opc. For the concrete mixes containing cement replacement materials, the ratio of the quantity of the mixing water to the amount of binder (i.e. cement plus replacement) was expressed as water-binder ratio (w/b). The proportions of the ten mixes and their test ages have already been presented in Table 4.1.

5.2 Results and discussion

In this section, the results obtained from the tests are presented and discussed. The main emphasis of the discussion is on the evaluation of the effectiveness of the test methods in assessing the chloride diffusivity.

The effects of the mix variables, such as w/b and the type of binder, on the test parameters are discussed first, which is followed by a discussion on the relationships between the different test parameters. The inference from these two sections is made use of in proposing a new test protocol for the Permit ion migration test. However, in order to ensure the experimental procedures to be as reliable as possible, certain changes made during the experiments are presented first.

5.2.1 Experimental observations

During a typical non-steady state diffusion test, the exposure solution (which had an initial concentration of 165g/litre of NaCl) was found to precipitate. This process left flakes of concentrated salt floating on the surface of the solution, which was considered to be due to the evaporation of water from the solution. Although the

effects of this on the measurements were not studied, in order to eliminate any effect the solution was stirred periodically on a daily basis and the box containing the cells were kept air tight to avoid any evaporation.

For both the steady and the non-steady migration tests, NaCl precipitation could occur at the upstream cell surface. This precipitation could be due to the evaporation of water from the upstream cell and hence care was taken to eliminate any such evaporation. Further, the break down of water in the upstream cell could cause a reduction in the solution volume (Prince and Gagne, 2001).

$$2H_2O + 2e^- \rightarrow H_2 \uparrow + 2(OH)^- \qquad \text{(Eq. 5.1)}$$

In such cases, it has been recommended that an average concentration of the upstream solution should be used for calculating the migration coefficient (Prince and Gagne, 2001). Although the average concentration was used in calculations for both steady and unsteady state migration tests, this phenomenon was observed mostly in the steady state migration tests.

The opc 0.42 specimens contained longer cavities, not evenly distributed. As a result, the specimens used for different test methods were not uniform in porosity.

5.2.2 Influence of mixes on test parameters

The influence of mix properties on chloride diffusivity of concrete has already been discussed in section 2.6. It was reported that the main mix factors affecting the diffusivity are the water/binder, the type of binder, the aggregates and the type of curing. However, it was not possible to discuss the effect of curing due to the lack of this information from the manufacturers of the concrete specimens. Therefore, the discussion of results here focuses mainly on the w/b ratio and the type of binder. Ideally it would have been better to have the same aggregate-cement ratio and the size of both fine and coarse aggregates in order to discuss the effect of the w/b and type of binder, but all these varied to some extent in the mixes tested because the mixes were manufactured at four different countries. These variations are highlighted before discussing the effects of mixes on test parameters.

Noticeable differences in aggregate size and proportions were present in opc 0.45, pfa 0.45 and ggbs 0.45 mixes (Table 4.1). In these mixes, a finer sand (≤ 6mm) was used compared to other mixes (≤ 8mm). Maximum size of the coarse aggregate used in pfa 0.45 mix was 25mm, while for all the other mixes it was closer to 15mm. The coarse aggregate to fine aggregate ratio was 0.88, 0.92, 1.2, 1.38, and 1.76 respectively for opc 0.50, opc 0.42, ggbs 0.45, opc 0.45 and pfa 0.45 mixes, and for other mixes, the ratio was 1.

All these variations might have contributed to the variations in diffusion/transport properties observed between different mixes. However, there was no way to isolate the individual contributions of various mix ingredients and, hence, these are not discussed here.

As an average of three results is reported for each measured parameter, the standard error (i.e. one standard deviation on either side of the mean) of the results is also reported in this section. This is used to highlight the repeatability of each test method. The average value of each test parameter along with the corresponding standard error is presented in Table 5.1.

5.2.2.1 Effect of mix variables on D_{nssd}, C_s and K_{cr}

Effect on D_{nssd}

The effect of the w/b and the type of binder on the non-steady state diffusion coefficient, D_{nssd}, is presented in Fig. 5.2 and Fig. 5.3 respectively. In Fig. 5.2, for each cement type, as the w/b increased the D_{nssd} also increased, with the exception of opc 0.42 mix. This trend was similar to the results reported by Kropp and Hilsdorf, (1995) and Xi *et al.*, (1994) and is considered to be due to the increased porosity with increase in w/b. As highlighted earlier, the opc 0.42 mix was highly porous, which is considered to be the reason why this mix did not follow the general trend. In this case the variability of the data (i.e. the standard error) was also higher compared to other mixes. For concretes containing supplementary cementitious materials, the influence of w/b was found to be significant in all cases. Lower diffusivity was observed for samples with lower w/b.

As far as the effect of type of binder is concerned, the lowest D_{nssd} was obtained for ggbs 0.42 sample, where the D_{nssd} was 1.31 x 10^{-12} m^2/s. The D_{nssd} obtained for pfa 0.42 and ms 0.40 samples was also lower, 1.44 x 10^{-12} m^2/s and 1.61 x 10^{-12} m^2/s respectively. Similar trends were obtained by Gilleece, (1996) and Nilsson *et al.*, (2000). Gilleece, (1996) found in his study of concrete mixes (w/b 0.52) subjected to cyclic ponding that the apparent diffusion coefficient obtained for ggbs concrete (50% cement replacement) was the lowest, followed by pfa concrete (30% cement replacement), ms mix (10% cement replacement) and opc. The results presented in Fig. 5.3 for w/b 0.42 and w/b 0.45 shows the same trend as reported by Gilleece, (1996). Nilsson *et al.*, (2000) reported a slightly lower apparent diffusion coefficient for ms concrete over the ggbs concrete at lower w/b (0.30). However, the trend got reversed at a higher w/b < 0.40 and in both types of binder there was an increase in diffusivity with increase in w/b.

The parameters reported in Figs. 5.2 and 5.3 are an average of three and the variation between the parameters is reported using the error bar. The standard error associated with opc 0.42 mix is much higher compared to other mixes. As mentioned earlier, the opc 0.42 concrete specimens contained larger and unevenly distributed cavities, which could have influenced their test parameters. The standard error associated with the mixes opc 0.45 and pfa 0.45 was relatively high. Interestingly these two concretes had more coarse aggregate compared to fine aggregate. As the D_{nssd} was calculated from the curve fitting of chloride profiles, the spatial variation of the profiles could have an effect on the coefficient obtained (Bentz and Feng, 2000; Nilsson *et al.*, 2000). For example, if the chloride content was determined from dust samples taken from an area with a higher aggregate concentration, the corresponding chloride content would be lower and hence the resulting profile would give a lower value of the diffusion coefficient.

Effect on C_s

The surface chloride concentrations determined by fitting curves to the chloride profiles are presented in Figs 5.4 and 5.5. The Fig. 5.4 suggests that the effect of w/b on the C_s was not apparent for any of the mixes. Even though the mean C_s values for pfa, ggbs and ms mixes indicate a decrease in trend with an increase in w/b, the results are not conclusive due to the high variability of the C_s values. This means that

no conclusion can be reached on the effect of w/b on C_s values. Nevertheless, the mean values can be used to discuss the effect of the binder on the C_s value (see Fig. 5.5), which is discussed next.

The high amount of the aluminate phase in pfa samples might have resulted in the binding of more chloride ions to form chloroaluminates (Delagrave *et al.*, 1997), which is considered to be the reason for the C_s value to be the highest for pfa mix. The lowest C_s was observed in the case of ggbs sample presumably due to the dense microstructure of this type of concrete as reported by Roy, (1989b). The difference in C_s between the mixes would indicate their relative ability to bind more chloride ions (CHLORTEST, 2006).

Effect on K_{cr}

The effect of w/b on the penetration parameter K_{cr} is presented in Fig. 5.6 and the effect of type of binder on the parameter is presented in Fig. 5.7. These figures suggest that the effect of w/b and type of binder on K_{cr} is the same as that obtained for D_{nssd} (see Figs. 5.2 and 5.3). The standard error for all mixes is lower than the corresponding values for D_{nssd}. K_{cr} is proportional to the square root of D_{nssd}, which means that theoretically the standard error in K_{cr} should be half of the standard error in D_{nssd}.

5.2.2.2 Effect of mix variables on D_{nssm}

The non-steady state migration coefficient, D_{nssm} for the mixes are presented in Fig. 5.8 and Fig. 5.9. It can be seen that D_{nssm} follows a very similar trend to that of D_{nssd} (see Figs. 5.2 and 5.3). In Fig. 5.8, for each cement type, as the w/b increased the D_{nssm} also increased, with the exception of 0.42 opc mix. As discussed earlier, this is considered to be due to the increased porosity with the increase in w/b. As previously mentioned, the opc 0.42 mix was highly porous and, hence, this mix showed the highest D_{nssm}.

For concretes containing cement replacement materials, the D_{nssm} increased in the following order of mixes: ggbs, pfa, ms and opc (see mixes with w/b 0.42 and 0.45 in Fig. 5.9). The lowest D_{nssm} was for ggbs 0.42 mix, this could be due to the dense microstructure of this type of concrete as reported by Roy (1989b).

The standard errors associated with the parameters for the opc 0.42 and the opc 0.45 were higher compared to that for all other mixes. In general, the standard error associated with D_{nssm} was comparatively lower than that associated with D_{nssd}. As discussed before, the spatial variations of chloride concentrations (and hence the chloride profiles) might be the reason for the higher standard error obtained for D_{nssd}, where as in the D_{nssm}, the chloride penetration depth was measured along the colour change boundary avoiding the aggregates (i.e. if an aggregate was present on the colour change boundary, the depth measurements were taken on both sides of the aggregate).

5.2.2.3 Effect of mix variables on D_{ssm}

The steady state migration coefficient, D_{ssm} for all the mixes are presented in Figs. 5.10 and 5.11. The effect of w/b was not obvious for the opc mixes, but a decreasing trend with an increasing w/b could be seen if the data for the opc 0.42 was neglected. The D_{ssm} value decreased with the increase in w/b for both the pfa and the ggbs mixes, but a substantial increase in D_{ssm} with an increase in w/b was observed for ms mixes. CHLORTEST, (2006), consortium also reported similar trends. However, previous research work by Halamickova *et al.*, (1995); Delagrave *et al.*, (1996) and Tong and Gjorv, (2001) found that D_{ssm} increases with an increase in w/b. A close examination of their work indicated that in all cases the sample thickness was greater than three times the maximum aggregate thickness, as suggested by Nilsson *et al.*, (1996) in order to eliminate the influence of the aggregate-paste interfacial transition zone on the transport of chloride ions. However, the thickness of specimens used in this study was 20mm, as recommended in the protocol for the Chlortest project. With the maximum aggregate size of 15mm in most cases and 25 mm for the pfa 0.45 mix, the aggregate-paste interface might have influenced the flow of chloride ions when the sample thickness was 20mm (i.e. less than three times the aggregate size). As the objective of the study was to compare different test methods, no further investigations were carried out to eliminate this effect, but for the results reported in Chapter 6 the specimens were cast at Queen's University Belfast and the thickness of the specimens used was three times the maximum aggregate size.

The mixes containing supplementary cementitious materials showed a reduced diffusivity compared to the opc mixes, except ms 0.42 sample. The coefficient D_{ssm} for ms 0.40 was the lowest and this could be due to the dense and less permeable microstructure associated with such concretes (Roy, 1989a). However, the D_{ssm} for ms 0.42 was the highest. As the microstructure of the concrete specimens was not studied, it is difficult to comment further on this high variation. For w/b 0.42, the D_{ssm} was the highest for ms, followed by opc, pfa and ggbs in decreasing order. As mentioned earlier, the dense microstructure in the case of concretes containing ggbs might have resulted in the reduction of chloride ion transport, thus resulting in a very low D_{ssm}. In the case of concretes containing pfa, the higher alumina content could increase the binding capacity, as discussed previously. The chloroaluminates formed due to the binding could get deposited in the available pore spaces, thus blocking the pores for further transport of chloride ions and thereby reducing the D_{ssm}.

The opc 0.35 mix showed a much higher D_{ssm} compared to all other mixes, except ms 0.42. As previously discussed, the decrease in w/b decreases the porosity of concrete and thereby decreases the diffusivity of concrete. Therefore, the increase in D_{ssm} for opc 0.35 compared to all other opc mixes of higher w/b was not expected.

5.2.2.4 Effect of mix variables on ρ_{bulk}

The bulk resistivity, ρ_{bulk} for all the mixes are presented in Figs. 5.12 and 5.13. In the bulk resistivity test, the current is carried by ions dissolved in the pore liquid. As the concrete specimens were saturated with $Ca(OH)_2$ solution prior to testing, the flow of current then depends on how wide and interconnected pore networks are (Polder, 2001). With the increase in w/b the porosity also increases, thus increasing the current flow. The higher the current flowing the lower is the resistivity of the material. That is for concretes with higher w/b the resistivity should decrease. In the case of concretes containing the supplementary cementitious materials, these pores are generally discontinuous, either due to the dense microstructure or due to the hydration products blocking the existing pores. Therefore, the resistivity of such concretes will be higher. The bulk resistivity is inversely related to the diffusivity of concrete (Andrade *et al.*, 2000). Therefore, the trend expected in the case of bulk resistivity would be the inverse to that of the diffusion parameters.

The effect of w/b on mixes was apparent (see Fig. 5.12), i.e. the ρ_{bulk} increased with a decrease in w/b, except for opc 0.35 and opc 0.42. The low ρ_{bulk} for opc 0.35 suggests that the diffusivity of the material would be high. As highlighted in the previous section, in fact the diffusivity D_{ssm} of this mix was very high, which was opposite to the trend that would be expected for this mix. Similar to the discussions in D_{ssm}, it is not possible to provide an explanation for the low value of ρ_{bulk} for opc 0.35 within the scope of this study. In the case of the opc 0.42 mix, the porous nature might have resulted in the lower ρ_{bulk}. For concretes containing the supplementary cementitious materials, the effect of w/b on the resistivity was apparent, the ρ_{bulk} decreased with an increase in w/b. However, for the pfa mixes the difference was negligible and it is highly likely that this was caused by the reason given next. The coarse aggregate to fine aggregate ratio of the pfa 0.45 was 1.76 compared to 1 for pfa 0.42. The resistivity of the coarse aggregate is much higher compared to the cement gel. In such a case, the pfa 0.45 with more coarse aggregates can be expected to have higher resistivity than a similar mix with less coarse aggregates.

The effect of the type of binder on the ρ_{bulk} is presented in Fig. 5.13. For w/b 0.42 the resistivity changed in the following order: opc>ms>pfa>ggbs. The trend was similar for w/b 0.45 as well. The ρ_{bulk} of concretes containing supplementary cementitious materials were generally higher than that for the corresponding opc concrete, presumably due to the reasons discussed earlier. Polder (1995) studied the electrical resistivity of concretes using embedded electrodes. Concrete mixes examined were opc (w/b 0.43) and concretes containing ggbs (w/b 0.43), pfa and ms together (w/b 0.43) and ms (w/b 0.43). The author observed that the resistivity increased in the following order: opc>ms>pfa>ggbs. The trend shown in Fig. 5.13 for both w/b 0.42 and 0.45 confirms the findings by Polder (1995).

5.2.2.5 Discussion on the diffusion parameters

The effect of w/b and type of binder on the diffusion parameters were discussed earlier. The effect of w/b on both D_{nssd} and D_{nssm} was similar, as discussed earlier. Both the parameters increased with the increase in w/b, except opc 0.42. In general, both parameters decreased for concretes containing supplementary cementitious materials compared to the corresponding opc concrete. Therefore, it can be

concluded that the non-steady state migration test and the non-steady state diffusion test determines the diffusivity of concrete in a similar manner and both vary similarly with the variations in the mix, such as the w/b and the type of binder. However, the standard error associated with the D_{nssm} was generally lower compared to D_{nssd}, which signifies that the non-steady state migration test can be used to substitute the non-steady state diffusion test.

The effects of w/b and type of binder on D_{ssm} were not apparent. The expected trend was that with the increase in w/b D_{ssm} should increase. Instead of this trend, the D_{ssm} for most mixes increased with the decrease in w/b. The presence of supplementary cementitious materials generally decreased the D_{ssm} compared to the opc counterpart, except in the case of ms 0.42. Although this trend was similar to the one obtained for D_{nssd} and D_{nssm}, it was not possible to distinguish the effect of w/b for each type of binder in the case of D_{ssm}.

As discussed earlier, the non-expected fluctuations in the D_{ssm} could have resulted from carrying out the steady state migration test with a 20mm thick specimen when the maximum aggregate size was 15mm and 25 mm. Therefore, it is considered that the test should be carried out with a thicker specimen (at least three times the maximum size of aggregate) in order to obtain reliable results.

The bulk resistivity ρ_{bulk} showed an inverse trend compared to the diffusivity parameters. The ρ_{bulk} decreased with an increase in w/b, except for opc 0.35 and opc 0.42. With the increase in w/b the ρ_{bulk} decreased and in the case of concretes containing supplementary cementitious materials the resistivity generally followed an increasing trend with the w/b. The standard errors associated with the mean value were low. Therefore, it can be concluded that the ρ_{bulk} can be used to identify the effect of mix variables on diffusivity of concretes.

5.2.3 Relationships between different test parameters

As mentioned in section 4.3, the concrete cores were cut from test slabs which were cast by the ready mix companies in Spain, Sweden and the Netherlands. Therefore, the project partners in the EU Chlortest programme did not have any control on both

the quality of the concrete supplied and the casting of the test specimens. From the point of view of a discussion of the mix ingredients on the measured properties, variations in aggregate size and the lack of information on curing (both of which are known to influence the chloride transport) limited any in-depth discussion. Furthermore, when the cores received were inspected, it was observed that some of them contained large and unevenly distributed cavities. This might have influenced most of the test results, and in particular, those from the steady state migration test, as a thinner concrete disc was used in this case compared to the other tests. However, due to the requirement to carry out tests on all concrete cores in the EU Project, the work was continued as planned. Given the limitations of the specimens received, it was necessary to isolate the outliers from the data before trying to establish relationships between measured properties.

From the visual inspection of the specimens, it was identified that specimens from the opc 0.42 mix contained large cavities, which were not evenly distributed. As a result, the specimens used for different test methods were not uniform in porosity. Therefore, results from this mix are considered as an outlier and were subsequently eliminated from the study of relationships. In addition, due to the reasons given in section 5.2.2.3 two more mixes (opc 0.35 and ms 0.42) were considered as outliers in the case of the steady state migration test. Therefore, these mixes are also not included in the analysis of the relationships between measured properties. The relationships between different diffusivity parameters obtained are presented in the following sections:

5.2.3.1 Relationship between D_{nssd} and D_{nssm}

The relationship between non-steady state diffusion coefficient, D_{nssd} and non-steady state migration coefficient, D_{nssm} is presented in Fig. 5.14 from which the following empirical equation was obtained.

$$D_{nssd} = 0.97 \, x \, D_{nssm} \qquad \text{(Eq. 5.2)}$$

where the unit of D_{nssd} and D_{nssm} is in m^2/s.

Due to the reasons mentioned earlier the opc 0.42 specimen was eliminated from the regression analysis. A coefficient of determination R^2 for the relationship was 0.93,

which suggests that for all practical purposes, the non-steady state migration test can be used as a substitute for the non-steady state diffusion test, with 93% confidence.

A similar relationship was reported by CHLORTEST (2006) and by Tang and Sorensen (2001). Furthermore, the D_{nssm} was recommended as a reliable substitute for the D_{nssd}. However, the results reported by Baroghel-Bouny *et al.* (2002) suggest that although D_{nssm} follows a similar trend to D_{nssd}, the former coefficient is always higher than the latter. This could be either due to the differences in either the test set-up or the concentration of the exposure solution. Baroghel-Bouny *et al.* (2002) used 0.51M NaCl solution, where as in this research work 2.8M and 2M NaCl solutions were used as exposure solutions for the non-steady state diffusion test and the non-steady state migration test, respectively.

Nevertheless, the results in this study indicate that the diffusivity of concrete can be evaluated rapidly using the non-steady state migration test and the D_{nssm} can be used as an alternative to D_{nssd} from the non-steady state diffusion test.

5.2.3.2 Relationship between D_{nssd} and D_{ssm}

Figure 5.15 shows the relationship between the non-steady state diffusion coefficient and the steady state migration coefficient. The Fig. 5.15 shows a reasonable correlation with a coefficient of determination R^2=0.68. The empirical relationship is given by the equation:

$$D_{nssd} = 9.6 \, x \, D_{ssm} \qquad \text{(Eq. 5.3)}$$

where the unit of D_{nssd} and D_{ssm} is in m^2/s.

The coefficients in Eq. 5.3 differ by a magnitude of 9.6. However, none of the mixes with cement replacement materials was closer to the regression line. Therefore, this relationship has limited use for any practical applications.

The relationship between the non-steady state diffusion coefficient and the steady state diffusion coefficient as proposed by Nilsson *et al.* (1996) is given below.

$$D_{nssd} = \frac{D_{ssd}}{\varepsilon \left(1 + \frac{\partial c_b}{\partial c_f}\right)} \qquad \text{(Eq. 5.4)}$$

where,

D_{nssd} is the non-steady state diffusion coefficient, m^2/s

D_{ssd} is the steady state diffusion coefficient, m^2/s

ε is the volumetric porosity,

$\frac{\partial c_b}{\partial c_f}$ is the binding capacity.

That is, the non-steady state diffusion coefficient is a function of the porosity of the concrete, the binding capacity and the steady state diffusion coefficient. Therefore, Eq. 5.4 suggests that a lower D_{nssd} could be obtained for concrete mixes with higher binding capacity such as ggbs and pfa. As the presence of such mineral additives reduces the porosity of concrete by the pozzolanic reaction, the resulting non-steady state diffusion coefficient (D_{nssd}) could be considerably low. Similarly higher D_{nssd} could be obtained for more porous concretes.

The results reported by Baroghel-Bouny *et al.* (2002) and Delagrave *et al.* (1996) support the above effects of both the porosity and the binding capacity. In their case, whilst the difference between D_{nssd} and D_{ssm} increased with increased porosity, the increased binding in concretes reduced the difference between both the coefficients. The above discussion can thus be used to explain the trend seen on Fig. 5.15, where the concretes containing the supplementary cement replacement materials showed a lower D_{nssd} compared to the opc only concretes.

5.2.3.3 Relationship between D_{nssm} and D_{ssm}

The relationship between D_{nssm} and D_{ssm} is presented in Fig. 5.16. Two of the outliers excluded from the regression analysis are the opc 0.35 and the ms 0.42 mix, in addition to the porous mix, opc 0.42. The relationship in Fig. 5.16 is:

$$D_{nssm} = 10.48 \, x \, D_{ssm} \qquad \text{(Eq. 5.5)}$$

where D_{nssm} and D_{ssm} are in m^2/s.

A closer examination of Fig. 5.16 would reveal that although there appear to have a reasonably acceptable relationship between the two coefficients, there are two data clusters, one representing the opc mixes and the other representing the mixes containing cement replacement materials. As explained in section 5.2.3.2, the lower

values of D_{nssm} and D_{ssm} for mixes containing cement replacement materials might have been the result of improved binding effect on the diffusivity for these mixes. However, for each of the data clusters, it is impossible to identify a clear trend between the two coefficients. This is considered to be due to the limitation of the D_{ssm} results, caused by the use of thin samples for the steady state migration test. Therefore, it is not advisable to conclude from the results in Fig. 5.16 that D_{nssm} is an alternative for D_{ssm}.

5.2.3.4 Relationship between D_{ssm} and ρ_{bulk}

The relationship between D_{ssm} and ρ_{bulk} is presented in Fig. 5.17, which shows an inverse relationship between the two parameters. The outliers excluded from the regression fit are the opc 0.35 and the ms 0.42 mix in addition to the porous opc 0.42 mix. The relationship between the two parameters is given by the equation:

$$\rho_{bulk} = 197.02 \, x \, D_{ssm}^{-0.76} \qquad \text{(Eq. 5.6)}$$

where ρ_{bulk} is in ohm.m,

and D_{ssm} is in m^2/s.

The coefficient of determination R^2 obtained was 0.37.

Andrade *et al.* (2000) suggest that the steady state migration coefficient can be calculated from the resistivity of concrete. The relationship suggested by Andrade *et al.* (2000) is given below:

$$\rho_{bulk} = 120 \, x \, D_{ssm}^{-1} \qquad \text{(Eq. 5.7)}$$

where ρ_{bulk} is bulk resistivity in ohm.m,

and D_{ssm} is the steady state migration coefficient (Catholyte 1M NaCl) in m^2/s.

Both Eqs. 5.6 and 5.7 suggest that the steady state migration coefficient can be calculated from the electrical resistivity of the concrete, but the degree of dependence in Fig. 5.17 is weak. This is considered to be due to the limitations of the D_{ssm} in this investigation (see section 5.2.2.3)

5.2.3.5 Relationship between D_{nssd} and ρ_{bulk}

The bulk resistivity ρ_{bulk} is plotted against D_{nssd} in Fig. 5.18. The coefficient of determination, R^2 for the relationship is 0.74 and the relationship is given by:

$$\rho_{bulk} = 721.16 x D_{nssd}^{-0.71} \qquad \text{(Eq. 5.8)}$$

where ρ_{bulk} is in ohm.m,

and D_{nssd} is in m^2/s.

Based on the investigations by Polder, (1995) on opc (0.40 w/c and 0.54 w/c) and ggbs (0.40 w/b) concretes, it has been suggested that the non-steady state diffusion coefficient obtained from the chloride profiles for samples immersed in 3.5% NaCl solution for 1.5 years is inversely proportional to the electrical resistivity. Furthermore, the product of both was found to be nearly a constant (290 ohm.m^3/s), with a variation of ± 85 ohm.m^3/s. The Eq. 5.8 suggests that the non-steady state diffusion coefficient can be calculated from the resistivity ρ_{bulk} with 74% confidence. The relationship obtained in Fig. 5.18 is close enough to an inverse relationship, however, with a much higher product (i.e. product of both parameters in Eq. 5.8) to that obtained by Polder (1995). The concentration of the exposure solution used in this study was 165g/litre of NaCl compared to 35g/litre used by Polder, (1995). As the concentration of the exposure solution has a considerable effect on the diffusivity, this could have influenced the relationship, so a comparison could be inappropriate.

5.2.3.6 Relationship between D_{nssm} and ρ_{bulk}

The relationship between the non-steady state migration coefficient, D_{nssm} and the bulk resistivity, ρ_{bulk} is presented in Fig. 5.19. The coefficient of determination, R^2 for the relationship is 0.85 and the relationship is given by:

$$\rho_{bulk} = 713 x D_{nssm}^{-0.75} \qquad \text{(Eq. 5.9)}$$

where ρ_{bulk} is in ohm.m,

and D_{nssm} is in m^2/s.

A good correlation was obtained between the two parameters, suggesting that the non-steady state migration coefficient can be determined using the ρ_{bulk} with 85% confidence. The better relationship found by Eq. 5.9 compared to the previous one in Eq. 5.8 is considered to be due to the fact that both the ρ_{bulk} and the D_{nssm} were

determined from the same concrete specimens. Therefore, any variations in the specimens due to the aggregate spacing, defects, etc would affect both the tests in a similar manner.

5.2.4 Discussion on the relationships of the test parameters

The relationships between different test parameters were discussed in section 5.2.3, the results presented suggests that:

1. The coefficient from the non-steady state migration test, D_{nssm}, correlates well with D_{nssd} from the non-steady state diffusion test. Therefore, D_{nssd} could be evaluated more rapidly using D_{nssm}. The magnitudes of the coefficients are similar.
2. The steady state migration coefficient, D_{ssm} could be obtained from the bulk resistivity, ρ_{bulk} using the empirical relationship given in Eq. 5.7 (see section 5.2.3.4).

Based on the experimental evaluation, it can be concluded that the following tests are most appropriate in terms of simplicity, rapidity and interpretation of results to evaluate the chloride ion diffusivity of concretes.

- The non-steady state migration test
- The bulk resistivity test

5.2.5 Findings relevant for the modification of the test protocol of the Permit ion migration test

One of the objectives of this research was to develop a new test protocol for the Permit ion migration test and to validate the test with other standard test methods (identified from the above Evaluation Programme) for a range of concrete mixes. The first part of this objective was achieved by conducting an evaluation of different test methods for measuring the chloride diffusivity of concrete, for which the results were discussed in the previous section. These measurement techniques used in these test are critically reviewed in this section to formulate a new test protocol for the Permit ion migration test which has good scientific basis. The validation of the new Permit ion migration test protocol (Validation Programme) will be discussed in Chapter 6.

5.2.5.1 Evaluation of electrical resistivity from current measurements

In a typical resistivity test set-up, an AC current is applied across the specimen and the drop in potential (due to the resistivity of the specimen) is measured and the resistance offered by the specimen is calculated using the Ohm's law (Eq. 5.10).

$$R_e = \frac{V}{I} \qquad \text{(Eq. 5.10)}$$

where,

R_e is the electrical resistance, ohms,

V is the potential drop measured, volts, and

I is the current applied, Ampere.

If the geometry of the concrete specimen influencing the current flow is known, the electrical resistivity of the concrete can be calculated using:

$$\rho = \frac{R_e A}{L} \qquad \text{(Eq. 5.11)}$$

where,

ρ is the electrical resistivity, ohm.m,

R_e is the electrical resistance, ohm,

A is the area of the concrete specimen, m^2,

L is the length of the concrete specimen, m.

As the current is carried by the ions present in the pore solution, the resistance to the flow of current can be related to the moisture content and the pore structure. Thus, the electrical resistivity provides an estimate of the ease with which the pores can conduct electricity. The results discussed in sections 5.2.3.4 to 5.2.3.6 show that the resistivity correlates with the chloride ion diffusivity of the concrete. The bulk resistivity in these cases was determined on concrete specimens saturated with $Ca(OH)_2$ solution, suggesting that if the concrete specimen can be saturated with ions, the voltage and current measurement can be used to obtain the resistance offered by the specimen, from which the resistivity or the diffusivity can be estimated.

In the steady state migration test, the peak current coincides with the onset of steady flow of chlorides through the concrete (Fig. 5.20). At this stage all the pores in concrete are filled with chloride ions and the current carried across the test specimen

is mainly due to the chloride flux, i.e., the peak current can be used to estimate the electrical resistance of the chloride saturated concrete. Andrews (1999) reported that the peak current obtained in Permit ion migration test coincided with the onset of the steady state condition. Furthermore, the value of the peak current correlated well with the *in situ* migration coefficient calculated using the slope of the steady state flow, Fig. 5.21. Similarly, Delagrave *et al.* (1996) reported a good correlation between the total current and the diffusing flow.

Therefore, the resistivity of concrete could be obtained from the current measurements in the Permit ion migration test, particularly using the peak current, provided the geometry influencing the current flow is known.

5.2.5.2 Conductivity measurements for the identification of the steady state

In Permit ion migration test the *in situ* migration coefficient is calculated using the slope of the concentration versus time graph corresponding to the steady flow of ions. Andrews (1999) used chloride ion selective electrodes (ise) to measure the chloride concentration in the anolyte. However, ise is sensitive to temperature and other measurement conditions, and hence it needs to be calibrated before the measurement. This makes it difficult to use for repetitive measurement in Permit ion migration test. Furthermore, the handling difficulty of the ise could contribute to increased experimental errors. As an alternative Castellote *et al.* (2001) measured the conductivity of the anolyte and found that the conductivity correlated well with the chloride concentration. Furthermore, for the steady state migration test the chloride concentration and the conductivity of the anolyte were related as presented below:

$$Cl^- = 11.45 \times \lambda_{25} - 1.71 \qquad \text{(Eq.5.12)}$$

where,

Cl^- is the chloride concentration of the anolyte, mmol/l,

λ_{25} is the conductivity of the anolyte at 25°C, mS/cm.

Along with the measurement of the conductivity of the anolyte, at regular intervals in the steady state migration test, liquid samples were collected from the anolyte and analysed for the chloride concentration using the potentiometric titration. The conductivity versus concentration relationship thus obtained is presented in Fig. 5.22.

The conductivity of the anolyte correlates well with the chloride concentration in this figure, with R^2=0.95, and the relationship between the two can be expressed by the following equation:

$$Cl^- = 9.43 \times \lambda_{25} + 0.13 \qquad \text{(Eq. 5.13)}$$

where the unit is same as Eq. 5.12.

This means that the measurement of conductivity is a good alternative to monitoring the concentration of the anolyte for identifying the onset of the steady state condition and determining the slope of the steady state chloride flux. The relationship between conductivity and concentration of the anolyte solution in both steady state migration test as well as Permit ion migration test are further discussed in detail in Chapter 6.

5.2.5.3 Modifications to the test protocol

Instead of measuring the chloride concentration, the conductivity of the anolyte solution could be used to identify the steady state flow as well as the rate of flow during the steady state condition. The current flowing between the anode and the cathode could be monitored continuously and the peak current obtained could be correlated with the electrical resistivity and diffusivity of the concrete.

5.2.6 Comparison of the rapid tests and the selection of test methods for the experimental Validation Programme

Based on the results from this evaluation three test methods were selected for the experimental validation (Validation Programme) of the new Permit test protocol. They are discussed in the following sections. However, a comparison of the various methods shall be first in order to highlight the specimen requirement, the test duration, the interpretation of results and the repeatability.

5.2.6.1 Comparison of the rapid test methods

A comparison of the different test methods studied is given in Table 5.2. The size of the specimen varies depending on the nature of the test. The non-steady state tests require thicker specimens. The non-steady state diffusion test required a sample thickness of 60mm, whereas it was 50mm for the non-steady state migration test. The resistivity test can be conducted on either the 50mm thick or the 60mm thick

(CHLORTEST, 2006). However, it is suggested that for measuring the resistivity the use of the thicker samples would reduce the effect of defects such as air voids or cavities on the measurements.

In the case of the steady state migration test, the inconsistencies reported earlier in the test parameter might have been due to the effect of smaller thickness of the test specimen (as discussed in section 5.2.2.3). Sugyama *et al.* (1996) considered a specimen thickness greater than the maximum size of the aggregate and Nilsson *et al.* (1996) suggested a test specimen thickness of three times the maximum aggregate size. Therefore, the maximum aggregate size in the concrete would determine the minimum thickness of the concrete specimen required for conducting the steady state migration test. However, the increase in thickness could increase the test duration.

When the complexity of the test set-up for each test is compared, the immersion tank required for the non-steady state diffusion is the simplest. However, the duration of the test and the chloride analysis after the test make the non-steady state diffusion test tedious and expensive. Furthermore, a non-linear curve fitting of the data is required to obtain D_{nssd} and C_s. For the bulk resistivity test, once a set of electrodes and power supply are set up, multiple tests could be done in a matter of minutes and the test parameter, ρ_{bulk} can be obtained using a simple calculation. Both the non-steady state migration test and the steady state migration test are done using similar perspex cells, therefore, the requirements are comparable, but the duration of the test is longer for the steady state migration test. In both cases calculations can be done using a scientific calculator to obtain the test parameter.

5.2.6.2 Selection of test methods for the experimental Validation Programme

Based on the experimental evaluation, it can be concluded that the non-steady state migration test and the bulk resistivity test are most appropriate in terms of simplicity, rapidity and interpretation of results to evaluate the chloride ion diffusivity of concretes. However, it is considered to be appropriate to include the steady state migration test as well for the comparative study of the Permit ion migration test presented in Chapter 6 because there were limitations with this test in this investigation. The thickness of the sample for the steady state migration test should

be decided on the basis of the aggregate size effect, as reported by Nilsson *et al.* (1996).

However, certain changes to the test protocol of the steady state migration test are considered in the Validation Programme in order to obtain data comparable with Permit ion migration test. They are discussed next.

Modifications to the steady state migration test protocol

Voltage

As the anolyte initially was de-ionized water, there was the absence of charge carrying ions in the anolyte, which meant that the actual voltage across the concrete was lower than the voltage applied. However, the average voltage during the steady state was used to calculate the migration coefficient, D_{ssm}. The ratio of the actual voltage as measured across the specimen to the applied voltage is presented in Fig. 5.23. This figure shows that the actual voltage varies randomly, but in order to compare the current flowing across the concrete sample it is necessary to maintain a constant voltage. So, in the new test protocol for the steady state migration test (already described in section 4.4.6.2) the voltage was applied closer to the concrete surface in order to reduce any voltage drop in the solution. Two voltage regimes were used in the validation programme, 12V and 60V.

Concentration of the catholyte

The concentration of the catholyte (exposure solution) recommended by Andrews (1999) was 0.55M NaCl (discussed in section 3.5.4). According to Tang (1999a) the concentration of the catholyte could affect the coefficient of diffusion obtained from either the migration test or the diffusion test. Therefore, 0.55M NaCl solution was used as the catholyte in the Validation Programme.

Measurement techniques

The following modifications were made to the measurement techniques:

1. The current flowing across the specimen was monitored regularly to calculate the charge passed.

2. The conductivity of the anolyte was monitored during the test and once the steady flow was established, liquid samples were extracted to obtain the chloride concentration of the anolyte.

The correlation between the modified steady state migration test and the Permit ion migration test is discussed in section 6.5.1.3. As both the Permit ion migration test and steady state migration test measure the chloride diffusivity in a steady state condition, the correlation is of great importance for practical applications.

5.3 Conclusions

In this Evaluation Programme, the performance of four rapid test methods, viz. a non-steady state diffusion test, a non-steady state migration test, a steady state migration test and a bulk resistivity test, was evaluated for determining the chloride diffusivity of concretes. The ability of the parameters obtained from the test methods to distinguish the variations in the mixes, mainly the w/b and type of binder, was used to assess the performance of each test. The following conclusions have been drawn from the results presented and discussed in this chapter.

1. The parameter obtained from the non-steady state diffusion test, D_{nssd} and the non-steady state migration test, D_{nssm}, both increased with increase in w/b and followed similar trends. Both the parameters decreased for concretes containing supplementary cementitious materials compared to their opc counterparts. Therefore, it can be concluded that either of these parameters would identify the effect of mix variations, such as w/b and type of binder, on chloride diffusivity.
2. The test parameter obtained from the steady state migration test, D_{ssm}, increased with a decrease in w/b, unlike the D_{nssd} and D_{nssm}. For concretes containing supplementary cementitious materials, the D_{ssm} was generally lower than the corresponding opc concretes. Unlike the D_{nssd} and D_{nssm}, the effect of both the w/b and type of binder was not recognisable using D_{ssm}. The lower thickness of the specimen used in this test is considered to be the reason for the unexpected trends stated above. Therefore, it is suggested that the steady state migration test should be carried out with a thicker test specimen, having a thickness at least equal to three times the maximum size of aggregate.

3. The bulk resistivity, ρ_{bulk}, showed an inverse relationship with the diffusivity parameters, D_{nssd} and D_{nssm}. Generally, with the increase in w/b the resistivity decreased, which agrees with the increase in diffusivity observed for similar concretes. The resistivity of concretes with cement replacement materials was higher than the corresponding opc concretes. Based on the results here, it can be concluded that the bulk resistivity test is an alternative to both the non-steady state diffusion test and the non-steady state migration test, in order to identify the variations in the mix such as w/b and type of binder.
4. The D_{nssd} and D_{nssm} showed similar trends with variations in the w/b and the type of binder and both these parameters were of similar magnitude. Therefore, the non-steady state migration test can be used as a substitute for the non-steady state diffusion test to determine D_{nssd}. This also enables the determination of D_{nssd} in a more rapid and inexpensive manner, using the non-steady state migration test.

Table 5.1 Average test parameter and the associated standard error

Mix	D_{nssd}(x10^{-12} m^2/s)		C_s (% weight of concrete)		K_{cr} (mm^2/year)		D_{nssm}(x10^{-12} m^2/s)		D_{ssm}(x10^{-12} m^2/s)		ρ_{bulk} (ohm.m)	
	Mean	Error	Mean	Error	Mean	Error	Mean	Error	Mean	Error	Mean	Error
opc 0.35	5.11	0.56	0.67	0.04	32.00	1.53	6.00	1.24	1.84	0.32	175.70	16.50
opc 0.42	17.53	9.74	0.75	0.11	60.33	15.31	17.40	2.63	1.24	0.04	68.33	5.13
opc 0.45	14.63	3.74	0.43	0.01	53.30	6.65	15.00	3.02	1.48	0.18	187.00	22.19
opc 0.50	16.56	1.82	0.72	0.05	58.00	2.52	16.70	0.99	1.26	0.08	56.00	12.77
pfa 0.42	1.44	0.27	0.97	0.10	19.00	1.53	1.70	0.13	0.76	0.09	323.70	40.07
pfa 0.45	7.38	2.43	0.92	0.18	48.00	7.55	3.70	0.54	0.35	0.05	291.40	4.61
ggbs 0.42	1.31	0.16	0.67	0.07	16.33	0.58	1.00	0.05	0.53	0.14	838.30	160.32
ggbs 0.45	3.19	1.35	0.62	0.26	25.00	3.21	2.20	0.25	0.55	0.06	469.80	17.25
ms 0.40	1.61	0.62	0.90	0.24	25.67	1.53	1.90	0.07	0.21	0.18	426.80	21.25
ms 0.42	4.88	0.58	0.84	0.03	32.67	1.53	6.90	0.50	1.96	0.29	236.30	31.00

Table 5.2 Comparison of different rapid test method for determining the chloride diffusivity

Test Method	Test requirements						
	Thickness of test specimen	Method of saturation of the test specimen	Test duration	Comparative work load (for 3 replicate specimens)	Test setup	Measurements	Method of calculation of the test parameters
Non-steady state diffusion test	60mm	$Ca(OH)_2$	35days	Heavy (16 Man hours)	Simple immersion in NaCl solution	Extremely complex, Profile grinder and chemical analysis of collected concrete dust	Complex, Non linear curve fitting for chloride profiles
Non-steady state migration test	50mm	Vacuum using $Ca(OH)_2$	1 day	Medium (6 Man hours)	Complex, Requires electrodes, prespex cells, power supply, provision for splitting the specimen, ammeter, thermometer and $AgNO_3$ solution	Complex, Check for leaks, need to measure current, temperature and chloride penetration depth	Simple, Need a scientific calculator
Steady state migration test	20mm	Vacuum using de-ionized water	7 days	Medium (8 Man hours)	Complex, Requires electrodes, prespex cells, power supply, conductivity meter, ammeter, thermometer	Complex, Check for leaks, need to measure voltage, temperature and conductivity	Simple, Need a scientific calculator
Bulk resistivity test	50mm	Vacuum using $Ca(OH)_2$	minutes	Easy (1 Man hour)	Simple, needs electrodes and an AC Databrige	Simple, Single measurement	Simple, Need a scientific calculator

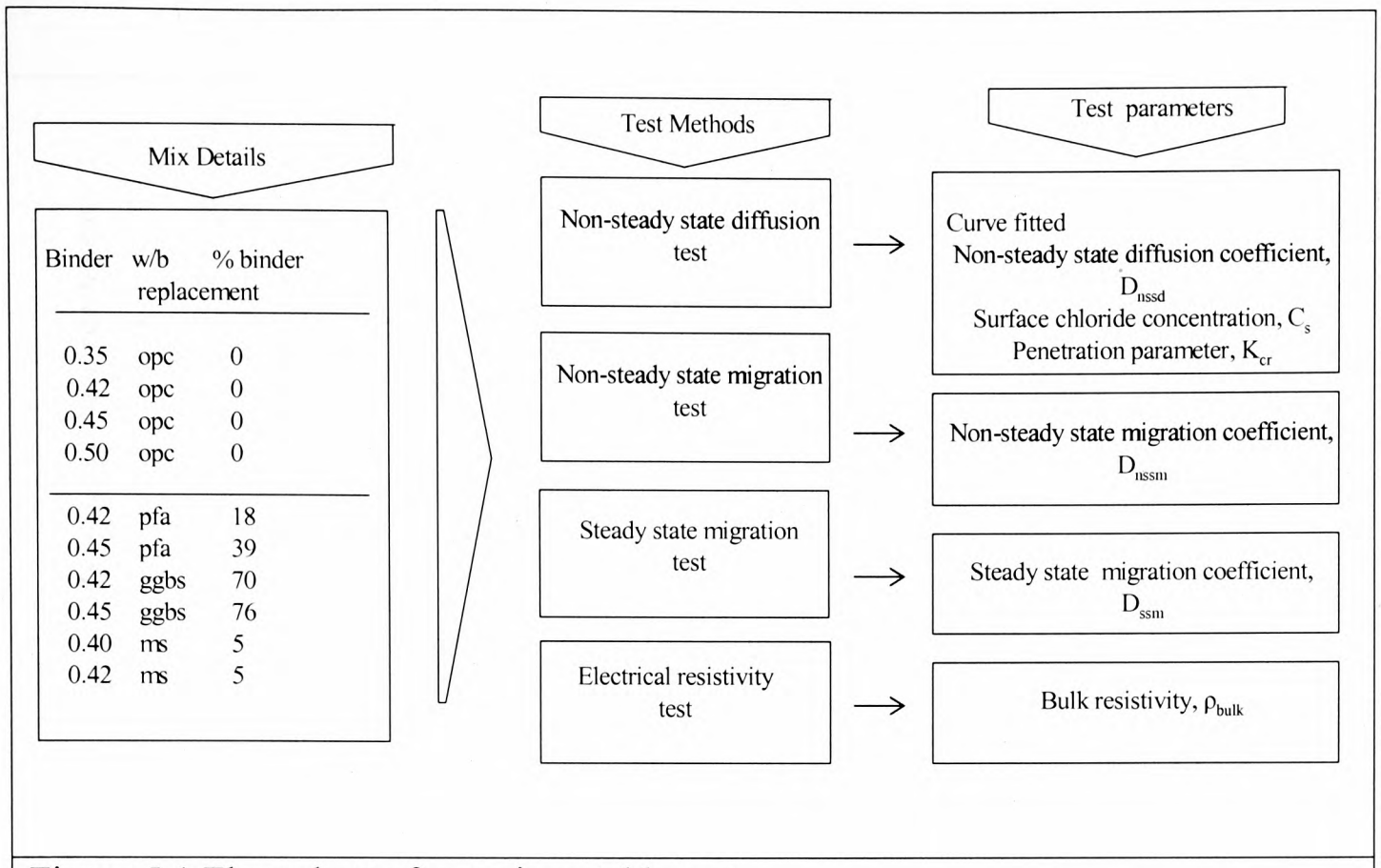

Figure 5.1 Flow chart of experimental layout

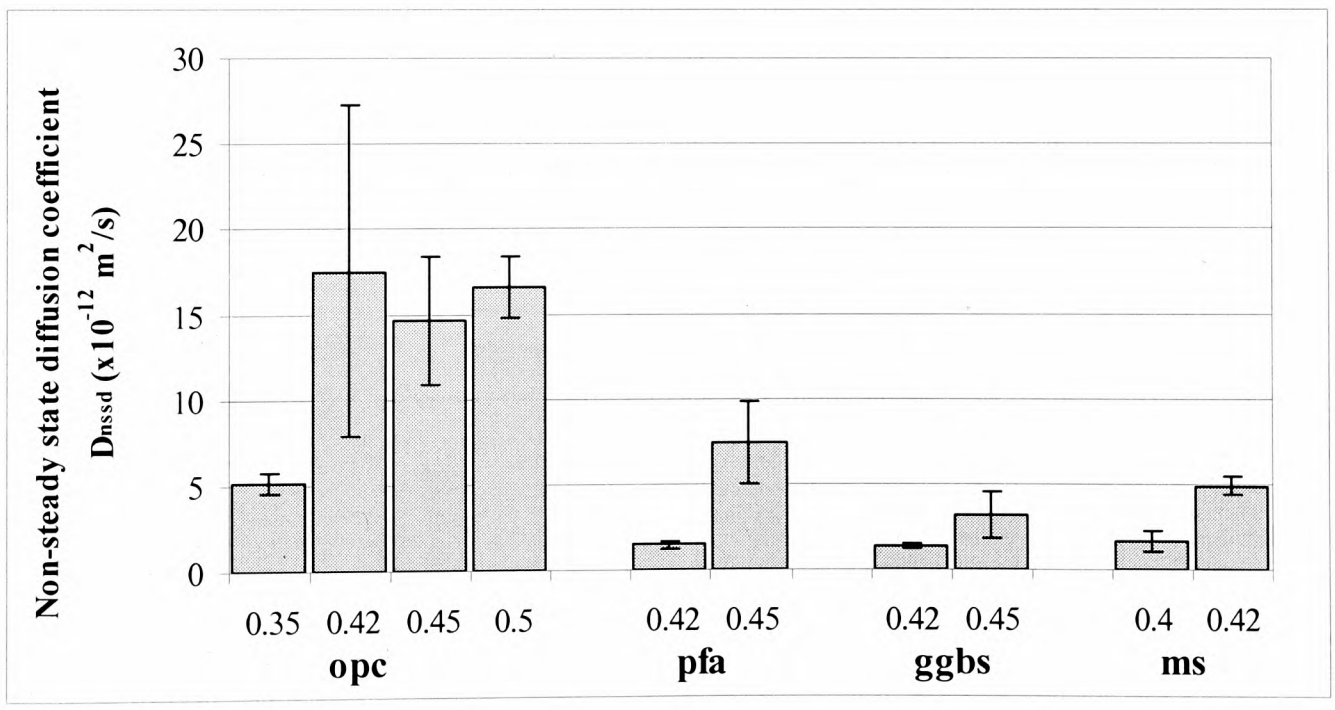

Figure 5.2 Effect of w/b on the non-steady state diffusion coefficient, D_{nssd}

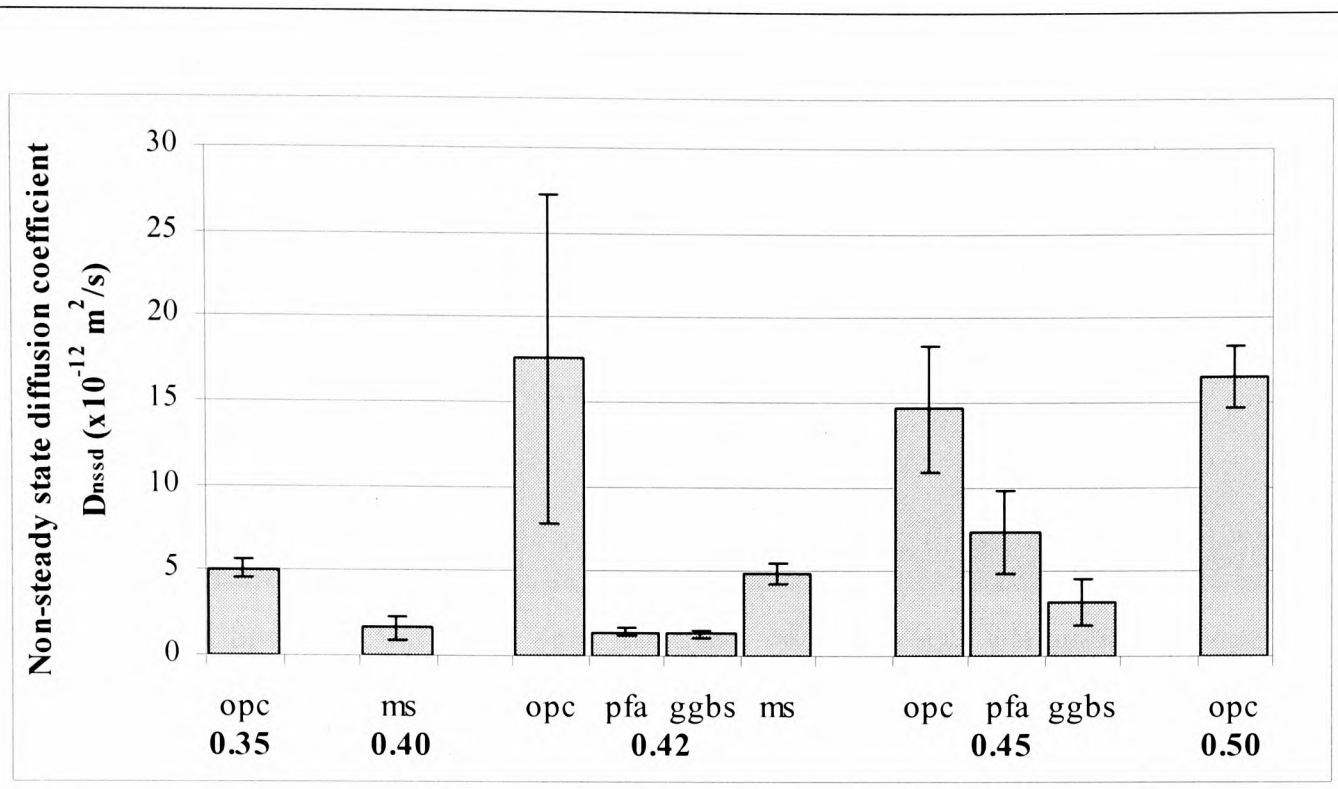

Figure 5.3 Effect of type of binder on the non-steady state diffusion coefficient, D_{nssd}

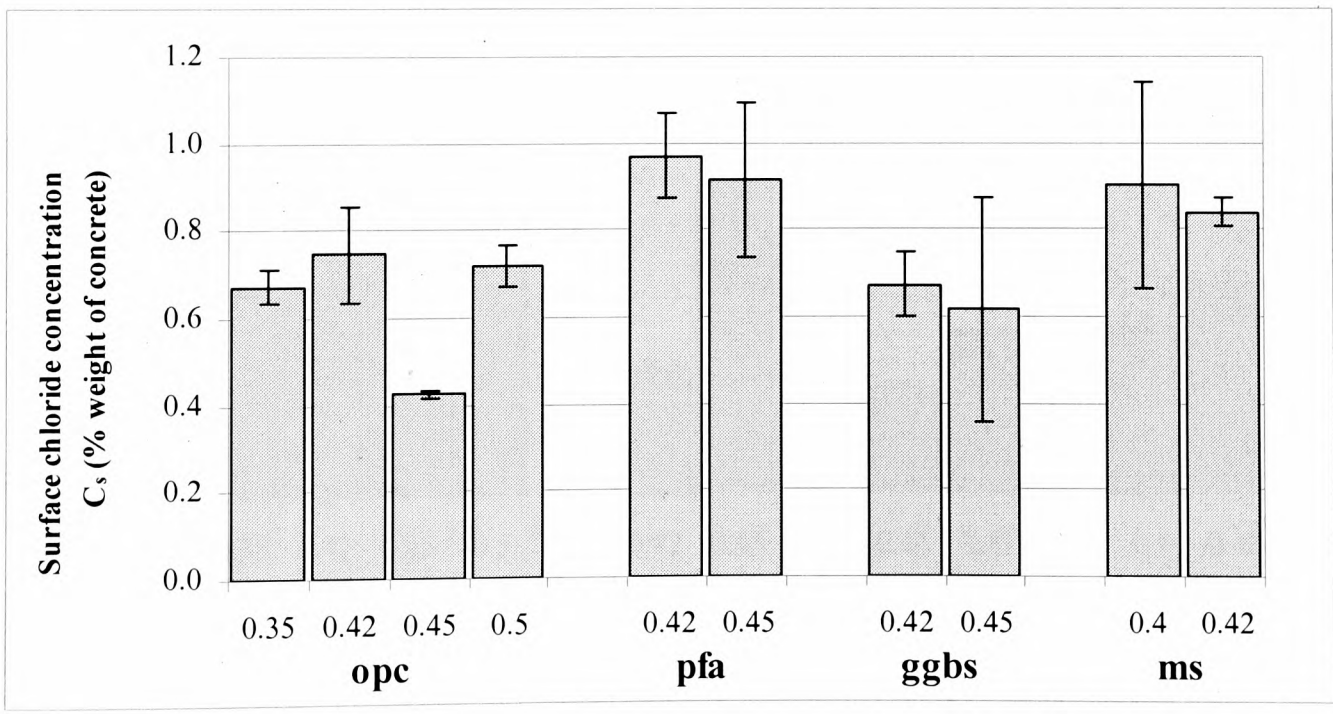

Figure 5.4 Effect of w/b on the surface chloride concentration, C_s

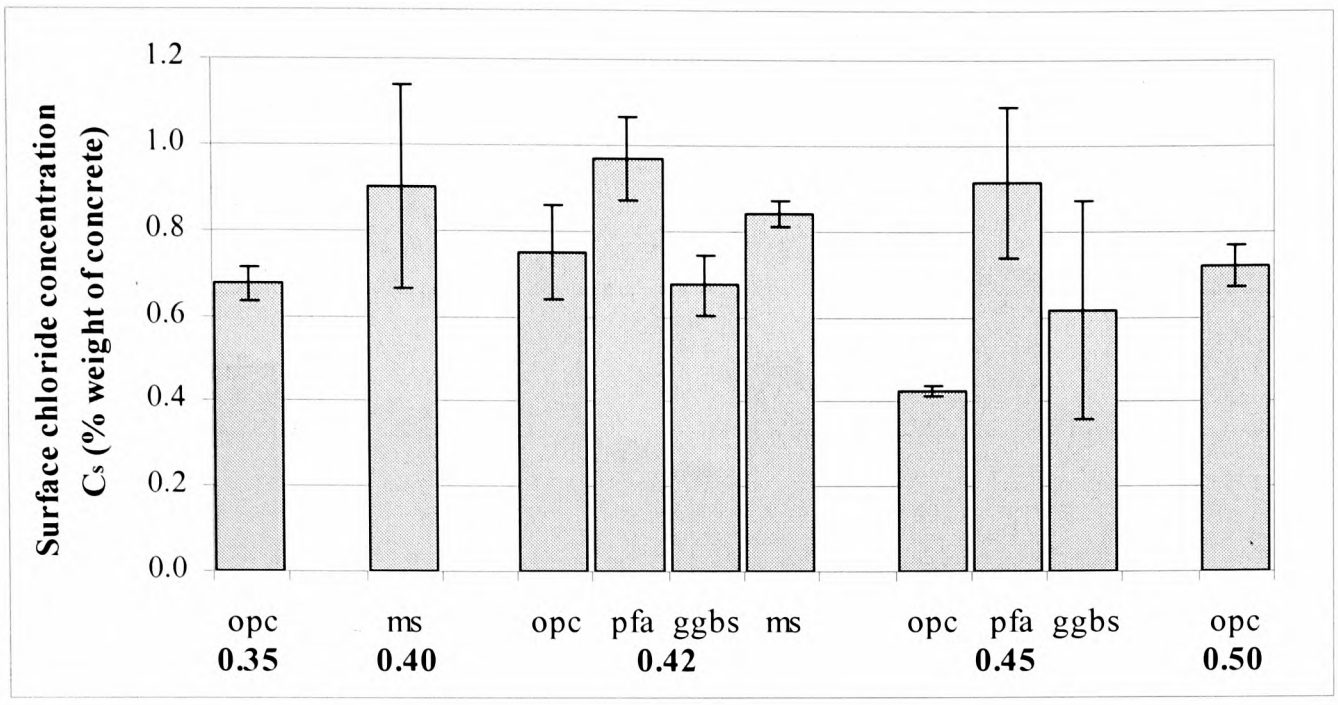

Figure 5.5 Effect of type of binder on the surface chloride concentration, C_s

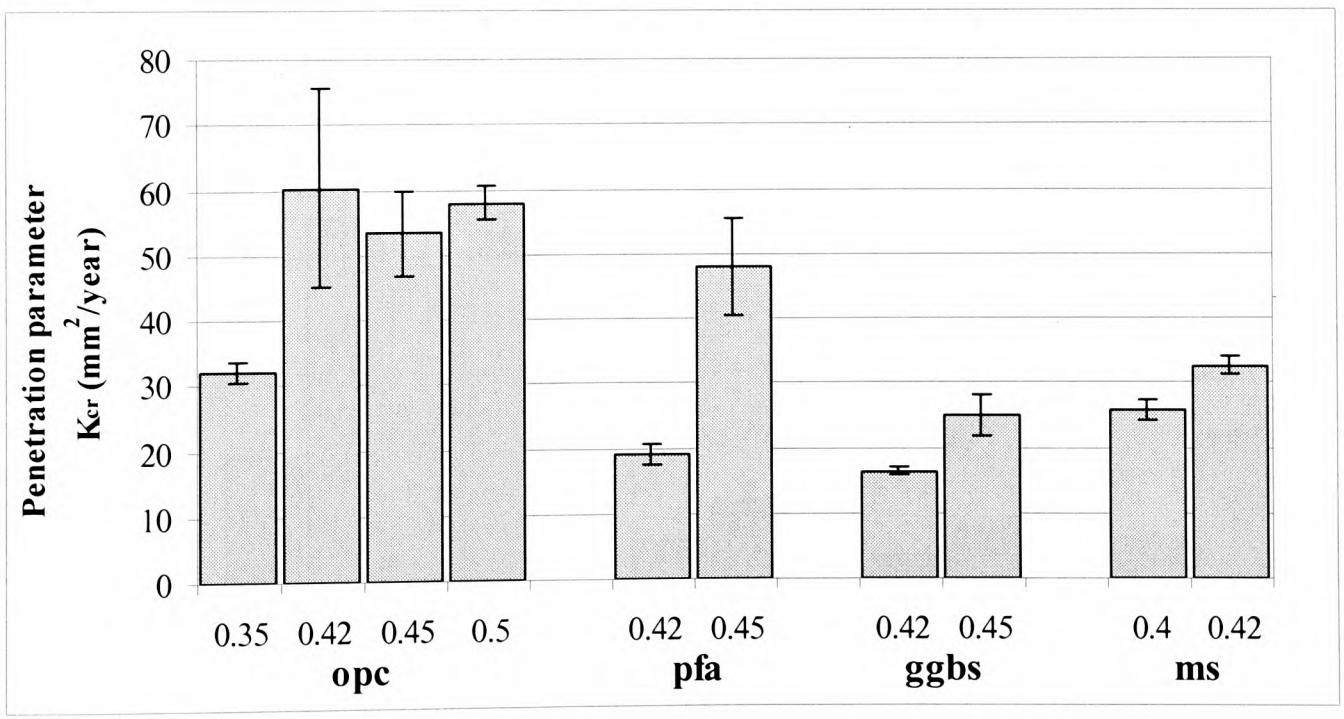

Figure 5.6 Effect of w/b on the penetration parameter, K_{cr}

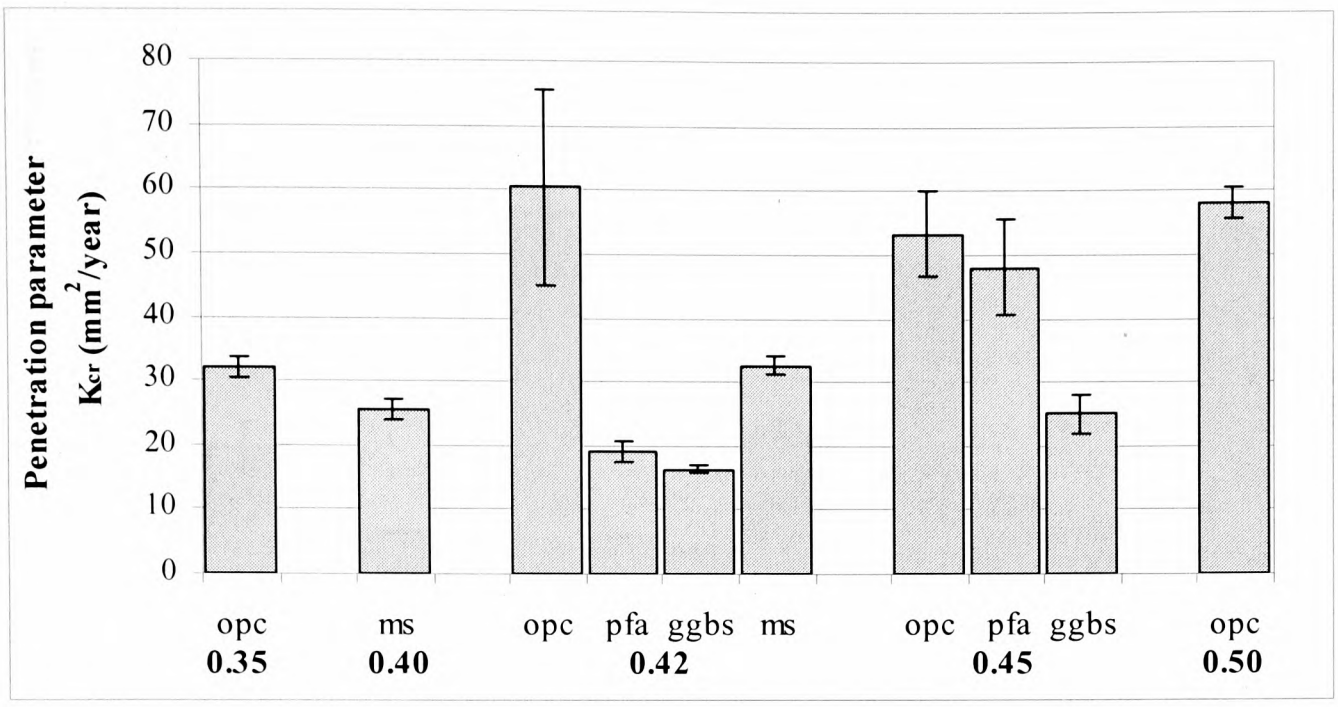

Figure 5.7 Effect of type of binder on the penetration parameter, K_{cr}

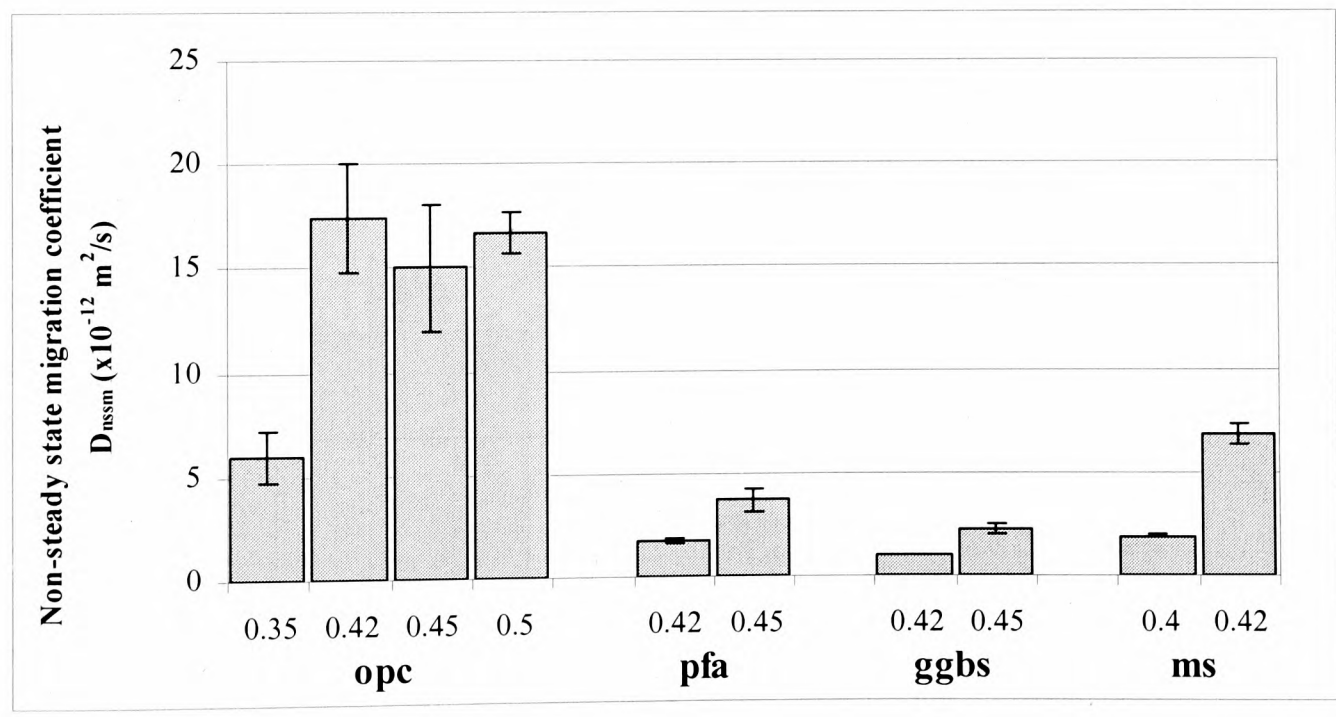

Figure 5.8 Effect of w/b on the non-steady state migration coefficient, D_{nssm}

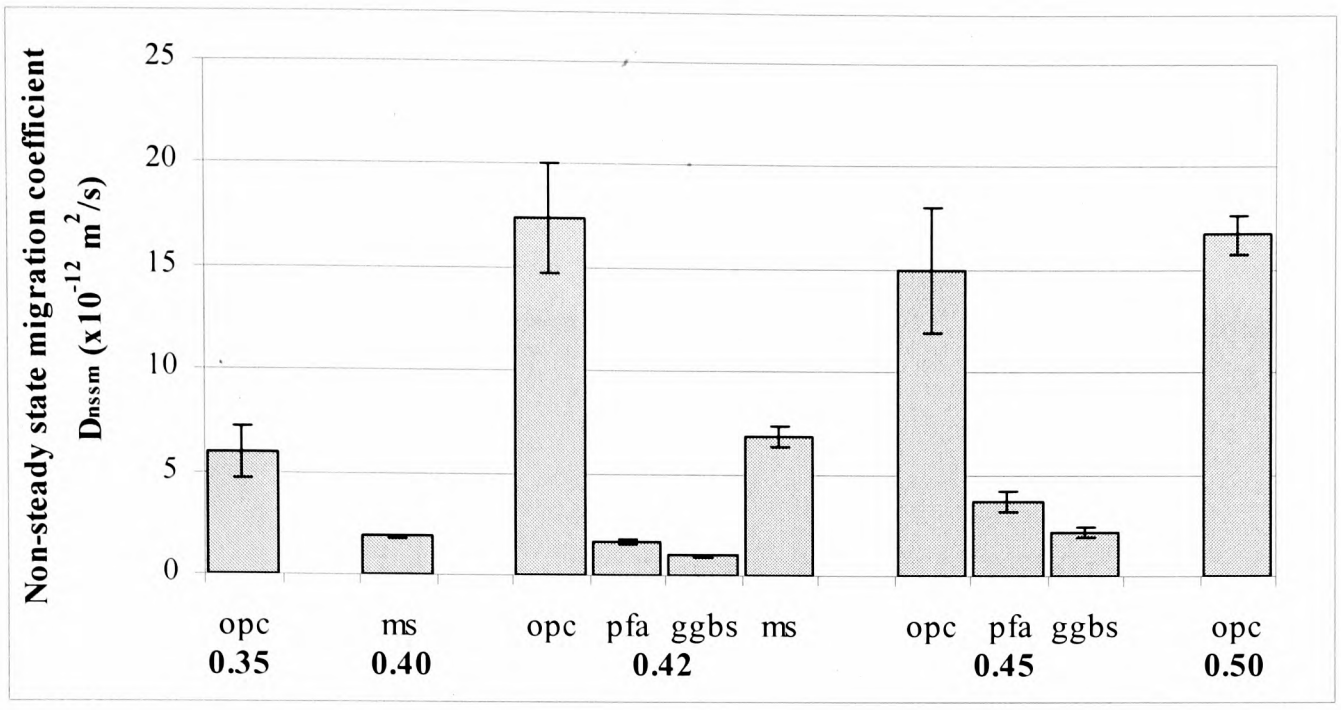

Figure 5.9 Effect of type of binder on the non-steady state migration coefficient, D_{nssm}

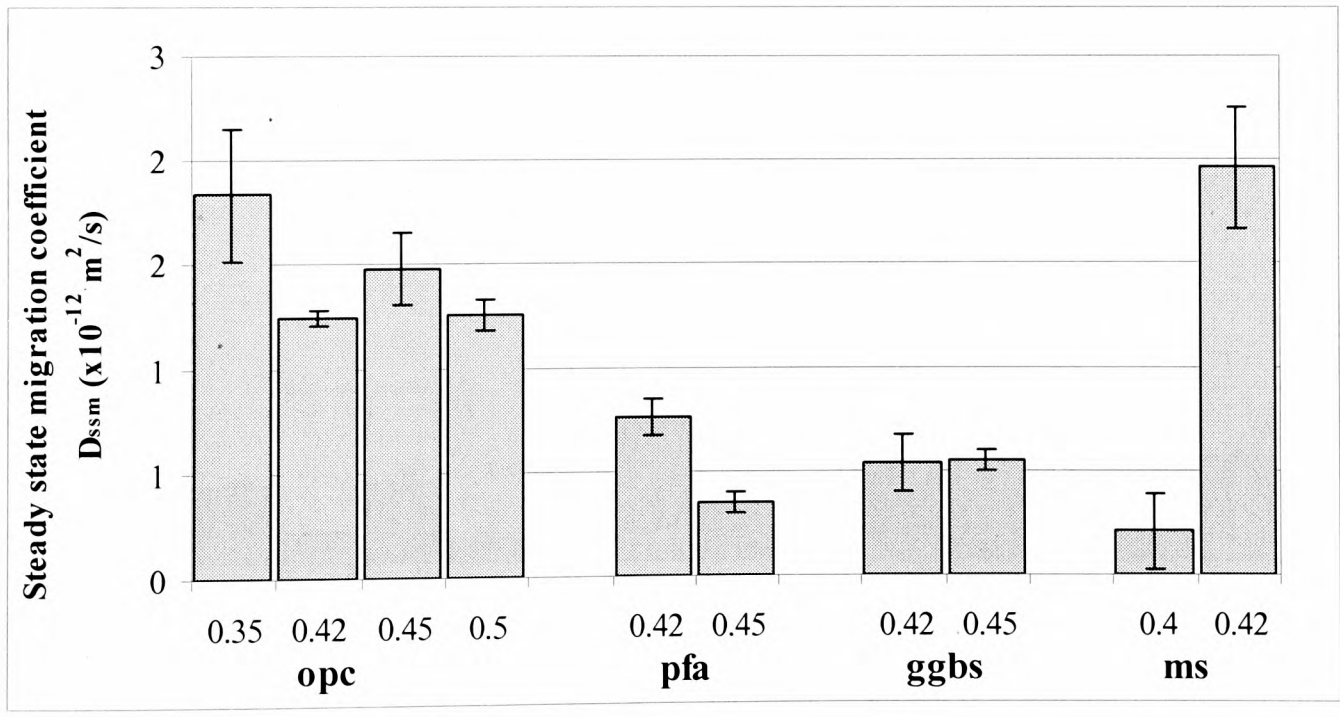

Figure 5.10 Effect of w/b on the steady state migration coefficient, D_{ssm}

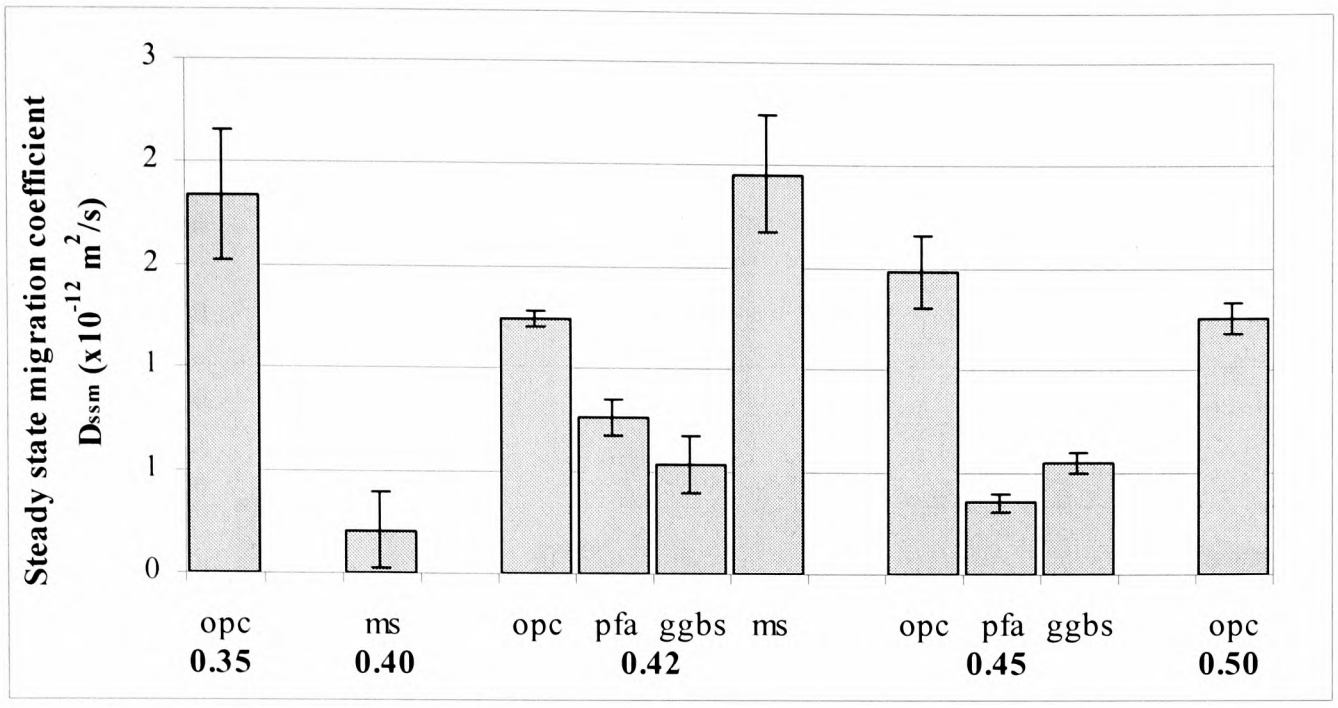

Figure 5.11 Effect of type of binder on the steady state migration coefficient, D_{ssm}

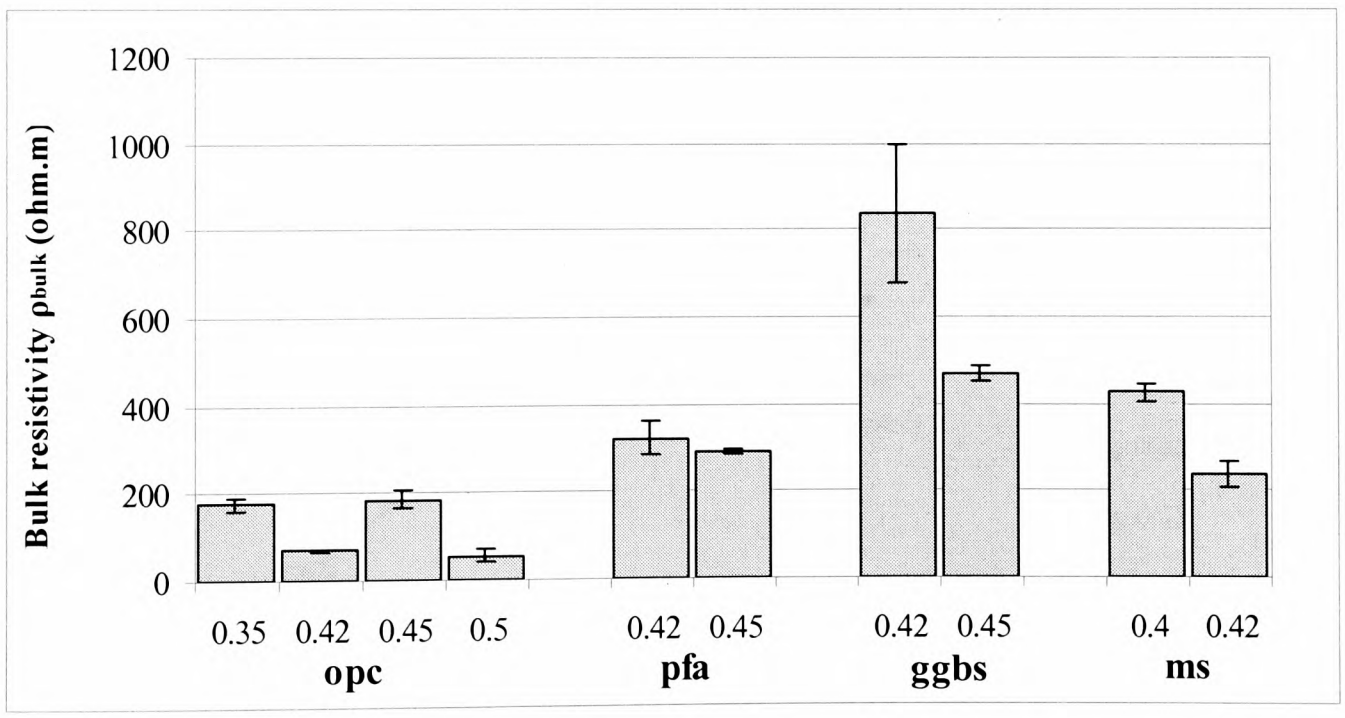

Figure 5.12 Effect of w/b on the bulk resistivity, ρ_{bulk}

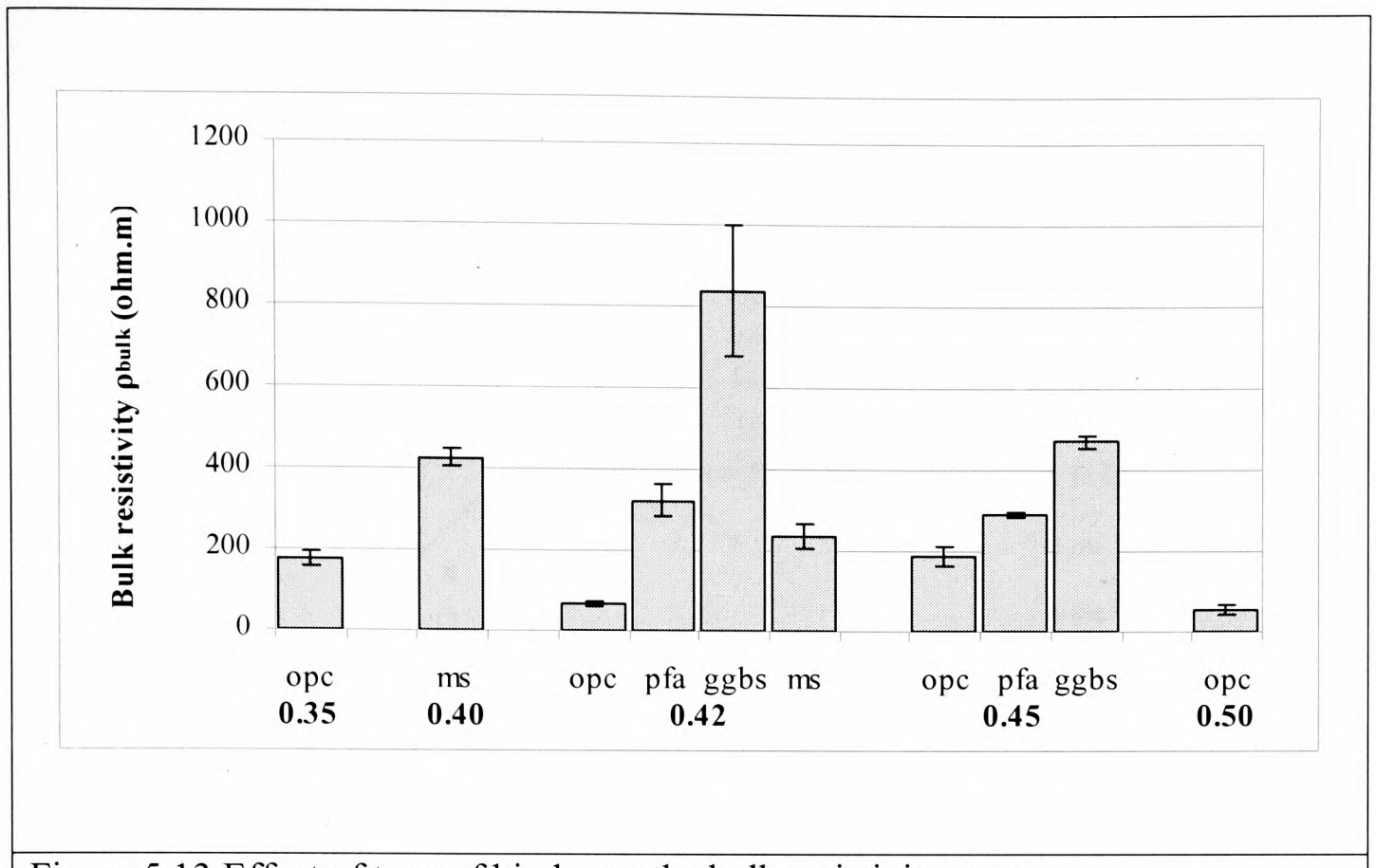

Figure 5.13 Effect of type of binder on the bulk resistivity, ρ_{bulk}

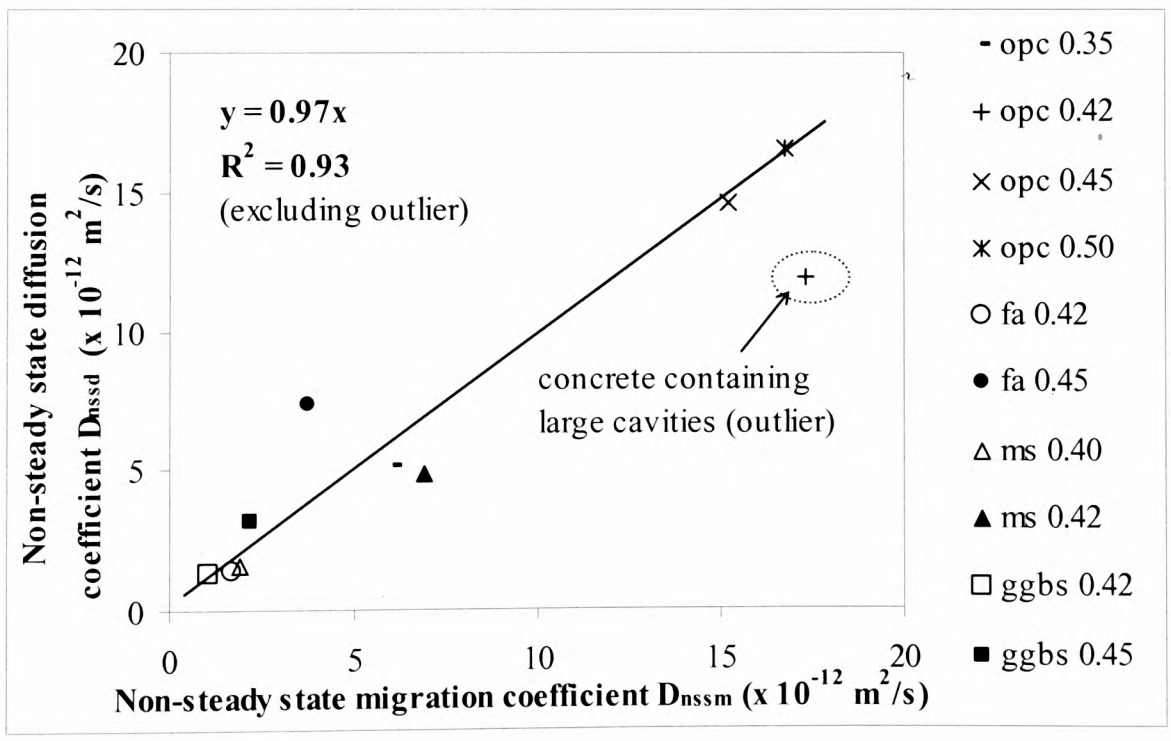

Figure 5.14 Relationship between the non-steady state diffusion coefficient, D_{nssd} and the non-steady state migration coefficient D_{nssm}

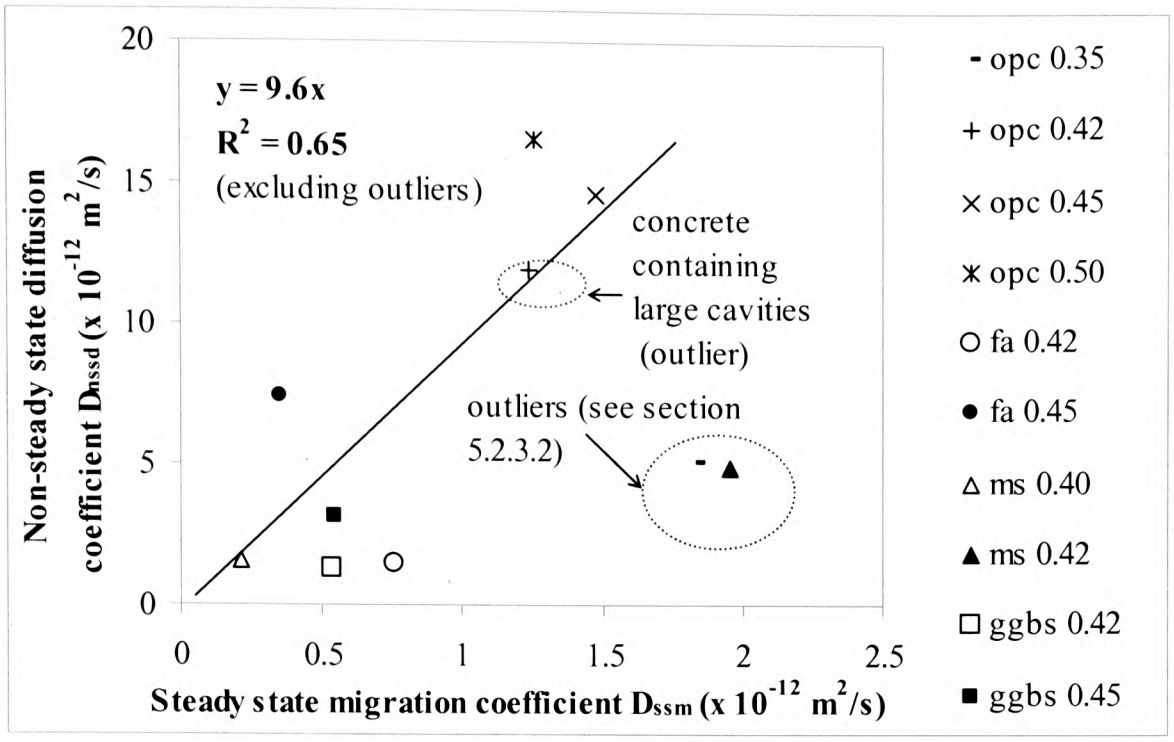

Figure 5.15 Relationship between the non-steady state diffusion coefficient, D_{nssd} and the steady state migration coefficient, D_{ssm}

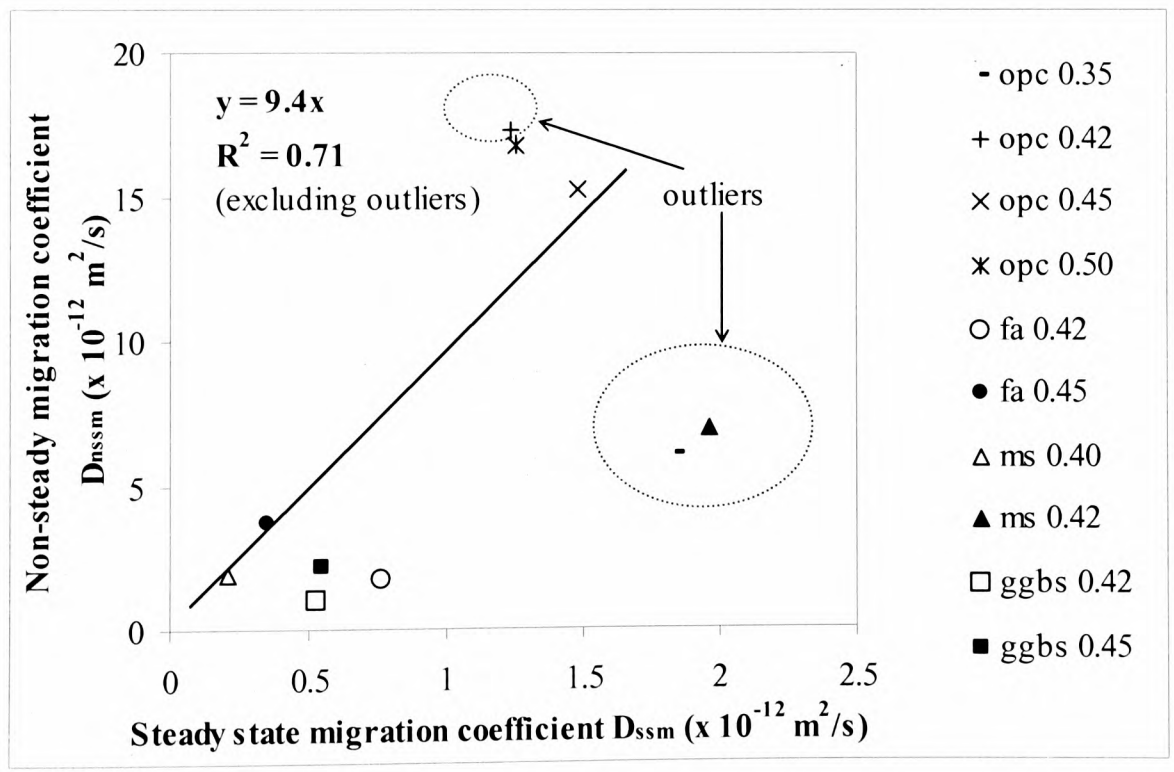

Figure 5.16 Relationship between the non-steady state migration coefficient, D_{nssm} and the steady state migration coefficient, D_{ssm}

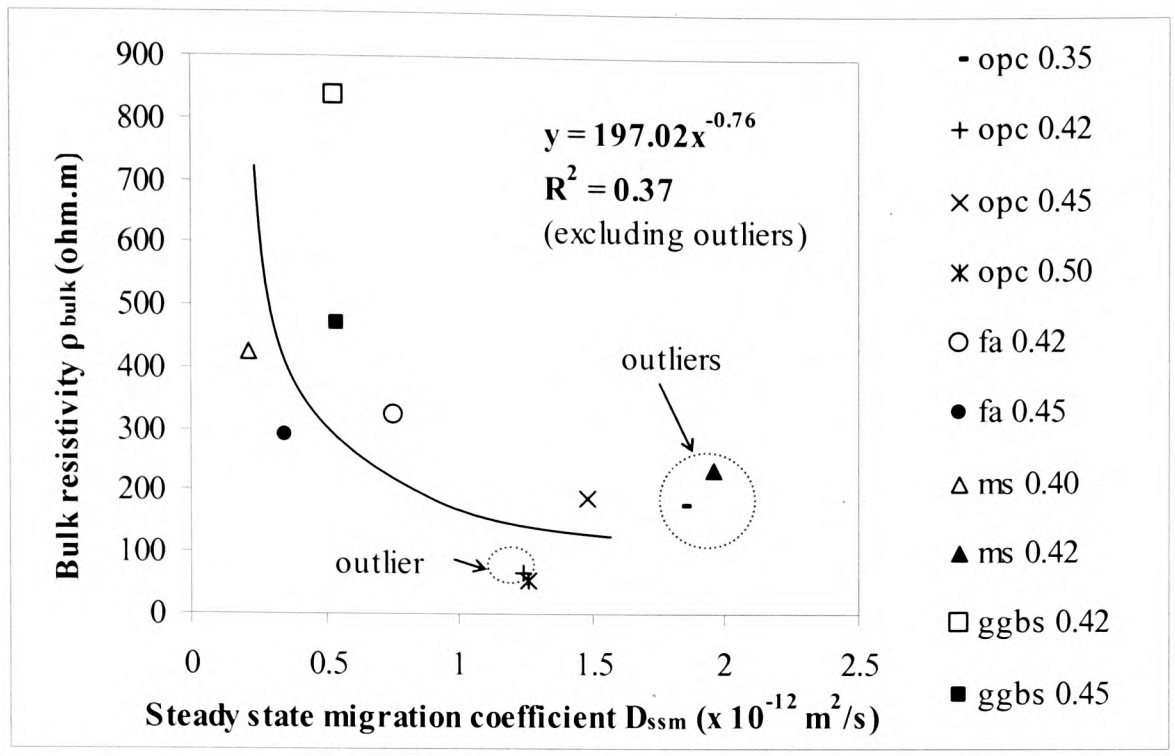

Figure 5.17 Relationship between the bulk resistivity, ρ_{bulk} and the steady state migration coefficient, D_{ssm}

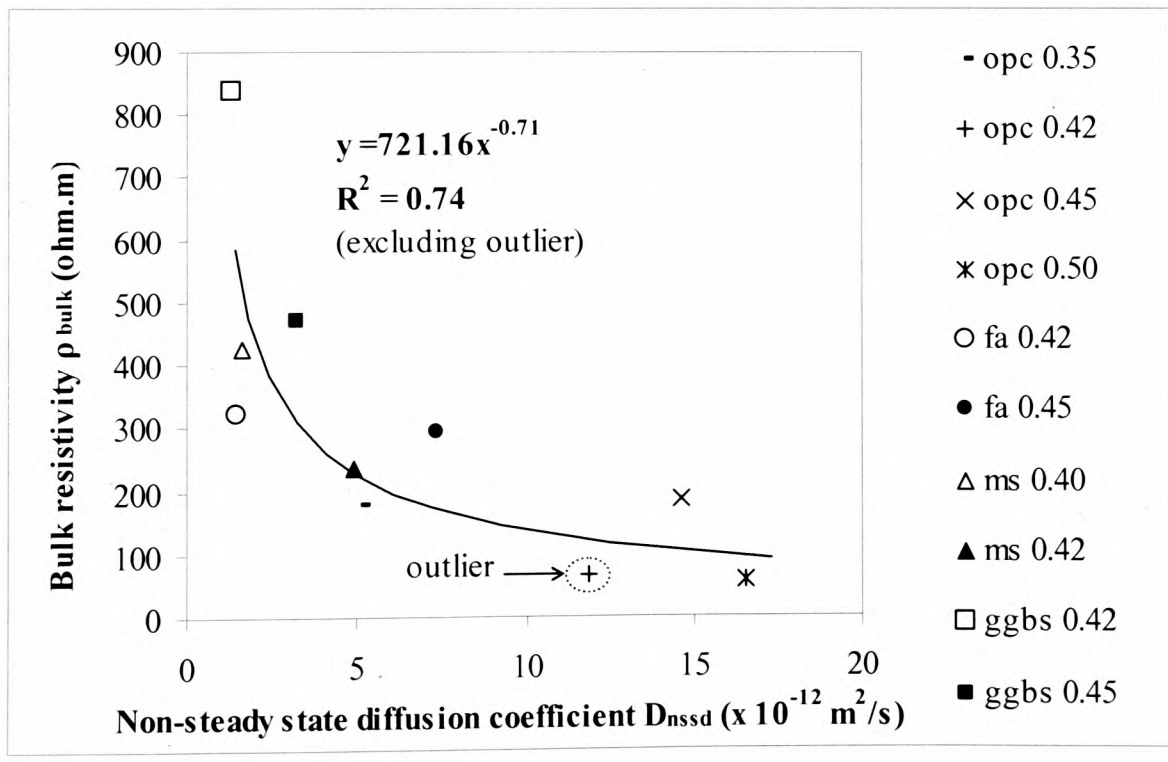

Figure 5.18 Relationship between the bulk resistivity, ρ_{bulk} and the non-steady state diffusion coefficient, D_{nssd}

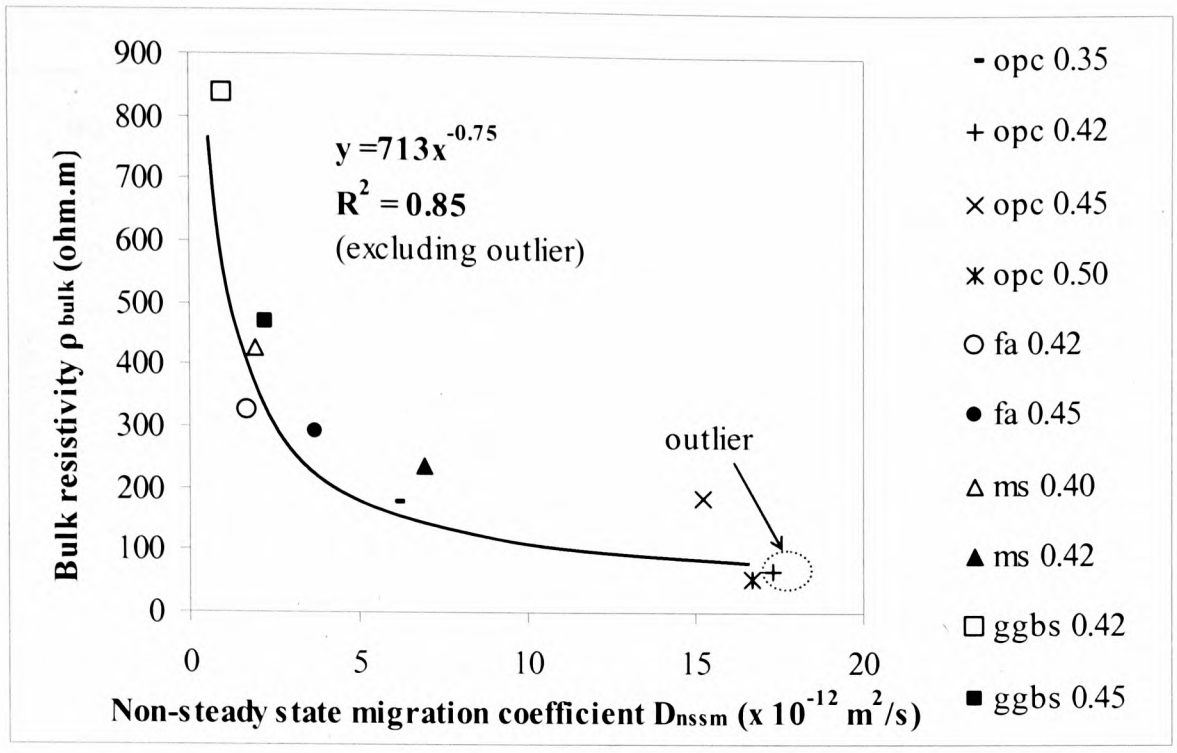

Figure 5.19 Relationship between the bulk resistivity, ρ_{bulk} and the non-steady state migration coefficient, D_{nssm}

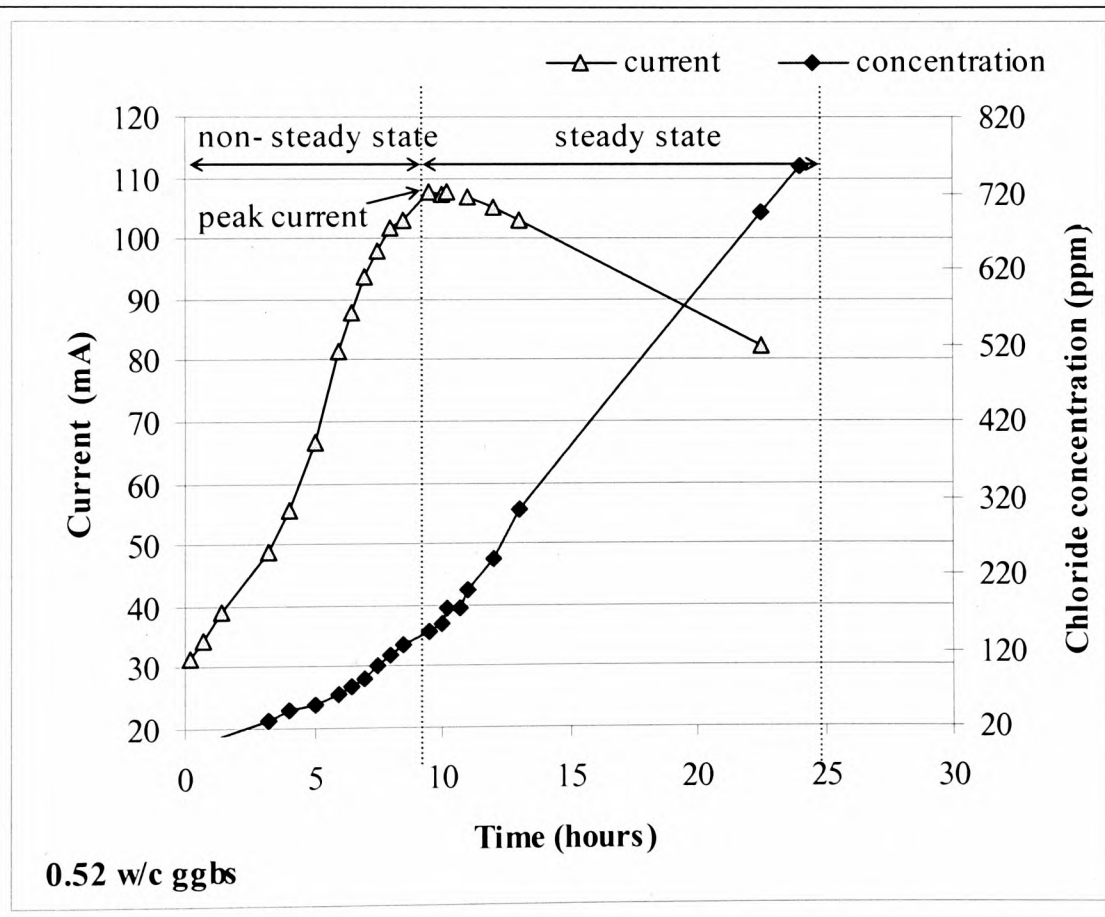

Figure 5.20 A typical current and concentration measurement from the steady state migration test (used in Validation Programme)

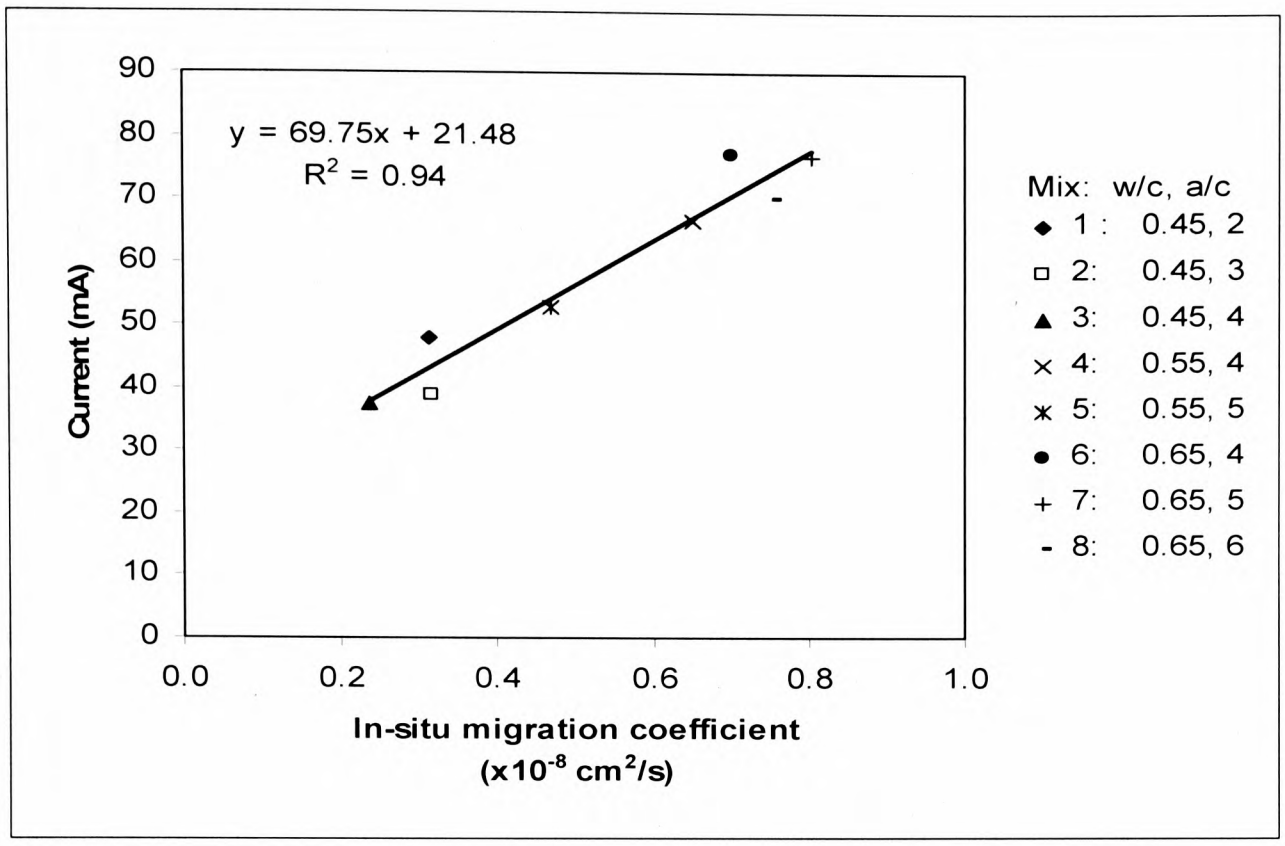

Figure 5.21 Relationship between the peak current and the *in situ* migration coefficient, $D_{in\ situ}$ (Andrews, 1999)

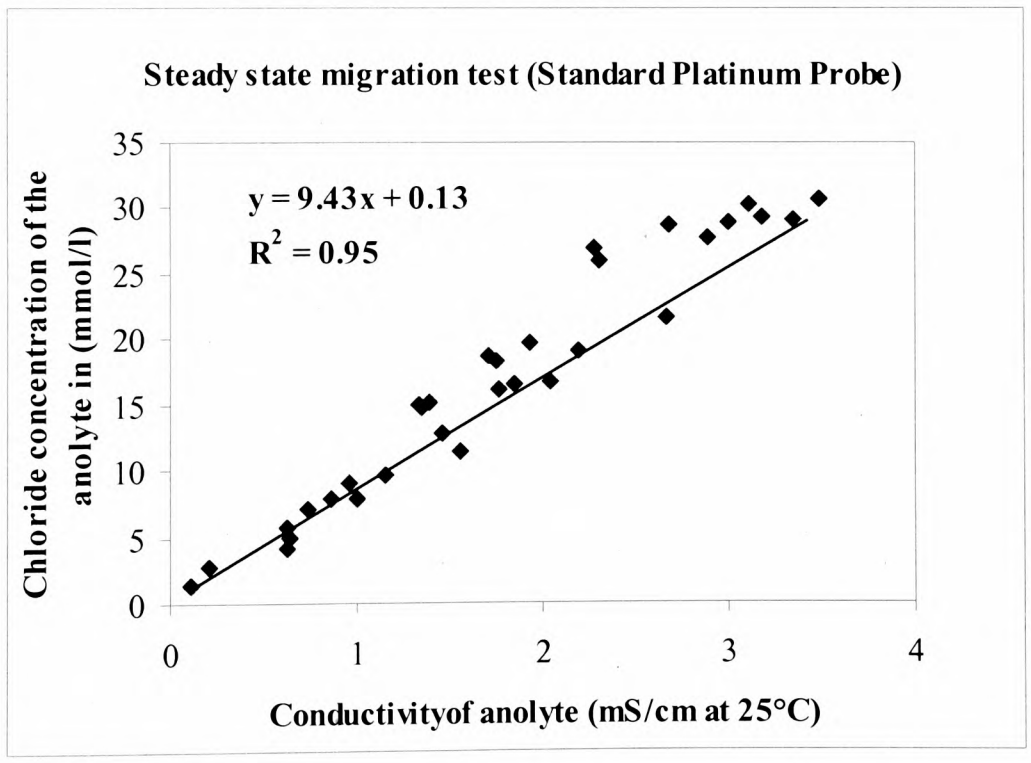

Figure 5.22 Relationship between the conductivity and the chloride concentration of the anolyte

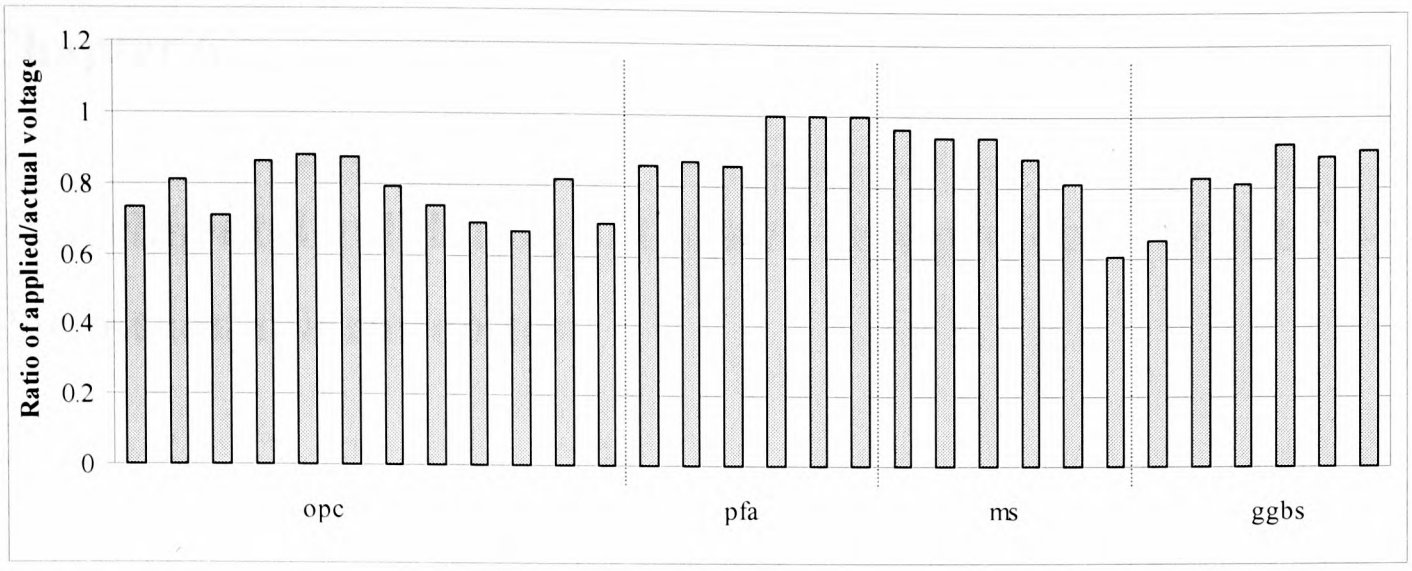

Figure 5.23 Ratio of applied voltage to actual voltage measured across the specimen from the steady state migration test during steady state

Chapter 6

Experimental validation of the new test protocol for the Permit ion migration test

6.1 Introduction

In this chapter, it is intended to validate experimentally the new test protocol from Chapter 5 for the Permit ion migration test. Therefore, the results of the laboratory based experimental programme (Validation Programme) described in Chapter 4 are discussed in order to assess the correlation between the Permit ion migration test and other reliable lab-based test methods identified in Chapter 5 from the Evaluation Programme.

6.1.1 Objectives of the experimental programme

The objectives of this experimental programme were as follows:

1. To identify and determine experimentally the flow path of chloride ions in the Permit ion migration test.
2. To compare the influence of mix variables, such as w/b and binder type on the *in situ* migration coefficient determined using the Permit ion migration test with other commonly used laboratory methods, such as non-steady state migration test, steady state migration test, bulk resistivity test and Wenner four probe resistivity test.
3. To determine the correlation between the *in situ* migration coefficient and the test parameters obtained from other test methods.
4. To establish the validity of the new test protocol using objective 3.
5. To identify relationships between different test parameters, such as concentration versus conductivity, concentration versus charge passed, etc. in both the Permit ion migration test and the steady state migration test.

6.2 Experimental details

As reported in Chapter 4, the test methods in the Validation Programme were the non-steady state migration test (section 4.4.6.1), the steady state migration test (section 4.4.6.2), the Permit ion migration test (section 4.4.6.3), the bulk resistivity test (section 4.4.6.5) and Wenner four probe resistivity test (section 4.4.6.4). The results obtained from these test methods are of different nature, therefore a general term 'test parameter' is used hereafter to refer to the results obtained from different test methods. The test parameters obtained from the different tests are described in the section 6.2.2. In addition to the tests mentioned here, standard quality control tests, such as the slump test, the air content and the compressive strength test were carried out, details of which can be found in section 4.4.5.

6.2.1 Test specimens

Eight different concrete mixes were used in this experimental programme. Details of the mix proportions are summarised in Table 4.2. The specimens with w/b 0.40 and 0.45 were tested at an age of 28 days and those with w/b 0.52 were tested at the age of 56 days so that a relationship between various diffusion-related properties could be established for concretes containing supplementary cementitious materials at different maturities. Details of the manufacture and curing of the test specimens have already been discussed in sections 4.4.2 and 4.4.3. As it can be seen from Table 4.2 the maximum size of coarse aggregate was 10mm for the mixes with w/b 0.40, whereas it was 6mm for the mixes with w/b 0.52. This was done to produce mixes which were comparable with those used in the Evaluation Programme described in Chapter 5. As a consequence, it was possible to obtain variations in chloride diffusivity and the related properties of concrete mixes with a range of mix constituents, ensuring that any trend obtained from this research would have high level of confidence. The conditioning of specimens for different tests was different and they can be found in sections 4.4.6.1 to 4.4.6.5.

6.2.2 Test parameters

The test parameters obtained for the different mixes and various test methods in the Validation Programme reported in Tables 6.1a, b & c. Details of the preparation of the test specimens, test set-up, procedure to carryout the various tests and the

methods used to calculate various properties have already been given in sections 4.4.6.1, 4.4.6.2, 4.4.6.3, 4.4.6.4 and 4.4.6.5.

Permit ion migration test

The test parameters obtained from the Permit ion migration test are as follows (see Table 6.1a):

- *Initial current*: the current obtained at the start of the test, generally initial current is measured within the first 5 minutes since the start of the migration.
- *Peak current*: the maximum current measured during a migration test.
- *6 hours charge passed*: the charge passed is obtained by integrating the area under the current – time graph, for the first 6 hours.
- *Charge passed till steady state*: obtained by integrating the area under current – time graph till steady state (obtained by extending the steady portion of the concentration – time graph to x axis). The time to reach steady state is always less than the time at which the current peaks.
- *Concentration*: the chloride concentration of the anolyte.
- *Conductivity*: the conductivity of the anolyte solution.
- $D_{in\ situ}$: the *in situ* migration coefficient (section 4.4.6.3).

Steady state migration test

The test parameters obtained from the steady state migration test are as follows (see Table 6.1b):

- *Initial current*: the current obtained at the start of the test, generally initial current is measured within the first 5 minutes since the start of the migration test.
- *Peak current*: the maximum current measured during a migration test.
- *Charge passed*: the area under the current – time graph.
- *Conductivity*: the conductivity of the anolyte solution.
- *Concentration*: the chloride concentration of the anolyte solution.
- $D_{1D\ ssm}$: the steady state migration coefficient (section 4.4.6.2).

Non-steady state migration test

The test parameter obtained from the non-steady state migration test is the non-steady state migration coefficient, D_{nssm} (see Table 6.1c).

Bulk resistivity test

The test parameter obtained from the bulk resistivity test is termed as the bulk resistivity, ρ_{bulk} (see Table 6.1c).

Wenner four probe resistivity test

The test parameter obtained from the Wenner four probe resistivity test is the Wenner resistivity, ρ_{Wenner} (see Table 6.1c).

6.3 Identification of the flow path in Permit ion migration test

The flow path of chloride ions in Permit ion migration test was determined theoretically as well as experimentally by Andrews (1999). The average flow path for Permit ion migration test was estimated to have an area (A) of 60 cm^2 and an effective length (L) of 2.72 cm (i.e., L/A = 4.53 m^{-1}) (see section 3.5.2). However, this was based on the following assumptions:

- The electric potential E is constant throughout the flow path.
- Average flow area is the average of the exposed area of the inner cell and that of the outer cell.
- The L/A is a constant, which only depends on the geometry of the Permit cell.

For a bulk concrete specimen similar to the one used for the Permit ion migration test, the intensity of electric field through the concrete depends much on the electrical resistivity of the material (Andrade, 1993). Therefore, the intensity of the electric field will diminish with distance from the source. The depths to which chloride ion reached were found to be different for different concretes, and this depth increases with the test duration (Andrews, 1999). Therefore, the assumption that L/A is a constant does not take into account the variations in L for different concretes or the test duration. Nevertheless, Andrews (1999) observed a good correlation between the *in situ* migration coefficient from Permit ion migration test (calculated using L/A = 4.53 m^{-1}) and other steady state test methods. This suggests that irrespective of the

variations in L for different test conditions, the value of L/A can be a constant, which would mean that the value of A may vary depending on the variations in L, or vice versa. Therefore, a new approach using the resistivity of the concrete is attempted here to define the L/A for different concretes as well as different test duration.

The following sections describe redefining the flow path L/A and the experimental verification of the L/A using the resistivity of the concrete mix obtained from various test methods.

6.3.1 Redefining flow path L/A

The average flow area and flow length for the steady state migration test is the face area of the concrete specimen exposed to the electrolytes (78.5 x 10^{-4} m^2) and the thickness of the concrete specimen perpendicular to the exposed face (20-30mm respectively). However, in Permit ion migration test the flow occurs or takes place in an axi-symmetric form, where both the flow length and the flow area depend on the strength of the electric potential represented by the equipotential lines. The schematic representation of the flow lines or the trajectory the chloride ions follow in Permit ion migration test are given in Fig. 6.1. The position of the inner cell and the outer cell is also shown in the figure. The average flow area is the curved surface area of the imaginary cylindrical surface perpendicular to the flow lines. The average flow length is the length of the equipotential line along which all the flow can be assumed to take place.

A finite element analysis of the flow pattern in Permit ion migration test, within the cover concrete has indicated that 90% of the flow takes place through the initial 15mm depth from the test surface (Basheer *et al.*, 2005). However, the chloride concentration in the concrete along the centreline up to a depth of 30mm at the completion of the test was the same. As the test progresses more chloride ions enter the concrete specimen from the inner cell. This increases the flow area by increasing the length of the imaginary cylinder (y). The increase in the flow area also increases the average flow length because chloride ions penetrating much deeper will take longer trajectory to reach the outer cell. So it can be assumed that this conjoint increase of both the average flow area (A) and the average flow length (L) maintains the L/A as a constant. However, the exact determination of the unknowns y and L is

difficult because the flow of ions depends on the resistance of the material and the pore structure.

As resistivity is the parameter characterising the ionic conductivity of the capillary pores in concrete (Andrade *et al.*, 2000), an approach using the resistivity of the concrete was used to estimate the flow path dimensions.

6.3.2 Determination of L/A

6.3.2.1 Theoretical background

During the migration test, the chloride front penetrates deeper through the concrete towards the anolyte side. In the one-dimensional migration test, the chloride front travels parallel to the exposed face and, in the case of the Permit ion migration test, the flow takes place from the inner cell to the outer cell. Andrews (1999) found that the hemispherical bulb of the chloride front (Fig. 6.1) expands with test duration. In the mean time, the resistance of the concrete specimen decreases as more chloride ions enter the specimen. When the flow reaches steady state, the bulb of concrete specimen influencing the flow will be saturated with chloride ions. Consequently, the resistance of the specimen decreases to a minimum, and provided the potential difference is maintained, the current increases to a maximum (peak current). Therefore, this peak current can be used to calculate the resistivity of the ion saturated concrete. This means that, in the case of the Permit ion migration test, the ion saturated path through which the flow takes place can be estimated once the resistance and the resistivity of the material are known. While the resistance can be estimated from the peak current, the resistivity can be determined from other tests on the same material.

6.3.2.2 Formulations to determine L/A from current flow (Ohm's law)

In case of the steady state migration test, where L is the thickness of the specimen, the resistivity of the sample, ρ_{1Dssm} (ohm.m) can be calculated from the peak current, using the following equation (Hassanein *et al.*, 1999):

$$\rho_{1D\,ssm} = \frac{Voltage}{Peak\ Current} \times \frac{Area}{Length} \qquad \text{(Eq. 6.1)}$$

where:

Voltage is the potential applied across the specimen, V

Area is the surface area of the test specimen exposed to migration, m^2

Peak current is the maximum current measured during the migration, A

Length is the thickness of the sample through which migration occurs, m.

In case of the Permit ion migration test, the resistance, $R_{in\ situ}$, can be calculated by dividing the applied voltage applied (60V) with the peak current obtained from the test.

$$R_{in\ situ} = \frac{Voltage}{Peak\ Current} \qquad \text{(Eq. 6.2)}$$

Figure 6.2 shows the relationship between the resistivity ρ_{1Dssm} and the resistance $R_{in\ situ}$. There is a linear relationship between the resistivity from the steady state migration test and the resistance of the concrete calculated from Permit ion migration test, (R^2=0.97), for a range of concrete mixes. The relationship is represented by the following equation:

$$R_{in\ situ} = 3.76 \text{ x } \rho_{1Dssm} \qquad \text{(Eq. 6.3)}$$

As the same concrete mix was used in both these tests, it can be assumed that both sets of specimens have the same resistivity. i.e., the resistivity of the concrete in Permit ion migration test is ρ_{1Dssm}. Therefore, it can be written that:

$$\rho_{in\ situ} = \rho_{1D\ ssm} = R_{in\ situ}\left(\frac{A}{L}\right) \qquad \text{(Eq. 6.4)}$$

Rearranging Eq. 6.4

$$R_{in\ situ} = \left(\frac{L}{A}\right)\rho_{1Dssm} \qquad \text{(Eq. 6.5)}$$

By comparing Eqs. 6.3 and 6.5, the dimensions of the flow net for the Permit ion migration test L/A can be obtained as $3.76m^{-1}$. This value of L/A was validated using the bulk resistivity of concrete (ρ_{bulk}) obtained from the bulk resistivity test as below.

The relationship between ρ_{bulk} and $R_{in\ situ}$ is presented in Fig. 6.3, which can be expressed by the following equation:

$$R_{in\ situ} = 3.77 \text{ x } \rho_{bulk} \qquad \text{(Eq. 6.6)}$$

where,

$R_{in\ situ}$ is the resistance calculated from Permit ion migration test using Eq. 6.2, ohm,

ρ_{bulk} is the bulk resistivity of the concrete specimen, ohm.m,

The value of R^2=0.88, suggesting that there exists a good relationship between the two. By comparing Eqs. 6.5 and 6.6, the value of L/A is found to be 3.77, compared to 3.76 obtained from the analysis of the steady state migration test data. As a higher degree of correlation (R^2=0.97) was obtained between the parameters in Eq. 6.3 compared to that in Eq. 6.6 (R^2=0.88), and also as the test set-up for the steady state migration test and the Permit ion migration test was similar, the L/A considered as the flow path dimension was 3.76 m^{-1}. Therefore, it can be stated that the value of 3.76m^{-1} for L/A can be used in Permit ion migration test. This L/A was used in calculating the $D_{in\ situ}$ (section 4.4.6.3).

The above relationship was evaluated based on the assumption that the resistivity obtained from the migration test compares to the actual resistivity of the concrete specimen. This assumption was further examined by comparing the resistivity obtained from the migration test with the bulk resistivity of the concrete in Fig. 6.4 and the relationship is represented in by the equation:

$$\rho_{bulk} = 0.99\rho_{1Dssm} \qquad \text{(Eq. 6.7)}$$

where,

ρ_{bulk} is the bulk resistivity of the concrete specimen, ohm.m,

ρ_{1Dssm} is the resistivity calculated from 1D steady state migration test using Eq. 6.1, ohm.m.

The coefficient of regression for the relationship was R^2=0.84. Eq. 6.7 suggests that both the resistivity values are comparable and they are of equal magnitude. This validates the assumption that the resistivity obtained from the migration test using the peak current is comparable to the actual resistivity of the concrete specimen.

6.3.3 Measurement of the chloride front

The actual chloride front was identified by spraying the silver nitrate solution after the completion of the test. The shape and dimensions of the chloride front in the form

of hemispherical bulb described earlier (see Fig. 6.1) for four concrete mixes were as shown in Fig. 6.5. The resistivity values of the mixes are also given in the figure. The volume of the chloride front bulb increased with the decrease in resistivity of the mix. The largest dimension was for the pfa mix while the smallest for the ggbs mix. Eq. 6.3 suggest that irrespective of the differences observed in the chloride front (and the mix), the L/A for the Permit ion migration test is a constant. This also validates the assumption that any increase in the average flow area could be associated with a conjoint increase in the average flow length, thereby keeping the L/A constant.

6.4 Influence of mix variables on test parameters

The material properties influencing the chloride diffusivity of concrete have been identified in section 2.6 to be the w/b, the type of binder, the aggregates and the curing regime. In this section the influence of the w/b and the type of binder on the test parameters obtained from the Validation Programme are discussed. As mentioned before the age of specimens at which tests commenced was 28 days for mixes with w/b 0.40 and 0.45 and it was 56 days for the mixes with w/b 0.52. Furthermore, the maximum size of coarse aggregate was also different for the various mixes. However, their efforts on any measured parameters have been ignored in the following discussion because the objective of the discussion is to compare the effects of two mix parameters, viz. w/ and the type of binder, on various measured parameters.

6.4.1 Effect of mixes on D_{nssm}

The effect of the w/b and the type of binder on the non-steady state migration coefficient, D_{nssm}, is presented in Fig. 6.6 and 6.7 respectively. Similar to the results discussed in section 5.2.2.2, the D_{nssm} was influenced by the w/b as well as the type of binder.

Figure 6.6 shows a trend of increase in the D_{nssm} with the increase in w/b, despite the fact that the test ages were 28 days for the 0.45 mixes and 56 days for the 0.52 mixes. This is considered to be due to the increase in the porosity of concrete with the increase in w/b (Neville, 1996). The increase in D_{nssm} with w/b was less pronounced

in the case of ggbs and ms mixes compared to other two mixes, presumably due to the better hydration of 0.52 w/b mixes at the age of 56 days.

The D_{nssm} measured for the ggbs and the ms mixes were the lowest for both w/b (see Fig. 6.7). This could be due to the dense microstructure observed generally in ggbs and ms mixes (Roy, 1989b). The D_{nssm} values obtained for the pfa mixes were the highest for both w/b. However, this can be attributed to testing the concrete at an early age of either 28 or 56 days. As the breakdown of the pfa particles takes time and required a pH $\geq$ 13.2, the pozzolanic reaction of the pfa is extremely slow at early ages. This improves with the release of $Ca(OH)_2$ into the pore solution due to the hydration of the opc. As a result, at early ages the pfa concretes exhibit higher diffusivities than opc and ms mixes of similar mix ratios (Roy, 1989b). For similar mixes, Gilleece (1996) reported the non-steady state diffusion coefficient obtained from chloride profiles and the chloride migration index. This study showed that the diffusion coefficient for the ggbs concrete was half of those obtained for the opc mix. A similar trend was observed for the chloride migration index. In the case of the pfa mix, a lower diffusion coefficient than that of opc was observed for the 12 months old specimen. However, the migration index showed a relatively very high difference in diffusivity for the 1 month old specimen and a moderate difference for the 12 months old specimen. Similar observations were reported by McPolin (2005) for 0.50 w/b pfa mix (6 months old specimens). At 0.52 w/b the D_{nssm} changed in the order pfa>opc>ms>ggbs (Fig. 6.7).

6.4.2 Effect of mixes on D_{1Dssm}

The steady state migration coefficient, D_{1Dssm} obtained for all the mixes are presented in Figs. 6.8 and 6.9. Unlike results in the Evaluation Programme in section 5.2.2.3, the value of the D_{1Dssm} was very much influenced by both the w/b and the type of binder in the Validation Programme.

Figure 6.8 shows that the value of D_{1Dssm} increases with the increase in w/b in all cases. The increase in D_{1Dssm} however was much more pronounced than D_{nssm} (section 6.4.1).

Figure 6.9 shows that the type of binder influenced the D_{1Dssm} to a considerable extent. For all the mixes with 0.52 w/b the D_{1Dssm} varied in the order pfa>opc>ms>ggbs. These results follow a trend similar to that reported by Delagrave *et al.* (1996), Halamickova *et al.* (1995) and Tong and Gjorv (2001). The lowest D_{1Dssm} was obtained for the 0.45 ggbs mix and the highest for the 0.52 pfa mix. Similar to the findings presented in section 6.4.1, the pfa mixes had the highest diffusivities for both w/b. Again, this could be the result of the slow early hydration of the pfa particles.

6.4.3 Effect on $D_{in\ situ}$

The effect of the w/b and the type of binder on the *in situ* migration coefficient is presented in Fig. 6.10 and Fig. 6.11 respectively. Figure 6.10 shows that the $D_{in\ situ}$ increased with the increase in w/b for all types of binders. Similar results were reported by Andrews (1999).

The use of supplementary cementitious materials generally decreased the $D_{in\ situ}$ at both w/b investigated (see Fig. 6.11). Whereas ggbs and ms mixes exhibited the lowest $D_{in\ situ}$, the pfa mixes had the highest $D_{in\ situ}$. As explained previously this could be due to the slow initial hydration of pfa particles. The trend shown in Fig. 6.11 is similar to that observed in Fig. 6.7 and Fig. 6.9 for the D_{nssm} and D_{1Dssm} respectively. Therefore, it can be stated that the $D_{in\ situ}$ distinguishes the variations in the mixes in a manner similar to that by D_{nssm} and D_{1Dssm}.

6.4.4 Effect on ρ_{bulk} and ρ_{Wenner}

6.4.4.1 Theoretical considerations

The electrical resistivity of the concrete specimens was obtained using the bulk resistivity test and the Wenner four probe resistivity test. The electrical conductivity, which is the inverse of the electrical resistivity, is related to diffusivity of specimen by the following equation (Streicher and Alexander, 1995):

$$\frac{D}{D_0} = \frac{\sigma}{\sigma_0} \qquad \text{(Eq. 6.8)}$$

where,

D is the diffusivity of ions through porous material (concrete specimen), m^2/s,

D_0 is the diffusivity of ions through pore solution, m^2/s,

σ is the conductivity of the porous material (concrete specimen), ohm.m,
σ_0 is the conductivity of the pore solution, ohm.m.

From the above equation it can be stated that, for a given pore solution with diffusivity equals D_0 and conductivity equals σ_0, the diffusivity, D of the material is directly related to its conductivity, σ. In other words, the resistivity, which is the inverse of the conductivity, is inversely proportional to the diffusivity. Andrade (2006), considered that for concretes under normal exposure conditions, the D_0 and σ_0 of different pore solutions are comparable and, hence, the resistivity, ρ, of concrete can be related to the diffusivity, D_{ssm} (steady state migration coefficient) by the following equation.

$$\rho = \frac{230}{D_{ssm}} \qquad \text{(Eq. 6.9)}$$

where,
ρ is the resistivity of the material, ohm.m,
D_{ssm} is the steady state migration coefficient (for catholyte NaCl 0.55M) in m^2/s without the multiplier 10^{-12}.

The following sections discuss the effect of the w/b and the type of binder on both the bulk resistivity and the Wenner resistivity. From the above discussion, it is expected that both the resistivity values will provide an inverse trend to that observed in the case of the migration coefficients (sections 6.4.1 to 6.4.3).

6.4.4.2 Effect of mixes on ρ_{bulk}

The effect of the w/b and the type of binder on the bulk resistivity, ρ_{bulk} is presented in Fig. 6.12 and Fig. 6.13 respectively. In Fig. 6.12, the ρ_{bulk} decreased with the increase in w/b for all mixes. As discussed previously in section 5.2.2.4, the increase in w/b increases the porosity and the connectivity between the pores. This would result in an increased current flow through the concrete, thus lowering the resistivity.

In Fig. 6.13, for w/b 0.45, the ρ_{bulk} was the highest for the ggbs mix and changed in the order ggbs>pfa>opc (note that the w/b of the microsilica mix was 0.4). For 0.52 w/b, ρ_{bulk} changed in the order ms>ggbs>pfa>opc, which indicates that the trends for both 0.45 and 0.52 w/b were similar. However, the difference in ρ_{bulk} values of the

opc and the pfa mix in 0.52 w/b was negligible. It is known that the pozzolanic reaction of the supplementary cementitious materials results in a discontinuous pore system and, hence, leads to a very high resistivity. This is evident in Fig. 6.13, that is, the resistivity generally increased for concretes containing supplementary cementitious materials. However, in the case of the pfa mixes, this effect probably did not result in a significant change in resistivity compared to the opc mixes, the reasons for which shall be explored further.

In general, similar to the bulk resistivity results discussed in section 5.2.2.4, when there was an increase in ρ_{bulk} with a change in mix parameter, correspondingly there was a decrease in diffusivity, (sections 6.4.1 - 6.4.3), except for the pfa mixes, which did not follow this general trend. Although the pfa mix was expected to show a lower resistivity than the corresponding opc mix, an opposite trend was obtained. The difference was more pronounced for the 0.45 w/b mixes. Two possible explanations for the increase in resistivity in the case of pfa mixes are as follows:

1. The bulk resistivity was measured with concrete specimens saturated with $Ca(OH)_2$ solution. The presence of the $Ca(OH)_2$ solution in the pore water could increase the dissolution of the unhydrated pfa particles and produce more C-S-H and C-A- H. As these new products block the pores in concrete, the resistivity could increase.
2. The intrinsic resistivity of the pfa particles could be higher than the corresponding opc particles. For example, Kokubu *et al.* (1974) suggested that the pfa particles show a hydrophilic nature. That is, they could absorb the water molecule and, hence, reduce the moisture content around them. This lack of moisture content could result in an increase in resistivity around the pfa particle, which will increase the resistivity of the concrete as a whole.

These findings are further explored whilst discussing the Wenner resistivity in section 6.4.4.3.

Polder (2001) provided a classification of concretes based on the electrical resistivity from site measurements (see Chapter 3, Table 3.5). However, for concretes containing supplementary cementitious materials, only guidelines were given. Nevertheless, when the resistivity values obtained from the bulk resistivity test

(Table 6.1c) are compared with classification given by Polder (see Chapter 3, Table 3.5), it can be seen that the resistivity values from this investigation lie at the lower end of the scale. This could be either because the specimens were saturated with $Ca(OH)_2$ solution prior to the measurement, which could lower the resistivity, or due to the fact that the test ages of 28 and 56 days were not sufficient for demonstrating the benefits of the supplementary cementitious materials on resistivity values.

6.4.4.3 Effect of mixes on ρ_{Wenner}

The effect of w/b and the type of binder on Wenner resistivity is presented in Fig. 6.14 and Fig. 6.15 respectively. Similar to the ρ_{bulk}, the Wenner resistivity, ρ_{Wenner} decreased with an increase in w/b for all mixes (see Fig. 6.14). However, the differences were less pronounced in the case of ρ_{Wenner}. In the case of ρ_{bulk}, the increase in w/b from 0.45 to 0.52 nearly halved the corresponding resistivity values. However, the case was not the same for ρ_{Wenner}, where a similar increase in w/b led to only a marginal decrease in ρ_{Wenner}.

The effect of the type of binder on the ρ_{Wenner} is shown in Fig. 6.15. This figure shows that, in the case of 0.45 w/b, the resistivity changed in the order ggbs>pfa>opc, with ggbs mix having resistivity 5.6 times higher than the corresponding opc mix. For 0.52 w/b mixes, the Wenner resistivity changed in the order ggbs>ms>opc>pfa, which highlights that the effects of w/b on ρ_{Wenner} for the two w/b were not the same. Furthermore, in the case of the bulk resistivity, in section 6.4.4.2, it was observed that the ρ_{bulk} was higher than that of the opc for 0.45 w/b and the difference was negligible for 0.50 w/b. In Fig. 6.15, the difference in ρ_{Wenner} for opc and pfa mixes is marginal for both w/b. However, when the individual values in Table 6.1c are compared with the effects in both Fig. 6.13 and 6.15, it can be concluded that the variations between pfa and opc mixes are not significant.

6.4.5 Effect of mixes on current in migration tests

In both the Permit ion migration test and the steady state migration test, a constant voltage was applied between the electrodes. Therefore, the current can be considered to be inversely proportional to the resistance of the concrete according to the Ohm's law (section 6.3.2.2, Eq. 6.2). As discussed in section 6.4.4.1, the resistivity of concrete can be considered to be inversely proportional to the migration coefficient

(Andrade *et al.*, 2000). Consequently, the current obtained from the migration tests should be directly proportional to the migration coefficient. That is, a discussion on the effects of mix variables on current is appropriate to study the effects of mix variables on the migration coefficients. The effects of the two mix variables on the initial and the peak current obtained from both the steady state migration test and the Permit ion migration test are discussed in the following sections.

6.4.5.1 Initial current from steady state migration test

As stated in section 4.4.6.2, the test voltage was decided on the basis of the resistivity of the specimens. The test voltage in the case of 0.52 w/b opc, pfa and ms mixes was 12V and for all other mixes it was 60V (see Table 6.1b). If the capillary pores were saturated with an ionic solution which is used to carry out the test, the initial current at 12V would have been $1/5^{th}$ of that at 60V, as per Ohm's law. However, in this case, initially the pores were saturated with de-ionised water, not with an ionic solution. Therefore, the above relationship cannot be applied to relate the initial current at 12V to that at 60V. However, for comparison purposes, the initial currents obtained at 12V are adjusted to 60V by multiplying with a factor of 5 and are presented in Figs. 6.16 and 6.17. The test voltage and the corresponding initial current for all the mixes are presented in Table 6.1b.

The effect of the w/b and the type of binder on the initial current is presented in Fig. 6.16 and Fig. 6.17 respectively. Figure 6.16 shows that the initial current increased with the increase in w/b for most cases, except that for the pfa mixes. As the porosity of concrete increases with an increase in w/b, the initial current is also expected to increase in a similar manner. The effect of w/b on the initial current was similar to that obtained for the migration coefficients discussed in sections 6.4.1 to 6.4.3 and had an inverse trend with that observed for the resistivity values in sections 6.4.4.2 and 6.4.4.3. As there are numerous interlinked effects causing the changes in initial current, the apparent spurious result for the pfa mixes cannot be explained without further investigation.

The effect of the type of binder on the initial current was not apparent (see Fig. 6.17). For 0.45 w/b mixes, the initial current changed in the order pfa>ggbs>opc and for 0.52 w/b the order was opc>ms>pfa>ggbs. The beneficial effect of ggbs or ms mixes

was not apparent in Fig. 6.17. The trend observed was not similar to that observed for the migration coefficients (sections 6.4.1 to 6.4.3). This apparent contradiction observed for the initial current is possibly due to the limitations discussed below.

(i) The thickness of the test specimens was different between the two different w/b by a significant margin and within each w/b there was a slight variation in thickness of the specimens (see Table 6.1b). An increase in thickness could result in an increase in resistance, which could decrease the current in the migration tests. However, as the thickness of specimens did not vary significantly for a given w/b, this is not considered to have influenced the initial current significantly for measurements carried out for each w/b, but this might have influenced the differences in initial current values between the two sets of data for the two w/b.

(ii) The resistance of the cell arrangement in a migration test (the specimen-electrolyte interface and the electrolyte-electrode interface) could have contributed to the actual resistance offered by the specimen. This resistance could be more influential in 12V tests when compared to 60V tests (McGrath and Hooton, 1996). As the cell resistance was not separated from the resistance of the specimen and, both were not measured, no further attempt is made here to explain the effects of the w/b or the type of binder on the initial current.

6.4.5.2 Initial current from Permit ion migration test

The effect of the w/b and the type of binder on the initial current from the Permit ion migration test is presented in Fig. 6.18 and 6.19 respectively. In general, an increase in w/b resulted in an increase in initial current significantly in all mixes except for both opc and ms mixes (see Fig. 6.18); in the latter cases, the difference between the initial currents obtained for the 0.45 and 0.52 w/b was negligible.

Figure 6.19 shows that the effect of the type of binder on the initial current was similar to that obtained for the migration coefficients (see sections 6.4.1 to 6.4.3). For the 0.45 w/b, ggbs mix showed the lowest initial current and the general trend was pfa>opc>ggbs. The trend was similar for 0.52 w/b mixes, with the highest initial current observed for the pfa mix, and other mixes exhibiting lower initial current with a trend pfa>opc>ms>ggbs.

The trend observed for the effect of w/b and type of binder on the initial current for all mixes was similar to that of the migration coefficients discussed in sections 6.4.1 to 6.4.3 and inverse to that of the resistivity values discussed in sections 6.4.4.2 and 6.4.4.3. However, the relative differences of the initial current in Figs. 6.18 and 6.19 between the mixes were marginal compared to that observed for the migration coefficients or resistivity values. Therefore, the initial current in Permit ion migration test is not appropriate to distinguish the mixes for their resistance to the transport of chloride ions. Furthermore, these results strengthen the argument that unless the pores are completely saturated with the ionic solution used to carry out the migration test, the initial current does not reflect the resistance of the concrete to the flow of ions.

6.4.5.3 Peak current from the steady state migration test

As mentioned in the section 6.4.5.1, the test voltage for the 0.52 w/b opc, pfa and ms mixes was 12V and that for all other mixes was 60V (see Table 6.1b). Therefore, the initial currents discussed in section 6.4.5.1 were adjusted before comparing with those obtained for tests carried out at 60V. A similar procedure was adopted in the case of the peak current. However, during the peak current, the pores are saturated with the ionic solution and, hence, it is reasonable to assume that the current is linearly proportional to the voltage. Therefore, in the case of the peak current, the adjustment applied to the 12V data can be justified with confidence. The adjusted peak current values are presented in Figs. 6.20 and 6.21, in order to identify the effect of the w/b and the type of binder respectively.

Figure 6.20 shows that with the increase in w/b the peak current increases for all mixes. With the increase in w/b, the porosity of concrete also increases (Neville, 1996). This results in a reduced resistivity, which leads to an increased current and chloride flow through the concrete. Therefore, the peak current and the diffusivity of concrete are expected to increase with the increase in w/b, while the resistivity is expected to decrease. This variation in the peak current with w/b shown in Fig. 6.20 is similar to that observed for the migration coefficients discussed in sections 6.4.1 to 6.4.3, and shows an opposite trend to that observed for the resistivity values discussed in sections 6.4.4.2 and 6.4.4.3.

Figure 6.21 shows that the effect of the type of binder influenced the peak current in a similar manner for both the w/b. For 0.45 w/b the peak current varied in the order pfa>opc>ggbs and for 0.52 w/b the peak current changed in the order pfa>opc>ms>ggbs. These trends are similar to those observed for the migration coefficients discussed in sections 6.4.1 to 6.4.3. The resistivity values for the pfa mixes were better than those for the opc mixes in Fig. 6.13, suggesting that the peak current values of the pfa mixes would be lower than that of the corresponding opc mixes. However, the trend in Fig. 6.21 was different; the pfa mixes exhibited the highest peak current values, conforming to the trend observed for the migration coefficients in Figs. 6.7, 6.9 and 6.11. This confirms that the effects of the w/b and the type of binder on the peak current and the migration coefficients are similar.

6.4.5.4 Peak current from Permit ion migration test

The effects of w/b and the type of binder on the peak current obtained from the Permit ion migration test for all the mixes are presented in Figs. 6.22 and 6.23 respectively. The effect of the w/b on peak current in Permit ion migration test was similar to that discussed in section 6.4.5.3 for the steady state migration test.

The effect of the type of binder on the peak current in Permit ion migration test is shown in Fig. 6.23. This figure shows that for the 0.45 w/b mixes the peak current varied in the order opc>pfa>ggbs. This variation was different to that of the peak current obtained for the steady state migration test (see section 6.4.5.3), for which the peak current varied in the order pfa>opc>ggbs. As the actual values in Permit ion migration test are relatively closer for the opc and pfa mixes, no further explanation is given for this apparent contradiction. However, for the 0.52w/b mixes, the variation in the peak current was similar to that for the steady state migration test, viz. pfa>opc>ms>ggbs.

Therefore, it can be concluded that the peak current observed in both the steady state migration test and the Permit ion migration test increases with an increase in w/b and decreases for mixes containing supplementary cementitious materials. This effect was very similar to that observed for the migration coefficients presented in sections 6.4.1 to 6.4.3 and the trend was opposite to that of the resistivity.

6.4.6 Effect of mixes on charge passed

In both the steady state migration test and the Permit ion migration test, the current flowing between the electrodes was used to calculate the charge passed. ASTM C1202 (1997) estimates the charge passed during the first six hours as a measure of the chloride ingress resistance of concrete. Therefore, the charge passed during the first six hours in both the steady state migration test and the Permit ion migration test was calculated for all mixes and the effect of mix variables on the charge passed is discussed.

The ASTM C1202 (1997) requires a test thickness of 50mm. However, the thickness of the test specimen used in the steady state migration test was different for different mixes (see Table 6.1b). The test is to be carried out at 60V according to ASTM C1202 (1997), whereas the steady state migration test was carried out at either 12V or 60V depending on the resistivity of the mix (see Table 6.1b for the test voltage). Therefore, the following procedure was used in order to calculate the charge passed during the six hours from the steady state migration test.

1. The charge passed at 12V was multiplied by a factor 7.5 to estimate the equivalent charge passed at 60V (justified according to Misra *et al.*, 1994).
2. The equivalent charge passed estimated using step 1 was adjusted to take account of the variation in the volume of the specimens, by multiplying with the corresponding thickness of the test specimen (as the diameter of the test specimens was the same) and a normalised charge passed was estimated.
3. In order to obtain the value of the charged passed during the first six hours an interpolation of the current obtained during the test was used to find the current at six-hour first, the current values up to six hours were then used to calculate the charge passed during the first six hours. Therefore, the number of points used for the interpolation might have influenced the accuracy of the calculated charge passed. Although, ideally it would have been better if the value of the current was available at six hours as well as at other times before this, the practical difficulties did not permit these measurements.

Due to the above limitations of the procedure used to calculate the six hour charge passed, the intention here is to see if there is any possibility of using the charge

passed to qualify the concretes rather than trying to correlate with the ASTM C 1202 classifications.

In case of the Permit ion migration test, the test was carried out on the concrete surface directly. Therefore, the thickness of 50mm specified by the ASTM C1202 was not applicable. The Permit ion migration test was carried out using 60V for all the mixes. Therefore, there was no need to adjust the value of the charge passed for the variation in the applied voltage, unlike in the case of the steady state migration test.

Besides the charge passed during the first six hours, the charge passed until both the commencement of the steady state (i.e. charge passed during the time lag in Fig. 3.8) and up to the peak current was calculated. However, the latter is not used in any further discussions because the charge passed up to the peak current followed trends similar to those of the former and between the two the former is more reliable to qualify the concrete due to the limitations of the current values during the steady state. In any case, further discussion of the charge passed during the steady state is given in section 6.5.5.

6.4.6.1 Normalised six-hour charge passed in the steady state migration test

The effect of the w/b and the type of binder on the normalised charge passed during the first six hours is presented in Fig. 6.24 and 6.25 respectively. Figure 6.24 shows that the charge passed during the first six hours increased with an increase in the w/b, except for the pfa mixes. As discussed in section 6.4.5.1, the increase in w/b increases the porosity of the concrete. This increases the flow of current through the concrete, thus resulting in an increased charge passed for a given test duration, with an increase in the w/b. In case of the pfa mixes, concrete with w/b 0.45 showed much higher charge passed than the one with w/b 0.52. The initial current presented in Fig. 6.16 showed that the mix with w/b 0.45 had a higher initial current than that with w/b 0.52. As stated in section 6.4.5.1, the apparent spurious trend cannot be explained without carrying out further detailed investigation on the pfa mixes.

The effect of the type of binder on the normalised six-hour charge passed in the steady state migration test is shown in Fig. 6.25. For the mixes with w/b 0.45, the

charge passed was the highest for the pfa mix followed by the opc mix and the ggbs mix in a decreasing order. In mix with w/b 0.52, the normalised six-hour charge passed varied in the order ms>opc>pfa>ggbs. The beneficial effect of concretes containing ms was not apparent in Fig. 6.25. Both the ms mixes showed higher charge passed compared to their opc counterparts. Interestingly the trend observed in the Fig. 6.25 is similar to that observed for the initial current, discussed in section 6.4.5.1. The initial current was considered to have limitations due to the fact that the measurements were made on concretes saturated with water rather than the ionic solution used to carry out the test. Other factors which might have influenced the initial current were also discussed in section 6.4.5.1. Therefore, the apparent lack of trend in Fig. 6.25 for the normalised six-hour charge passed can also be related to these limitations.

6.4.6.2 Six hour charge passed in Permit ion migration test

The effect of the w/b and the type of binder on the effect of the charge passed during the first six hours in Permit ion migration test is shown in Fig. 6.26 and Fig. 6.27 respectively. Figure 6.26 shows that the charge passed during the first six hours increased with an increase in the w/b only for the ggbs mixes and in all other cases an opposite trend was observed. It must be noted here that all the mixes with w/b 0.45 contained 10mm maximum size aggregates as opposed to 6mm in mixes with w/b 0.52 and the steady state condition was reached in the former cases before six hours. Therefore, some of the results in Fig. 6.26 contained data corresponding to the non-steady state condition and some others incorporated data beyond the steady state. As a result, it is not desirable to make use of the six-hour charge data to distinguish the mixes in Permit ion migration test. However, for the completeness of the discussions, the effect of the type of binder on the six-hour charge passed in Permit ion migration test is presented in Fig. 6.27. Interestingly, the effect of the mixes in both w/b was found to follow the similar trends, which is pfa>opc>ggbs for the mixes with w/b 0.45 and pfa>ggbs>opc>ms for mixes with w/b 0.52.

From the results discussed above for both the steady state migration test and the Permit ion migration test, it can be stated that the charge passed during the first six hours cannot be used to distinguish the effect of mix variables on the chloride diffusivity.

6.4.6.3 Charge passed until steady state in the steady state migration test

The effect of the w/b and the type of binder on the normalised charge passed until steady state is presented in Fig. 6.28 and Fig. 6.29 respectively. The charge passed increased with an increase in the w/b, except for the ggbs mixes. The trend was opposite for the ggbs mixes (i.e. with an increase in the w/b from 0.45 to 0.52, the charge passed was nearly halved). The results presented in sections 6.4.1 to 6.4.3 suggest that the chloride diffusivity of the 0.45 ggbs mix is lower than that of the 0.52 ggbs mix. In section 6.4.4, the resistivity of the 0.45 ggbs mix was higher than that of the 0.52 ggbs mix. The initial current discussed in section 6.4.5.1 also demonstrated that the 0.52 ggbs mix is more permeable than the 0.45 ggbs mix. Considering all these data, the decrease in charge passed with the increase in the w/b for the ggbs mix in Fig. 6.28 cannot be explained.

The effect of type of binder in Fig. 6.29 shows that the charge passed was the highest for the opc mix, followed by ggbs and pfa in the decreasing order for the mixes with w/b 0.45. For the mix with w/b 0.52, the charge passed varied in the following order opc>ms>pfa>ggbs. Based on the resistivity values for the mixes with w/b 0.45 in Fig. 6.13, the ggbs mix was expected to show a low charge passed. Once again, this apparent spurious trend cannot be explained without further investigation. The charge passed in the case of 0.45 pfa mix was lower compared to the corresponding opc mix. The bulk resistivity presented in section 6.4.4.2 suggests that the pfa mix is more resistive compared to the opc mix. Therefore, the trend in Fig. 6.29 for the 0.45 pfa and opc mixes can be expected.

The changes in the charge passed for the mixes with w/b 0.52 are very similar to those of both the initial current (section 6.4.5.1, Fig. 6.17) and the normalised six-hour charge passed (section 6.4.6.1, Fig. 6.25). When the effect of the supplementary cementitious materials on the charge passed until steady state is considered for the mix with w/b 0.52, there was a reduction due to the addition of the supplementary cementitious materials in all cases except for the ms mix. Therefore, it can be stated that similar to the normalised six-hour charge passed, the charge passed until steady state also failed to identify the beneficial effects of the ms mix.

Due to the unexpected variations in trends of the data presented in Figs. 6.28 and 6.29, it is difficult to draw any definite conclusions using the charge passed till steady state. Nevertheless, the trends discussed in section 6.4.6.1 and the current section suggests that the charge passed failed to identify the beneficial effects of the ms mixes.

6.4.6.4 Charge passed until steady state in Permit ion migration test

The effect of the w/b on the charge passed until steady state in Permit ion migration test is presented in Fig. 6.30. This figure shows that with an increase in the w/b, the charge passed also increased for all the mixes, despite the fact that the mixes with w/b 0.45 were tested at an age of 28 days and the mixes with w/b 0.52 were tested at the age of 56 days. Therefore, it can be concluded that the charge passed until steady state is capable of identifying the mix effect caused by the change in the w/b irrespective of the type of binder in the Permit ion migration test.

Figure 6.31 shows the effect of the type of binder on the charge passed until steady state. It is evident from the figure that the charge passed for concrete containing ggbs was the lowest for both the w/b. For both the w/b the charge passed increased for pfa and opc mixes in this order compared to the ggbs mixes, with the ms mix showing values closer to that of the pfa mix in the case of the mixes with w/b 0.52. In section 6.4.4.2 it was found that the resistivity of the 0.52 ms mix was higher than the corresponding pfa mix (Fig. 6.13) and in Figs. 6.9 and 6.11 the migration coefficients also demonstrated correspondingly lower values for ms mixes compared to the pfa mixes. Therefore, the charge passed until steady state for the pfa mix should have been higher than that of the ms mix. However, such a trend was not observed in Fig. 6.31, which demonstrates again the limitation of using the charge passed to distinguish the mixes.

6.4.7 Conclusions on the influence of mixes on test parameters

On the basis of the effects of both the w/b and the type of binder on various measured properties, the following conclusions can be drawn:

(i) The non-steady state migration coefficient, D_{nssm}, the steady state migration coefficient, D_{1Dssm} and the *in situ* migration coefficient, $D_{in\ situ}$ increased with an

increase in the w/b irrespective of the mixes and the differences in the test ages. In general, the aforementioned three parameters decreased for concretes containing supplementary cementitious materials compared to their opc counterparts, except for the pfa mixes, which showed a higher D_{nssm}, D_{1Dssm} and $D_{in\ situ}$ compared to other mixes for both the w/b studied. From the results discussed, it can be observed that the effects of mixes on the non-steady state migration coefficient, the steady state migration coefficient and the *in situ* migration coefficient were similar.

(ii) The bulk resistivity, ρ_{bulk} and the Wenner resistivity, ρ_{Wenner} decreased with an increase in the w/b, which is opposite to the trend reported in (i). The resistivity values were high for concretes containing supplementary cementitious materials, except for the pfa, which did not show any consistent trend. For mixes with w/b 0.45, the pfa concretes showed slightly higher ρ_{bulk} and ρ_{Wenner} compared to the corresponding opc mixes, but both sets were similar for the mixes with w/b 0.52. These anomalies are considered to have been caused due to the way pfa concretes responded to the method of saturating them with water and saturated $Ca(OH)_2$ solution. Nevertheless, it can be concluded that the bulk resistivity and the Wenner resistivity can be used to distinguish the variations in the mixes.

(iii) The effect of the mixes on the initial current observed from the steady state migration test for most of the mixes was similar to that found for the migration coefficients. The pfa mixes were an exception to this general trend. As many interlinked factors were considered to have influenced the initial current measured from the steady state migration test, this was not considered to be a good test parameter to distinguish the effect of both the w/b and the type of binder on the chloride transport. The effect of mixes was more apparent for the initial current from the Permit ion migration test compared to that observed for the steady state migration test. Nevertheless, the trends were not sufficiently clear to consider this property to distinguish the mix effects.

(iv) The effect of the mixes on the peak current measured from both the steady state migration test and the Permit ion migration test was varied similar to that obtained for the corresponding migration coefficients. Therefore, it can be

concluded that the peak current is a useful parameter to study the effect of mixes on the chloride transport resistance of concretes.

(v) The six-hour charge passed for the steady state migration test and the Permit ion migration test did not show any clear trends due to the variations in the w/b or the type of binder. As a consequence, this was not considered to be a reliable measure of the chloride transport resistance of concretes.

(vi) In general, the charge passed until steady state from both the steady state migration test and the Permit ion migration test increased with the increase in w/b and this was lower for concretes containing supplementary cementitious materials compared to their opc counterparts. However, the charge passed was relatively higher for ms concretes compared to the pfa concretes; this trend should have been reversed according to the resistivity values of these mixes. As there was a reasonably good agreement in trend between the resistivity values and the migration coefficients in both these tests, it was considered that the apparent anomaly in charge passed for the pfa and the ms mixes was due to the limitations of the charge passed in distinguishing the mix effects.

6.5 Relationships between different test parameters

In this section, the relationships between different test parameters assessing the resistance of concrete to chloride transport are discussed first. This is followed by a critical comparison of the charge passed with the migration coefficients, which is used to evaluate critically the usefulness of expressing charge passed as a measure of the chloride ion penetration resistance. These are followed by a discussion on other properties from tests which can be used to estimate the chloride ion penetration resistance. Finally, methods to improve the test protocol used in Permit ion migration test are presented.

6.5.1 Relationships between D_{nssm}, D_{1Dssm} and $D_{in\ situ}$

6.5.1.1 Relationship between D_{nssm} and D_{1Dssm}

The relationship between D_{nssm} and D_{1Dssm} is presented in Fig. 6.32. In this figure, a satisfactory correlation between the two parameters, with a coefficient of determination, R^2 of 0.67 can be seen. The relationship is represented by the equation:

$$D_{nssm} = 4.42 \times D_{1Dssm} \qquad \text{(Eq. 6.10)}$$

where both D_{nssm} and D_{1Dssm} are in m^2/s.

This equation shows that the non-steady state migration coefficient was 4.42 times the steady state migration coefficient, which is in agreement with the relationship reported by Delagrave *et al.* (1996). As discussed in section 5.2.3.2, the non-steady state migration coefficient is a function of the porosity of the concrete, the binding capacity and the steady state diffusion coefficient. Therefore, the difference between the magnitudes of the coefficients in the above relationship can be considered to be due to a factor representing both the binding capacity and the porosity of the mixes.

The relationship between the D_{nssm} and D_{1Dssm} from the Evaluation Programme was discussed in section 5.2.3.3. Compared to the relationship discussed in section 5.2.3.3 and Chlortest (2006), a better relationship was observed in Eq. 6.10, presumably due to the use of a thickness of three times the maximum aggregate size for specimens used in the steady state migration test. This supports the argument that a thicker test specimen needs to be used to carry out the steady state migration test.

6.5.1.2 Relationship between D_{nssm} and $D_{in\ situ}$

Figure 6.33 shows the relationship between $D_{in\ situ}$ and D_{nssm}. There is a good relationship between the two parameters (R^2 = 0.82) expressed by the following equation:

$$D_{in\ situ} = 0.11 \times D_{nssm} \qquad \text{(Eq. 6.11)}$$

where,

D_{nssm} is the steady state migration coefficient, m^2/s,

$D_{in\ situ}$ is the *in situ* migration coefficient, m^2/s.

Similar to the relationship discussed above, the magnitude of D_{nssm} was higher than the $D_{in\ situ}$ (i.e. D_{nssm} was 9.1 times $D_{in\ situ}$). The reason for this difference is the same as that discussed in the above section.

Andrews (1999) reported a good correlation between the non-steady state diffusion coefficient (or the apparent diffusion coefficient) and the *in situ* migration coefficient for opc concretes. The non-steady state migration coefficient was found to correlate well with the non-steady state diffusion coefficient (section 5.2.3.1, (Chlortest 2006)). Therefore, the relationship presented in Eq. 6.11 establishes further that the $D_{in\ situ}$ can estimate the non-steady state migration coefficient for concretes containing cement replacement materials, without removing the cores for testing in a laboratory.

6.5.1.3 Relationship between D_{1Dssm} and $D_{in\ situ}$

The relationship between $D_{in\ situ}$ and the $D_{1D\ ssm}$ is presented in Fig. 6.34. There is an excellent correlation between the two migration tests (R^2=0.93), showing that the chloride diffusivity determined by the Permit ion migration test was similar to that determined by the more established steady state migration test. However, the former value differed by the latter by a factor of 0.55, as shown in Eq. 6.12:

$$D_{in\ situ} = 0.55 \times D_{1D\ ssm} \qquad \text{(Eq. 6.12)}$$

where,

$D_{1D\ ssm}$ is the steady state migration coefficient, m^2/s,

$D_{in\ situ}$ is the *in situ* migration coefficient, m^2/s.

According to Andrews (1999), the $D_{in\ situ}$ was 0.271 times D_{1Dssm}. This would mean that the value of $D_{in\ situ}$ that is predicted from D_{1Dssm} (Eq. 6. 12) would be higher than that calculated based on the equation given by Andrews (1999). As shown in section 6.3, the L/A value used in this research was $3.76m^{-1}$ and Andrews used a value of $4.53m^{-1}$. Therefore, as per Eq. 4.20 for a given concrete, when a measured chloride flux J is multiplied by each of the above L/A values to calculate the corresponding $D_{in\ situ}$, a lower value will be yielded from this research compared to that from Andrews. As stated above, but the trend was opposite. This is considered to be due to the increase in the volume of the catholyte chamber (and hence the quantity of

chloride ions available for the transport) in this research compared to that by Andrews.

In Eq. 6.12, a lower value for $D_{in\ situ}$ compared to D_{1Dssm} was obtained. This indicates that the chloride flux in Permit ion migration test is lower than that in the steady state migration test. As highlighted in section 3.5.3, the top 15mm layer of concrete contributed to 85% of the flow in Permit ion migration test and the rest of the flow took place through the next 25mm depth (Basheer *et al.*, 2005). In the calculation of $D_{in\ situ}$ an equal contribution of all layers to the flow was assumed, which obviously has limitations, as per Basheer *et al.* (2005). However, in the steady state migration test the whole cross section contributes equally to the transport.

As a good relationship between the *in situ* migration coefficient and the steady state migration coefficient was obtained for a range of opc mixes (Andrews, 1999) and concretes containing supplementary cementitious materials in this research (Eq. 6.12), it can be concluded that irrespective of the type of binder, the Permit ion migration test could reliably determine the diffusivity of concrete. Furthermore, the Permit ion migration test eliminates the need to remove cores for determining this property and tests can be completed within a day compared to up to seven days required for the steady state migration test.

6.5.2 Relationship of migration coefficients with resistivity

6.5.2.1 Relationship between D_{1Dssm} and ρ_{bulk}

The relationship between steady state migration coefficient, D_{1Dssm} and the bulk resistivity, ρ_{bulk} is presented in Fig. 6.35. An inverse relationship, given by Eq. 6.13, was obtained between the two parameters, with a coefficient of determination, R^2, of 0.87.

$$\rho_{bulk} = 191 x D_{1Dssm}^{-0.84} \qquad \text{(Eq. 6.13)}$$

where ρ_{bulk} is in ohm.m,

and D_{1Dssm} is in m^2/s (without the multiplier 10^{-12}).

The above relationship is similar to that reported by Polder (1995); Andrade *et al.* (2000) and Chlortest (2006) and an explanation of the relationship is given below.

Andrade (2006) suggested that the steady state migration coefficient can be calculated from the resistivity of concrete using the relationship in Eq. 6.9. This is plotted along with the data in Fig. 6.35 for comparison purposes. It is evident from this figure that the relationship suggested by Andrade (2006) is very close to that represented by Eq. 6.13. Therefore, it can be concluded that the steady state migration coefficient can be determined using a simple resistivity measurement with a high degree of confidence (87% of the variability of D_{1Dssm} is explained by ρ_{bulk}). The reason for the high degree of dependence between the two parameters is that the bulk resistivity measurements were carried out when the pores were saturated with $Ca(OH)_2$ and the ionic conductivity of such a concrete is what was obtained in the steady state migration test.

6.5.2.2 Relationship between $D_{in\ situ}$ and ρ_{bulk}

Figure 6.36 shows the relationship between the *in situ* migration coefficient, $D_{in\ situ}$ and the bulk resistivity, ρ_{bulk}. A very good relationship, with a coefficient of determination, R^2, equals 0.87, was obtained (Eq. 6.14).

$$\rho_{bulk} = 117.14 D_{in\ situ}^{-0.81} \qquad \text{(Eq. 6.14)}$$

where,

ρ_{bulk} is in ohm.m,

$D_{in\ situ}$ is in m^2/s (without the multiplier 10^{-12}).

This relationship is similar to that obtained for the results discussed in the previous section. Equation 6.14 suggests that ρ_{bulk} can be assessed with 87% confidence using the $D_{in\ situ}$ and *vice versa*. Therefore, the resistivity of the concrete in a structure can be predicted from the Permit ion migration test, without removing cores from the structure and testing them in a laboratory.

6.5.2.3 Relationship between D_{1Dssm} and ρ_{Wenner}

The relationship between D_{1Dssm} and ρ_{Wenner} is presented in Fig. 6.37, which shows an inverse relationship between these two test parameters. The relationship is given by the following equation, with an R^2 value of 0.55:

$$\rho_{Wenner} = 217.43 \times D_{1Dssm}^{-0.74} \qquad \text{(Eq. 6.15)}$$

where the ρ_{Wenner} is in ohm.m,
and D_{1Dssm} is in m^2/s (without the multiplier 10^{-12}).

The general trend observed is that with an increase in ρ_{Wenner}, the D_{1Dssm} of concrete decreases. Although the relationship presented in Eq. 6.15 is similar to that in Eq. 6.13, a lower coefficient of determination R^2 was obtained for the relationship in Eq. 6.15. This is considered to be due to the following reasons. The ρ_{Wenner} depends much on the degree of contact made by the wooden plugs with the concrete surface in Wenner four probe resistivity test. Further, any small defects at the point of contact of the concrete surface could affect the resistivity value. This is not that much of an issue in the bulk resistivity test as the resistivity is measured across the whole of the test specimen. In addition to these effects, it must be noted that the Wenner four probe resistivity test was carried out on concrete specimens saturated with de-ionised water instead of $Ca(OH)_2$ solution. In such a case, the resistivity will be influenced by the nature of the pore solution (Polder, 2001). All these factors are considered to have influenced the relationship in Eq. 6.15.

6.5.2.4 Relationship between $D_{in\ situ}$ and ρ_{Wenner}

The relationship between the *in situ* migration coefficient, $D_{in\ situ}$ and the Wenner probe resistivity, ρ_{Wenner} is presented in Fig. 6.38. The regression relationship is presented by the following equation:

$$\rho_{Wenner} = 142.57 D_{in\ situ}^{-0.82} \qquad \text{(Eq. 6.16)}$$

where,
$D_{in\ situ}$ is in m^2/s (without the multiplier 10^{-12}),
ρ_{Wenner} is in ohm.m.

The coefficient of determination R^2 obtained in this case was 0.74, lower value than that obtained for the relationship in Eq. 6.13 between the *in situ* migration coefficient and the bulk resistivity. It can be seen from Fig. 6.38 that the data points are not closer to the regression curve. As there existed an excellent regression relationship between $D_{in\ situ}$ and both D_{1Dssm} and ρ_{bulk}, the limitations discussed in section 6.5.2.3 for the Wenner four probe resistivity tests are considered to be the reasons for the poor relationship in Eq. 6.16.

6.5.3 Relationship of migration coefficients with initial current and peak current

6.5.3.1 Relationship between D_{1Dssm} and initial current in the steady state migration test, $i_{initial\text{-}1Dssm}$

The relationship between the D_{1Dssm} and the initial current obtained from the steady state migration test, $i_{initial\text{-}1Dssm}$, is presented in Fig. 6.39. The relationship is given by Eq, 6.17:

$$i_{initial-1Dssm} = 6.4 \times D_{1Dssm} + 40.5 \qquad \text{(Eq. 6.17)}$$

where $i_{initial\text{-}1Dssm}$ is in mA and D_{1Dssm} is in m^2/s (without the multiplier 10^{-12})

The coefficient of determination of the relationship is very low (R^2=0.11). The regression curve did not pass through the origin, which is normally expected in a migration test because when the diffusivity of the concrete is zero, the resistivity of it should tend to be infinity (or the current should tend to be zero).

As discussed in section 6.4.5.1, the initial current in the steady state migration test could be affected by the differences in thickness of the test specimens, the cell resistance and the different voltages used for testing different mixes. Therefore, it is difficult to assign any set of specific reasons for the poor relationship in Fig. 6.39.

6.5.3.2 Relationship between $D_{in\ situ}$ and initial current in Permit ion migration test, $i_{initial\text{-}in\ situ}$

The relationship between the $D_{in\ situ}$ and the initial current for Permit ion migration test, $i_{initial\text{-}in\ situ}$ is presented in Fig. 6.40. As can be seen from this figure, the relationship could be best expressed with a straight line, with an R^2 value of 0.82 (Eq. 6.18):

$$i_{initial-in\ situ} = 7.26\, D_{in\ situ} + 28 \qquad \text{(Eq. 6.18)}$$

where,

$D_{in\ situ}$ is the *in situ* migration coefficient, in m^2/s, (without the multiplier x 10^{-12}),

$i_{initial\text{-}in\ situ}$ is the initial current is current measured at the start in the Permit ion migration test (mA).

Although the coefficient of determination obtained for the relationship is good, the regression curve did not pass through the origin. As discussed in section 6.4.5.2, the initial current measured in the Permit ion migration test could have been influenced by the cell resistance. This could have resulted in the y-intercept in Eq. 6.18. However, as the cell resistance was not measured, no attempt is made here to quantify the effect of the cell resistance on the initial current or the relationship presented in Eq. 6.18.

6.5.3.3 Relationship between D_{1Dssm} and the peak current in the steady state migration test, $i_{peak\text{-}1Dssm}$

Figure 6.41 shows the relationship between D_{1Dssm} and the peak current in the steady state migration test, $i_{peak\text{-}1Dssm}$. Equation 6.19 shows the relationship between these two parameters:

$$i_{peak-1Dssm} = 95.38\, D_{1Dssm} \qquad \text{(Eq. 6.19)}$$

where,

D_{1Dssm} is the steady state migration coefficient, in m^2/s (without the multiplier 10^{-12}),

$i_{peak\text{-}1Dssm}$ is the current measured when it was the maximum during the steady state migration test, in mA.

The coefficient of determination R^2 for the above relationship is 0.88. The regression curve passes through the origin in this case, as expected. When the test specimen is fully saturated with the ionic solution used in the migration test (which happens at the steady state condition), the resistivity of the test specimen is the lowest and the conductivity (and hence both the transport and the current) is the highest. As a result, the steady state diffusion coefficient obtained using the chloride flux during the steady state condition correlates well with the peak current and the regression curve passes through the origin.

Delagrave *et al.*, (1996) and Yang and Weng, (2003) also obtained good correlation between the peak current and the steady state migration coefficient. The good correlation between these two parameters in Eq. 6.19 suggests that the different mixes might have reached relatively similar pore solution conductivities when the peak current was reached. Therefore, the peak current is indicative of the physical

resistance of the concrete to the ionic transport, which also directly relates to the steady state migration coefficient.

6.5.3.4 Relationship between $D_{in\ situ}$ and the peak current in Permit ion migration test, $i_{peak\text{-}in\ situ}$

The relationship between the *in situ* migration coefficient and the peak current from the Permit ion migration test, $i_{peak\text{-}in\ situ}$ is shown in Fig. 6.42. As can be seen from this figure there is a very good linear relationship (R^2=0.92) between the two parameters and the regression line passes through origin. The regression relationship is given by:

$$i_{peak-in\ situ} = 127.76 D_{in\ situ} \qquad \text{(Eq. 6.20)}$$

where,

$i_{peak\text{-}in\ situ}$ is the current measured when it was the maximum in the Permit ion migration test, in mA,

$D_{in\ situ}$ is in m^2/s (without the multiplier 10^{-12}).

Andrews (1999) also reported a good correlation (R^2=0.94) between the peak current and the *in situ* migration coefficient for his investigations of eight concrete mixes containing normal Portland cement. Therefore, it can be concluded that the peak current in Permit ion migration test provides a measure of the physical resistance offered by the concrete to ionic transport, which also influences the *in situ* ion migration coefficient. In addition, the the peak current can be determined in Permit ion migration test by just measuring the current between the electrodes. This can considerably reduce the workload and simplify the test procedure.

The relationship between the *in situ* migration coefficient and the peak current was better than that between the *in situ* migration coefficient and the initial current. The ionic saturation of the concrete specimens with chloride ions for the peak current measurements is considered to be the reason for the excellent regression relationship in Fig. 6.42. Therefore, it can be argued that if the concrete specimen could be saturated with the ionic solution used to carry out the Permit ion migration test, the initial current could also result in a good relationship with the corresponding migration coefficient.

6.5.4 Relationship between both D_{1Dssm} and $D_{in\ situ}$ and the corresponding charge passed

6.5.4.1 Relationship between D_{1Dssm} and six-hour charge passed

The variation of D_{1Dssm} with the normalised six-hours charge passed (see section 6.4.6.1 for details) in the steady state migration test is presented in Fig. 6.43. This figure shows no apparent relationship between the two test parameters. A linear regression between the two parameters can be represented by the equation:

$$6\,hours\,charge\,passed = 2.63 \times D_{1Dssm} + 30 \qquad \text{(Eq. 6.21)}$$

where, 6 hours charge passed is in coulombs.m,

D_{1Dssm} is in m^2/s (without the multiplier 10^{-12}).

The lack of any relationship could have been resulted from the limitations of the charge passed during the first 6 hours as discussed in section 6.4.6.1. Therefore, no further discussion on the relationship in Fig. 6.43 can be made here. However, it may be noted that the data corresponding to 0.45 pfa concrete is obviously an outlier and the possible reasons for this were presented in section 6.4.4.2. The removal of this data would have improved the regression relationship.

6.5.4.2 Relationship between $D_{in\ situ}$ and six-hour charge passed

The relationship between the *in situ* migration coefficient, $D_{in\ situ}$ and the charge passed during the first six-hours in Permit ion migration test is presented in Fig. 6.44. As in the case of the data presented in Fig. 6.43, there is no relationship between the two parameters in Fig. 6.44.

A closer examination of Fig. 6.44 would highlight that concretes with very high resistivity values, such as ms and ggbs mixes, show a different trend to concretes with low resistivity values, such as pfa and opc mixes. These are represented by the two different dotted lines in this figure. However, both the trends are unexplainable because they show a decrease in charge passed with an increase in *in situ* migration coefficient, which is not normally expected. Therefore, it can be concluded that, as in the case of the steady state migration test, the charge passed during the first six-hours

cannot be used to predict the corresponding *in situ* migration coefficient in Permit ion migration test.

6.5.4.3 Relationship between D_{1Dssm} and charge passed until steady state

The relationship between D_{1Dssm} and the normalised charge passed until steady state (see section 6.4.6.1 for details) in the steady state migration test is presented in Fig. 6.45. This figure shows that the charge passed increases with an increase in the steady state migration coefficient and the relationship is given by the equation:

$$Charge\ passed\ until\ steady\ state = 60.7 \times D_{1Dssm} + 166 \qquad \text{(Eq. 6.22)}$$

where, the normalised charge passed until steady state is in coulombs.m,
D_{1Dssm} is in m^2/s (without the multiplier 10^{-12}).

The coefficient of determination R^2 for this relationship is 0.50 and the regression line does not pass through the origin. The positive value for the y intercept suggests that the steady state of flow was reached after certain amount of charge had passed. A better relationship was observed in Fig. 6.45 compared to Fig. 6.43. This would suggest that the relationship between the steady state migration coefficient and the charge passed improved as the concrete specimens became saturated with the ions used in the migration test.

As reported by Castellote *et al.* (2000), the relative charge carried by the chloride ions will vary during the migration test. This is known as the transference number of the chloride ions. The presence of other mobile ions can reduce the transference number of the chloride ions (Castellote *et al.*, 2000). This means that if other conductive ions are present in the pore fluid, the charge carried by them will be greater compared to the chloride ions (Andrade, 1993). During the initial six hours, different conductive ions are present in the pore fluid and their concentration is relatively higher than that of the chloride ions. Therefore, there exists a weak correlation between the charge carried by all the ions and the chloride penetration resistance of concrete. However, as the test progresses the chloride ions become dominant in the pore fluid. As a result, the relative charge carried by chloride ions increases. This is considered to be the reason for the improved relationship between the charge passed and the steady state migration coefficient in Fig. 6.45 compared to

that in Fig. 6.43. Furthermore, the excellent regression relationships obtained in the case of the peak currents with the corresponding migration coefficients confirm the argument that the charge passed correlates better with the chloride penetration resistance of concrete, provided the pores are saturated with chloride ions.

6.5.4.4 Relationship between $D_{in\ situ}$ and charge passed until steady state

Figure 6.46 shows the relationship between $D_{in\ situ}$ and the charge passed until steady state in Permit ion migration test. As in Fig. 6.46, the charge passed increases with an increase in the *(in situ)* migration coefficient. The relationship between the two test parameters is given by the equation:

$$Charge\ passed\ until\ steady\ state = 219.51 \times D_{in\ situ} + 1047 \qquad \text{(Eq. 6.23)}$$

where, charge passed until steady state is in coulombs,

$D_{in\ situ}$ is in m^2/s, (without the multiplier 10^{-12})..

Similar to the results from steady state migration test discussed in section 6.5.4.3, the charge passed until steady state showed a better relationship with the *in situ* migration coefficient, compared to charge passed during first six-hours presented in Fig. 6.44. This would suggest that the relationship between the charge passed and the chloride penetration resistance improves as the flow reaches the steady state.

From the discussions in section 6.5.4.3 and 6.5.4.4, it can be concluded that the relationship between the charge passed and the migration coefficient improves when the pore system becomes saturated with chlorides (corresponding to the steady state condition). Therefore, the relationship between the charge passed and the chloride transport during the steady state is discussed further in the next section.

6.5.5 Relationship between charge passed and chloride flux

The charge passed in both the steady state migration test and the Permit ion migration test was calculated from the current flow. The charge passed was determined by integrating the area under the current versus time graph, using:

$$Q = \int I(t)dt \qquad \text{(Eq. 6.24)}$$

where,

Q is the charge passed, coulombs,

$I_{(t)}$ is the time dependent current, A,

t is the elapsed time, seconds.

The charge passed and the chloride concentration arriving at the anolyte during the migration tests changed continuously. A typical result showing both the charge passed and the chloride concentration of the anolyte in Permit ion migration test is presented in Fig. 6.47. The charge passed follows a trend similar to that of the chloride concentration and the relationships between these two in both the steady state migration test and the Permit ion migration test corresponding to the steady state condition are discussed in the following sub-sections.

6.5.5.1 Charge versus chloride flux in steady state migration test

The relationship between the charge passed and the chloride concentration in the steady state migration test for all the mixes is presented in Fig. 6.48. The relationship ($R^2 = 0.41$) is represented by the equation.

$$Cl^- = 0.15 + 0.0018 \; x \; charge\ passed \qquad \text{(Eq. 6.25)}$$

where,

Cl^- is the chloride concentration of the anolyte, in mmol/l,

Charge passed was calculated from the area under the current versus time graph, in coulombs.

Although, the correlation between these two parameters was low for all the mixes together in the graph, the relationship was excellent for each of the mixes separately (see Table 6.2). For example, it can be seen in Fig. 6.49 that the relationship was excellent for the 0.52 w/b ggbs mix. The equation representing the relationship between these two parameters for each of the mixes separately is presented in Table 6.2. The slope (m) and the x intercept vary between mixes. Therefore, combining the data points for all mixes to obtain a generalised relationship can be expected to weaken the strength of the regression, as seen on Fig. 6.48. The variations in regression coefficients in Table 6.2 is considered to be due to the differences in thickness of the test specimens and the test voltages used in the steady state migration test.

The data presented in Table 6.2 shows that there is a positive x intercept in all cases (except for the 0.45 pfa mix). This means that a certain amount of charge had passed before the chloride ions entered the anolytic solution and this amount of charge passed was different for different concretes. Due to numerous factors influencing the charge passed during the time lag, it is difficult to provide an explanation for the behaviour of different mixes. Nevertheless, the slope of the relationship presented in Table 6.2 shows that, irrespective of the type of concrete mixes, the value of slope is comparable (i.e. 0.0031mmol/l/coulombs). This means that, even though the charge passed until the chloride ions reached the anolyte solution did not give any clear trends, the rate of change of concentration with respect to the rate of change of charge can be considered to be a constant. Therefore, by measuring the rate of change of charge, it is possible to determine the rate of change of chloride concentration. This aspect is discussed next.

Rate of change of chloride concentration versus rate of change of charge

As shown in Fig. 6.47, both the chloride concentration and the charge passed varied with time in a similar manner. Therefore, the rate of change of charge and the rate of change of chloride concentration were compared to determine any possible relationship between them and to validate the earlier discussion. The relationship between the rate of change of charge and the rate of change of chloride concentration is given in Fig. 6.50. Equation 6.26 describes the relationship between these two parameters and the coefficient of determination R^2 was 0.64.

$$\frac{dQ}{dt} = 237.28\frac{dc}{dt} \qquad \text{(Eq. 6.26)}$$

where,

$\frac{dQ}{dt}$ is the rate of change of charge during the steady state, coulombs/s,

$\frac{dc}{dt}$ is the rate of change of chloride concentration during the steady state, mol/m^3.s,

Equation 6.26 suggests that the rate of change of chloride concentration can be estimated with 64% confidence using the value of the rate of change of charge. A similar conclusion was reached by Yang (2004). The degree of confidence of the

relationship could have been affected by the variations in carrying out the steady state migration test, (described in section 6.4.6).

Theoretically, the rate of change of charge gives current. This current value can be considered as an average current value during the steady state. The rate of change of chloride concentration is used to estimate the steady state migration coefficient. Therefore, the relationship discussed above can be used to qualify the relationship between the peak current and the steady state migration coefficient discussed in section 6.5.3.3.

6.5.5.2 Charge versus chloride flux in Permit ion migration test

The relationship between the charge passed and the chloride concentration in Permit ion migration test for all mixes is presented in Fig. 6.51. The relationship is represented by the equation:

$$Cl^- = -4.78 + 0.0038(Charge\ passed) \qquad \text{(Eq. 6.27)}$$

where,

Cl^- is the chloride concentration of the anolyte, mmol/l,

Charge passed calculated from area under the current versus time graph, coulombs.

The coefficient of determination, R^2, for the relationship in Eq. 6.27 was 0.91. Similar to the relationship in steady state migration test, the charge passed correlated with the chloride concentration in Permit ion migration test, but the degree of dependence improved for the latter. The improved relationship in Permit ion migration test is considered to have been contributed by the constant test voltage (60 V DC) and specimen dimensions used. The equation representing the relationship between the two parameters for each of the mixes separately is presented in Table 6.2. The x intercept and the slope of the different relationships (given in Table 6.2) varied much less compared to the corresponding values for the steady state migration test. This could have also contributed to the better regression relationship seen in Fig. 6.51.

Similar to the relationship discussed in the steady state migration test, the rate of change of charge was compared to the rate of change of chloride concentration for

the Permit ion migration test (Fig. 6.52). The regression relationship in Fig. 6.52 is represented by Eq. 6.28, with a coefficient of determination (R^2) of 0.85.

$$\frac{dQ}{dt} = 210.81\frac{dc}{dt} \qquad \text{(Eq. 6.28)}$$

where the unit of $\frac{dQ}{dt}$ and $\frac{dc}{dt}$ is the same, as given in Eq. 6.26.

Equation 6.28 suggests that the rate of change of chloride concentration can be estimated with 85% confidence using the value of the rate of change of charge. The implication of this conclusion is that by measuring the current, the rate of change of chloride concentration can be estimated in Permit ion migration test. Such a change would not only simplify the test procedure, but also reduce the cost of manufacturing the test equipment.

6.6 Method of identification of the onset of the steady state condition

In a migration test, the identification of whether the state of flow is steady or non-steady is made by plotting the chloride concentration of the anolyte against the elapsed time. This means that liquid samples should be taken at regular intervals to analyse for the chloride concentration. This could not only deplete the volume of the anolyte, but also make the test labour intensive. Therefore, an alternative approach is needed to identify the steady state of flow. Three approaches could be used to identify the onset of the steady state condition:

1. The relationship between the chloride concentration and the conductivity could be used to identify the onset of steady state flow.
2. The current flowing through the system would reach a peak value closer to (or soon after) the onset of the steady state condition.
3. The temperature also follows a trend similar to that of current, i.e., the peak in temperature would be observed closer to the steady state condition.

In the following sections the usefulness of these approaches is discussed.

6.6.1 Identification of the steady state from the conductivity of the anolyte

A typical graph showing both the conductivity and the chloride concentration of the anolyte in Permit ion migration test is shown in Fig. 6.53. As discussed in section

5.2.5.2, the conductivity of the anolyte correlated well with the chloride concentration. Therefore, the conductivity measurements could effectively be used to identify the onset of the steady state condition. This shall be discussed further in section 6.7.

6.6.2 Identification of the steady state from the current measurements

The current generated in a migration test provides an excellent overview of the resistance of the specimen to migration. Typical current measurements along with the corresponding chloride concentrations in the anolyte in Permit ion migration test are presented in Fig. 6.54. This figure shows that the current increased during the migration test, to reach a maximum value (peak current), and in most cases, the peak current was observed just as the chloride flow was in steady state. A similar observation was made by Andrade and Sanjuan (1994) in their steady state migration test. They considered that, by the time the peak current was observed, the chloride front would have moved through the whole sample, saturating the entire sample with chloride ions. This would cause a reduction in resistivity, resulting in a maximum current. Fig. 6.54 shows that this property of the current (i.e. to result in a peak value of current at steady state) can be used to identify the onset of the steady state.

6.6.3 Identification of the steady state from the temperature generated in the anolyte

The temperature change (heat) developed in a migration test is a function of the current flowing:

$$Heat = I^2 R_e t \qquad \text{(Eq. 6.29)}$$

where,

Heat is the heat generated in a migration test, Joule,

I is the current flowing across the cells, A,

R_e is the resistance of the specimen, ohm,

t is the time, seconds.

The trend for temperature is similar to that of the current measured in a migration test (see Fig. 6.55). The peak of temperature as well as current occurred more or less at the same time and this coincided with the onset of the steady state. However, the

absolute value of the peak temperature could depend also on the temperature of the surrounding.

6.7 Method of determining the steady state chloride flux

The usefulness of the conductivity measurements to monitor the change in chloride concentration of the anolyte was identified in the pervious chapter in section 5.2.5.2. Although, a very good linear relationship was obtained, the coefficients (Eq. 5.13) were slightly different to that reported by Castellote *et al.* (2001). Further, the Permit ion migration test uses a larger concrete specimen compared to that is used in the steady state migration test. Therefore, the amount of ions available in the pore fluid could be relatively higher in the case of the Permit ion migration test. As these ions could influence the conductivity of the anolyte, it was considered to be necessary to study the effectiveness of the relationship between these two parameters. Therefore, an in depth discussion on the relationship between the two parameters obtained from both the steady state migration test and the Permit ion migration test for a range of concrete mixes is given in this section.

The relationship between conductivity and chloride concentration in the anolyte solution for the steady state migration coefficient and the Permit ion migration coefficient is presented in Figs. 6.56 and 6.57 respectively. Both these figures show an excellent correlation between the two parameters.

The relationship between the two parameters in the steady state migration test is given by the equation:

$$Cl^- = 3.97 \times \lambda_{25} \qquad \text{(Eq. 6.30)}$$

where, Cl^- is the chloride concentration in mmol/l,

λ_{25} is the conductivity at reference temperature 25°C (refer Eq. 3.25) in mS/cm.

The relationship between the two parameters in Permit ion migration test is given by:

$$Cl^- = 6.01 \times \lambda_{25} \qquad \text{(Eq. 6.31)}$$

where, the parameters are the same as in Eq. 6.30.

The relationship between the test parameters suggested by Castellote *et al.* (2001) is presented in Eq. 6.32.

$$Cl^- = 11.45 \times \lambda_{25} - 1.71 \qquad \text{(Eq. 6.32)}$$

where, the parameters are the same as in Eq. 6.30.

The slope of the regression relationship in Eq. 6.30 and Eq. 6.31 is 3.95 and 6.01 respectively. The lower value of slopes compared to that in Eq. 6.32 could be mainly due to the difference in the conductivity probe used. While Castellote *et al.* (2001) used a standard platinum probe, a stainless steel two-rod probe was used in both the steady state migration test and the Permit ion migration test to measure the conductivity.

In order to use the relationship given by Eq. 6.31 to estimate the chloride concentration using the conductivity measurement in Permit ion migration test, a "confidence analysis" on the data was carried out (see Fig. 6.57). A good degree of dependence between the two parameters was obtained for all the mixes together, R^2=0.94. The standard error obtained for the y-intercept was 0.2367; the standard error for the slope (m) was 0.1279, and the residual standard deviation was 3.5628. Considering that the deviations were created by a few data points and the fact that these tests were carried out on a material which is known to have high natural variability, the correlation represented in Eq. 6.31 can be considered to be good.

Whilst comparing Eq. 6.30 with Eq. 6.31 it can be seen that a small increment in conductivity would result in a slightly more increase in chloride concentration in Permit ion migration test represented by Eq. 6.31 compared to the steady state migration test represented by Eq. 6.30. In other words, the influence of chloride ions on conductivity measurements in Permit ion migration test was greater than that in the steady state migration test. However, this cannot be concluded as a definite trend because the chloride concentration and the conductivity were the only measured parameters and presence of other ions, which could influence the conductivity, was not tested.

The relationships presented in this section establish that the conductivity of the anolyte in a migration test is linearly related to the chloride concentration. The coefficient of regression obtained in both cases is high suggesting that the mix variations have not affected the relationship. Therefore, in Permit ion migration test the relationship given by Eq. 6.31 could be used to calculate the equivalent chloride concentration. This eliminates the need to measure the chloride concentration in order to calculate the *in situ* migration coefficient. Therefore, the test can be carried out automatically by measuring the conductivity of the anolyte.

6.8 Conclusions

In this Validation Programme, the performance of five rapid test methods, viz. a non-steady state migration test, a steady state migration test, Permit ion migration test, a bulk resistivity test and Wenner four probe resistivity test was evaluated for determining the chloride diffusivity of concretes. The ability of the parameters obtained from the test methods to distinguish the variations in the mixes, mainly the w/b and type of binder, was used to assess the performance of each test. In addition, the relationship between the different test parameters was studied and the usefulness of the different test parameters was identified. The following conclusions have been drawn from the results presented and discussed in this chapter.

1. The hemispherical bulb within which the flow of chloride ions takes place in the Permit ion migration test was identified using the electrical resistivity of the concrete. The average flow length, L, to the average flow area, A, is used to define the hemispherical bulb, the ratio of which was found to be $3.76m^{-1}$. The chloride front measured for different concretes suggested that the dimensions of the hemispherical bulb decreased with the increase in electrical resistivity of the concrete. However, this variation did not affect the L/A value, which was found to be a constant for all the mixes. This suggests that irrespective of the variations in L and A, the ratio remains a constant and, hence, a value of $3.76m^{-1}$ could be used in calculations.
2. The *in situ* migration coefficient, the non-steady state migration coefficient and the steady-state migration coefficient increased with the increase in w/b. The coefficients were lower for mixes containing supplementary cementitious materials, with the exception of the pfa mix. As all the coefficients showed similar trends due to the variations in the mixes as a result of both w/b and

type of binder, it was concluded that the Permit ion migration test is an alternative method for the *in situ* determination of the chloride diffusivity of concrete.

3. Both the bulk resistivity and the Wenner resistivity decreased with the increase in w/b and increased with the addition of supplementary cementitious materials. It was observed that the electrical resistivity followed an inverse trend with the diffusivity parameters.
4. The *in situ* migration coefficient correlated well with the steady-state migration coefficient, the non-steady state migration coefficient and the resistivity obtained from both the bulk resistivity and the Wenner Four Probe resistivity for the different types of concrete studied. This would mean that a reliable prediction of these coefficients could be made by carrying out the Permit ion migration test.
5. The peak currents obtained from both the Permit ion migration test and the steady-state migration test were influenced by the w/b of the mix and the type of binder in a manner similar to the related migration coefficients. The peak current in each type of test also correlated well with both the corresponding migration coefficient and the bulk resistivity. This suggests that the estimation of the diffusivity of concrete can be made by measuring the peak current.
6. The charge passed during the first six-hours in both the Permit ion migration test and the steady-state migration test was not found to be influenced in any consistent manner by either the w/b or the type of binder. In the case of the steady state migration test there were limitations in the reported charge passed. Therefore, no attempt was made to evaluate critically the effectiveness of the charge passed during the first six hours in assessing the chloride penetration resistance of concretes. Although these limitations were not applicable to the six-hours charge passed reported in Permit ion migration test, the relationship did not improve much. Therefore, it was concluded that the charge passed during the first six hours cannot be used to quantify the chloride penetration resistance of concrete.
7. The charge passed until the steady state was also studied in both the steady state migration test and the Permit ion migration test. The trends obtained for this parameter was better compared to the six-hour charge passed. The

relationship between the charge passed until steady state and the corresponding migration coefficient was better in comparison with the relationship observed by the charge passed during the first six hours.

8. The charge passed and the chloride flux during the steady state in both steady state migration test and Permit ion migration test showed a liner relationship, with a higher degree of correlation observed for the relationship in Permit ion migration test.

The relationship between the conductivity and the chloride concentration of the anolyte was studied. The results suggest that there is an excellent correlation between the conductivity and the chloride concentration of the anolyte. That is, the conductivity values can be converted to concentration values using an empirical equation, which in turn can be used to calculate the slope of the steady state portion of the concentration versus time graph, and, thereby, the *in situ* ion migration coefficient. The correlation between the conductivity and the chloride concentration of the anolyte was not affected by the variations in the mix (due to both w/b and the type of binder).

Table 6.1a Test parameters from the Permit ion migration test

Mix	Permit ion migration test										
	$D_{in\ situ}$ (x 10^{-12} m^2/s)		Initial current (mA)		Peak current (mA)		Charge passed for 6hours (Coulombs)		Charge passed until steady state (Coulombs)		Time lag (hours)*
0.45 opc	0.76	0.99	39.12	39.62	174.00	191.00	1597	1562	1449	1592	5.24
	1.18		62.43		205.00		830		1565		4.12
	1.02		17.30		194.00		2258		1761		5.43
0.52 opc	2.28	2.68	40.16	43.08	412.00	400.67	705	791	1700	2033	7.86
	3.40		-		385.00		1074		3300		5.78
	2.36		46.00		405.00		593		1100		6.34
0.45 fa	1.72	1.36	32.80	41.60	196.40	182.87	1815	2220	802	994	4.42
	0.72		37.00		162.15		2796		1107		6.79
	1.62		55.00		190.06		2050		1073		3.93
0.52 fa	4.00	3.84	53.30	58.10	440.00	437.25	1046	1515	1450	1582	8.36
	3.82		71.30		446.75		2519		1701		6.99
	3.72		49.70		425.00		980		1595		10.14
0.4 ms	0.40	0.44	26.95	35.29	79.00	79.00	639	790	1218	1405	8.94
	0.54		40.21		84.50		955		1516		8.55
	0.39		38.71		73.50		776		1480		9.65
0.52 ms	1.58	1.49	44.30	35.68	179.00	161.33	614	475	1436	1578	11.12
	1.59		34.90		163.00		430		1719		15.11
	1.31		27.83		142.00		381		-		25.19*
0.45 ggbs	0.30	0.30	22.31	24.56	52.80	45.33	766	734	434	559	3.83
			21.97		42.00		705		592		5.22
	0.29		29.40		41.20		730		650		5.44
0.52 ggbs	0.85	0.78	31.62	33.19	105.30	107.10	557	932	1452	1241	10.18
	0.78		36.33		108.00		1145		1071		5.78
	0.73		31.62		108.00		1095		1200		6.34

* Time taken to reach steady state, calculated by extending the steady state portion of the concentration time graph to the x axis.

Table 6.1b Test parameters from the steady state migration test

Mix	Test voltage	Thickness of specimen (mm)	$D_{1D\,ssm}$ (10^{-12} m^2/s)		Current (mA)				Charge passed (coulombs)		Normalised charge passed (coulombs.m)	
					Initial current		Peak current		6 hours	until steady state	6 hours	until steady state
0.45 opc	60V	32.0	1.2	1.1	9.0	7.7	157.4	145.4	363	7465	11.46	244.59
		32.5	1.1		6.0		145.0					
		34.2	1.1		8.0		133.7					
0.52 opc	12V	16.3	6.0	5.9	20.0	16.7	101.0	96.7	308	5466	38.22	675.16
		18.6	6.0		17.0		85.0					
		15.7	5.8		13.0		104.0					
0.45 pfa	60V	29.8	2.7	2.2	130.0	140.3	241.0	223.7	3917	9923	114.65	193.63
		28.7	1.4		156.0		180.0					
		29.7	2.5		135.0		250.0					
0.52 pfa	12V	16.7	6.4	6.4	15.0	11.0	125.0	122.7	287	3485	34.39	422.93
		15.4	5.6		10.0		123.0					
		16.3	7.1		8.0		120.0					
0.4 ms	60V	31.7	0.8	0.9	62.8	53.6	80.0	77.7	1511	11191	31.85	231.85
		30.6	1.0		38.7		78.0					
		31.2	0.9		59.2		75.0					
0.52 ms	12V	16.5	1.8	2.1	17.0	15.0	65.0	67.3	357	4285	43.31	515.92
		15.7	2.3		16.0		69.0					
		16.0	2.2		12.0		68.0					
0.45 ggbs	60V	31.6	0.6	0.7	8.4	8.9	42.5	42.8	257	7465	7.64	224.20
		29.3	0.5		8.9		40.8					
		29.0	0.7		9.3		45.0					
0.52 ggbs	60V	16.3	2.3	1.8	38.6	36.2	257.0	236.3	665	6322	11.46	107.01
		18.0	1.1		36.0		219.0					
		16.5	2.1		33.9		233.0					

Note: Due to the difference in the thickness of the test specimen and the test voltage, the charge passed was normalised by multiplying the thickness of the specimen after converting charge passed at 12V to that equivalent at 60V ($Q_{60V} = Q_{12V}$*7.5 (Misra *et al.*, 1994))

Table 6.1c Test parameter from the non-steady state migration test and resistivity tests

Mix	Non-steady state migration test		Resistivity tests			
	D_{nssm} (10^{-12} m^2/s)		Wenner Resistivity (Ω-m)		Bulk Resistivity (Ω.m)	
0.45 opc	10.00	10.07	72.50	69.00	98.13	97.08
	9.40		67.00		104.05	
	10.80		67.50		89.06	
0.52 opc	20.30	20.20	59.00	58.50	29.90	38.75
	19.70		58.50		37.76	
	20.60		58.00		48.60	
0.45 pfa	21.70	21.07	79.50	79.50	137.38	133.08
	20.50		78.00		122.57	
	21.00		81.00		139.28	
0.52 pfa	28.90	29.73	57.50	51.50	36.75	39.92
	29.30		51.00		36.81	
	31.00		46.00		46.19	
0.4 ms	3.90	3.93	295.00	286.33	246.06	247.31
	3.90		273.00		250.56	
	4.00		291.00		245.32	
0.52 ms	7.10	8.00	174.00	171.67	99.38	120.66
	8.50		171.50		145.80	
	8.40		169.50		116.80	
0.45 ggbs	5.30	5.00	379.00	386.67	337.03	300.15
	5.20		399.00		309.22	
	4.70		382.00		254.19	
0.52 ggbs	6.00	6.03	285.00	291.17	104.20	107.37
	6.40		303.50		108.35	
	5.70		285.00		109.56	

Table 6.2 Regression analysis of charge passed versus chloride concentration in migration tests

Mix	Chloride concentration = c + m x charge passed							
	Steady state migration test				Permit ion migration test			
	m	c (mmol/l)	x intercept (coulombs)	R^2	m	c (mmol/l)	x intercept (coulombs)	R^2
0.45 opc	0.0021	-16.92	8055	0.98	0.0030	-5.44	1813	0.92
0.52 opc	0.0033	-18.03	5464	0.95	0.0038	-5.70	1499	0.95
0.45 pfa	0.0008	19.43	-2428	0.52	0.0037	-3.20	864	0.99
0.52 pfa	0.0035	-8.39	2396	0.86	0.0046	-5.98	1299	0.98
0.4 ms	0.0039	-43.72	11209	0.97	0.0022	-2.18	991	0.82
0.52 ms	0.0035	-12.94	3696	0.97	0.0045	-7.35	1634	0.94
0.45 ggbs	0.0044	-22.51	5115	0.95	0.0018	-0.38	213	0.82
0.52 ggbs	0.0036	-5.53	1535	0.95	0.0035	-4.10	1172	0.99

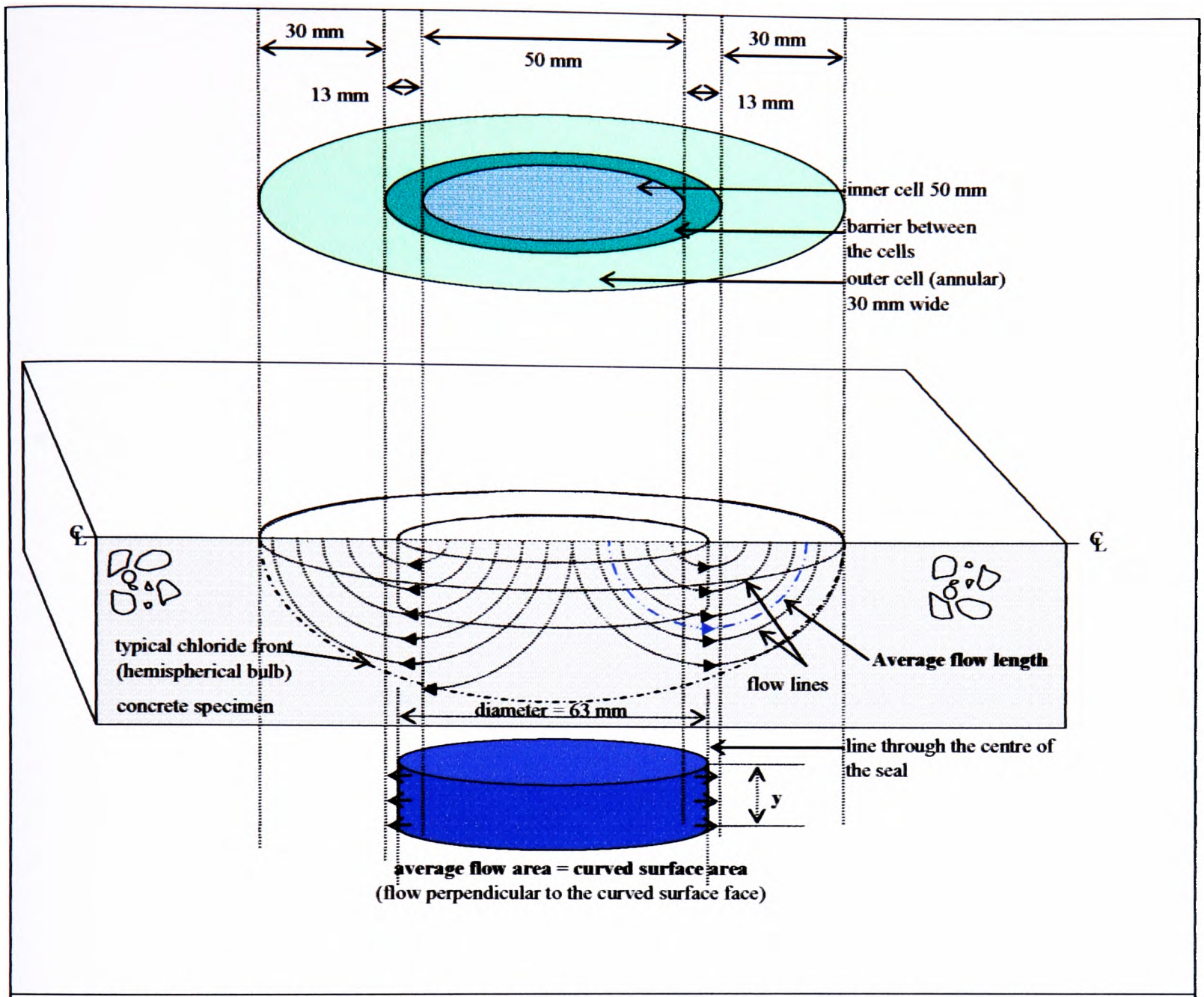

Figure 6.1 Schematic diagram of the flow path in Permit ion migration test

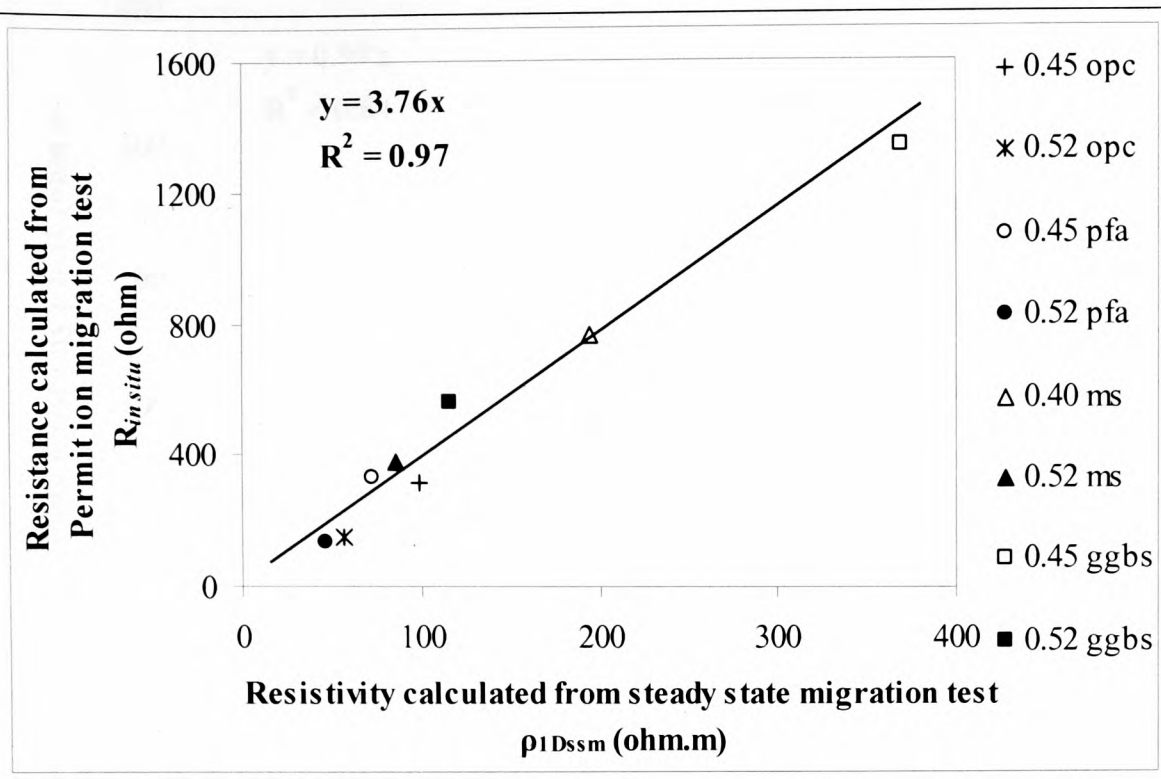

Figure 6.2 Relationship between $R_{in\ situ}$ and ρ_{1Dssm}

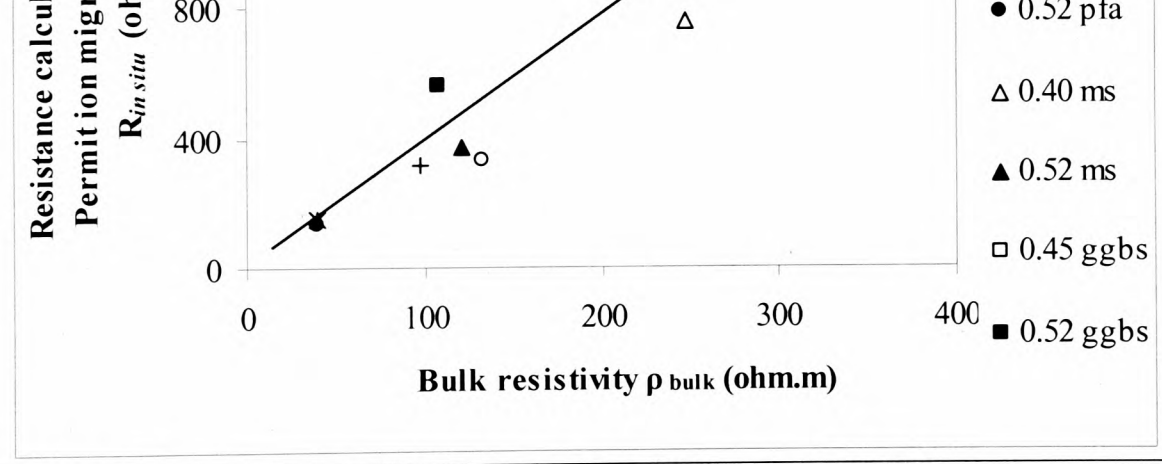

Figure 6.3 Relationship between $R_{in\ situ}$ and ρ_{bulk}

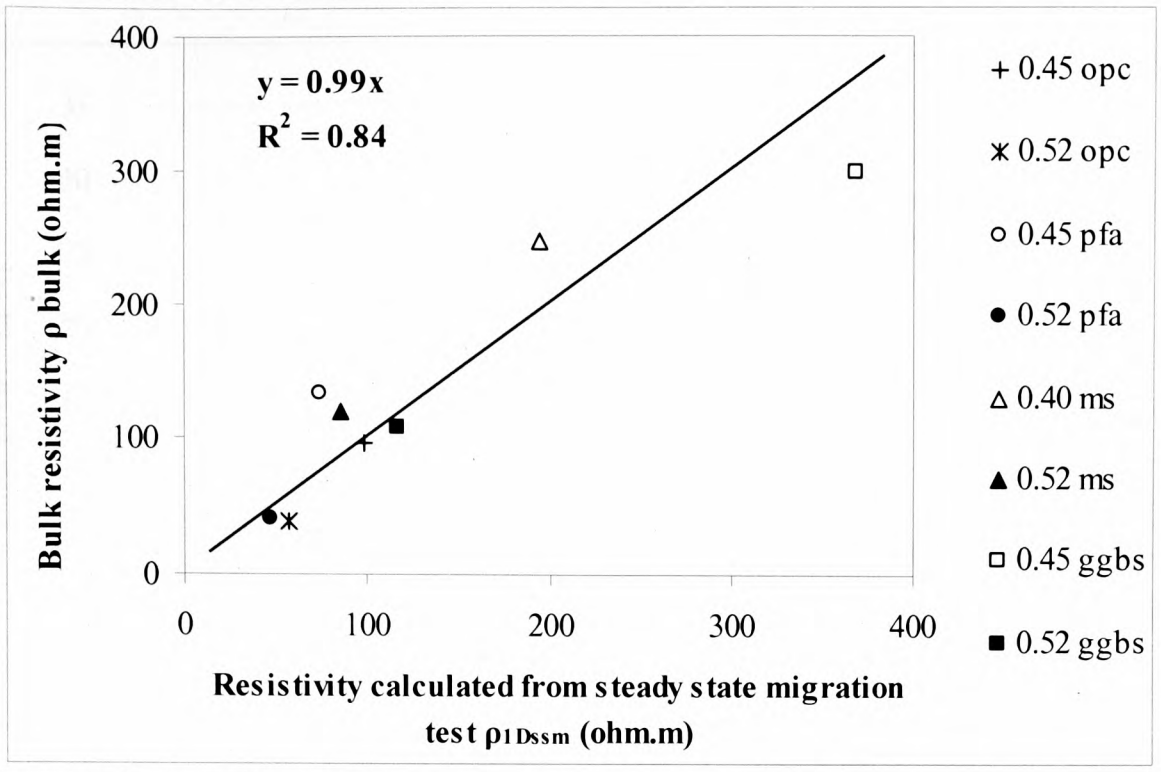

Figure 6.4 Relationship between ρ_{1Dssm} and ρ_{bulk}

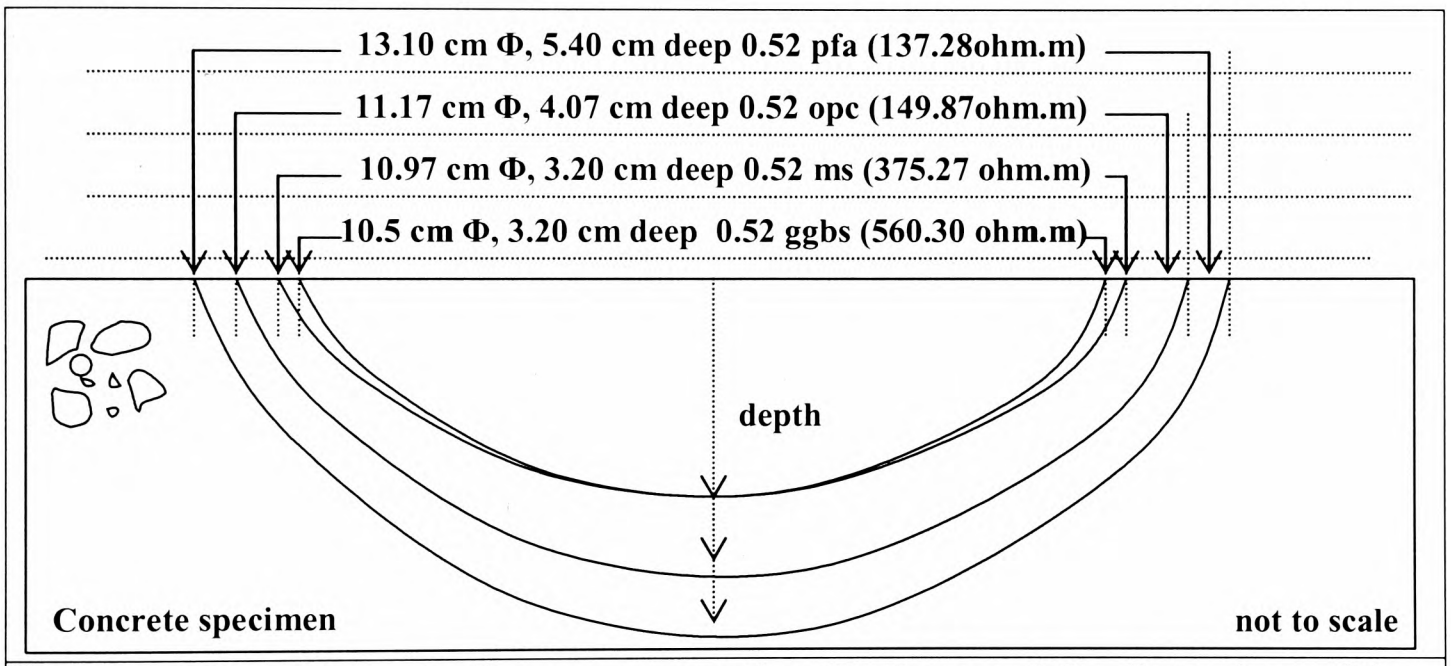

Figure 6.5 The schematic diagram representing the shape and the dimensions of the chloride front in different specimens tested with Permit ion migration test

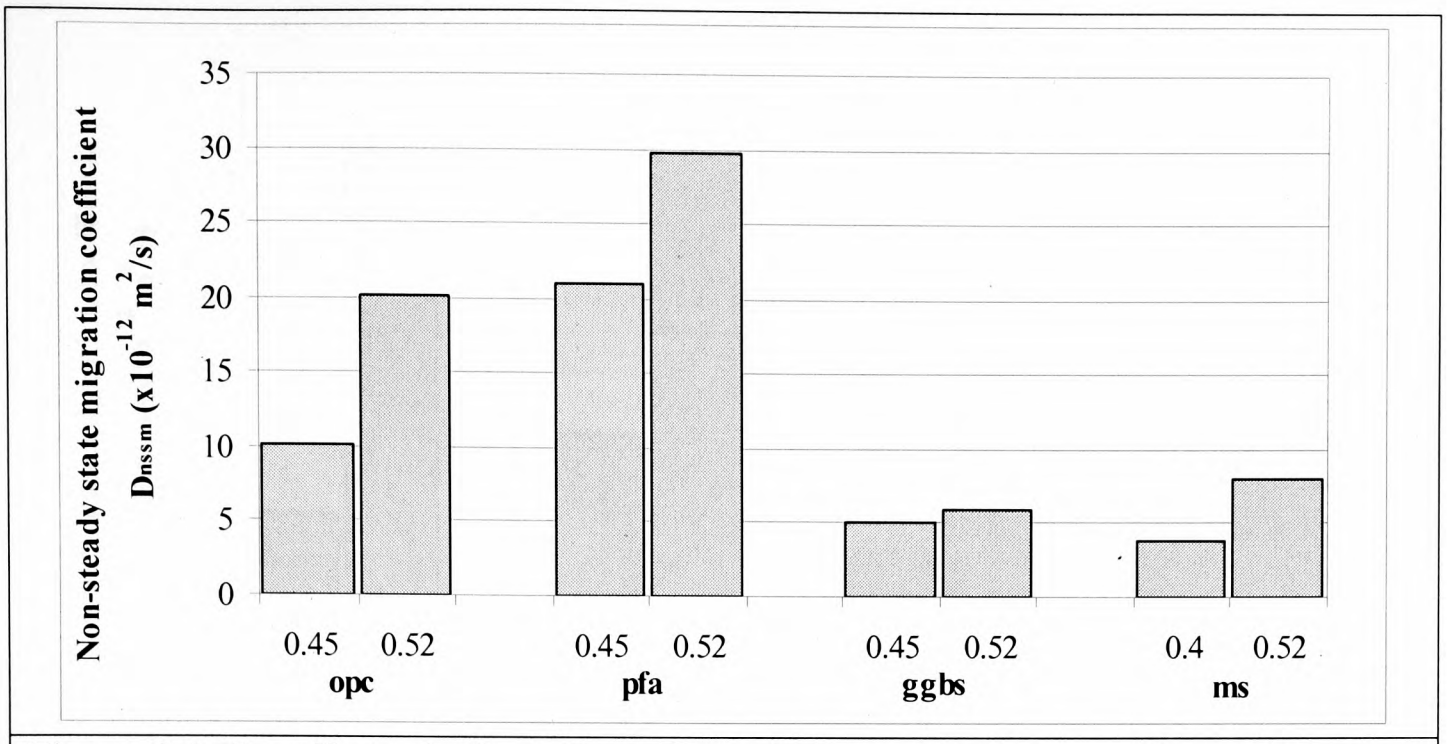

Figure 6.6 The effect of w/b on the non-steady state migration coefficient, D_{nssm}

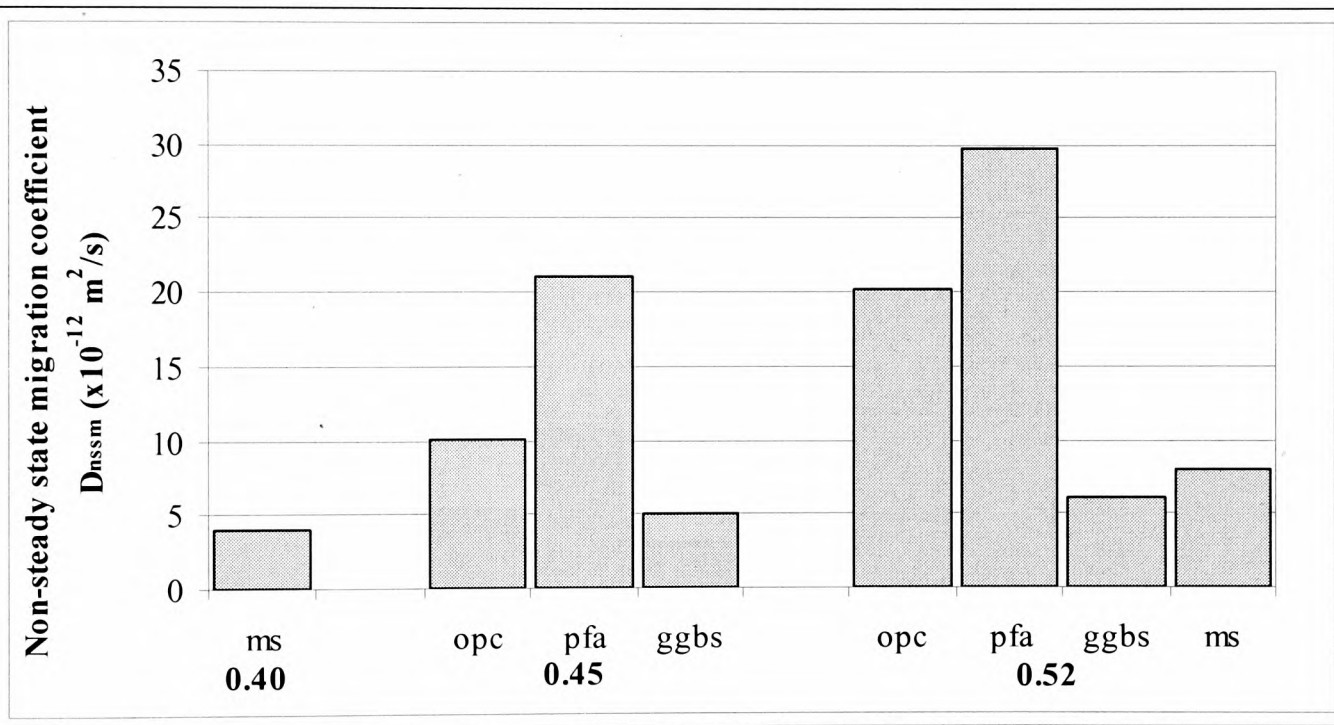

Figure 6.7 The effect of type of binder on the non-steady state migration coefficient, D_{nssm}

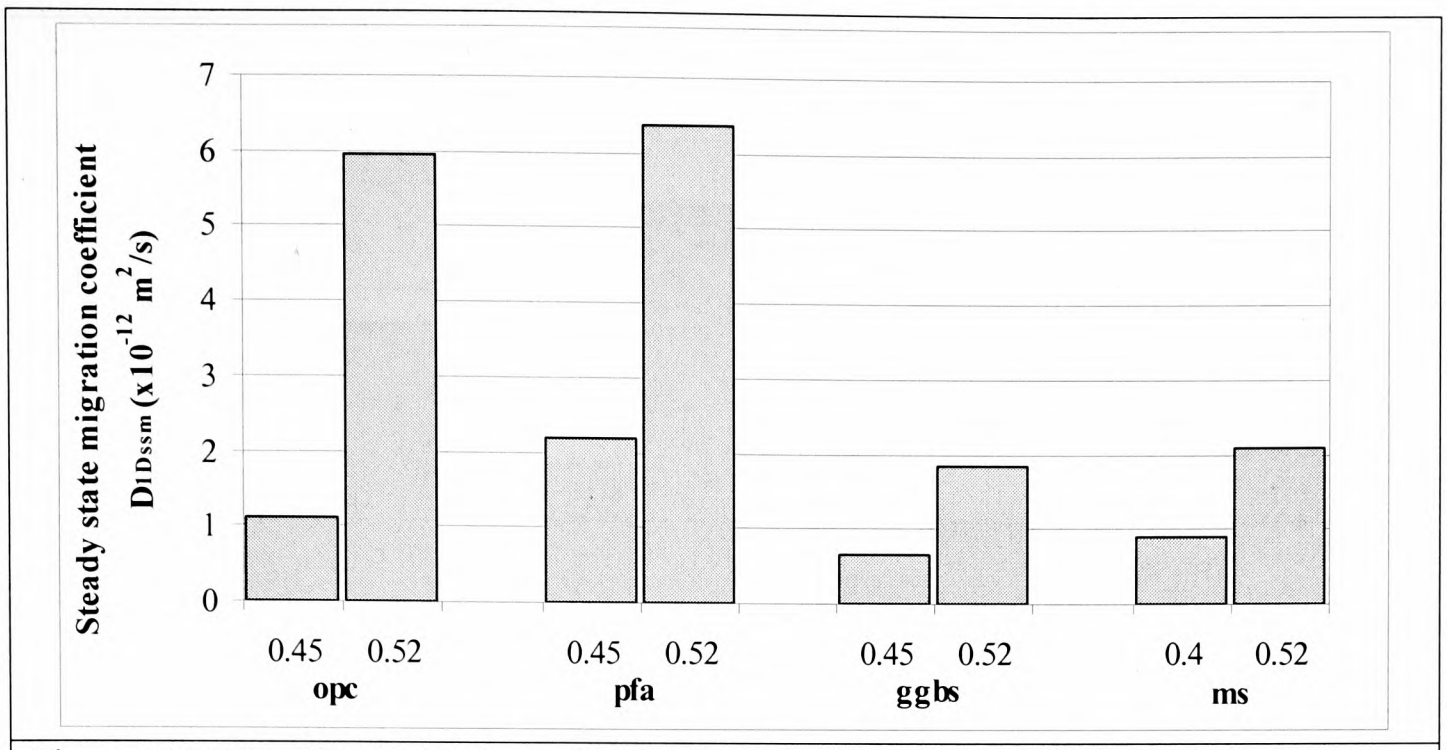

Figure 6.8 The effect of w/b on the steady state migration coefficient, D_{1Dssm}

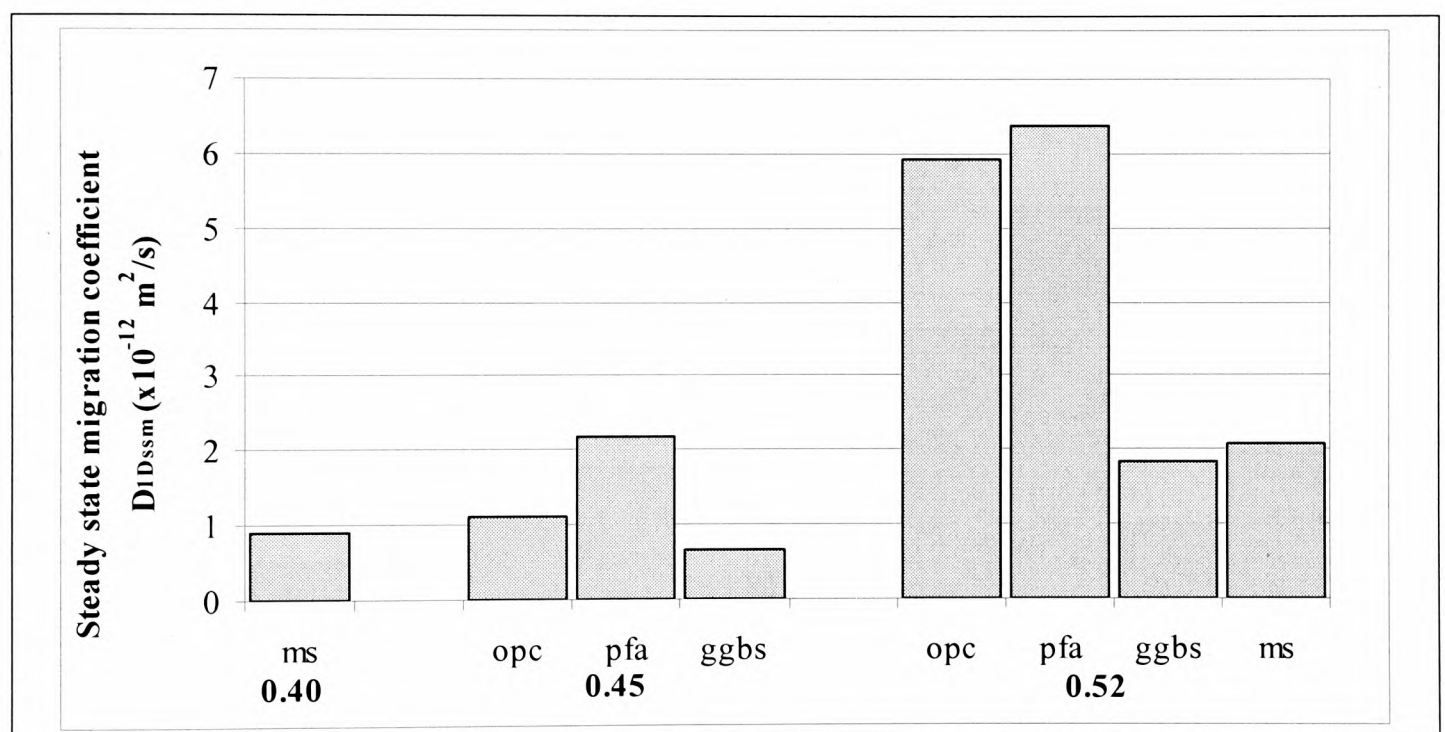

Figure 6.9 The effect of type of binder on the steady state migration coefficient, D_{1Dssm}

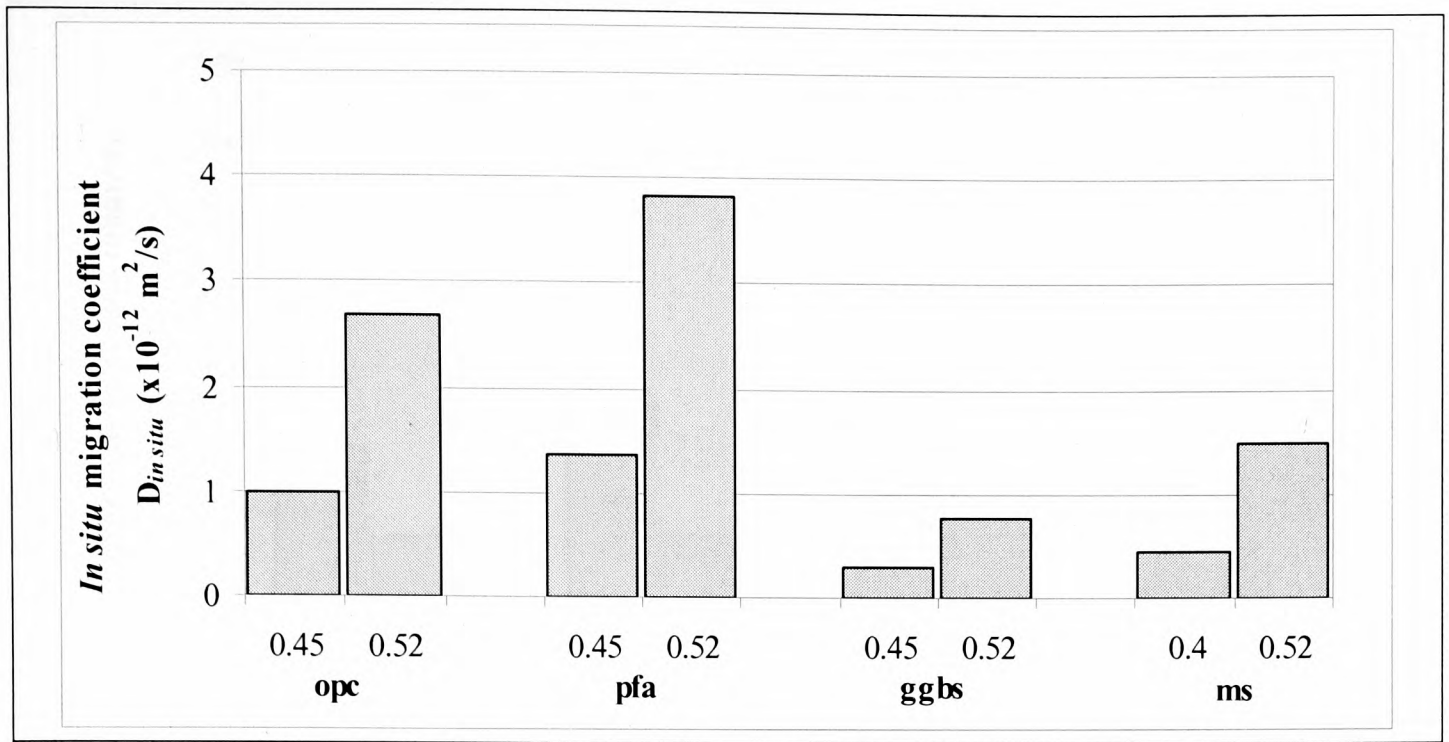

Figure 6.10 The effect of w/b on the *in situ* migration coefficient, $D_{in\ situ}$

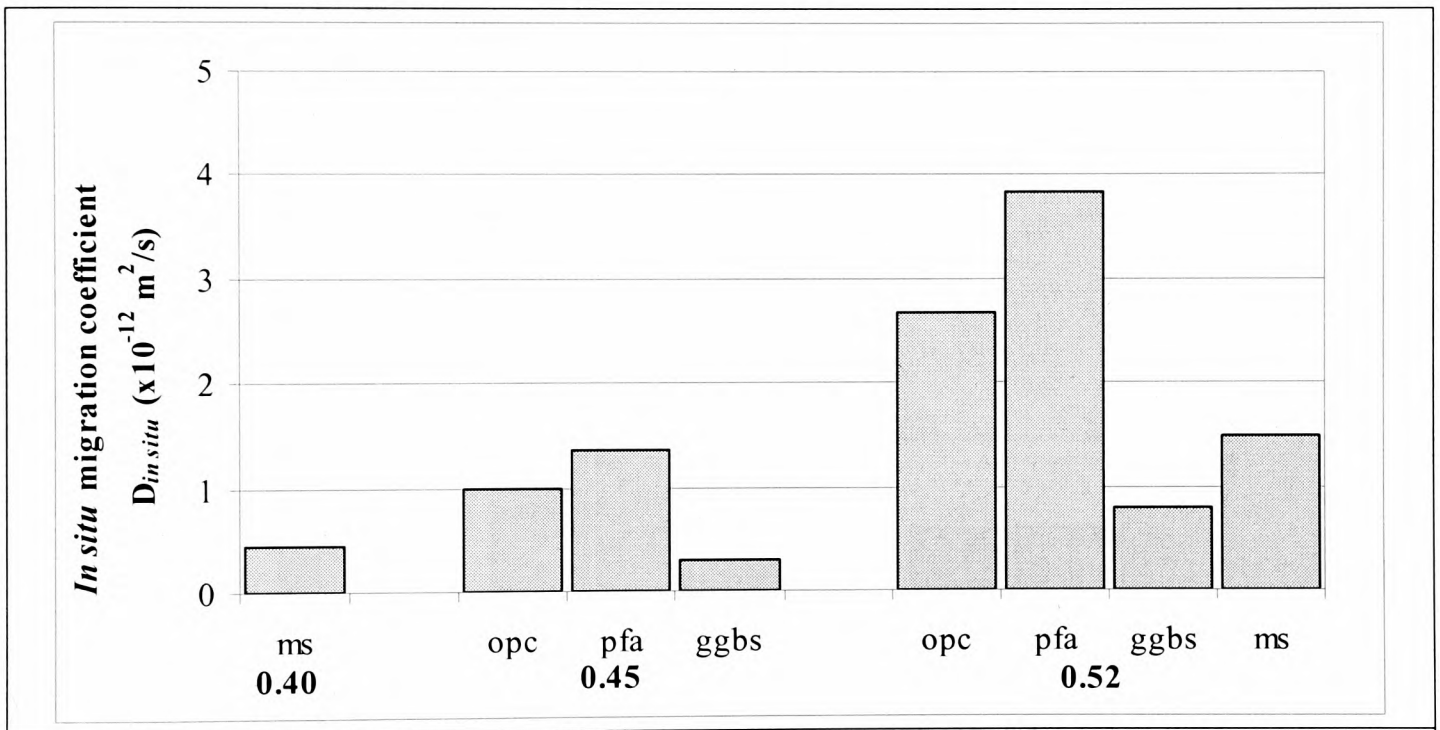

Figure 6.11 The effect of type of binder on the *in situ* migration coefficient, $D_{in\ situ}$

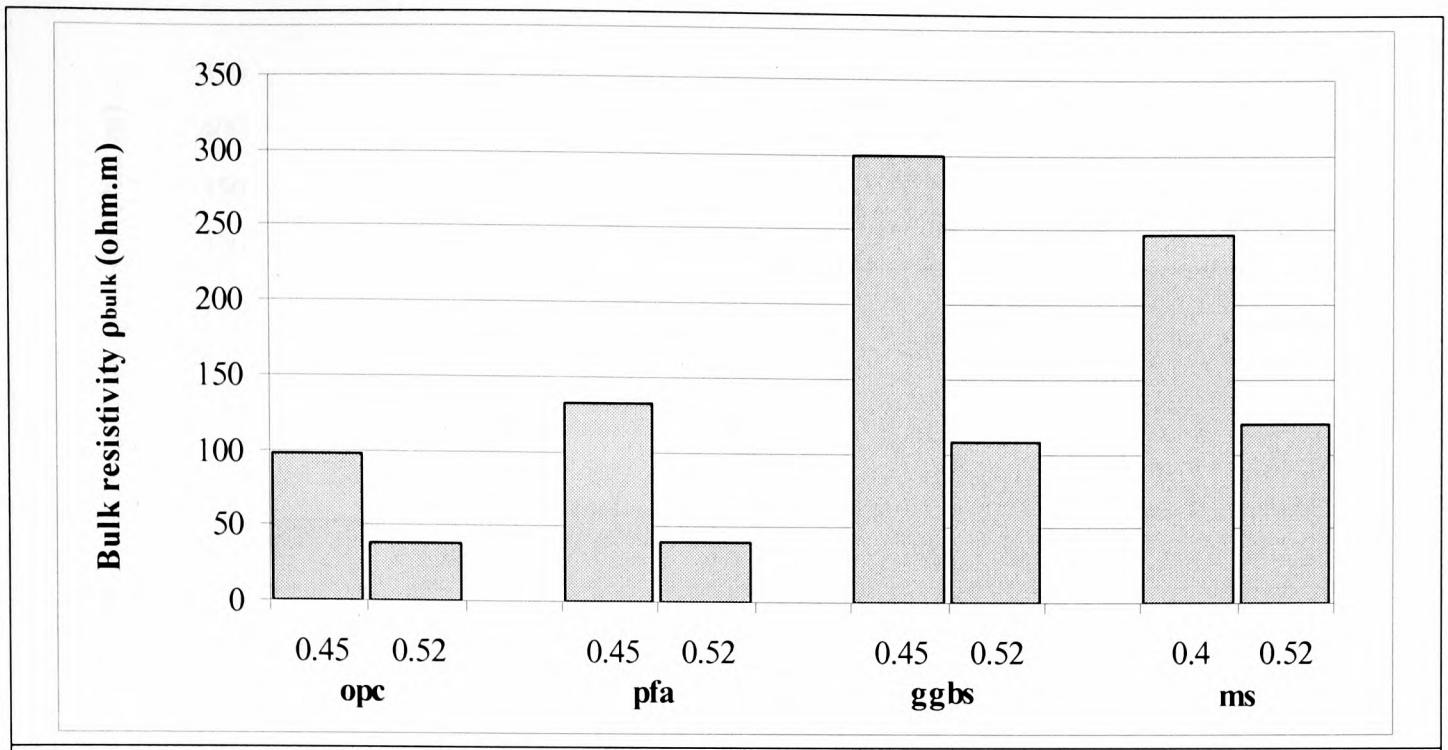

Figure 6.12 The effect of w/b on the bulk resistivity, ρ_{bulk}

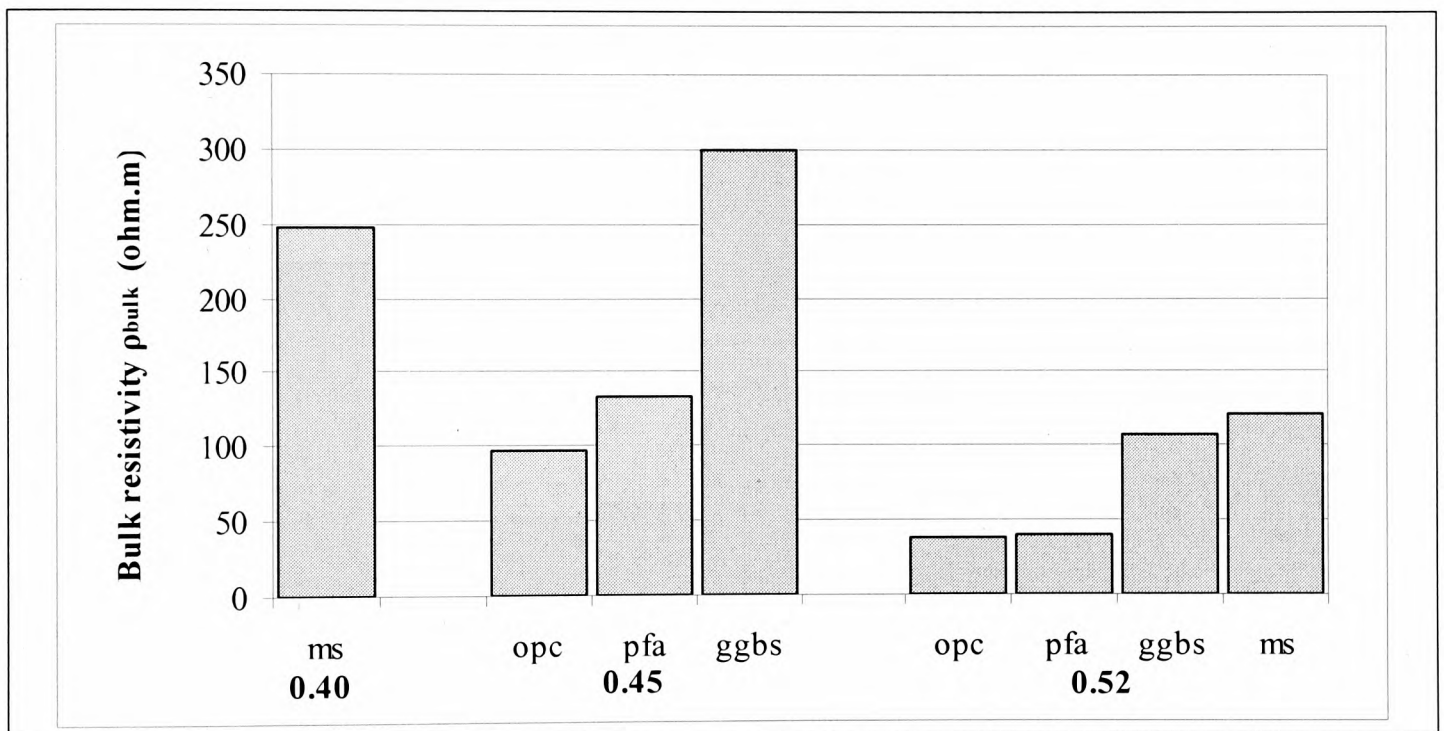

Figure 6.13 The effect of type of binder on the bulk resistivity, ρ_{bulk}

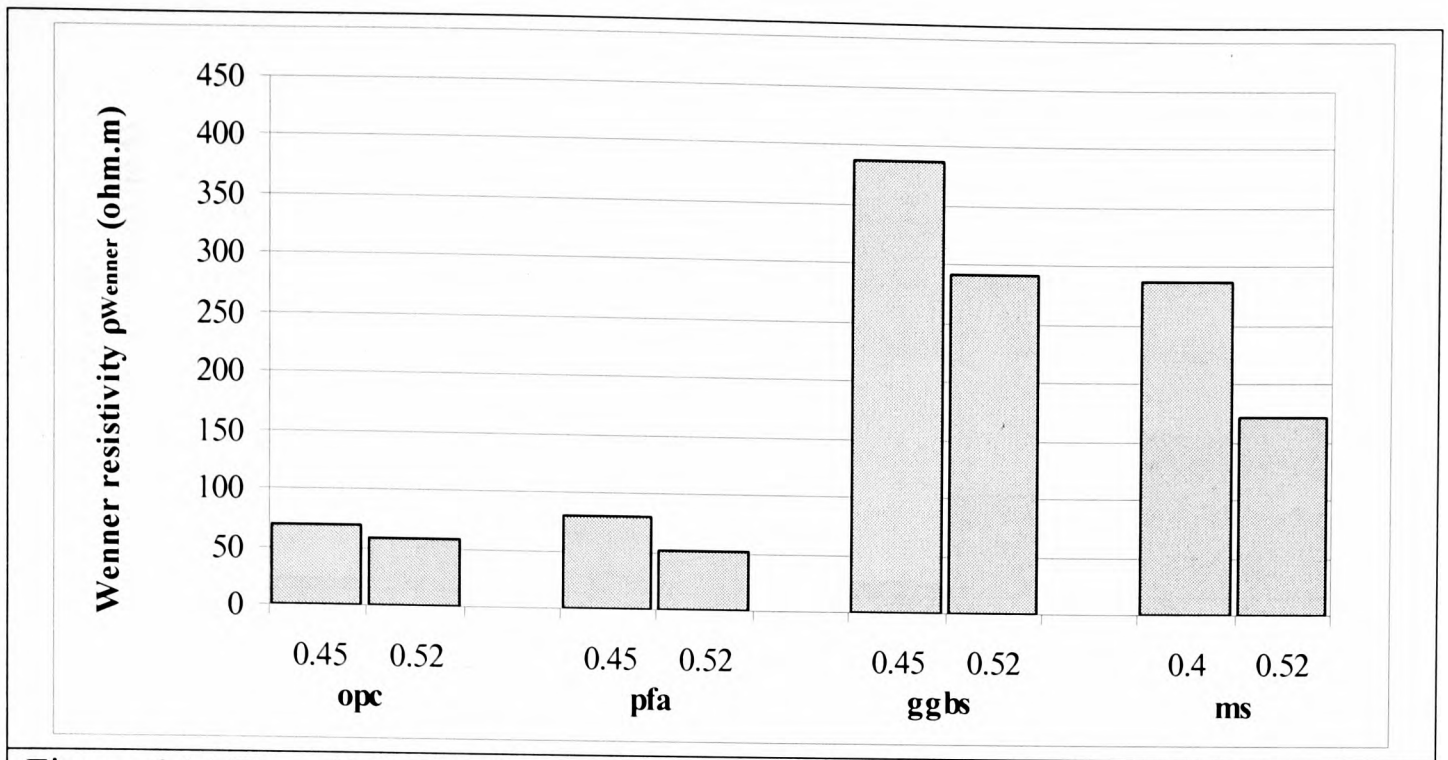

Figure 6.14 The effect of w/b on the Wenner resistivity, ρ_{Wenner}

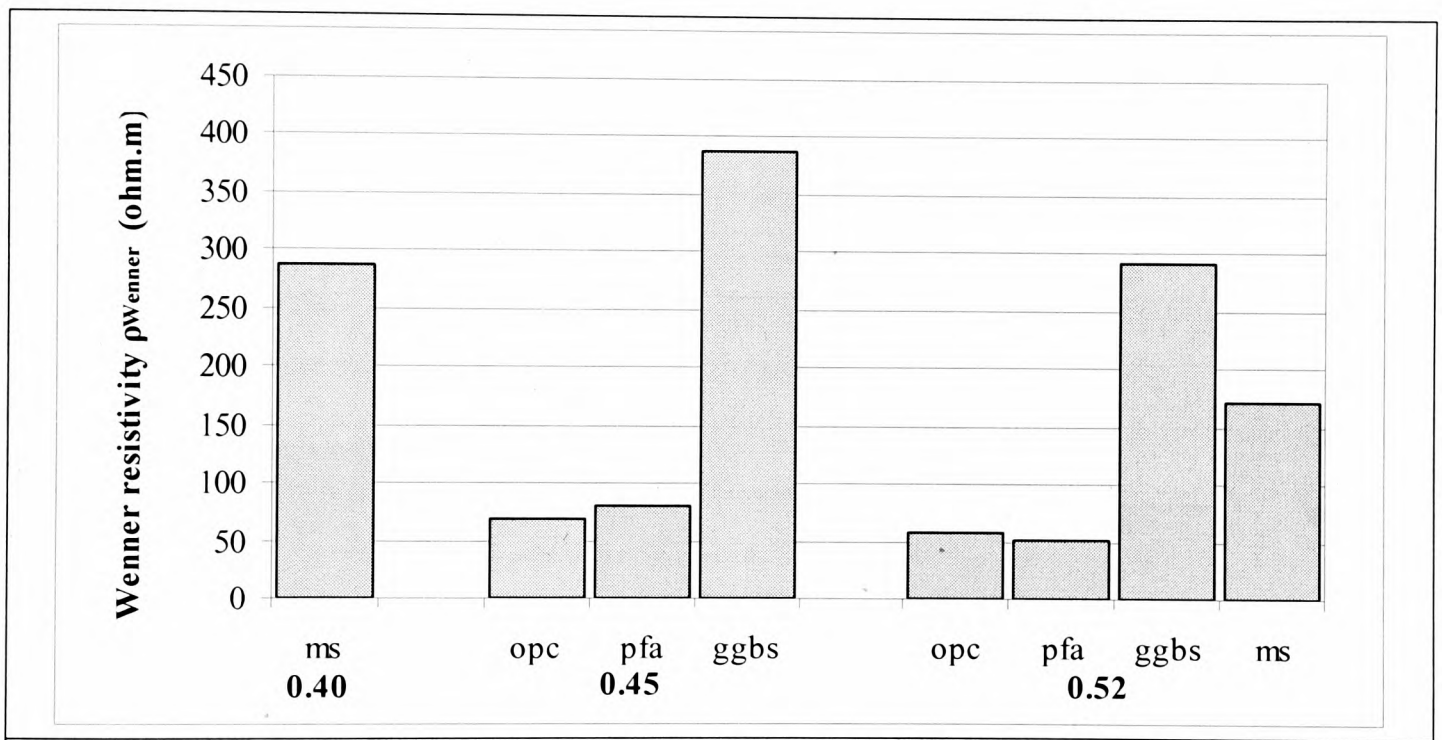

Figure 6.15 The effect of type of binder on the Wenner resistivity, ρ_{Wenner}

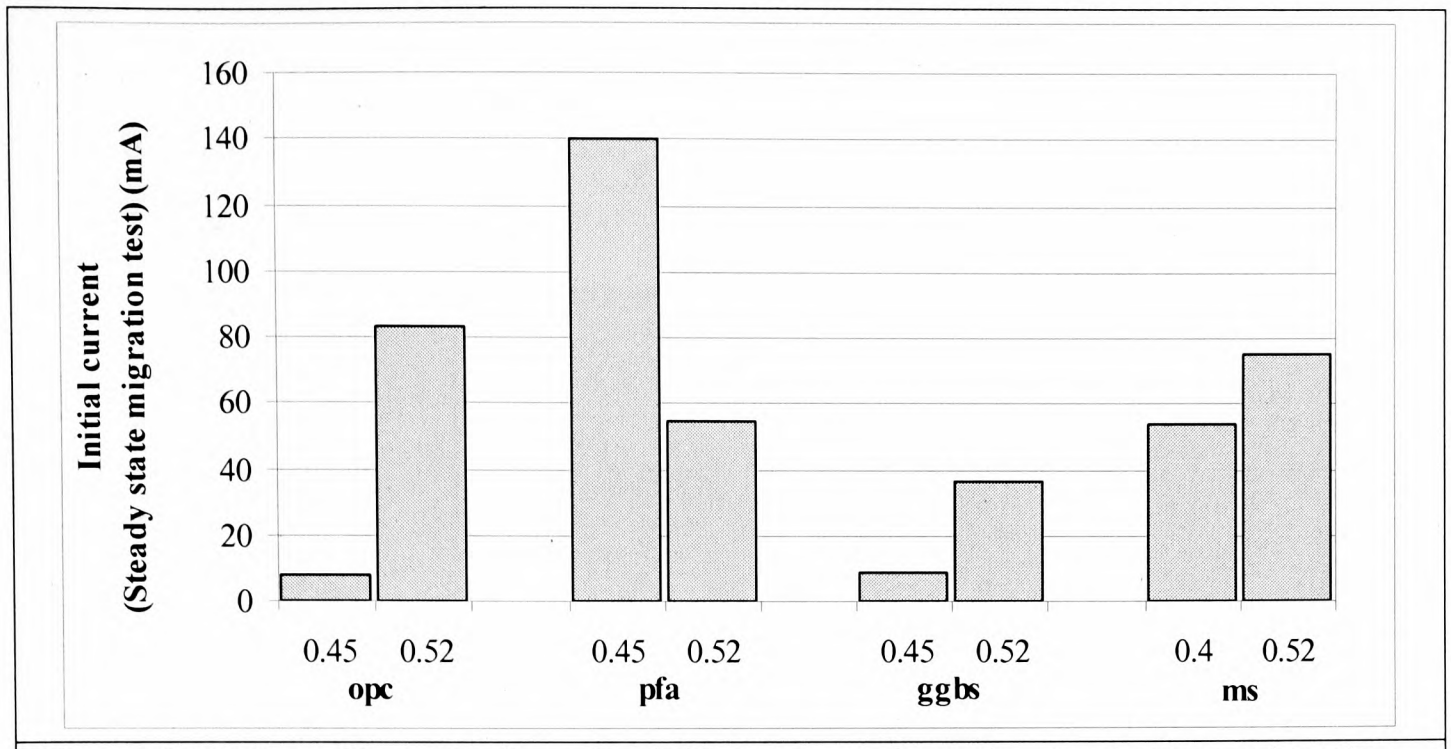

Figure 6.16 The effect of w/b on the initial current from the steady state migration test

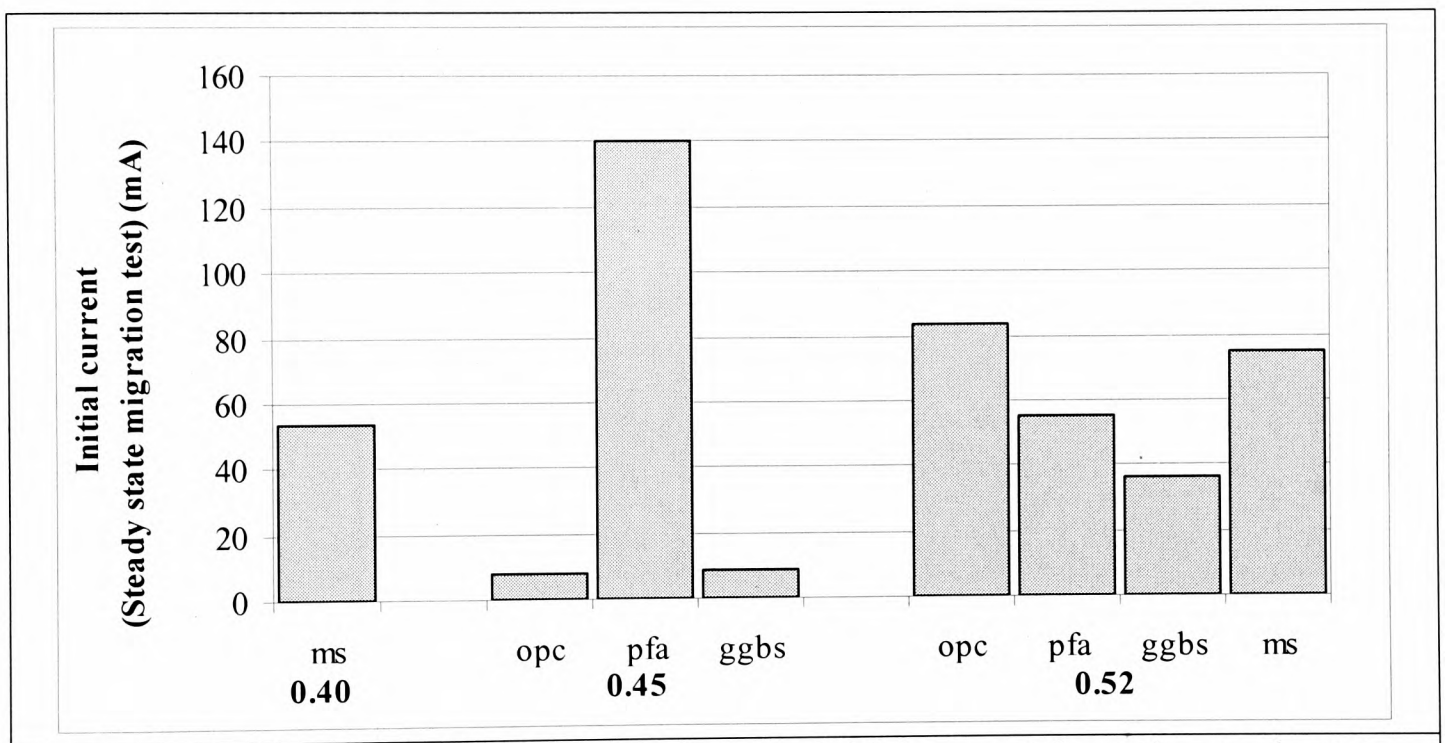

Figure 6.17 The effect of type of binder on the initial current from the steady state migration test

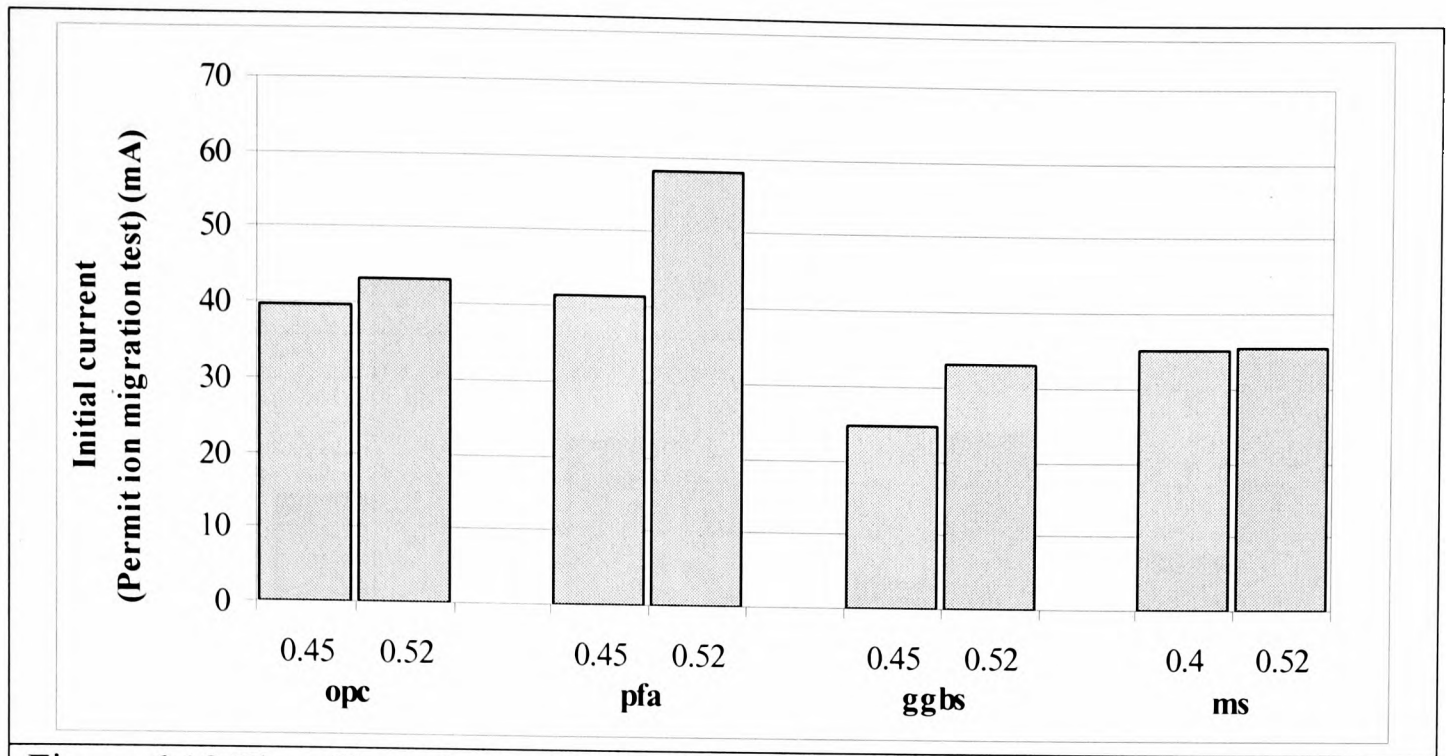

Figure 6.18 The effect of w/b on the initial current from the Permit ion migration test

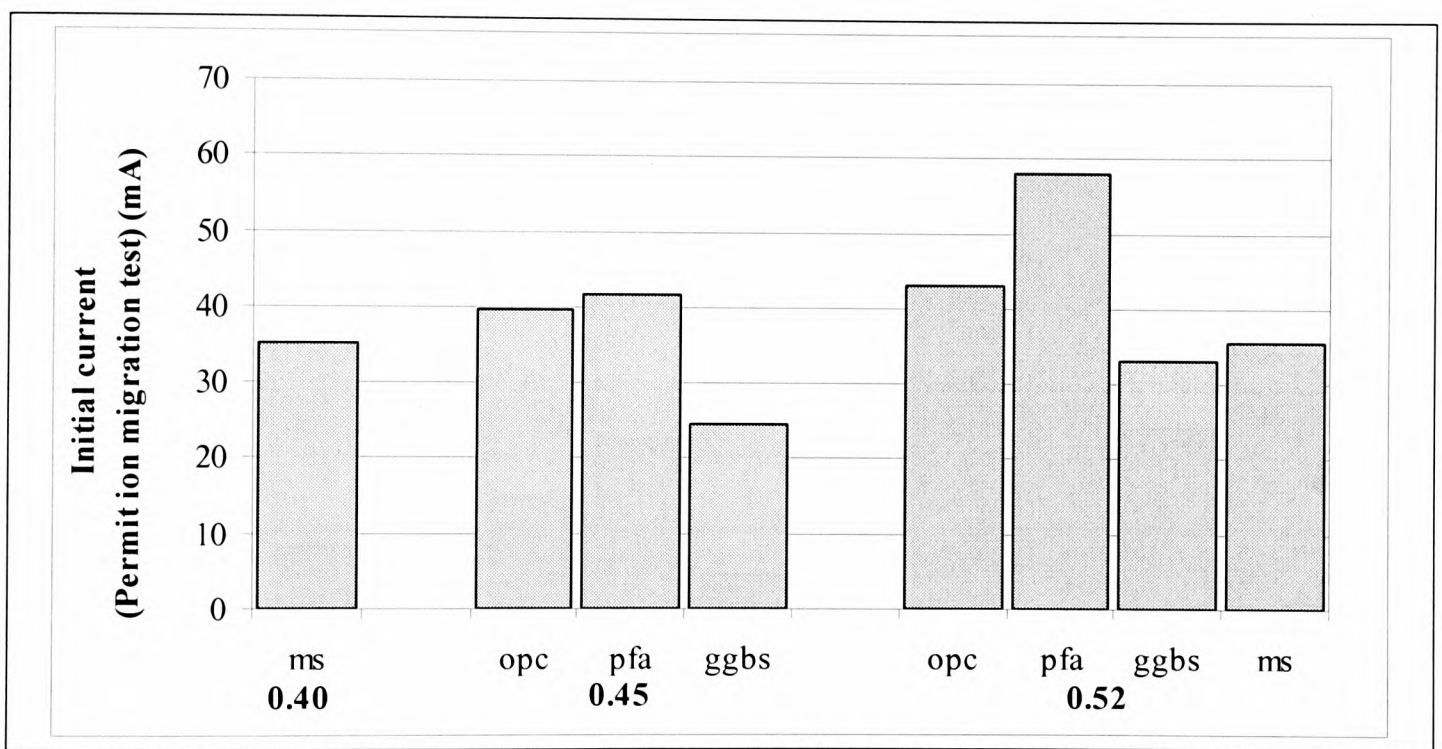

Figure 6.19 The effect of type of binder on the initial current from the Permit ion migration test

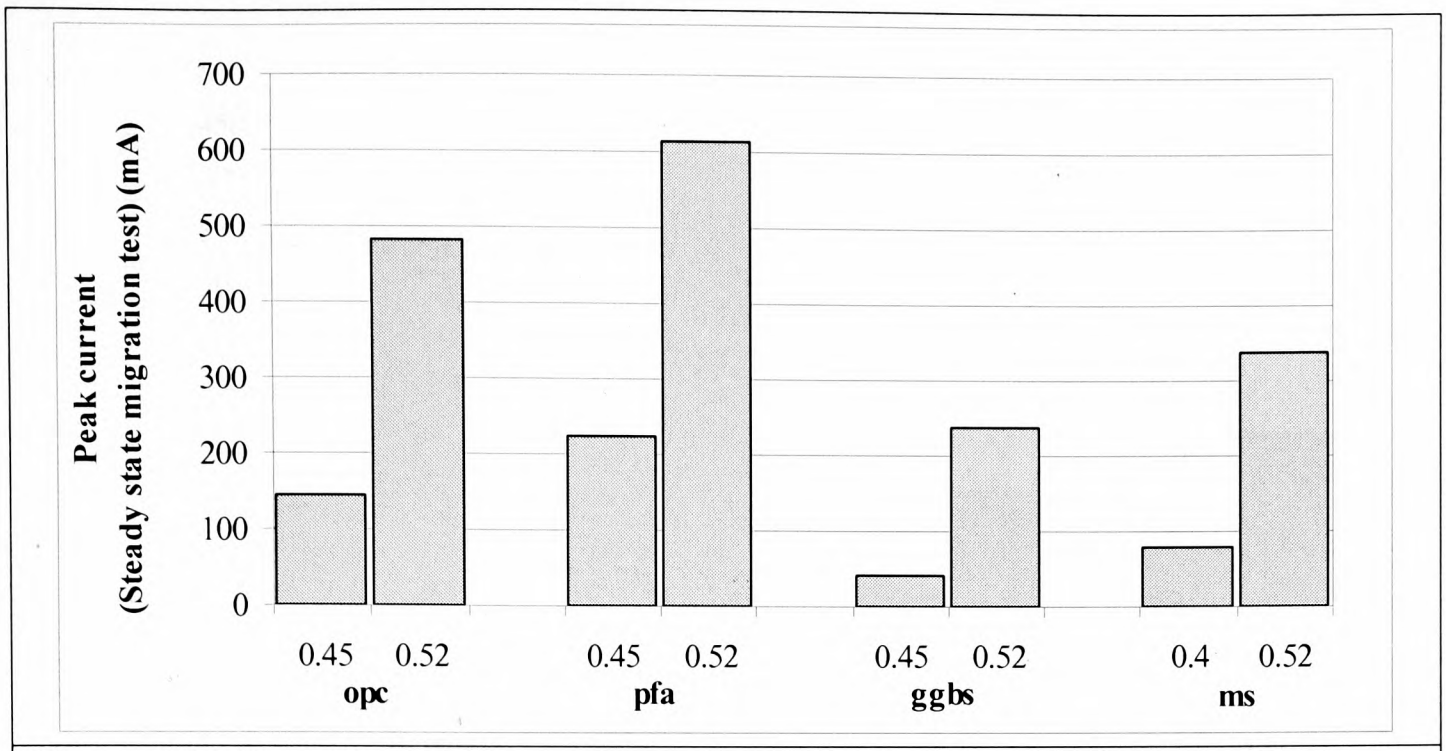

Figure 6.20 The effect of w/b on the peak current from the steady state migration test

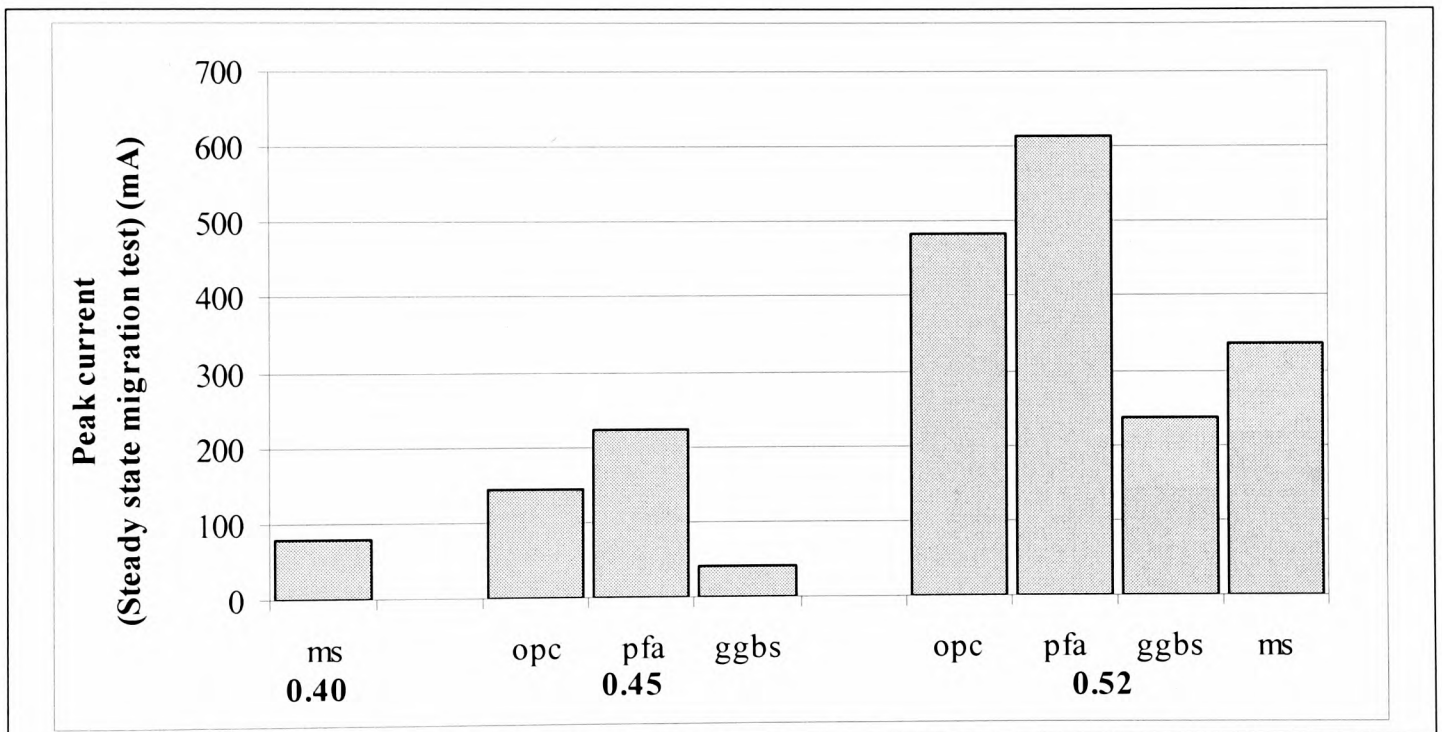

Figure 6.21 The effect of type of binder on the peak current from the steady state migration test

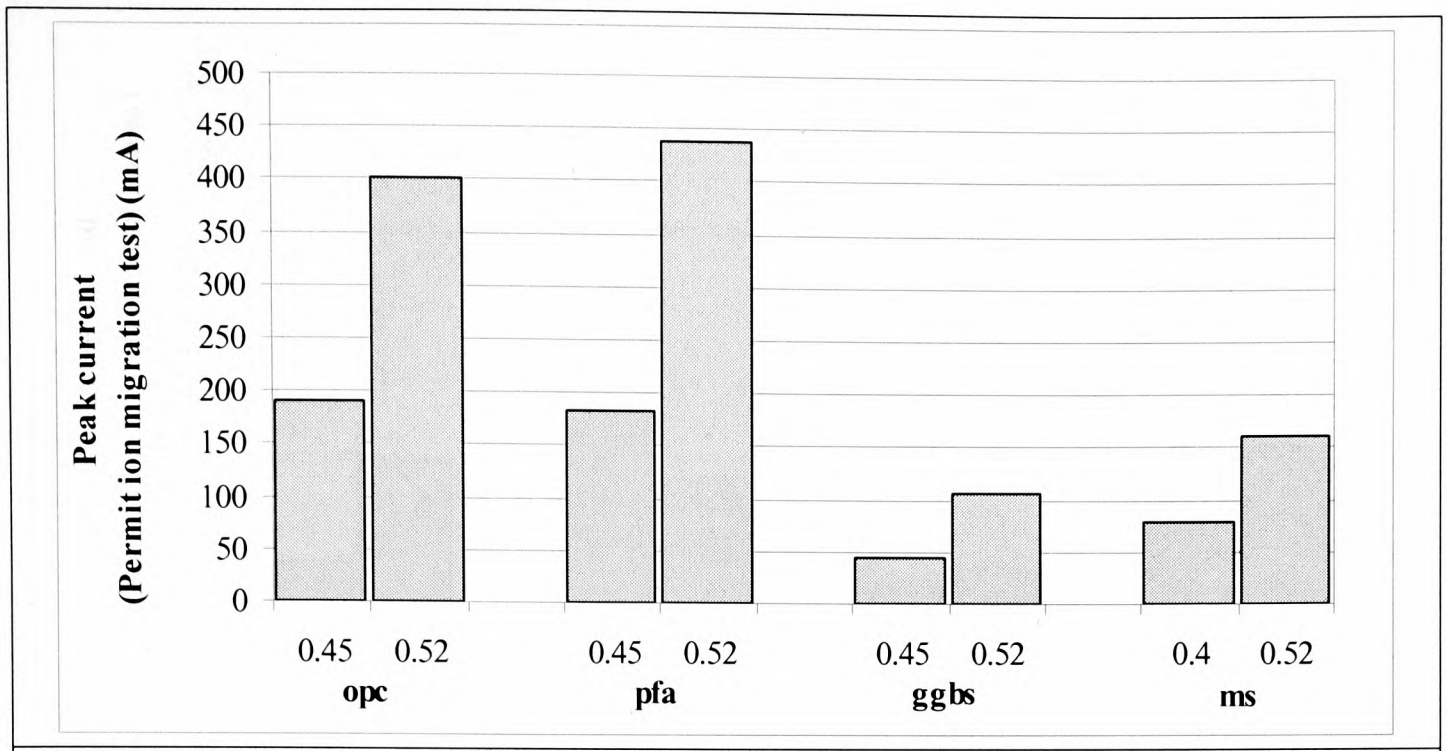

Figure 6.22 The effect of w/b on the peak current from the Permit ion migration test

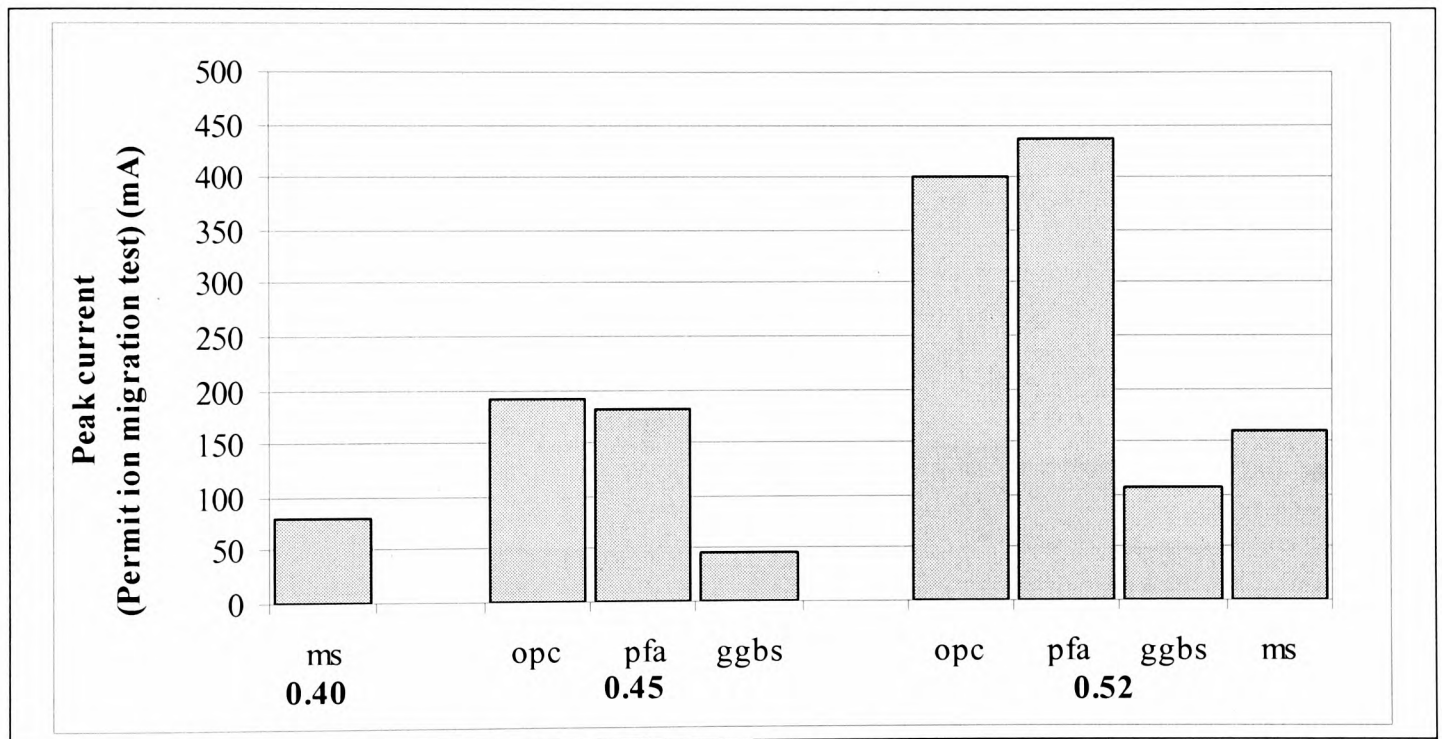

Figure 6.23 The effect of type of binder on the peak current from the Permit ion migration test

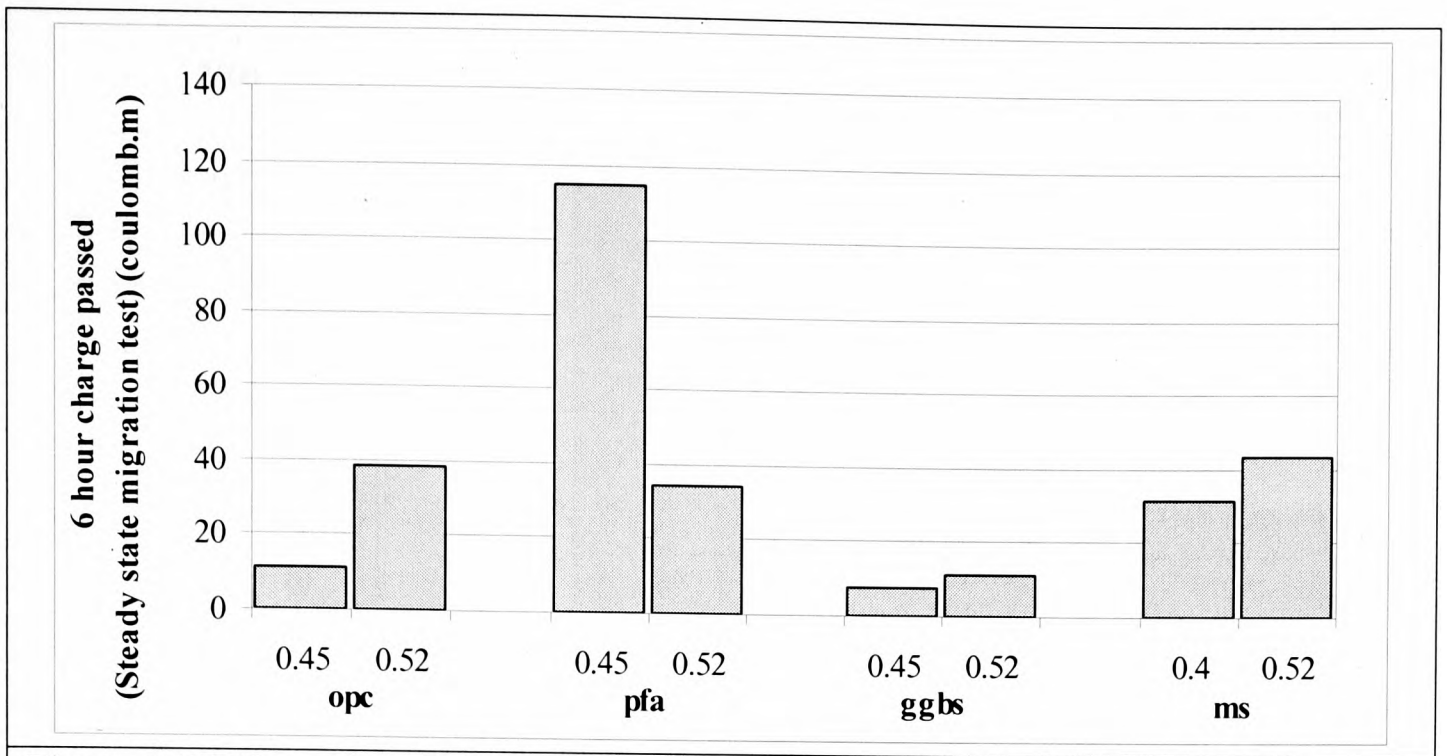

Figure 6.24 The effect of w/b on the 6 hours charge passed from the steady state migration test

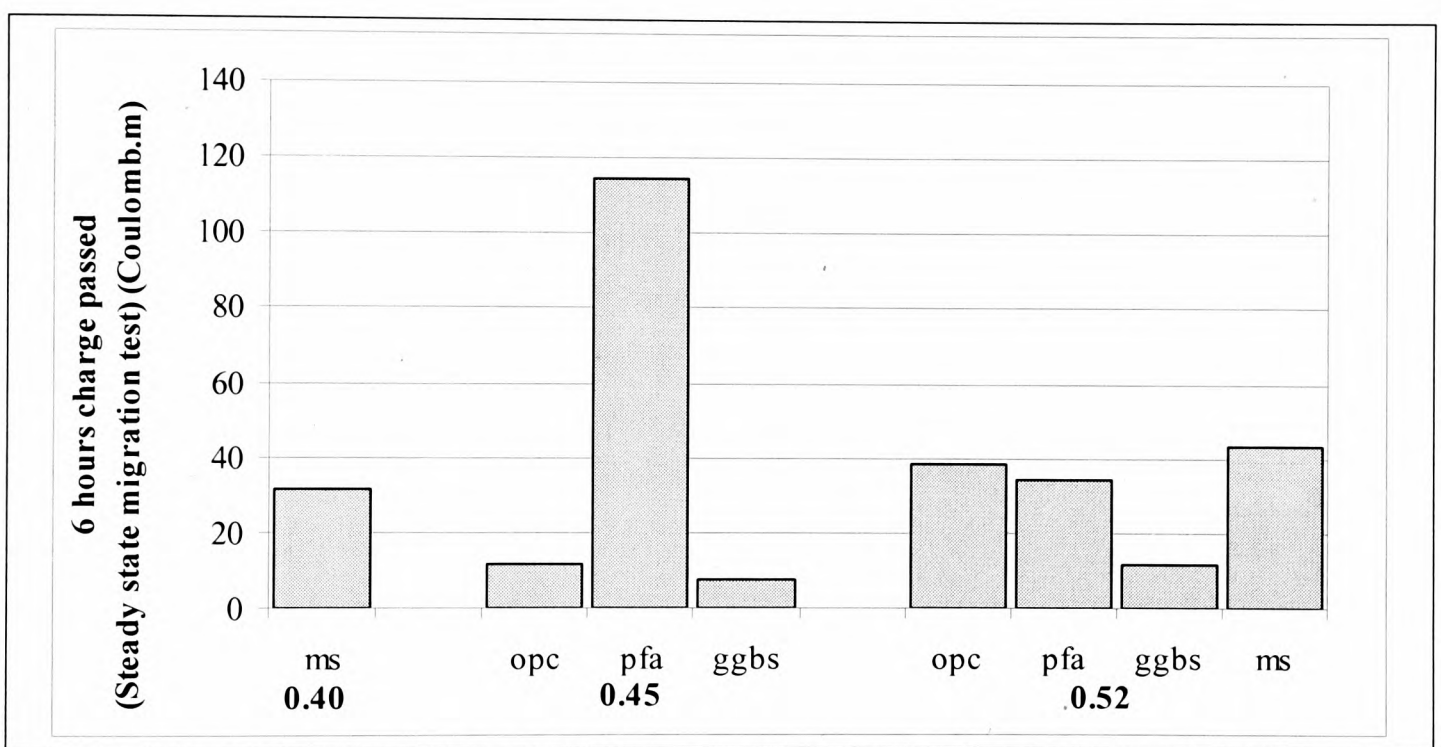

Figure 6.25 The effect of type of binder on the 6 hours charge passed from the steady state migration test

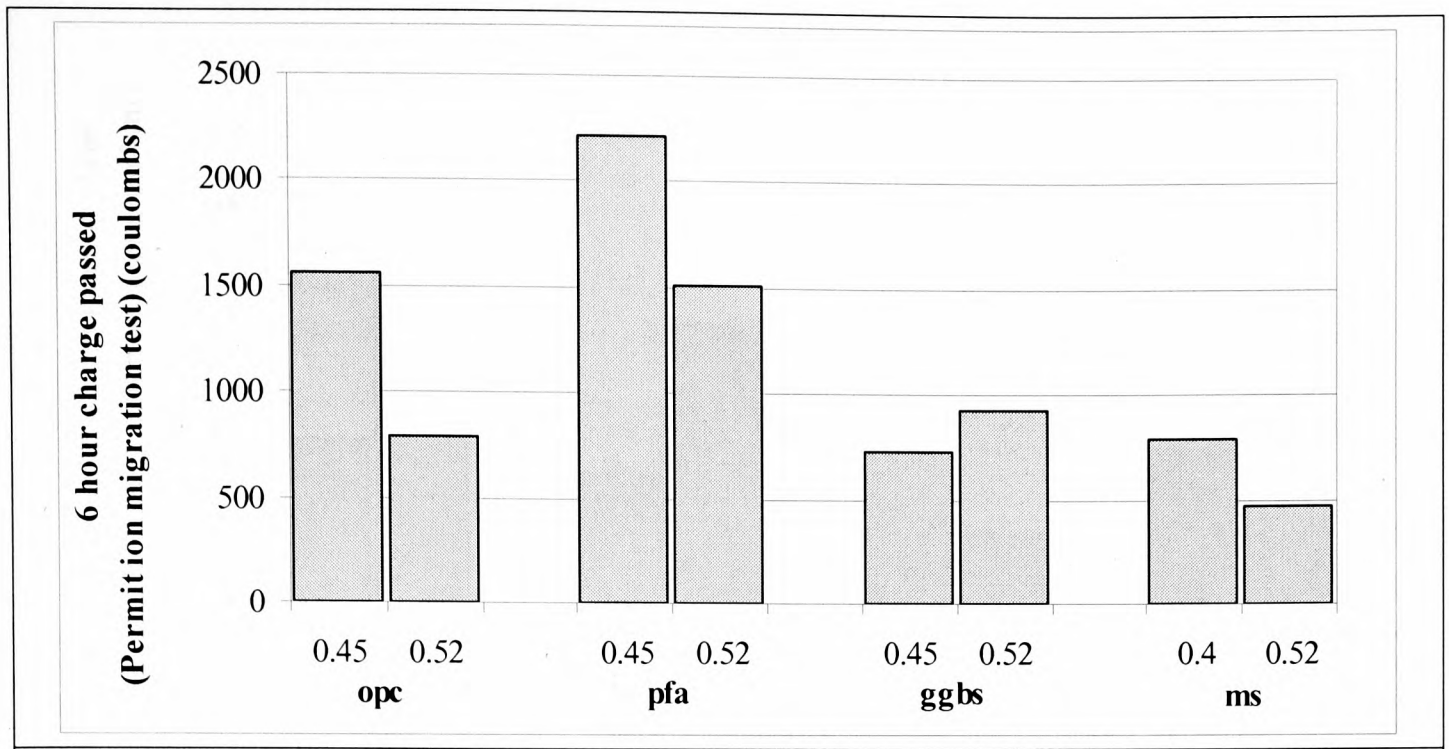

Figure 6.26 The effect of w/b on the 6 hours charge passed from the Permit ion migration test

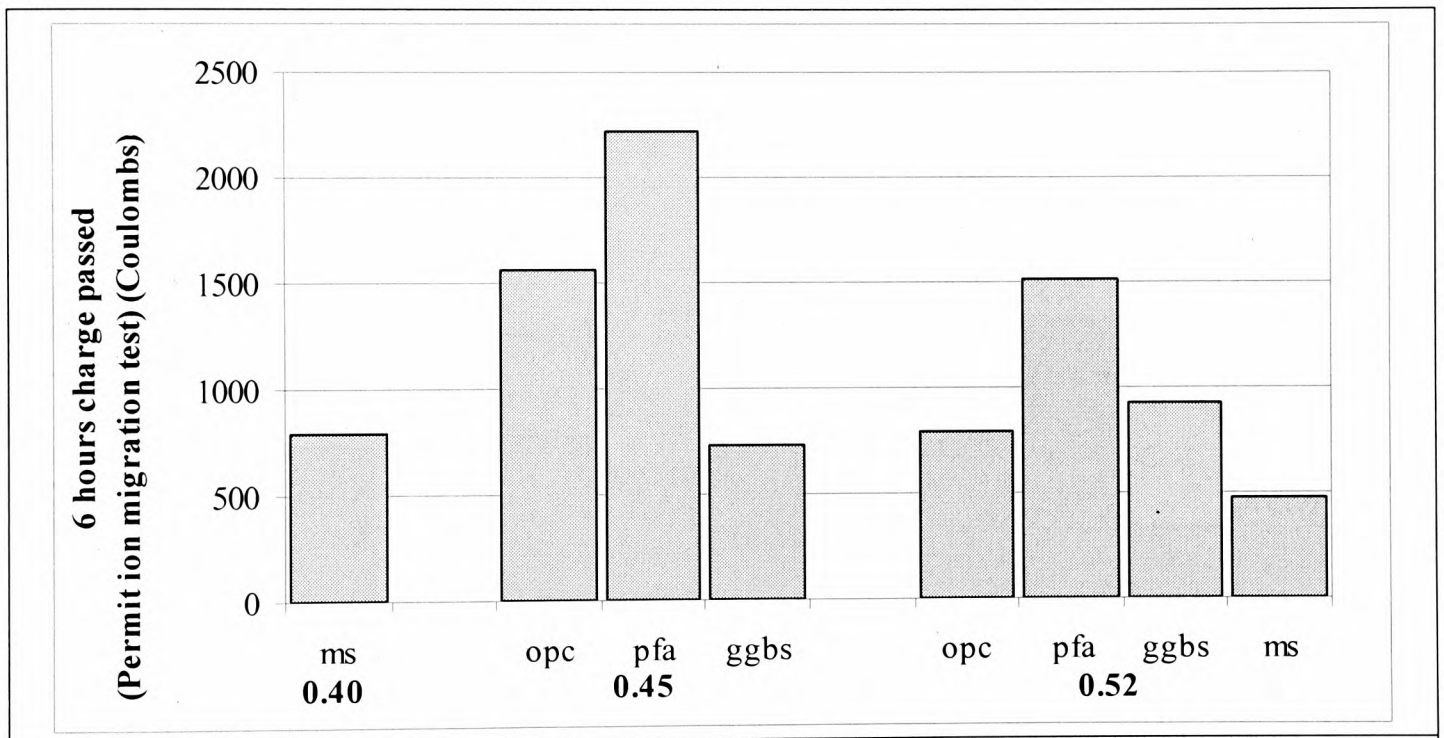

Figure 6.27 The effect of type of binder on the 6 hours charge passed from the Permit ion migration test

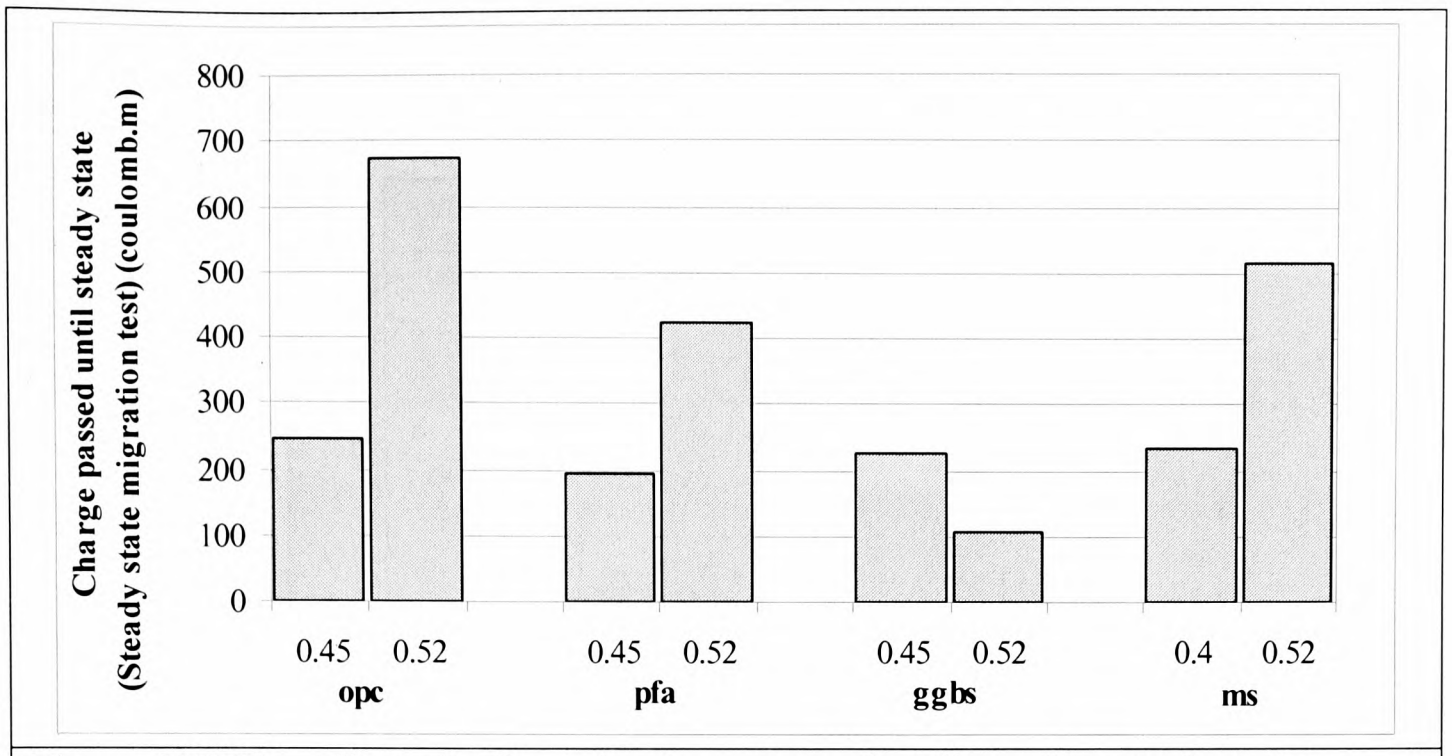

Figure 6.28 The effect of w/b on the charge passed until steady state from the steady state migration test

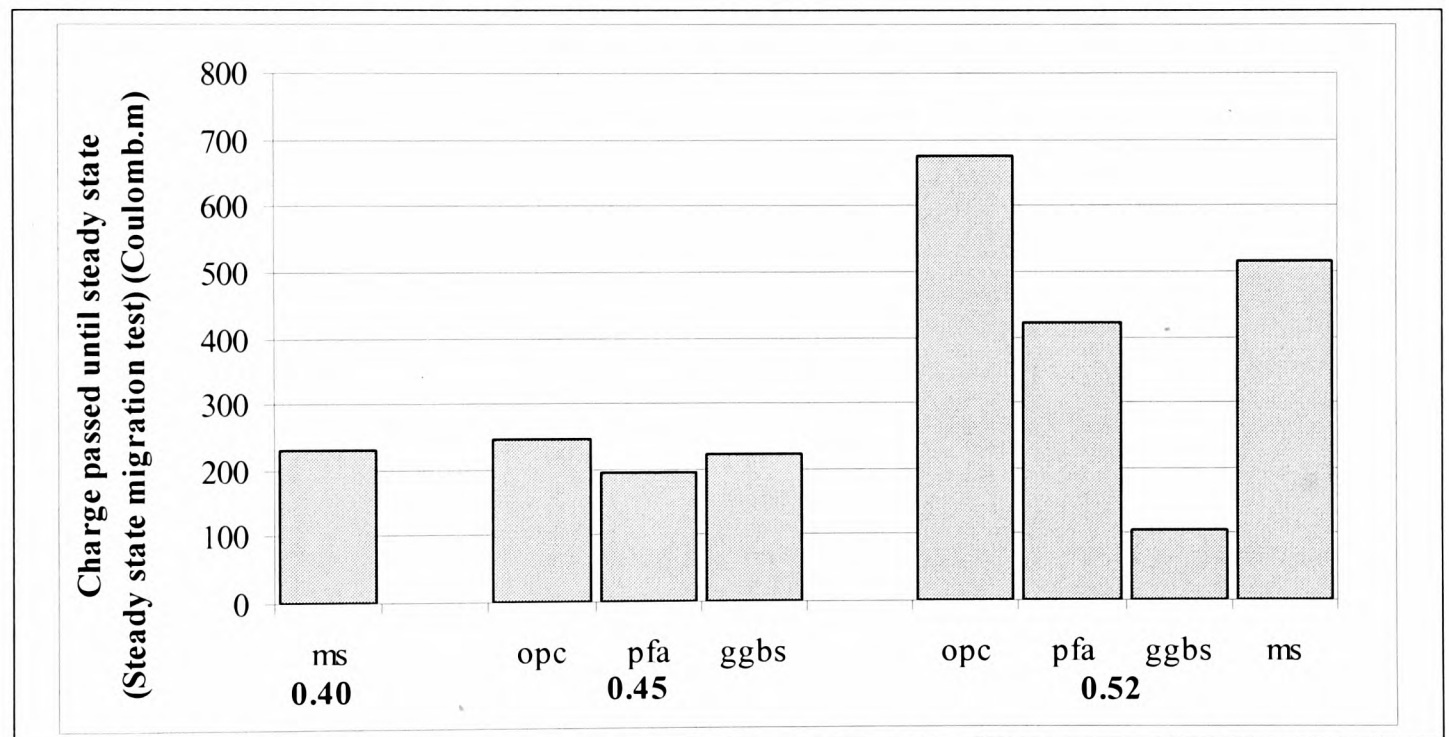

Figure 6.29 The effect of type of binder on the charge passed until steady state from the steady state migration test

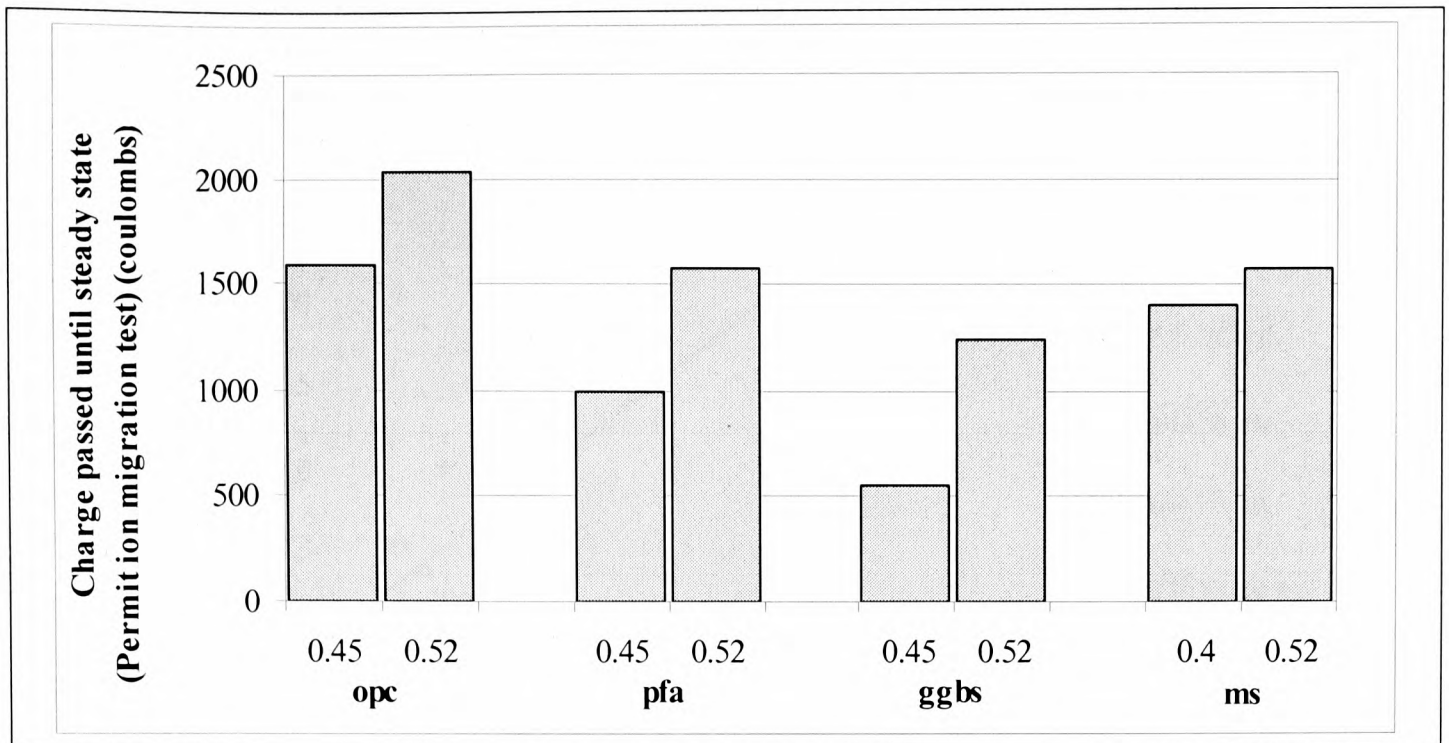

Figure 6.30 The effect of w/b on the charge passed until steady state from the Permit ion migration test

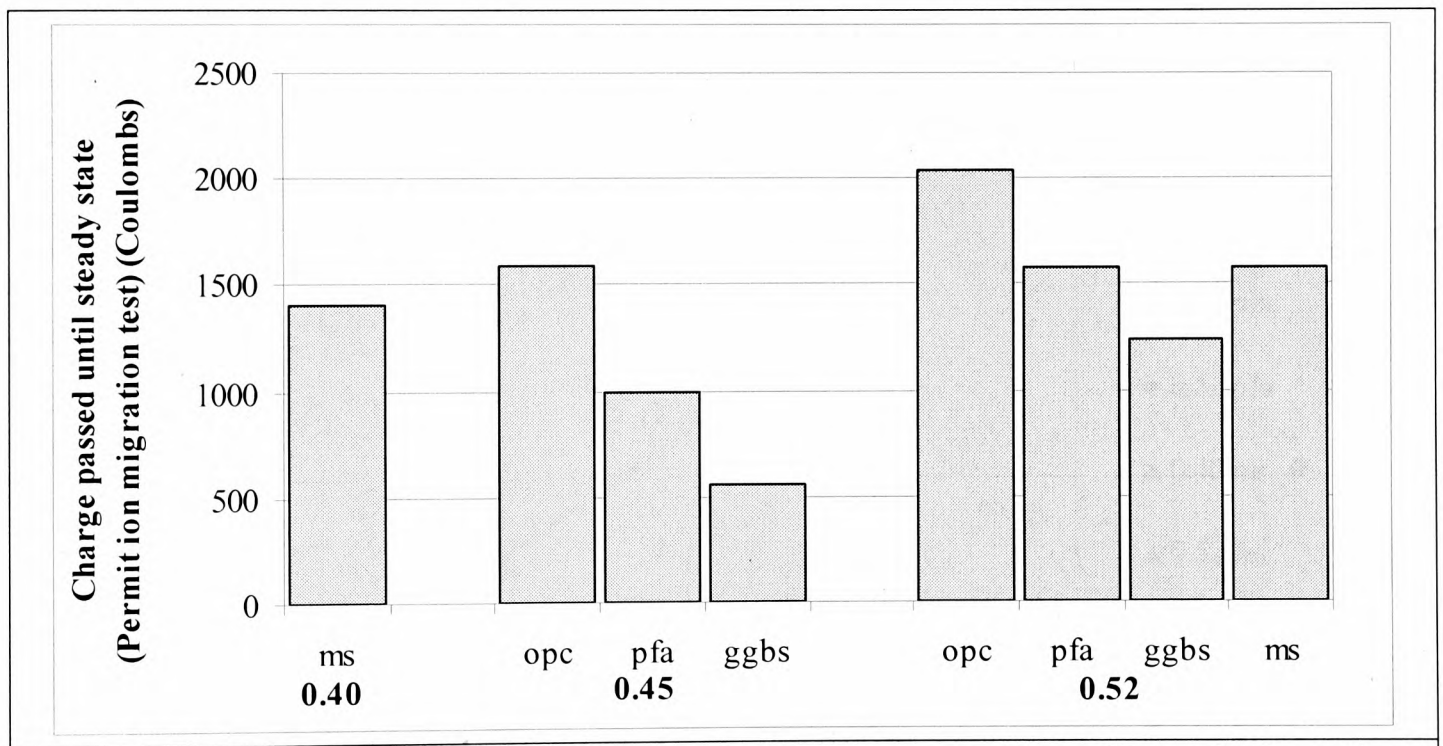

Figure 6.31 The effect of type of binder on the charge passed until steady from the Permit ion migration test

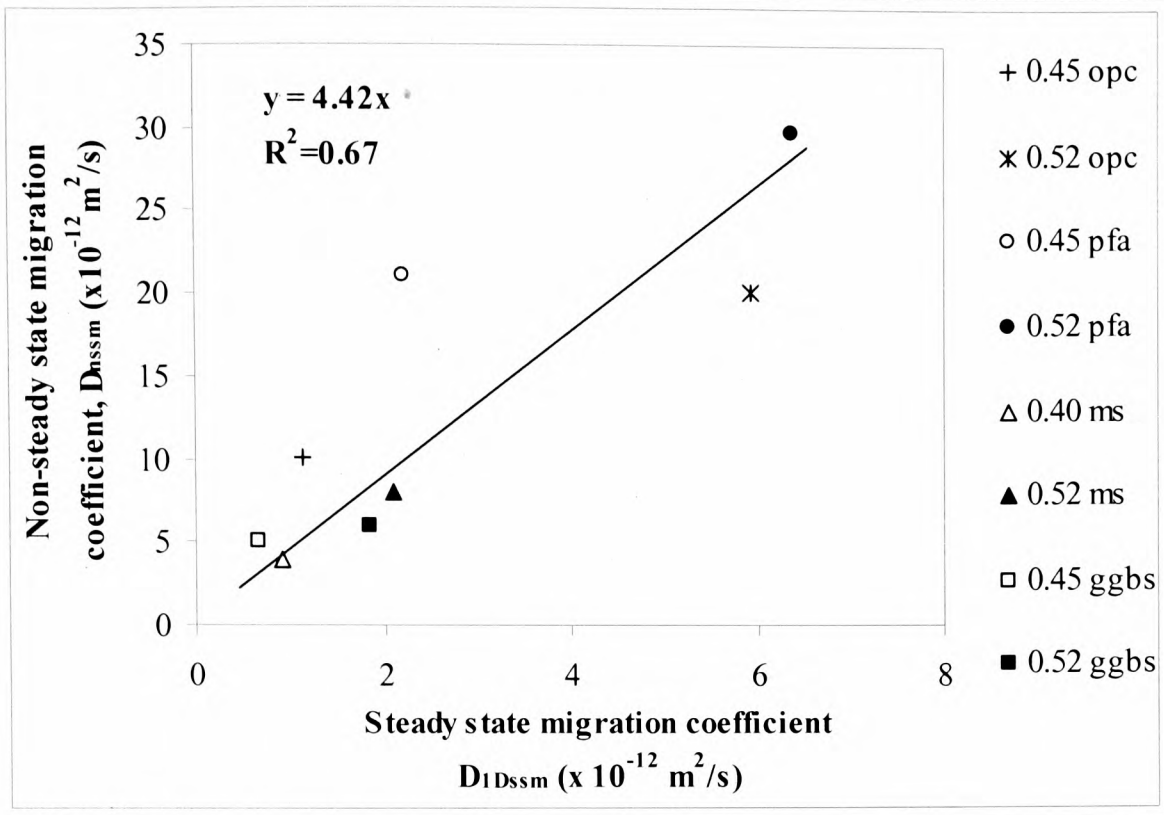

Figure 6.32 Relationship between D_{nssm} and D_{1Dssm}

Figure 6.33 Relationship between D_{nssm} and $D_{in\ situ}$

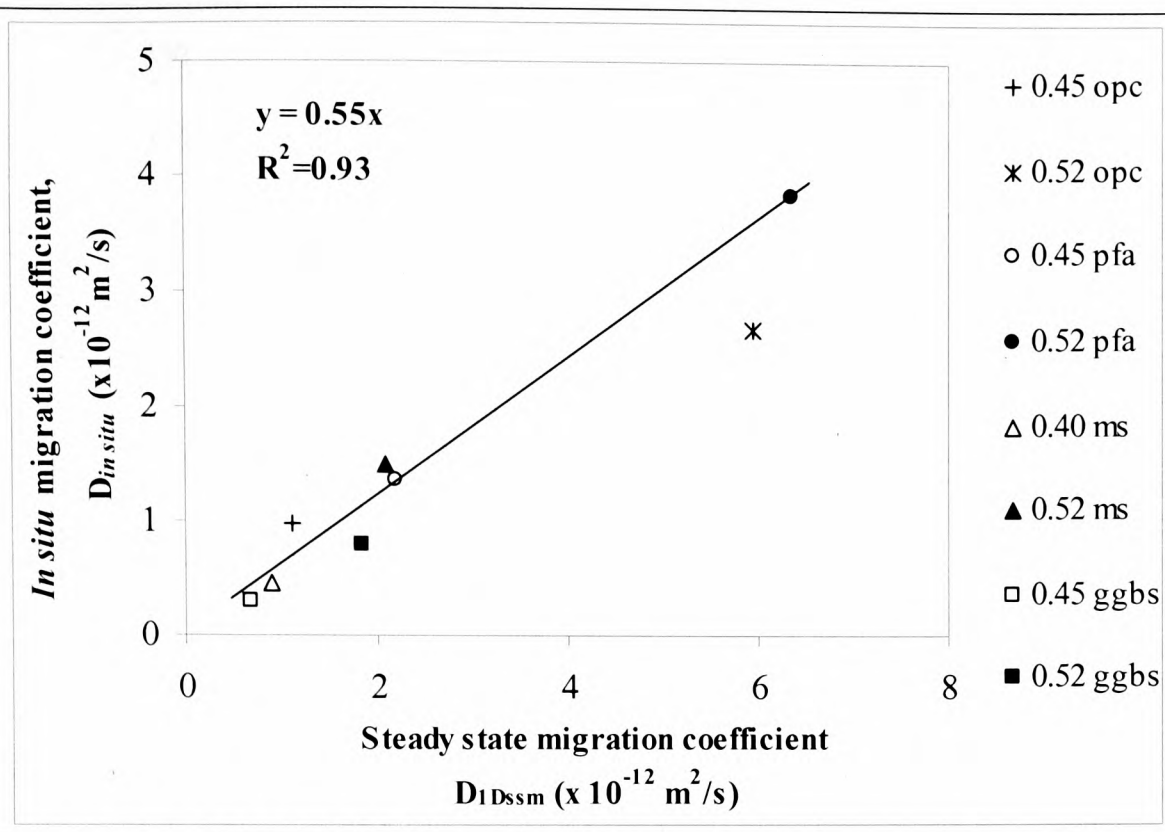

Figure 6.34 Relationship between D_{1Dssm} and $D_{in\ situ}$

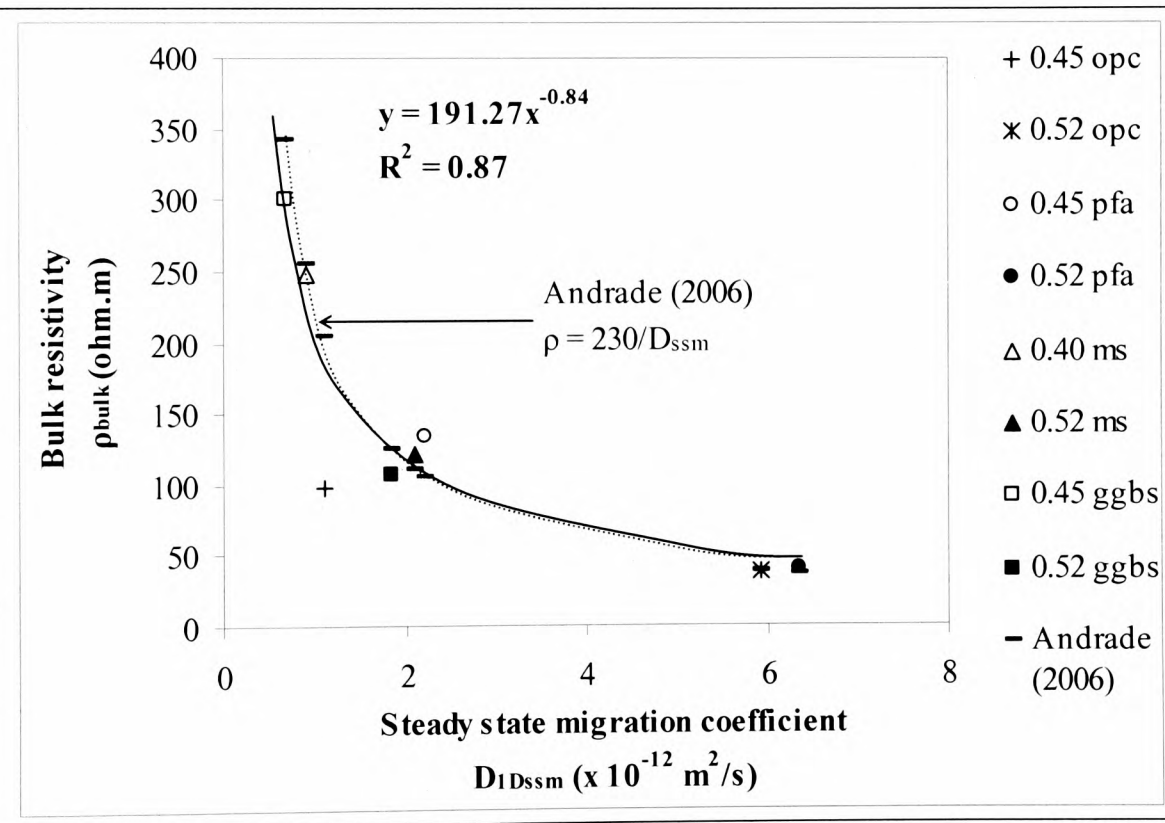

Figure 6.35 Relationship between D_{1Dssm} and ρ_{bulk}

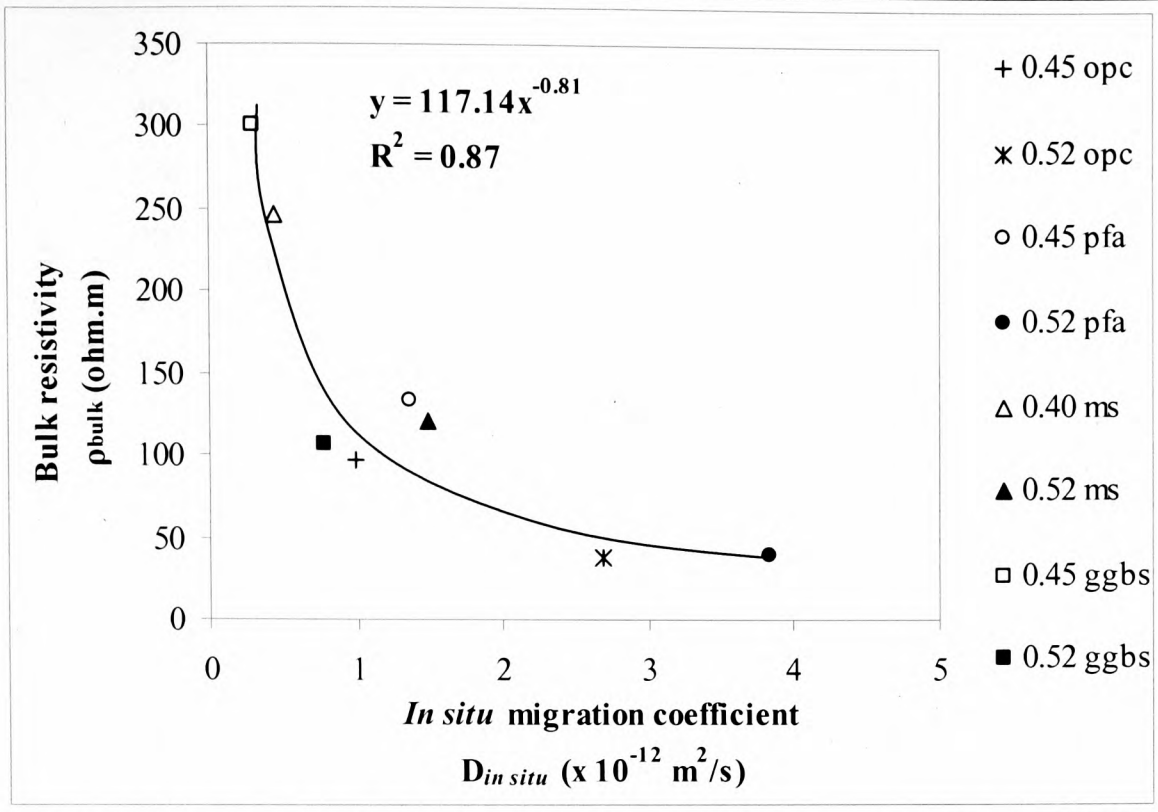

Figure 6.36 Relationship between $D_{in\ situ}$ and ρ_{bulk}

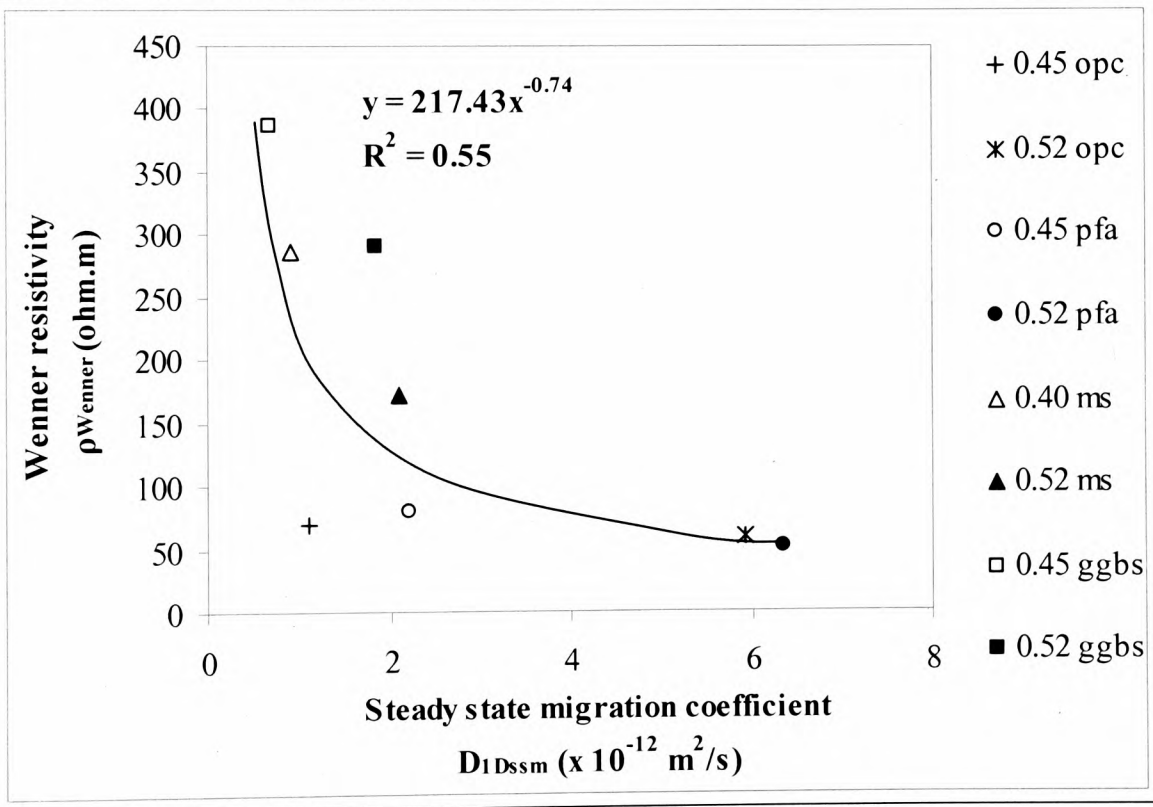

Figure 6.37 Relationship between D_{1Dssm} and ρ_{Wenner}

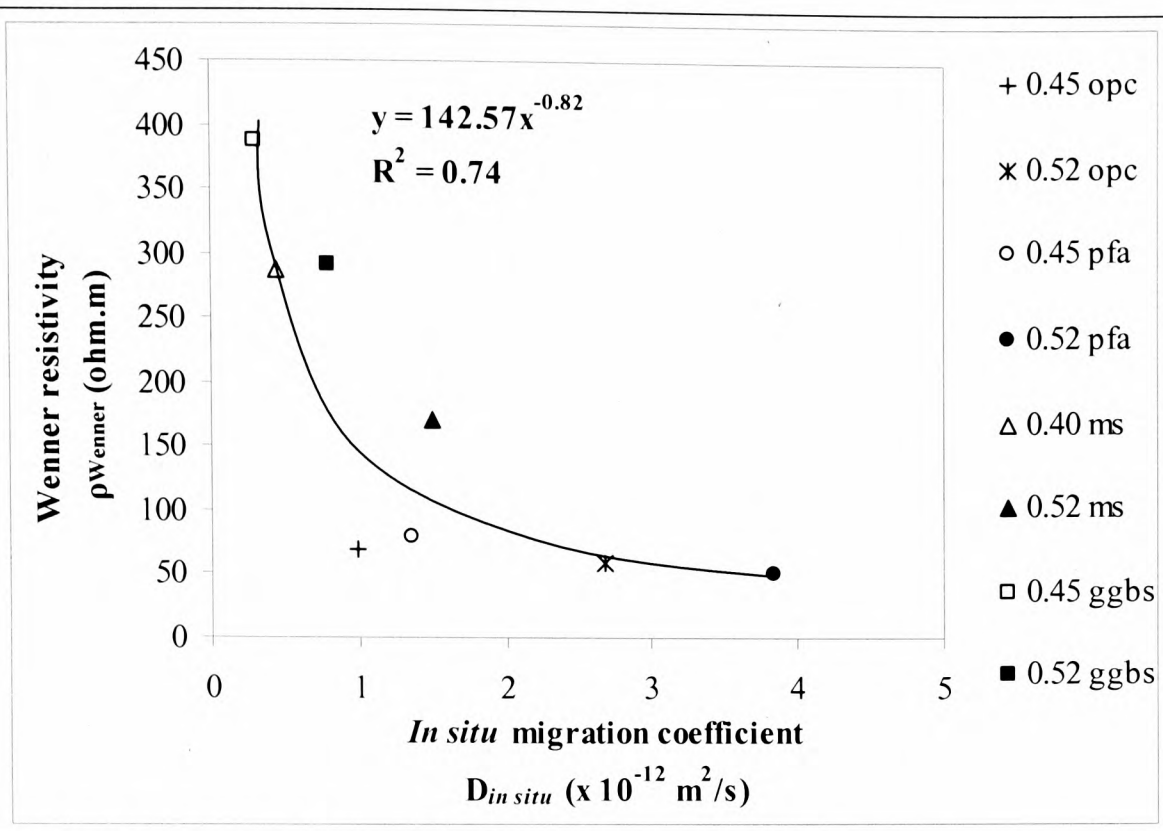

Figure 6.38 Relationship between $D_{in\ situ}$ and ρ_{Wenner}

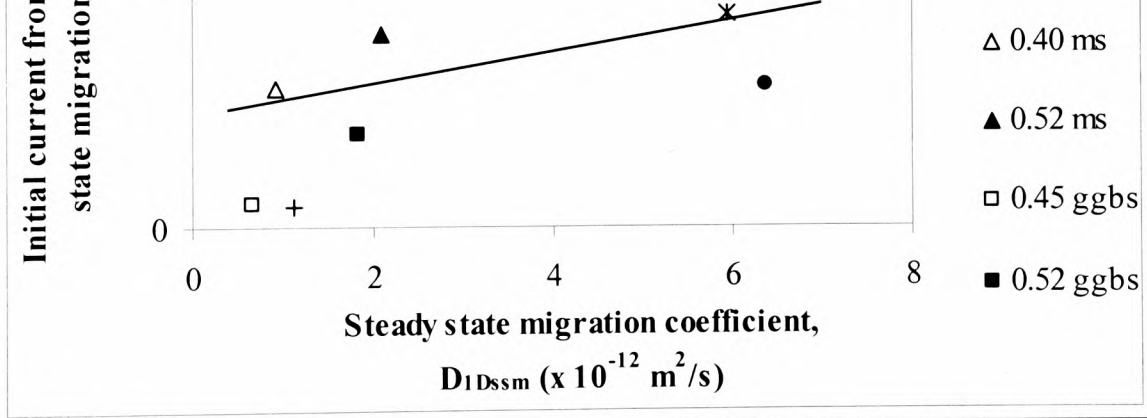

Figure 6.39 Relationship between D_{1Dssm} and initial current from the steady state migration test

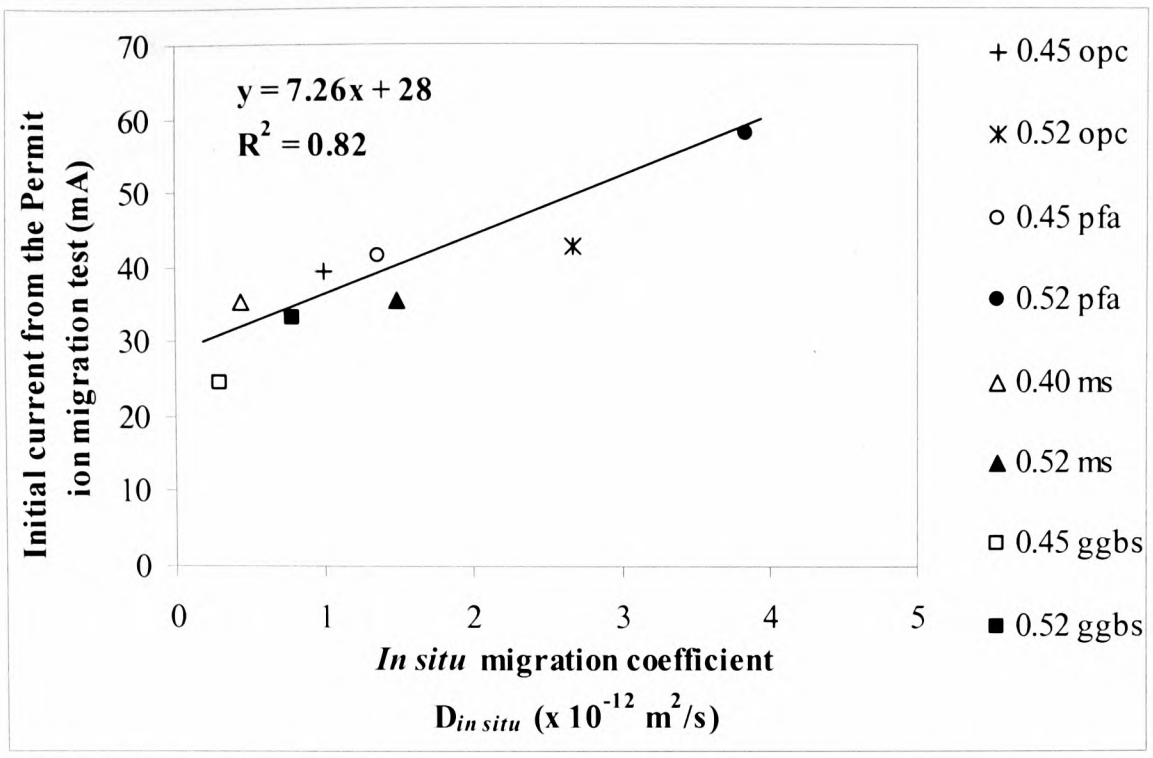

Figure 6.40 Relationship between $D_{in\ situ}$ and initial current from the Permit ion migration test

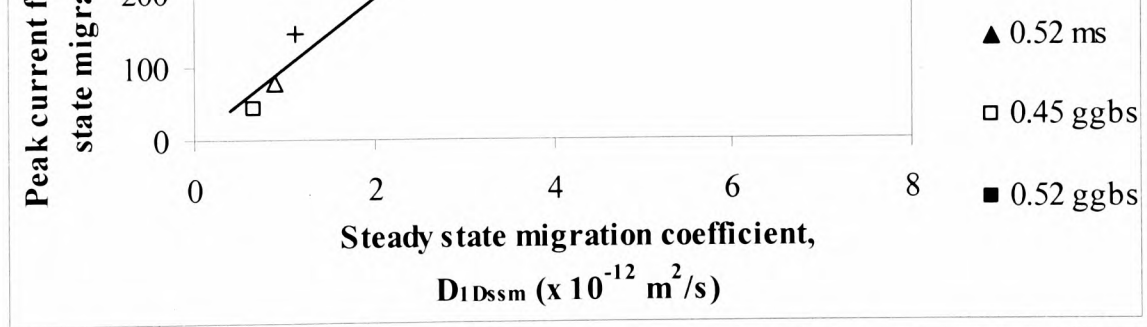

Figure 6.41 Relationship between D_{1Dssm} and peak current from the steady state migration test

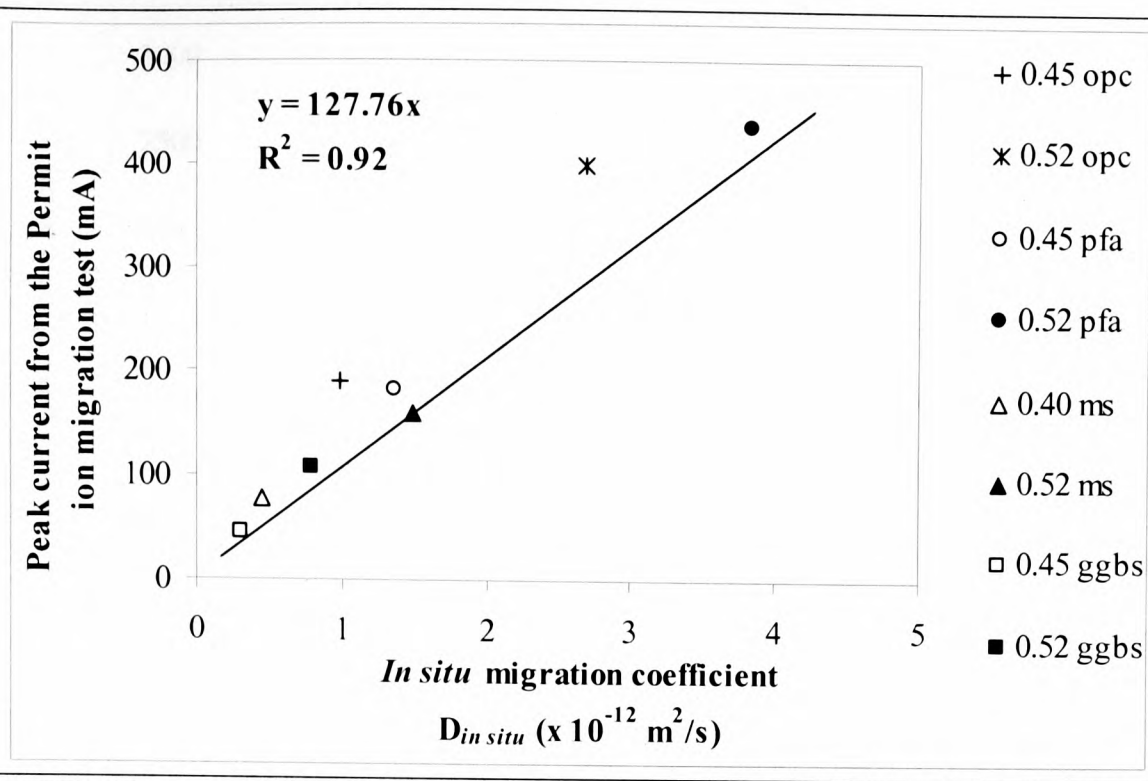

Figure 6.42 Relationship between $D_{in\ situ}$ and peak current from the Permit ion migration test

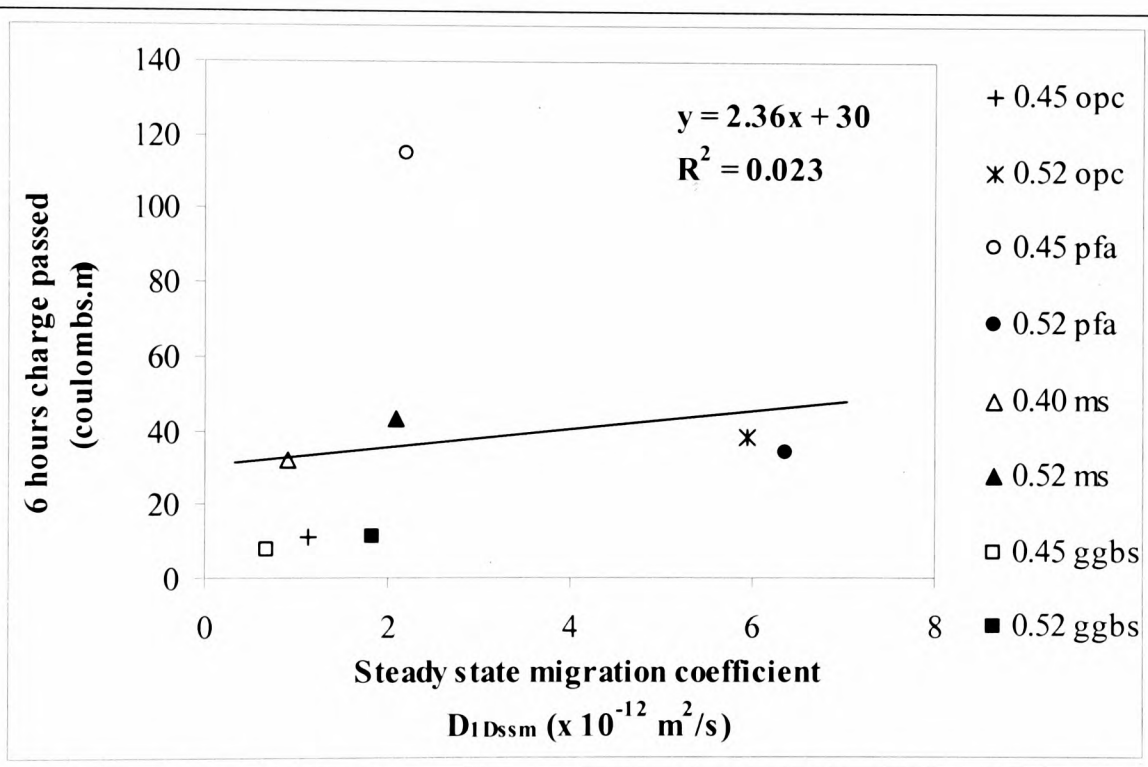

Figure 6.43 Relationship between D_{1Dssm} and 6 hours charge passed from the steady state migration test

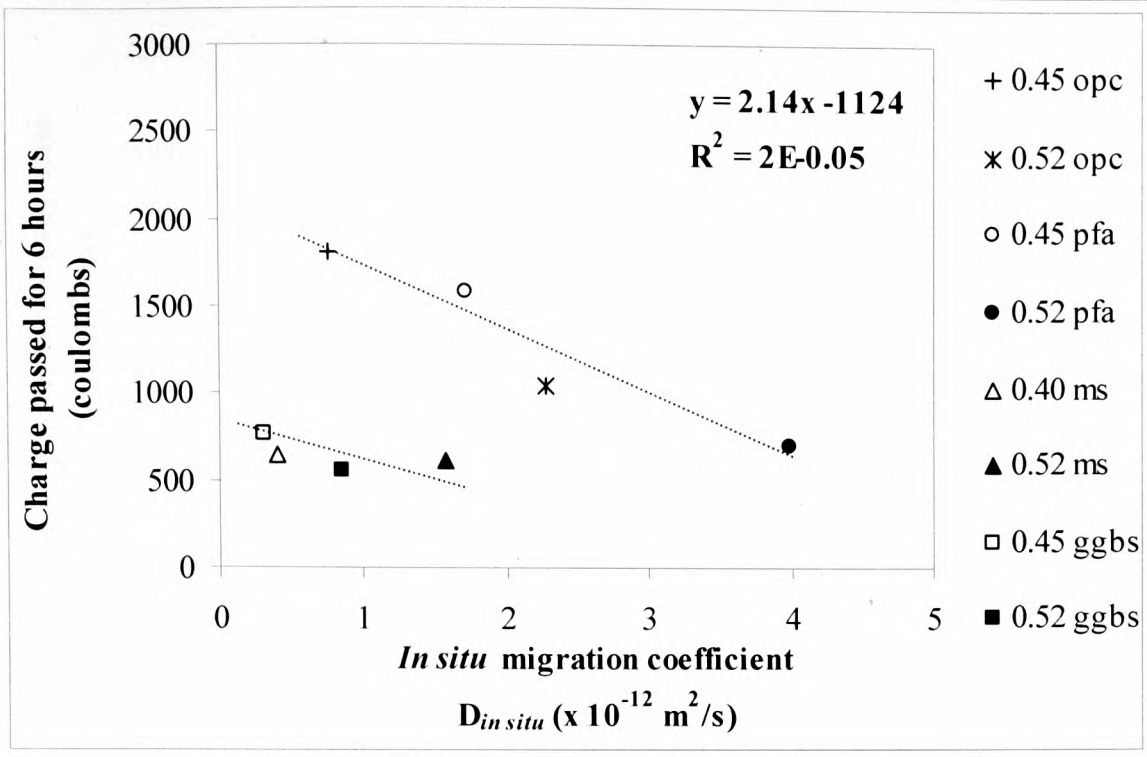

Figure 6.44 Relationship between $D_{in\ situ}$ and 6 hours charge passed from the Permit ion migration test

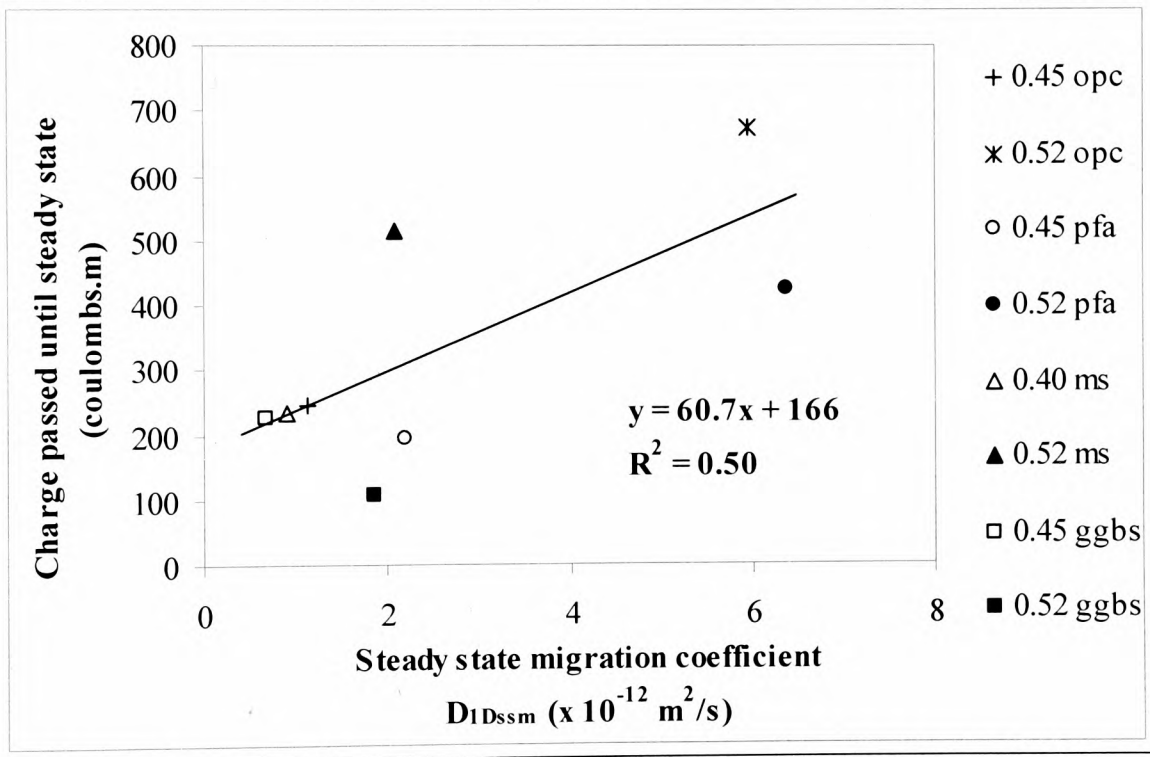

Figure 6.45 Relationship between D_{1Dssm} and charge passed till steady state from the steady state migration test

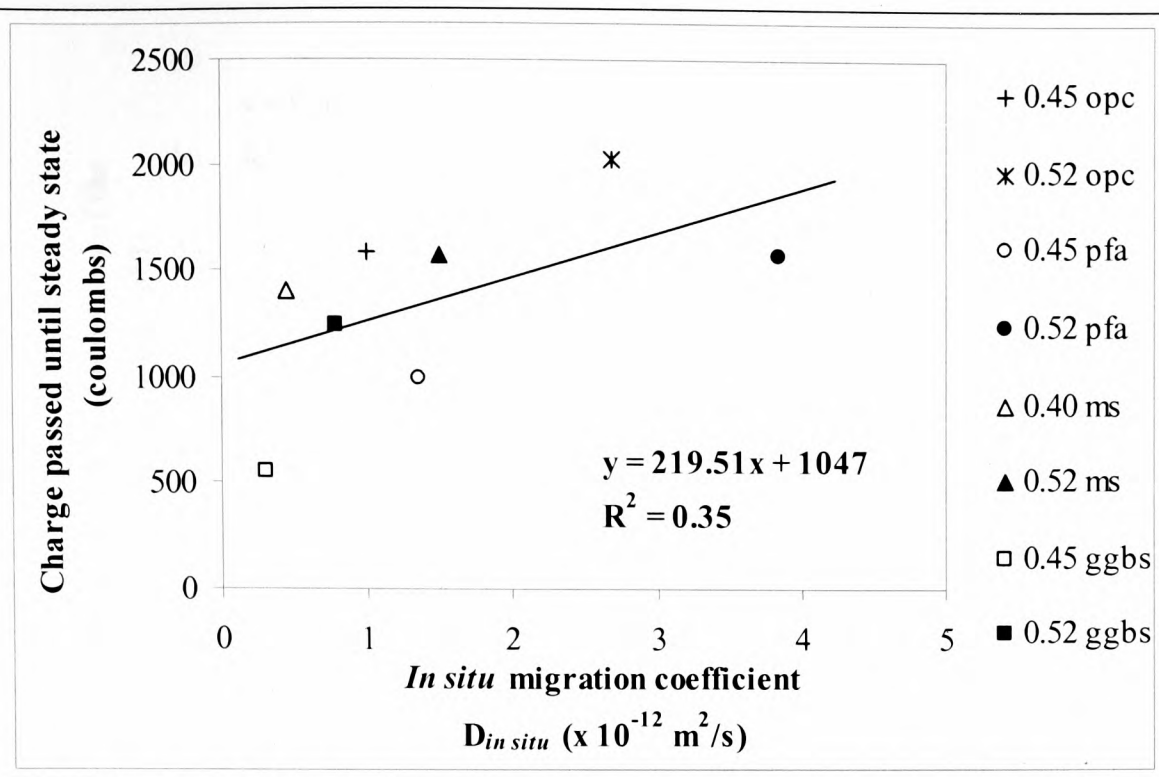

Figure 6.46 Relationship between $D_{in\ situ}$ and charge passed till steady state from the Permit ion migration test

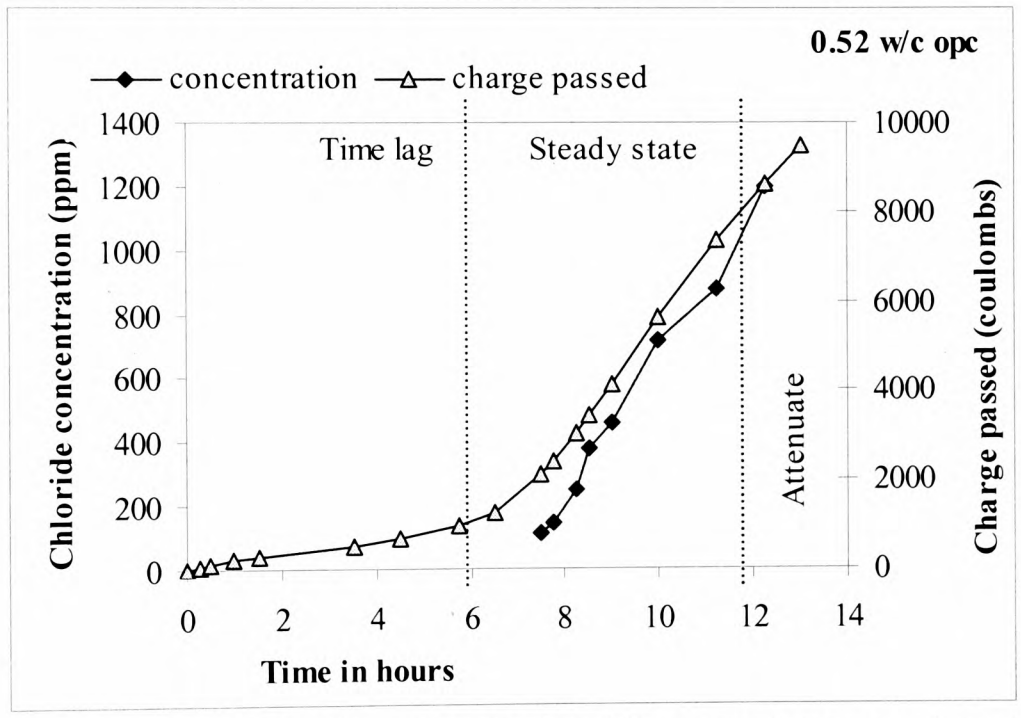

Note: The chloride concentration was obtained from anolyte samples taken during the steady state, this is why there are no chloride concentration data points during time lag

Figure 6.47 A typical graph of chloride concentration in the anolyte and the charge passed in Permit ion migration test

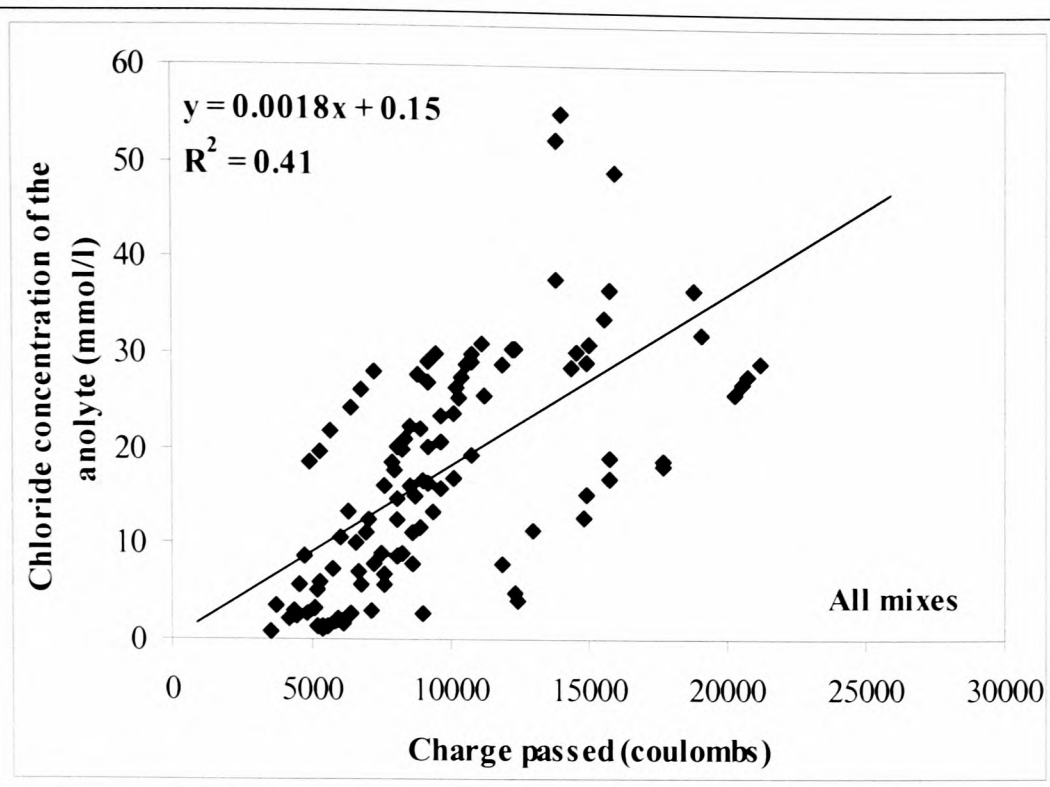

Figure 6.48 Relationship between charge passed and concentration at steady state condition for steady state migration test

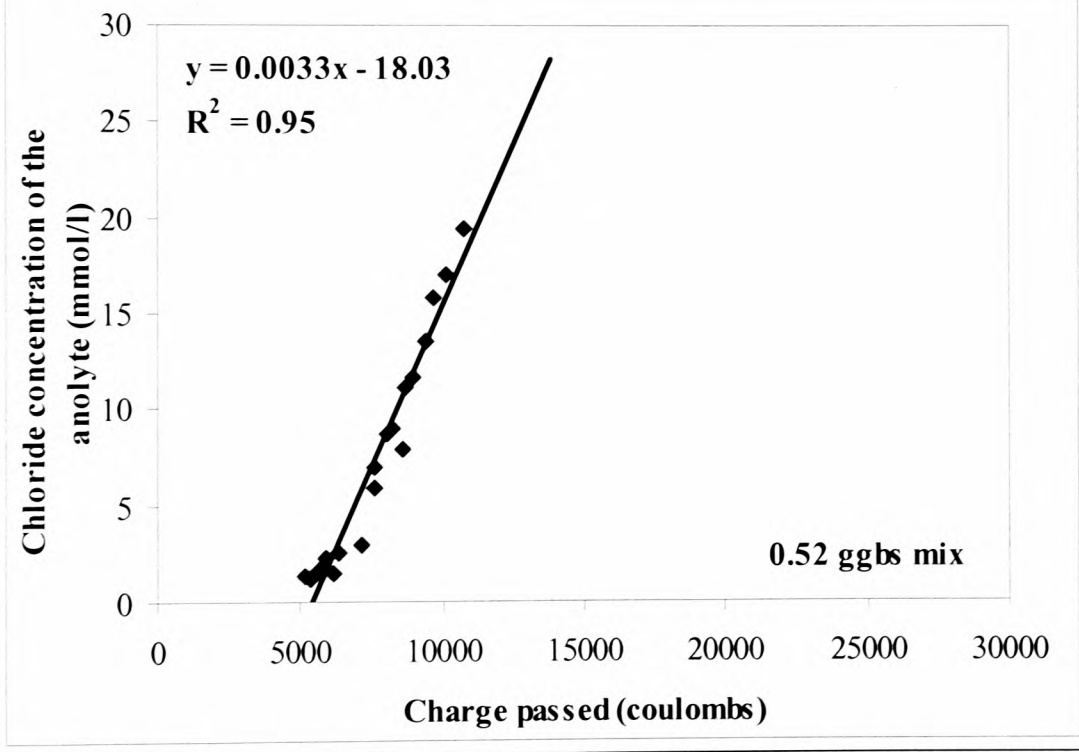

Figure 6.49 A typical graph showing the relationship between charge passed and concentration at the steady state condition for steady state migration test

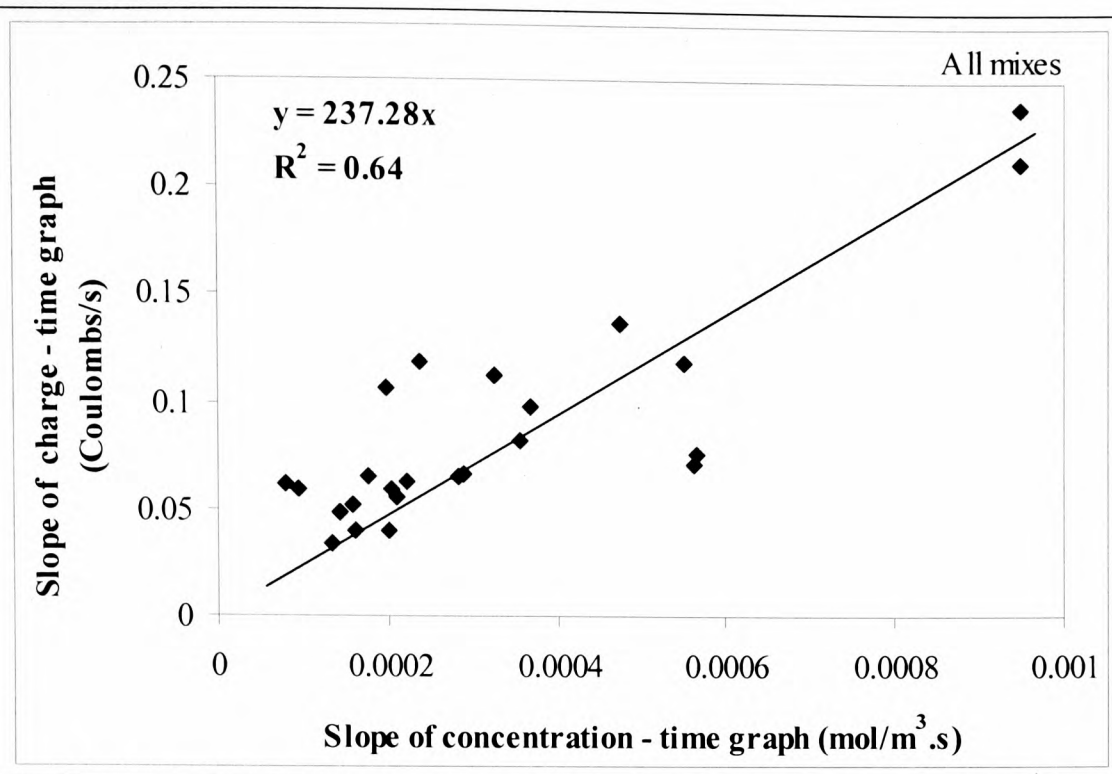

Figure 6.50 Relationship between rate of change of charge and rate of change of chloride concentration in the steady state migration test

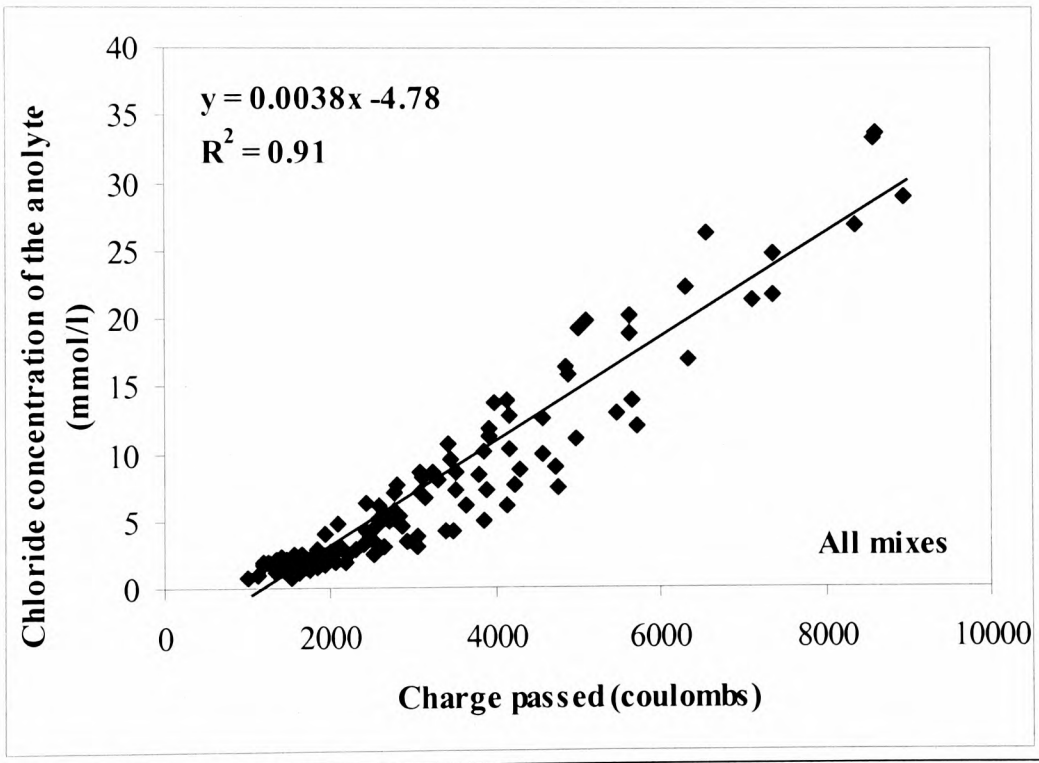

Figure 6.51 Relationship between charge passed and concentration at the steady state condition for Permit ion migration test

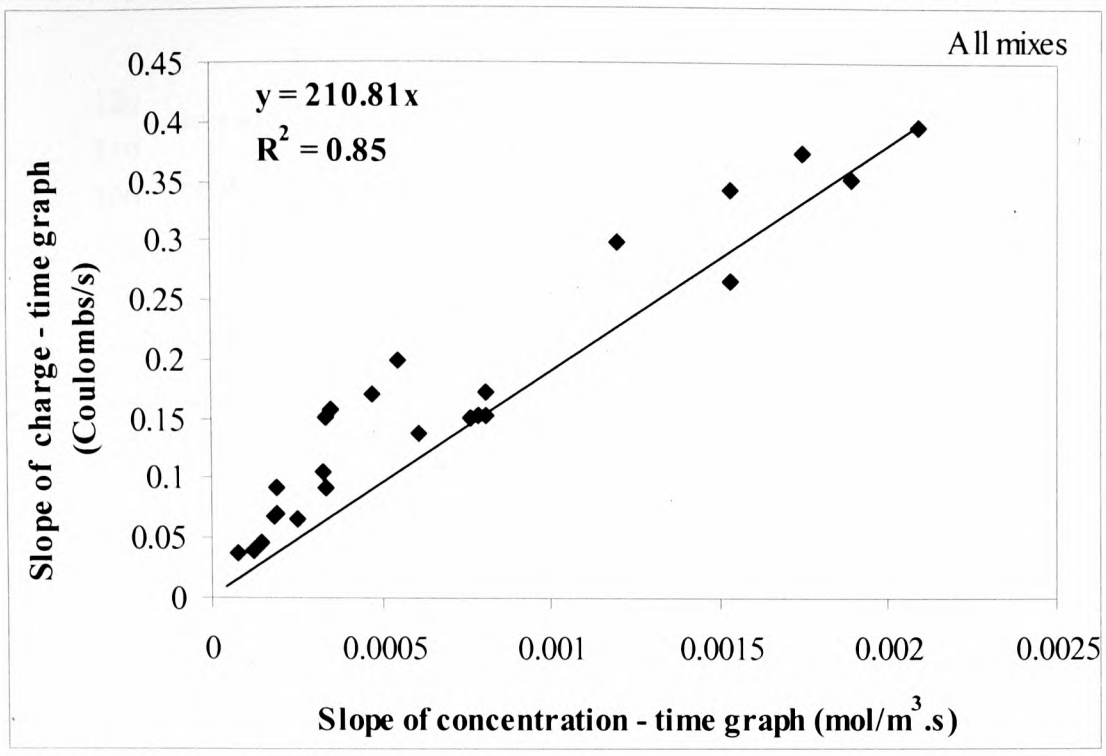

Figure 6.52 Relationship between rate of change of charge and rate of change of chloride concentration in Permit ion migration test

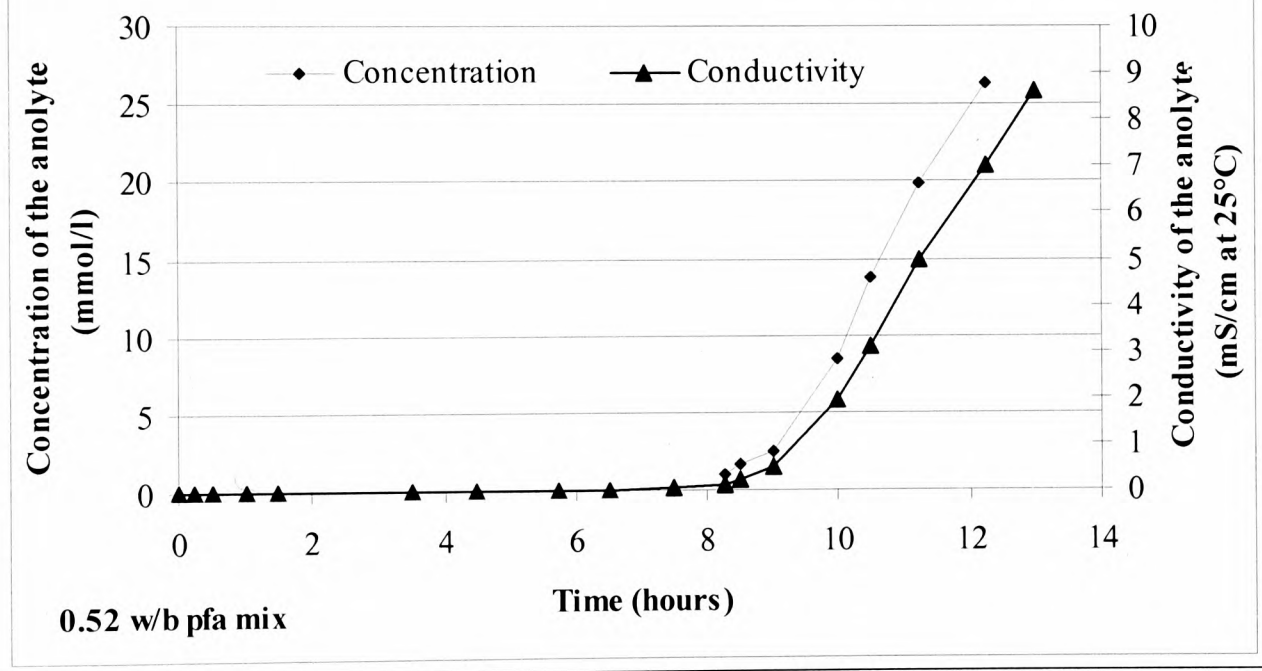

Figure 6.53 A typical concentration and conductivity measurement in the Permit ion migration test

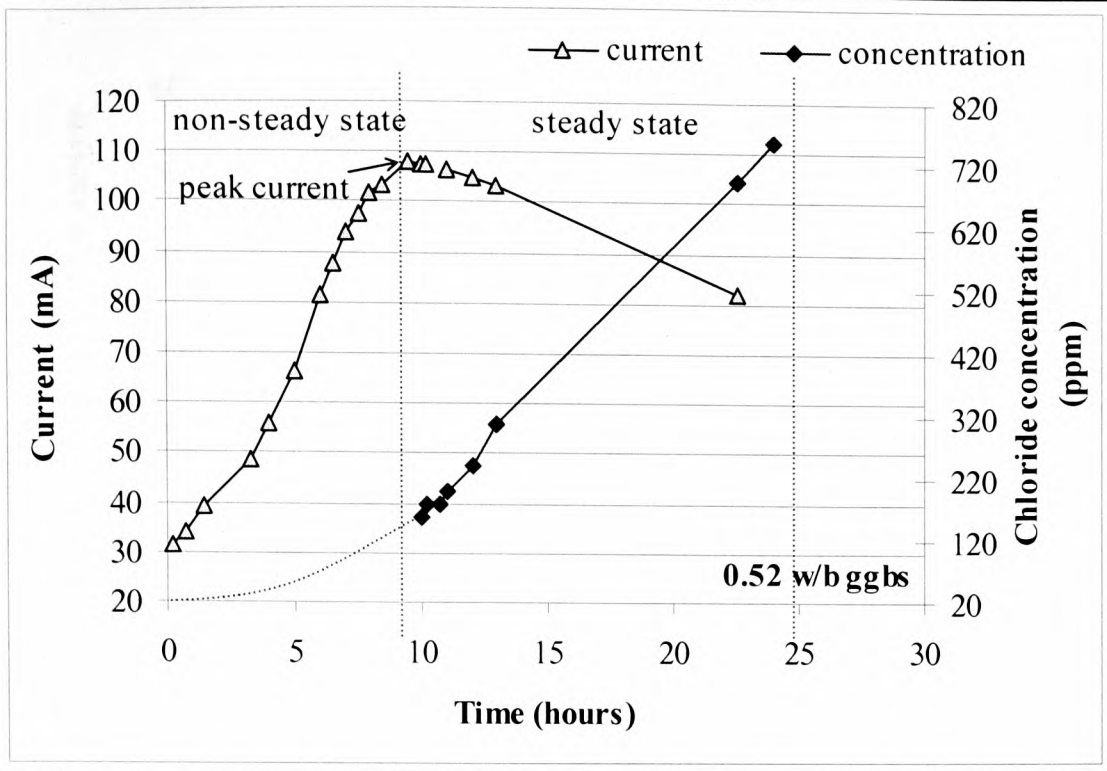

Figure 6.54 Typical current and concentration measurements in Permit ion migration test

Figure 6.55 Typical temperature and current measurement in Permit ion migration test

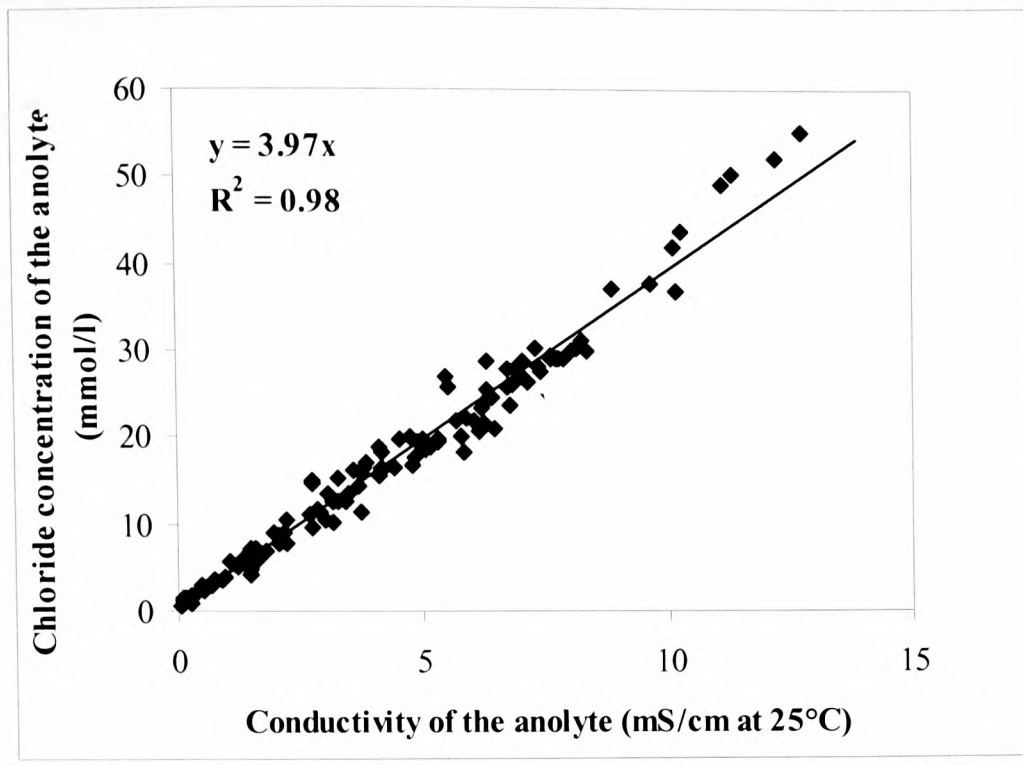

Figure 6.56 The relationship between conductivity and concentration in the steady state migration test

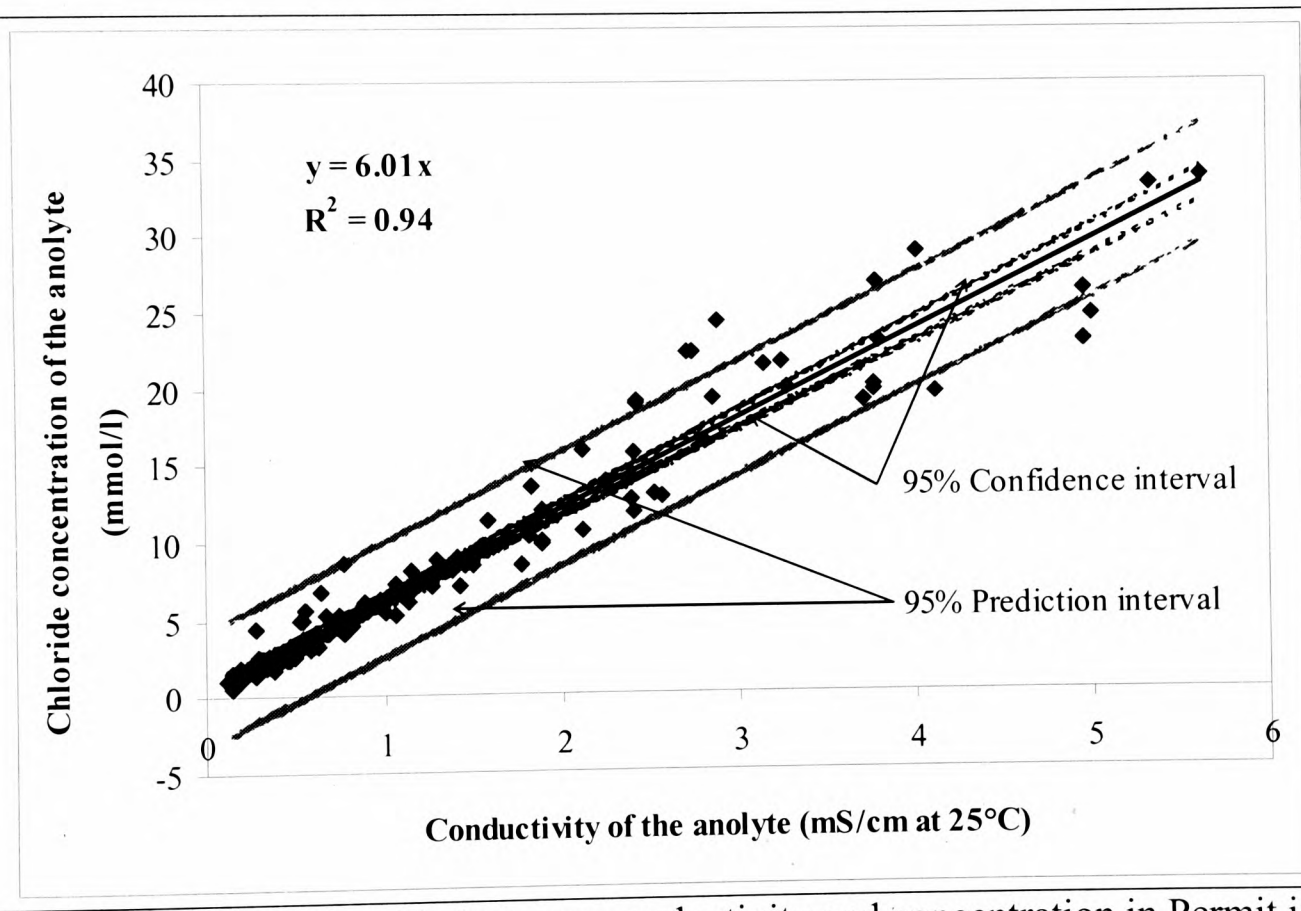

Figure 6.57 The relationship between conductivity and concentration in Permit ion migration test (all mixes)

CHAPTER 7

Developing the Permit ion migration test for use on site

CHAPTER 7 HAS BEEN REMOVED

FROM THE PDF DUE TO

CUSTOMER REQUEST.

Chapter 8

Conclusions and recommendations for further research

8.1 Conclusions

The following conclusions have been drawn from the results presented and discussed in this thesis.

Evaluation of rapid test methods for determining the chloride diffusivity of concrete

1. The performance of four rapid test methods, viz. a non-steady state diffusion test, a steady state migration test, a non-steady state migration test and a bulk resistivity test, was evaluated for determining the chloride diffusivity of concrete. The ability of the parameters obtained from the test methods to distinguish the variations in the mixes, mainly w/b and type of binder, was used to assess the performance of each test. Based on the findings, it was identified that the non-steady state diffusion test, the non-steady state migration test and the bulk resistivity test could be used to assess the chloride diffusivity of concrete, but the steady state migration test failed to distinguish the test variables.
2. The non-steady state diffusion coefficient and the non-steady state migration coefficient showed similar trends with the variations in w/b and the type of binder. The coefficients obtained from both these tests correlated well (R^2=0.93), and, they were of similar magnitude. Therefore, it was concluded that the non-steady state migration test could be carried out as a substitute for the non-steady state diffusion test. This would also mean that the chloride diffusivity of concrete can be estimated in a more rapid and inexpensive way using the former method.
3. In the case of the steady state migration test, the test parameter (i.e. the steady state migration coefficient) failed to demonstrate the effects of both the w/b

and the type of binder. It was considered that the inconsistencies could be due to the smaller thickness of the test specimen used in this test. Therefore, it is suggested that in order to carry out the steady state migration test, a thicker test specimen (i.e., minimum thickness equals three times the maximum size of aggregate, as used in this thesis) should be used.

4. The bulk resistivity was included in the Experimental Programme as an indirect test for estimating the diffusivity of concrete. The bulk resistivity decreased with the increase in w/b. The resistivity of concrete mixes containing cement replacement materials was generally higher than that for the opc concrete. The bulk resistivity showed an inverse relationship with the diffusion parameters (i.e. non-steady state diffusion coefficient and both steady and non-steady migration coefficients). The bulk resistivity correlated well with both the non-steady state diffusion coefficient and the non-steady state migration coefficient, but the coefficient of determination obtained for the latter was higher. Although the relationship between the bulk resistivity and the steady state migration coefficient was similar to that obtained with the non-steady state migration and diffusion coefficients, the coefficient of determination was low. This was considered to be due to the inconsistencies mentioned earlier for the steady state migration test. Nevertheless, based on all the results, it can be concluded that the bulk resistivity test is a reliable method for assessing the chloride diffusivity of concrete. Other attractions of this test are that it requires a simple test set-up and can determine the resistivity of multiple specimens in a short time.

Experimental validation of a new test protocol for the *in situ* ion migration test

5. A new test protocol was developed for the *in situ* ion migration test, with the conductivity of the anolyte being measured as an alternative for the tedious chloride concentration measurement. The conductivity of the anolyte was also used to identify the onset of the steady state condition. The results from this test programme suggest that there is an excellent correlation between the conductivity and the chloride concentration of the anolyte. That is, the conductivity values can be converted to concentration values using an empirical equation, which in turn can be used to calculate the slope of the steady state portion of the concentration versus time graph, and, thereby, the

in situ migration coefficient. The correlation between the conductivity and the chloride concentration of the anolyte was not affected by the variations in the mix (due to both w/b and the type of binder). This new method has been termed as Permit Ion Migration Test.

6. The hemispherical bulb within which the flow of chloride ions takes place in the Permit ion migration test was identified using the electrical resistivity of the concrete. The average flow length, L, to the average flow area, A, is used to define the hemispherical bulb, the ratio of which was found to be $3.76m^{-1}$. The chloride front measured for different concretes suggested that the dimensions of the hemispherical bulb decreased with the increase in electrical resistivity of the concrete. However, this variation did not affect the L/A value, which was found to be a constant for all the mixes. This suggests that irrespective of the variations in L and A, the ratio remains a constant and, hence, a value of $3.76m^{-1}$ could be used in calculations.
7. The *in situ* ion migration coefficient, the non-steady state migration coefficient and the steady state migration coefficient increased with the increase in w/b. The coefficients were lower for mixes containing supplementary cementitious materials, with the exception of the pfa mix. As all the coefficients showed similar trends due to the variations in the mixes as a result of both w/b and type of binder, it was concluded that the Permit *in situ* ion migration test is an alternative method for the *in situ* determination of the chloride diffusivity of concrete. In these comparative tests, the thickness of the sample used for the steady state migration test was three times the size of the coarse aggregate, which was found to yield coefficients that distinguish the mix effects.
8. Both the bulk resistivity and the Wenner Four Probe resistivity decreased with the increase in w/b and increased with the addition of supplementary cementitious materials. It was observed that the electrical resistivity followed an inverse trend with the diffusivity parameters. This also confirms the conclusion 4 that the electrical resistivity can be used to assess the diffusivity of concrete.
9. The *in situ* migration coefficient correlated well with the steady state migration coefficient, the non-steady state migration coefficient and the resistivity obtained from both the bulk resistivity and the Wenner Four Probe

resistivity for the different types of concrete studied. This would mean that a reliable prediction of these coefficients could be made by carrying out the Permit ion migration test. This would allow not only faster estimation of these properties, but also a repetitive assessment of the property on site after different periods of exposure in a service environment.

10. The peak currents obtained from both the Permit ion migration test and the steady state migration test were influenced by the w/b of the mix and the type of binder in a manner similar to the related migration coefficients. The peak current in each type of test also correlated well with both the corresponding migration coefficient and the bulk resistivity. This suggests that by measuring the peak current, the estimation of the diffusivity of concrete can be made and as the test duration is shorter for the determination of the peak current, it is faster than the determination of the migration coefficient.
11. The charge passed during the first six-hours in both the Permit ion migration test and the steady-state migration test was not found to be influenced in any consistent manner by either the w/b or the type of binder. In the case of the steady state migration test there were limitations in the reported charge passed. Therefore, no attempt was made to evaluate critically the effectiveness of the charge passed during the first six hours in assessing the chloride penetration resistance of concretes. Although these limitations were not applicable to the six-hours charge passed reported in Permit ion migration test, the relationship did not improve much. Therefore, it was concluded that the charge passed during the first six hours cannot be used to quantify the chloride penetration resistance of concretes.
12. The charge passed until the steady state was also investigated thoroughly in both the steady state migration test and the Permit ion migration test. In comparison with the charge passed during the first six hours, the charge passed until steady state distinguished the effect of both the w/b and the type of binder better for all mixes. The relationship between the charge passed until steady state and the corresponding migration coefficient also was better than that between the charge passed during the first six hours and the corresponding migration coefficient.
13. The charge passed during the steady state was linearly related to the corresponding chloride flux in both the steady state migration test and the

Permit ion migration test and the degree of correlation was better for the Permit ion migration test. In view of conclusions 11 and 12, these results would suggest that the procedure used in ASTM C1202 to determine the chloride ion penetration resistance of concretes needs to be revisited and the better correlation observed between the charge passed during the steady state and the corresponding chloride flux made use of in order to assess the chloride diffusivity of concretes.

Development of the Permit ion migration test for the site use

14. Based on conclusion 5, the measurements in the new test protocol of the Permit ion migration test were automated and the instrument was modified to make it more user-friendly for site applications. The new version, termed as the in situ version of the Permit ion migration test, contains a Permit body made of durable cast plastic and a control unit. The preparations for carrying out a test can be completed in 5 minutes and, once the test is started, the instrument can be left unattended. The control unit measures, records and displays the data. A laptop can be connected to the control unit at any time to download the data. Therefore, it is possible to carry out multiple tests with little increase in workload. The *in situ* version eliminates the possibility of human errors affecting the measurements and reduces the cost of carrying out the test considerably.

8.2 Recommendations for further research

Based on the research presented in this thesis the following areas have been identified for further investigation:

1. At present in Permit ion migration test, chloride ion solution is used as the catholyte. This, however, introduces more chlorides into the structure being tested. Although the chloride ions can be removed from the test zone by electrochemical extraction using Permit ion migration test itself (Andrews, 1999), it may take up to 4 days to complete this procedure. Therefore, as an alternative, different ion sources, such as nitrites, iodides or hydroxides instead of chlorides should be investigated. As these ions will be introduced into the concrete while testing, the long-term effect of the presence of such ions in concrete needs to be studied as well.

2. It was observed that the volume of the chloride source solution has an influence on the *in situ* migration coefficient determined using the Permit ion migration test. This effect needs to be studied further for a given chloride source solution in order to establish an optimum cell volume for the inner cell of the Permit.
3. The experimental results showed that the peak current correlated with the diffusivity. As the current peaks, the flow of ions through concrete is in a steady state, suggesting that the entire flow path is saturated with chloride ions. If a similar situation can be achieved by saturating the concrete by other ionic solutions, such as $Ca(OH)_2$, this would enable a quick measurement of the equivalent peak current using the Permit ion migration test. It has to be established whether or not the equivalent peak current measured in this case would correlate with the diffusivity of concrete. In addition, the presence of other ions could influence this result; therefore, this topic needs to be thoroughly investigated.
4. It was observed that for concretes with lower resistivity the current flowing through the electrodes in Permit ion migration test was very high. This would not only overheat the test specimen and test instrument, but also creates inaccuracies in the test result. Therefore, it is necessary to reduce the test voltage based on the resistivity of the test specimen. This need to be investigated further to create a classification of concretes based on the electrical resistivity and the recommended test voltage.
5. To assess effectively the diffusivity of concrete on site the new test needs to be carried out on structures exhibiting different degrees of deterioration. This will enable reliable estimates to be made of the future durability of structures exposed to a chloride environment.

References

-A-

Andrade, C., Calculation of chloride diffusion coefficients in concrete from ionic migration measurements, *Cement and Concrete Research*, Vol. 23, No. 3, 1993, pp.724-742.

Andrade, C. and Sanjuan, M.A., Experimental procedure for the calculation of chloride diffusion coefficients in concrete from migration tests, *Advances in Cement Research*, Vol. 6, 1994, pp. 127-134.

Andrade, C., Alonso, C., Arteaga, A. and Tanner, P, Methodology based on the electrical resistivity for the calculation of reinforcement service life, *Fifth CANMET/ACI International Conference on Durability of Concrete*, 2000, pp. 899-915.

Andrade, C., Private communications, 2006 (as included in Chlortest, 2006).

Andrews, R., *Design and Development of an In-situ Chloride Migration Test*, Ph.D Thesis, Queen's University of Belfast, 1999, pages. 388.

Arsenault, J., Bigas, J.P. and Ollivier, J.P., Determination of chloride diffusion coefficient using two different steady-state methods: Influence of concentration gradient, *RILEM International Workshop on Chloride Penetration into Concrete*, Saint-Remy-Les-Chevreuse, France, 1995, pp. 150-151.

Arya, C., Buenfeld, N.R. and Newman, J.B., Factors influencing chloride-binding in concrete, *Cement and Concrete Research*, Vol. 20, No. 2, 1990 pp. 291-300.

Arya, C. and Xu, Y., Effect of cement type on chloride binding and corrosion of steel in concrete, *Cement and Concrete Research*, Vol. 25, No. 4, 1995, pp. 893-902.

ASTM C 1152, *Standard Test Method for acid soluble chloride in mortar and concrete*, American Society for Testing and Materials, 1990, pp. 613-4.

ASTM C 1543-02, *Standard Test Methods for Determining the Penetration of Chloride Ion into Concrete by Ponding*, American Society for Testing Materials, 2002.

ASTM C 1556-04, *Standard Test Method for Determining the Apparent Chloride Diffusion Coefficient of Cementitious Mixtures by Bulk Diffusion*, American Society for Testing and Materials, 2004.

ASTM C1202, *Electrical Indication of Concrete's Ability to Resist Chloride Ion Penetration*, Annual Book of American Society for Testing Materials Standards, 1997.

Atzeni, C., Massidda, L., and Sanna, U., Effect of water/cement ratio on pore size distribution in hardened cement pastes - Porosity-strength relationship, *Materials Engineering*, Vol. 1, No. 2, 1989, pp. 467-473.

-B-

Bamforth, P.B. and Chapman-Andrews, J.F., Long term performance of R.C. elements under UK coastal exposure conditions, *Proceedings of International Conference, Corrosion and Corrosion protection of Steel in Concrete*, Ed. Swamy, R.N., Vol. 1, Sheffield, 1994, pp. 139-156.

Bamforth, P.B., Price, W.F. and Emerson, M., An international review of chloride ingress into structural concrete, Contractor Report 359, Transport Research Laboratory, Edinburgh, 1997, pages.162.

Baroghel-Bouny, V., Belin, P., Castellote, M., Rafai, N. and Rougeau, P., Which toolkit for Durability Evaluation as regards Chloirde ingress into concrete?, Part I: Comparison between various methods for assessing the chloride diffusion coefficient of concrete in saturated conditions, Testing and Modelling Chloride Ingress into Concrete, *Proceedings of the 3rd International RILEM Workshop*, Pro 38, 2002, pp. 105-136.

Basheer, P.A.M., Andrews, R.J., Robinson, D.J. and Long, A.E., 'PERMIT' ion migration test for measuring the chloride ion transport of concrete on site, *NDT & E International*, Vol. 38, No. 3, 2005, pp. 219-229.

Beaudoin, J.J., Ramachandran, V.S. and Feldman, R.F., Interaction of chloride and C-S-H, *Cement and Concrete Research*, Vol.20, No. 6, 1990, pp.875-883.

Bentz, D.P. and Feng, X., Time-dependent diffusivities: Possible misinterpretation due to spatial dependence, Testing and Modelling Chloride Ingress into Concrete, *Proceedings of the 2nd International RILEM Workshop*, Pro. 19, 2000, pp. 225-233.

Bockris, J.O. and Reddy, A.K.N., *Modern electrochemistry*, Macdonald & Co Ltd, London, Vols. 1-2, 1970, pages. 1432.

British Standard 882, *Specification for aggregates from natural sources for concrete*, British Standard Institution (BSI), London, 1992.

British Standard 1881-125, *Testing concrete- Part 125: Methods for mixing and sampling fresh concrete in the laboratory*, British Standard Institution (BSI), London, 1988.

British Standard 3892-1, *Pulverised fuel ash- Part 1: Specification for pulverized-fuel ash for use with Portland cement*, British Standard Institution (BSI), London, 1997.

British Standard 6699, *Pulverised fuel ash- Part 1: Specification for ground granulated blast-furnace slag for use with Portland cement*, British Standard Institution (BSI), London, 1992.

British Standard 8500, *Complementary British Standard to BS EN 206-1, Part 1 Method of specifying and guidance for the specifier*, British Standard Institution (BSI), London, 2002.

British Standard EN 197-1, *Cement- Part 1: Composition, specifications and conformity criteria for common cements*, British Standard Institution (BSI), London, 2000.

British Standard EN 206-1, *Specification, performance, production and conformity*, British Standard Institution (BSI), London, 2000.

British Standard EN 1008, *Mixing water for concrete: Specification for sampling, testing and assessing the suitability of water, including water recovered from processes in the concrete industry, as mixing water for concrete*, British Standard Institution (BSI), London, 2002.

British Standard EN 12350-2, *Testing fresh concrete- Part 2: Slump test*, British Standard Institution (BSI), London, 2000.

British Standard EN 12350-7, *Testing fresh concrete- Part 7: Air content- Pressure methods*, British Standard Institution (BSI), London, 2000.

British Standard EN 12390-3, *Testing hardened concrete- Part 3: Compressive strength of test specimens*, British Standard Institution (BSI), London, 2000.

British Standard EN 13263-1, *Silica fume for concrete- Part 1: Definitions requirements and conformity criteria*, British Standard Institution (BSI), London, 2005.

British Standard EN 13396, *Products and systems for the protection and repair of concrete structures, Test methods- Measurement of Chloride Ion Ingress by Diffusion of Repair Mortars and Concretes*, British Standard Institution (BSI), London, 2004.

Broomfield, J.P., *Corrosion of steel in concrete,* E&FN Spon, London, 1997, pages. 240.

Buenfeld, N.R., *Permeability of concrete in marine environment*, Ph.D Thesis, London University, 1984.

Buenfeld, N.R. and Newman, J.B., The permeability of concrete in a marine environment, *Magazine of Concrete Research*, Vol. 36, No. 127, 1984, pp. 67-80.

Buenfeld, N.R. and Newman, J.B., Examination of three methods for studying ion diffusion in cement pastes, mortars and concrete, *Materials and Structures*, Vol. 20, 1987, pp. 3-10.

Byfors, K., Influence of silica fume and fly ash on chloride diffusion and pH values in cement paste, *Cement and Concrete Research*, Vol. 17, No. 1, 1987, pp 115 – 130.

-C-

Castellote, M., Andrade, C. and Alonso, C., Phenomenological mass-balance-based model of migration tests in stationary conditions: Application to non-steady-state tests, *Cement and Concrete Research*, Vol. 30, No. 12, 2000, pp. 1885-1893.

Castellote, M., Andrade, C. and Alonso, C., Measurement of the steady and non-steady-state chloride diffusion coefficients in a migration test by means of monitoring the conductivity in the anolyte chamber, Comparison with natural diffusion tests, *Cement and Concrete Research*, Vol. 31, No. 10, 2001, pp. 1411-1420.

Chatterji, S., On the non-applicability of unmodified Fick's law to ion transport through cement based materials, Chloride penetration into concrete, *RILEM International Workshop on Chloride Penetration into Concrete*, Saint-Remy-Les-Chevreuse, France, 1995, pp. 64-73.

Chindaprasirt, P., Chotithanorm, C., Cao, H.T. and Sirivivatnanon, V., Influence of fly ash fineness on the chloride penetration of concrete, *Construction and Building Materials*, Vol. 21, No. 2, 2007, pp. 356-361.

Chlortest Resistance of concrete to chloride ingress-from laboratory test to in-field performance, CHLORTEST, Final Technical Report EU FP5 Growth Initiative (GRD1-2002-71808), 2006.

Crank, J., *The mathematics of Diffusion*, 2nd Edition, Claredon Press, Oxford, 1975, pages. 414.

-D-

Decter, M.H., Short, N.R., Page, C.L. and Higgins, D.D., Chloride ion penetration into blended cement pastes and concrete. SP114 - 68. Fly Ash, Silica Fume, Slag and Natural Pozzolans in Concrete, *Proceedings 3rd International Conference*, Trondheim, Norway, Vol. 2, Ed. V.M. Malhotra, 1989, pp. 1399 - 1412.

Delagrave, A., Marchand, J. and Samson, E., Prediction of diffusion coefficients in cement-based materials on the basis of migration experiments, *Cement and Concrete Research*, Vol. 26, No. 12, 1996, pp.1831-1842.

Delagrave, A., Marchand, J., Ollivier, J., Julien, S. and Hazrati, K., Chloride binding capacity of various hydrated cement paste systems, *Advanced Cement Based Materials*, Vol. 6, 1997, pp. 28-35.

Dhir, R.K., Jones, M.R., Ahmed, H.E.H. and Senevirantne, A.M.G., Rapid estimation of chloride diffusion coefficient in concrete, *Magazine of Concrete Research*, Vol. 42, No. 152, 1990, pp. 177-185.

-E-

El-Belbol, S.M.T. and Buenfeld, N.R., Accelerated chloride ion diffusion test (ACID), *Materials Research Society Symposium Proceedings 137*, 1989, pp. 203-208.

El-Belbol, S.M.T., *Acceleration of Chloride Ion Diffusion in Concrete*, Ph D Thesis, University of London, 1990.

-F-

Feldman, R., Prudencio Jr, L.R. and Chan, G., Rapid chloride permeability test on blended cement and other concretes: correlations between charge, initial current and conductivity, *Construction and Building Materials*, Vol. 13, No. 3, 1999, pp. 149-154.

Fidjestol, P. and Tuutti, K., Proceedings of International Conference, *Concrete under Severe Conditions 2: Environment and Loading*, CONSEC'98, Eds. Gjorv, O.E., Banthia, N. and Sakai, K., Norway, 1998, pp. 133-142.

-G-

Garboczi, E.J. and Bentz, D.P., *Journal of Material Science*, Vol. 27, 1992, pp. 2083-2092.

Gilleece, P.R.V., *An Investigation of Chloride Penetration into Modified Concretes*, Ph.D Thesis, Queen's University Belfast, United Kingdom, 1996, pages. 391.

Gjorv, O.E. and Sakai, K., Testing of Chloride Diffusivity for Concrete, *Concrete Under Severe Conditions, Environment and Loading*, CONSEC'95, Vol. 1, 1995, pp. 655-666.

Goto, S. and Roy, D.M., Diffusion of ions through hardened cement pastes, *Cement and Concrete Research*, Vol. 11, Nos. 5-6, 1981, pp 751-757.

Guimaraes, A.T.C. and Helene, P.R.L., Chloride diffusion and the influence of the saturation degree of the concrete, Testing and Modelling Chloride Ingress into Concrete, *Proceedings of the 3rd International RILEM Workshop*, Pro. 38, 2002, pp. 237-256.

-H-

Halamickova, P., Detwiler, R.J., Bentz, D.P. and Garboczi, E.J., Water permeability and chloride ion diffusion in portland cement mortars: Relationship to sand content and critical pore diameter, *Cement and Concrete Research*, Vol. 25, No. 4, 1995, pp. 790-802.

Hansson, C.M. and Berke, N.S., Chlorides in concrete, *Proceedings of Materials Research Society Symposium, Pore Structure and Permeability of Cementitious Materials*, Vol. 137, Boston, 1989, pp. 253-270.

Hassanein, A.M., Glass, G.K. and Buenfeld, N.R., Effect of intermitted cathodic protection on chloride and hydroxyl concentration profiles in reinforced concrete, *Corrosion Review*, Vol. 17, No. 5, 1999, pp. 423–441.

Hewlett, P.C., *Lea's Chemistry of Cement and Concrete*, 4th Edition, Butterworth-Heinemann, Oxford, 1998, pages. 1057.

-J-

Johnson, M.A., Miltenberger, M.A. and Amey, S.L., Determining chloride diffusion coefficients for concrete using accelerated test methods, *Proceedings of the 3rd CANMET/ACI International Conference on Concrete in marine environment*, Supplementary Papers, St Andrews by-the-sea, Canada, 1996, pp. 95-114.

-K-

Kayyali, O.A., Strength and porosity of Portland cement paste subjected to chloride penetration, *Journal of Materials in Civil Engineering*, Vol. 1, 1989, pp.10-18.

Kropp, J., State of the art and progress made by RILEM Committee TC 178-TMC, Testing and Modelling Chloride Ingress into Concrete, *Proceedings of the 3rd International RILEM Workshop*, Pro. 38, 2002, pp. 19-28.

Kropp, J. and Hilsdorf, H.K., *Performance criteria for concrete durability*, State-of-the-Art-Report prepared by RILEM Technical committee TC 116-PCD, RILEM Report 12, 1995, pages. 327.

Kokubu, M. and Yamada, Y., *Proceedings of the 6th International Congress Chemistry of Cement*, Moscow, Vol. 3, 1974, pages. 95.

Kosmatka, S., Kerkhoff, B. and Panarese, W., *Design and Control of Concrete Mixtures*, 14th Edition, Portland Cement Association, Skokie, USA, 2002.

Kumar, A. and Roy, D.M., Pore structure and ionic diffusion in admixtures blended Portland cement systems, *8th International Symposium on the Chemistry of Cement*, 1986, pp. 73 - 79.

-M-

Maagee, M., Helland, S., Poulsen, E., Vennesland, O. and Carlsen, J.E., Service life prediction of existing concrete structures exposed to marine environment, *ACI Materials Journal*, Vol. 93, No. 6, 1996, pp. 602-608.

MacDonald, K.A. and Northwood, D.O., Experimental measurements of chloride ion diffusion rates using a two-compartment diffusion cell: Effect of materials and test variables, *Cement and Concrete Research*, Vol. 25, No. 7, 1995, pp. 1407-1416.

McCarter, W.J., Ezirim, H. and Emerson, M., Absorption of water and chloride into concrete, *Magazine of Concrete Research*, Vol. 44, No. 158, 1992, pp. 31-37.

McCarter, W.J., Emerson, M. and Ezirim, H., Properties of concrete in the cover zone: developments in monitoring techniques, *Magazine of Concrete Research*, Vol. 47, No. 172, 1995, pp. 243-251.

McCarter, W.J., Ezirim, H. and Emerson, M., Properties of concrete in the cover zone: water penetration, sorptivity and ionic ingress, *Magazine of Concrete Research*, Vol. 48, No. 176, 1996, pp. 149-156.

McGrath, P.F. and Hooton, R.D., Influence of voltage on chloride diffusion coefficients from chloride migration tests, *Cement and Concrete Research*, Vol. 26, No. 8, 1996, pp. 1239-1244.

McPolin, D., *Profiling of carbonation and chloride distributions in concretes and development of novel fibre optic sensors*, Ph D Thesis, Queen's University of Belfast, United Kingdom, 2005, pages. 322.

Mehta, P.K. and Monteiro, P.J.M., *Concrete, Microstructure, Properties and Materials*, 2nd Edition, The McGraw-Hill Companies, London, 1993, pages. 548.

Millard, S.G., Harrison, J.A. and Edwards, A.J., Measurement of the electrical resistivity of reinforced concrete structures for the assessment of corrosion risk, *British Journal of Non-Destructive Testing*, Vol. 31, No. 11, 1990, pp. 617-621.

Misra, S., Yamamoto, A., Tsutsumi, T. and Motohashi, K., Application of Rapid Chloride Permeability Test to quality control of concrete, *Proceedings of 3rd ACI/CANMET International Conference on Durability of Concrete*, SP-145, Nice, France, 1994, pp. 487-502.

Monaghan, G., *Development of an in situ chloride migration apparatus for concrete*, BEng Dissertation, Queen's University Belfast, 1993.

-N-

Nanukuttan, S.V., Basheer, P.A.M. and Robinson, D.J., Developments on testing chloride transport of concrete on-site using Permit Ion Migration Test, International Conference on World of Innovations in Structural Engineering, Hyderabad, India, 2004, CD Rom.

Nanukuttan, S. V., Basheer, P. A. M., McCarter, W. J. and Robinson, D. J., Effect of duration and conditions of exposure on chloride diffusion, *International Conference on Concrete Repair Rehabilitation and Retrofitting*, Cape Town, South Africa, Nov 2005.

Nanukuttan, S.V., Basheer, P.A.M. and Robinson, D.J., Further development of the Permit ion migration test for determining the chloride diffusivity of concrete, Structure Faults and Repair, Eleventh International conference and exhibition, Edinburgh, 2006, CD Rom.

Newman, J. and Choo, B.S., *Advanced concrete technology: Constituent materials*, Published by Elsevier publications, London, 2003, page 3/37.

Neville, A.M., *Properties of Concrete*, 4th Edition, published by Longman Group Ltd, London, 1996, pages. 844.

Nilsson, L., Andersen, A., Tang, L. and Utgenannt, P., Chloride ingress data from field exposure in a Swedish road environment, Testing and modelling the chloride ingress into concrete, *Proceedings of the 2nd International RILEM Workshop*, Pro. 19, 2000, pp. 69-83.

Nilsson, L., Poulsen, E., Sandberg. P., Sorensen, H.E. and Klinghoffer, O., HETEK, *Chloride penetration into concrete*, State-of-the-art-report, Transport processes, corrosion initiation, test methods and predition models, Report No. 53, 1996, pages. 151.

NT BUILD 208, *Concrete, Hardened: Chloride Content*, NORDTEST Method 2nd Edition, 1984.

NT BUILD 443, *Concrete, Hardened: Accelerated Chloride Penetration*, NORDTEST Method, 1995.

NT BUILD 492, *Concrete, Mortar and Cement Based Repair Materials: Chloride Migration Coefficient from Non-steady State Migration Experiments*, NORDTEST Method, 1999.

-P-

Page, C.L., Short, N.R. and El-Tarras, A., Diffusion of chloride ions in hardened cement pastes, *Cement and Concrete Research*, Vol. 11, 1981, pp. 395-406.

Page, C.L. and Vennesland, O., Pore solution composition and chloride binding capacity of silica fume cement pastes, *Materials and Structures*, Vol. 1, 1983, pp. 19-25.

Page, C.L., Lambert, P. and Vassie, P.R.W., Investigations of reinforcement corrosion. 1, The pore electrolyte phase in chloride-contaminated concrete, Materials and Structures, Vol. 24, 1991, pp. 243-252.

Poulsen, E., *The chloride diffusion characteristics of concrete*, Nordic Concrete Research Publication, No. 9, 1990, pp. 124-133.

Polder, R.B., Chloride diffusion and resistivity testing of five concrete mixes for marine environment, *RILEM International Workshop on Chloride Penetration into Concrete*, Saint-Remy-Les-Chevreuse, France, 1995, pp. 225-233.

Polder, R.B., Test methods for on site measurement of resistivity of concrete - a RILEM TC-154 technical recommendation, *Construction and Building Materials*, Vol. 15, 2001, pp. 125-131.

Prince, W. and Gagne, R., The effects of types of solutions used in accelerated chloride migration tests for concrete, *Cement and Concrete Research*, Vol. 31, 2001, pp. 775-780.

prEN 13396, *Products and systems for the protection and repair of concrete structures, Test methods - Measurement of chloride ion ingress*, Pre European Standard, 2002, (now updated as BS EN 13396).

-R-

Roy, D.M., Fly ash and silica fume chemistry and hydration, Fly Ash, Silica Fume, Slag and Natural Pozzolans in Concrete, *Proceedings of third International Conference*, Norway, Volume 1, SP-114, 1989a, pp. 117-138.

Roy, D.M., Hydration, Microstructure, and Chloride Diffusion of Slag-Cement Pastes and Mortars, Fly Ash, Silica Fume, Slag and Natural Pozzolans in Concrete, *Proceedings of third International Conference*, Norway, Volume 2, SP-114, 1989b, pp. 1265-1281.

-S-

Schiessl, P. and Hardtl, R., Relationship between durability and pore structure properties of concretes containing fly ash, *Proceedings of Mehta, P.K., Symposium on Durability of Concrete*, Nice, France, 1994, pp. 99-118.

Sergi, G., Yu, S.W. and Page, C.L., Diffusion of chloride and hydroxyl ions in cementitious materials exposed to a saline environment, *Magazine of Concrete Research*, Vol. 44, No. 158, 1992, pp. 63-69.

Shi, C., Stegemann, J.A. and Caldwell, R.J., Effect of supplementary cementing materials on the specific conductivity of pore solution and its implications on the rapid chloride permeability test (AASHTO T277 and ASTM C1202) results, *ACI Materials Journal*, Vol. 95, No. 4, 1998, pp. 388-394.

Stanish, K.D., Hooton, R.D. and Thomas, M.D.A., Testing the Chloride Penetration Resistance of Concrete: A Literature Review, *FHWA Contract DTFH61-97-R-00022*, University of Toronto, Canada, 2000, pages. 31.

Streicher, P.E. and Alexander, M.G., A critical evaluation of chloride diffusion test methods for concrete, *Proceedings of 3rd CANMET/ACI International conference on Durability of Concrete*, Supplementary papers, 1994, pp. 517-530.

Streicher, P.E. and Alexander, M.G., A chloride conduction test for concrete, *Cement and Concrete Research*, Vol. 25, No. 6, 1995, pp. 1284-1294.

Sugiyama, T., Tsuji, Y., Bremner, T.W. and Hashimoto, C., Determination of chloride diffusion coefficient of high-performance concrete by electrical potential technique, *Proceedings, 3rd CANMET/ACI International Conference on Concrete in marine environment*, St Andrews by-the-sea, Canada, 1996, pp. 339-354.

Suryavanshi, A.K., Scantlebury, J.D. and Lyon, S.B., Pore size distribution of OPC and SRPC mortars in presence of chlorides, *Cement and Concrete Research*, vol. 25, No. 5, 1995, pp. 980-988.

-T-

Tang, L., On chloride diffusion coefficients obtained by using the electrically accelerated methods, Chloride penetration into concrete, *RILEM International Workshop on Chloride Penetration into Concrete*, Saint-Remy-Les-Chevreuse, France, 1995, pp. 126-134.

Tang, L., Concentration dependence of diffusion and migration of chloride ions: Part 1. Theoretical considerations, *Cement and Concrete Research*, Vol. 29, 1999a, pp. 1463-1468.

Tang, L., Concentration dependence of diffusion and migration of chloride ions: Part 2. Experimental evaluations, *Cement and Concrete Research*, Vol. 29, 1999b, pp. 1469-1474.

Tang, L. and Andersen, A., Chloride ingress data from five years field exposure in a Swedish marine environment. Testing and modelling the chloride ingress into concrete, *Proceedings of the 2nd International RILEM Workshop*, Pro. 19, 2000, pp. 105-119.

Tang, L. and Nilsson, L., Chloride diffusivity in high strength concrete at different ages, *Nordic Concrete Research-11*, 1992a, pp. 162-171.

Tang, L. and Nilsson, L., Rapid Determination of the Chloride Diffusivity in Concrete by Applying an Electrical Field, *ACI Materials Journal*, Vol. 89, No. 1, 1992b, pp. 49-53.

Tang, L. and Nilsson, L.O., A rapid method for measuring chloride diffusivity by using an electric field - theory and current experience, *Nordic Mini-Seminar*, Ed. Nilsson, L.O., Jan 1993, pp 26-35.

Tang, L. and Sorensen, H.E., Precision of the Nordic Test Methods for Measuring the Chloride Diffusion/Migration Coefficients of Concrete, *Materials and Structures*, Vol. 34, 2001, pp. 479-485.

Tong, L. and Gjorv, O.E., Chloride diffusivity based on migration testing, *Cement and Concrete Research*, Vol. 31, 2001, pp. 973-982.

Truc, O., Ollivier, J.P. and Carcasses, M., A new way for determining the chloride diffusion coefficients in concrete from steady state migration test, *Cement and Concrete Research*, Vol. 30, 2000, pp. 217-226.

-W-

Whiting, D., *Rapid measurement of the chloride permeability of concrete*, Federal Highway Administration, Washington, D.C. FHWA/RD-81/119, 1981, pages. 166.

Whittington, H.W., McCarter, W.J. and Forde, M.C., The conduction of electricity through concrete, *Magazine of Concrete Research*, Vol. 33, No. 114, 1981, pp. 48-60.

-X-

Xi, Y., Bazant, Z.P., Molina, L. and Jennings, H.M., Moisture Diffusion in Cementitious Materials, *Advanced Cement Based Materials*, Vol. 1, 1994, pp. 258-266.

-Y-

Yamamoto, A., Motohashi, K., Misra, S. and Tsutsumi, T., Proposed Durability Design for RC Marine Structures, *Concrete Under Severe Conditions, Environment and Loading*, CONSEC'95, 1995, Vol. 1, pp. 544-553.

Yang, C.C. and Weng, T.L., Using charge passed to determine the chloride diffusion coefficient in mortar from accelerated chloride migration test, *Construction and Building Materials*, Vol. 17, 2003, pp. 231-238.

Yang, C.C., Relationship between migration coefficient of chloride ions and charge passed in steady state, *ACI Materials Journal*, Vol. 101, No. 2, 2004, pp. 124-130.

Young, J.F., A review of pore structure of cement paste and concrete and its influence on permeability, ACI, SP108: *Permeability of concrete*, 1988, pp. 1-18.

-Z-

Zhang, J.Z. and Buenfeld, N.R., Development of the accelerated chloride ion (ACID) test, *Proceedings, International Conference on Corrosion and Corrosion Protection of Steel in Concrete*, Ed. Swamy, R.N., Vol. 1, 1994, pp. 395-403.

Zhang, T. and Gjorv, O.E., An electrochemical method for accelerated testing of chloride diffusivity in concrete, Chloride penetration into concrete, *RILEM International Workshop on Chloride Penetration into Concrete*, Saint-Remy-Les-Chevreuse, France, 1995a, pp. 105-114.

Zhang, T. and Gjorv, O.E., Diffusion behavior of chloride ions in concrete, Chloride penetration into concrete, *RILEM International Workshop on Chloride Penetration into Concrete*, Saint-Remy-Les-Chevreuse, France, 1995b, pp. 53-63.

Zhang, T. and Gjorv, O.E., Diffusion behavior of chloride ions in concrete, *Cement and Concrete Research*, Vol. 26, No. 6, 1996, pp. 907-917.

Zhang, T. and Gjorv, O.E., Migration testing of chloride diffusivity in concrete, *Proceedings of International Conference, Concrete under Severe Conditions 2: Environment and Loading*, CONSEC'98, Eds. Gjorv, O.E., Banthia, N. and Sakai, K., Norway, 1998.